

AD-A122 061

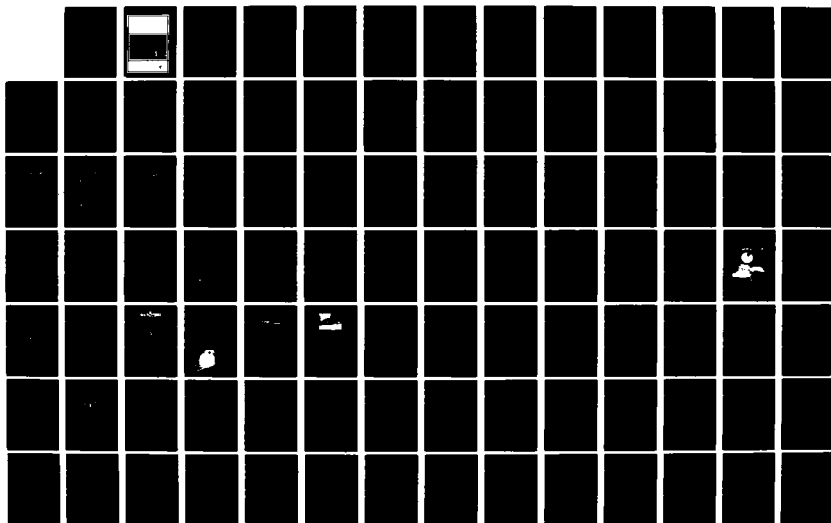
AIRCRAFT DYNAMIC RESPONSE TO DAMAGED AND REPAIRED  
RUNWAYS(U) ADVISORY GROUP FOR AEROSPACE RESEARCH AND  
DEVELOPMENT NEUILLY-SUR-SEINE (FRANCE) AUG 82  
AGARD-CP-326

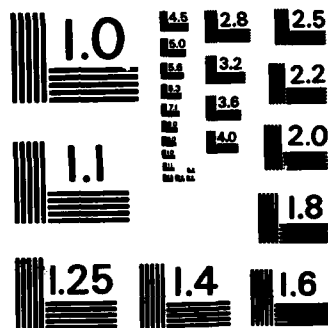
1/3

UNCLASSIFIED

F/G 1/5

NL





MICROCOPY RESOLUTION TEST CHART  
NATIONAL BUREAU OF STANDARDS-1963-A

AGARD-CP-326

AGARD-CP-326

# AGARD

ADVISORY GROUP FOR AEROSPACE RESEARCH & DEVELOPMENT

7 RUE ANCELLE 92200 NEUILLY SUR SEINE FRANCE

AGARD CONFERENCE PROCEEDINGS No. 326

## Aircraft Dynamic Response to Damaged and Repaired Runways

This document has been approved  
for public release and sale; its  
distribution is unlimited.

DTIC  
ELECTE  
DEC 3 1982  
S A

NORTH ATLANTIC TREATY ORGANIZATION



DISTRIBUTION AND AVAILABILITY  
ON BACK COVER

AD A 122061

FILE COPY

**NORTH ATLANTIC TREATY ORGANIZATION**  
**ADVISORY GROUP FOR AEROSPACE RESEARCH AND DEVELOPMENT**  
**(ORGANISATION DU TRAITE DE L'ATLANTIQUE NORD)**

**AGARD Conference Proceedings No.326**  
**AIRCRAFT DYNAMIC RESPONSE**  
**TO DAMAGED AND REPAIRED RUNWAYS**



Accession For	
NTIS GRA&I	<input checked="" type="checkbox"/>
NTIS TAB	<input type="checkbox"/>
Unannounced	<input type="checkbox"/>
Justification	
Availability Codes	
Avail and/or	
Dist	Special
A	



## THE MISSION OF AGARD

The mission of AGARD is to bring together the leading personalities of the NATO nations in the fields of science and technology relating to aerospace for the following purposes:

- Exchanging of scientific and technical information;
- Continuously stimulating advances in the aerospace sciences relevant to strengthening the common defence posture;
- Improving the co-operation among member nations in aerospace research and development;
- Providing scientific and technical advice and assistance to the North Atlantic Military Committee in the field of aerospace research and development;
- Rendering scientific and technical assistance, as requested, to other NATO bodies and to member nations in connection with research and development problems in the aerospace field;
- Providing assistance to member nations for the purpose of increasing their scientific and technical potential;
- Recommending effective ways for the member nations to use their research and development capabilities for the common benefit of the NATO community.

The highest authority within AGARD is the National Delegates Board consisting of officially appointed senior representatives from each member nation. The mission of AGARD is carried out through the Panels which are composed of experts appointed by the National Delegates, the Consultant and Exchange Programme and the Aerospace Applications Studies Programme. The results of AGARD work are reported to the member nations and the NATO Authorities through the AGARD series of publications of which this is one.

Participation in AGARD activities is by invitation only and is normally limited to citizens of the NATO nations.

The content of this publication has been reproduced  
directly from material supplied by AGARD or the authors.

Published August 1982

Copyright © AGARD 1982  
All Rights Reserved

ISBN 92-835-0316-2



Printed by Technical Editing and Reproduction Ltd  
5-11 Mortimer Street, London, W1N 7RH

## **PREFACE**

During 1981 and 1982 the AGARD Structures and Materials Panel held two technical meetings on "Aircraft Dynamic Response to Damaged and Repaired Runways". The 1981 meeting focused on the environment of damaged airfields, while the 1982 Specialists' Meeting focused on aircraft dynamic response. The meetings had two main goals: (1) to review the programs and methods within the AGARD countries for dynamic analysis and testing of taxiing aircraft, and (2) to encourage the exchange of information on aircraft dynamic response, thereby improving the interoperability of NATO military aircraft.

The meetings met the first goal in serving as an intermediate milestone in the prediction and measurement of dynamic response of NATO aircraft. Yet it became clear that two questions remain partially unanswered — what is the expected state of NATO airfields after attack, and what are the structural and dynamic limitations of the existing fleet of aircraft?

The meetings also met the second goal in that the participating nations each agreed to determine the dynamic response of many of their aircraft to a hypothetical "three-patch" test, developed by M.Hacklinger of Germany. The reporting and evaluation of those results remain as future actions for the AGARD/SMP which should form a basis for evaluating interoperability of NATO aircraft.

**JAMES J. OLSEN**  
Chairman, Sub-Committee on  
Dynamic Response to  
Damaged Runways

## CONTENTS

	Page
<b>PREFACE</b> by J.J.Olsen	iii
	Reference
<b><u>PART 1</u></b>	
<b>MINIMUM OPERATING STRIP SELECTION PROCEDURE</b> by W.S.Strickland and L.R.Caldwell	1
<b>DEVELOPMENT STATUS OF NEW CONSTRUCTION PROCEDURES FOR RAPID REPAIR OF DAMAGE TO AIRCRAFT OPERATING SURFACES IN WARTIME*</b> by D.Kempf	2
<b>PROPOSED SPECIFICATIONS FOR INTERNATIONAL INTEROPERABILITY ON REPAIRED BOMB DAMAGED RUNWAYS</b> by L.R.Caldwell and A.G.Gerardi	3
<b><u>PART 2</u></b>	
<b>Specialists Meeting</b>	
<b><u>SESSION I - OVERVIEWS</u></b>	
<b>ADVANCED RAPID RUNWAY REPAIR - A STABLE AND FLUSH REPAIRED RUNWAY SURFACE</b> by R.J.Bergholz	4
<b>EVALUATION OF THE PILOT PAPERS FROM THE SPRING 1981 SMP MEETING</b> by A.Krauss	5
<b>APPLICATION OF SEMI-RIGID PAVEMENTS IN RAPID RUNWAY REPAIR</b> by A.F.Tovar de Lemos	6
<b>THE REPAIRED RUNWAY CLEARANCE ENVIRONMENT</b> by C.Brain	7
<b>THE 'HAVE BOUNCE' PROGRAM</b> by J.E.Holpp	8
<b><u>SESSION II - MATHEMATICAL MODELLING OF AIRCRAFT DYNAMIC RESPONSE</u></b>	
<b>INFLUENCE OF MATHEMATICAL MODELLING OF UNDERCARRIAGES ON THE PREDICTION OF AIRCRAFT LOADS DUE TO DAMAGED AND REPAIRED RUNWAYS</b> by A.Krauss, O.Bartsch and G.Kempf	9
<b>DEVELOPMENT OF A COST EFFECTIVE APPROACH TO MODELLING AIRCRAFT RESPONSE TO REPAIRED RUNWAYS</b> by B.W.Payne, A.E.Dudman, B.R.Morris and M.Hockenhull	10
<b>STATUS OF COMPUTER SIMULATIONS OF USAF AIRCRAFT AND AN ALTERNATIVE SIMULATION TECHNIQUE</b> by A.G.Gerardi and L.Minnetyan	11
<b>METHODE DE SIMULATION NUMERIQUE DU SYSTEME AVION ATTERRISSEUR</b> par C.Petiau et A.Celler	12

**SESSION III – TEST METHODS AND CORRELATION WITH ANALYSES****PREDICTED AND MEASURED LANDING GEAR LOADS FOR THE NF-5 AIRCRAFT  
TAXIING OVER A BUMPY RUNWAY**

by H.H.Ottens

13

**LABORATORY TESTING SYSTEMS FOR STRUCTURAL DYNAMIC RESPONSE TO  
LARGE-SCALE DISTURBANCES**

by J.W.Piraino

14

**SESSION IV – DESIGN AND CLEARANCE****THE PROBLEM OF DESIGN CRITERIA FOR AIRCRAFT LOADS DUE TO ROUGH  
RUNWAY OPERATION**

by M.Hacklinger

15

**LANDING GEAR SHOCK ABSORBER DEVELOPMENT TO IMPROVE AIRCRAFT  
OPERATING PERFORMANCE ON ROUGH AND DAMAGED RUNWAYS**

by G.H.Haines

16

**ROUGHNESS CONSIDERATIONS FOR TRANSPORT AIRCRAFT**

by B.M.Crenshaw

17

**A FIGHTER LANDING GEAR FOR THE 1980's**

by R.F.Buttles and R.D.Renshaw

18

**PART 1**

**PAPERS PRESENTED AT THE 52nd PANEL MEETING**

**SPRING 1981**

**PART 1**

**PAPERS PRESENTED AT THE 52nd PANEL MEETING**

**SPRING 1981**

# MINIMUM OPERATING STRIP SELECTION PROCEDURE

William S. Strickland  
HQ AFESC/RDCR  
Tyndall AFB, FL 32403  
USA

Lt Col Lapsley R. Caldwell  
HQ AFESC/RDCR  
Tyndall AFB, FL 32403  
USA

## SUMMARY

This report provides Minimum Operating Strip (MOS) selection procedures for use in post attack launch and recovery operations. These procedures are based on interim surface roughness guidance found in Reference 1 and are provided pending development of finalized procedures under the USAF Rapid Runway Repair (RRR) program. Although the specific details and examples contained herein are given for the an F-4 aircraft, the general procedures can be applied to MOS selection for any aircraft at any particular airfield.

## I INTRODUCTION

1.0 OBJECTIVE. The objective of this MOS selection criteria is to minimize the time required to repair a MOS, prevent damage to the aircraft, and optimize the flexibility in selection of a MOS. The price that must be paid for these benefits is the complexity of the crater repair and the associated MOS selection process. This report defines five levels of repair quality, for AM-2 mat and crushed stone repairs, together with a repair spacing criteria for the F-4 aircraft. These definitions are used to select the MOS and define its repair quality.

2.0 ASSUMPTIONS. In the process of preparing this selection procedure, it was necessary to limit the scope and complexity of the analysis by making several assumptions. These assumptions are:

2.1 Emergency Use Only: These criteria will only be used under conditions of war.

2.2 F-4 Aircraft: The procedures contained herein are based primarily upon structural performance and test data for the F-4E aircraft. These criteria have been extended to other F-4 versions by analysis. Similar procedures could be developed for other aircraft.

2.3 Take Off Gross Weight: An F-4 take off gross weight of 57,000 pounds has been utilized for preparation of MOS selection criteria. Use of these criteria for F-4 aircraft lighter than 57,000 pounds will yield conservative results.

2.4 Landing Gross Weight: These criteria assume that the landing aircraft is approximately 38,000 pounds, which permits a small fuel reserve. Landing the aircraft at gross weights several thousand pounds heavier on a runway that meets the minimum roughness criteria could result in exceeding aircraft design limit loads.

2.5 Aborts: Since these criteria are intended for use under conditions of war no provision is made for Take Off aborts. A Take Off abort over a runway repaired to the minimum requirements of this criteria will result in exceeding main landing gear (MLG) structural design limit loads as well as tire design limit loads. No standards for aborting aircraft have been developed at this time.

2.6 Repairs: These criteria assume that all repairs are made with either AM-2 mats or the crushed stone technique discussed in References 2, 3, and 4.

2.7 Take Off Power: These criteria use nominal aircraft performance data and assume maximum power for take off.

3.0 PARAMETER DEFINITION. Referring to the simplified example of a repaired crater in Figure 1, the following parameters are defined:

3.1 REPAIR UPHEAVAL. The height of the repair above the original pavement elevation. It occurs where the pavement has been raised by the explosion around the edge of the crater or by overfill in the crater during the repair operation. Upheaval includes the height of a FOD cover or a repair mat such as the US AM-2.

3.2 SAG. The vertical distance between the low points of a repair and an "imaginary repair surface". In order to measure sag, the "imaginary repair surface" must be established by stretching a string across the repair so that it contacts the

pavement just outside the start of the upheaval, as shown in Figure 2. Then the vertical distance from the repair surface to the string must be measured. Sag will probably increase with aircraft traffic as the fill settles.

**3.3 DAMAGE LENGTH.** The length, parallel to the MOS centerline, including upheaved pavement, of the damaged pavement. If the repair has an FOD cover or a mat with a significant thickness then the damage length includes the cover or mat. The measurement includes all material including upheaved pavement, repair mats, etc., that may not be at the original pavement level and would result in surface roughness.

**3.4 CHANGE IN SLOPE.** The deviation of the repair grade from the original pavement grade. For example, since an AM-2 mat ramp rises 1.5 inches above the original grade in 3.75 feet, an AM-2 ramp represents a slope change of:  $(1.5) \text{ divided by } (3.75 \times 12)$  equals 0.033 or 3.3 percent. A special tool is provided in the repair kit for measuring the change in slope of the upheaved pavement around a crater.

**3.5 APPARENT CRATER DIAMETER.** The apparent diameter is the visible diameter of the crater, inside edge to inside edge, prior to debris being removed.

**3.6 ACTUAL DAMAGE DIAMETER.** The diameter across the upheaved pavement from the start of upheaval on one side of the crater to the end of upheaval on the far side of the crater.

## II MOS SELECTION PREPARATION

Successful conduct of MOS selection will be dependent on proper personnel, training, and equipment. The purpose of this section is to identify required personnel, graphical aids, and training.

**1.0 PERSONNEL.** Four civil engineering personnel will be required to perform the MOS identification and selection process. All four will be located in the Survival/Recovery Center (SRC), with supportive explosive ordnance disposal (EOD) and Disaster Preparedness (DP) personnel.

**1.1 Data Recorder.** This individual will be responsible for receiving and posting coordinates of damage and unexploded ordnance (UXO).

**1.2 Data Plotter.** This individual will be responsible for plotting damage and Unexploded Ordnance (UXO) locations on the airfield map.

**1.3 MOS Selector.** This individual will utilize templates and overlays to identify a potential MOS and the access routes to the MOS.

**1.4 Team Chief.** This individual will perform quality control of the MOS selection process, calculate estimated time to repair for a potential MOS, time to repair for MOS access routes, and will recommend the final MOS to the SRC Commander. The team chief will also make recommendations to the SRC Commander for damage and EOD reconnaissance when it affects the MOS selection process. One example would be a case where excessive damage would make it appear unprofitable to continue reconnaissance of one taxiway when a second route is available.

**2.0 TRAINING.** The MOS selector and the team chief should be familiar with References 1, 2, and 3. All individuals (and alternates) should receive a minimum of 16 hours of training and practice. The training should be conducted periodically with simulated exercises at each individual base.

**3.0 EQUIPMENT.** In coordination with the BRAAT team, several graphical aids must be prepared for the specific base.

**3.1 Airfield Map.** A scale drawing of the airfield pavement area must be prepared for recording and displaying airfield damage, UXO, and making the MOS selection. The suggested scale is 1 inch to 100 feet.

**3.2 Crater Damage Template.** A 1-inch to 100-foot scale clear plastic template that permits plotting of estimated crater damage diameter circles can be prepared using Figure 3. The template will automatically scale reported apparent crater diameter to maximum expected damage diameter. A drawing of the template is included in Appendix F.

**3.3 MOS Template.** A transparent template that represents the 50- x 5000-foot (1/2- x 50-inch) MOS should be fabricated. This template will be used to outline a potential 50- x 5000-foot MOS.

**3.4 Repair Spacing Templates.** Colored or shaded transparent overlays must be prepared to assist in MOS selection. These spacing templates should be prepared (Reference 1) for either expected, or a "worst case low" density ratio at the specific airfield. Estimated rotation distance should be marked on these templates for the expected take off combat loads. The expected density ratio (in tenths) and rotation distance are available from operations personnel. Templates have been prepared for density ratios of 0.9 (110°F, 500ft), 1.0 (51°F, 500ft), and 1.1 (4°F, 500ft). Rotation distance on the templates is based upon a planned F-4E take off weight of 57,000 lbs and a 33 percent center of gravity (c.g.) location.



### III MOS SELECTION PROCEDURES

This section describes how to use surface roughness criteria for selection of a 50-x 5000-foot Minimum Operating Strip (MOS) as shown in Figure 4, using the general procedures of Reference 1. These MOS selection procedures have been modified so that repairs made with both AM-2 mat and repairs made with crushed stone can be used on the same MOS. It must be stressed that MOS selection procedures will be ineffective unless adequate preplanning and practice have been performed.

**1.0 MAJOR PROCEDURAL STEPS.** Five major steps are involved in selection of an MOS. These steps (a detailed flow chart and checklist is included in Appendix C) are:

- (a) plotting the airfield pavement damage (to include UXO),
- (b) identification of several potential MOS locations,
- (c) selection of an access route to each MOS location,
- (d) calculation of the repair time for each potential MOS location and its associated access route,
- (e) comparison of the potential MOS locations.

**2.0 DAMAGE PLOTTING.** The repairs on the runway, taxiways and ramp areas should be plotted on the map using preselected coordinate systems. An example is shown in Figure 5. The damage assessment teams should identify the center of damage locations to the SRC. They should also report the type of damage; as a spall, small crater, large crater or camouflet and the apparent diameter of the crater. The damage plotter must convert apparent crater diameter to estimated actual damage diameter using the crater damage template discussed in paragraph 3.2 of Section II. The plotter should write the apparent crater diameter on the map as a 1, 2, 3 etc., for a crater less than 10 ft, 20 ft, 30 ft. Spalls and UXO should also be plotted. When a potential MOS is selected it will be identified by its direction and the coordinates of its starting point, (x,y). An example would be 23-(3000, -75) as shown in Figure 5.

**3.0 IDENTIFICATION OF POTENTIAL MOS LOCATIONS.** The MOS selection is based upon satisfying spacing criteria and defining five repair qualities along the length of a potential MOS. These five qualities are different for AM-2 mat repair and crushed stone repair. The detailed specifications are discussed in Reference 1 and 2 and a summary is included in Appendix A and B.

**3.1** The surface roughness criteria are direction sensitive, and a MOS repaired to the minimum surface roughness criteria will not be satisfactory for use in the direction opposite to the design direction. A bidirectional MOS will normally require more time to repair than a unidirectional MOS. Base operations should be asked for the required runway direction and the probability that the take off direction would change. Take off by an F-4E in the opposite direction, which results in operation over category "E" and "D" repairs before rotation, will result in exceeding design limit loads.

**3.2** Next the expected density ratio should be determined from Base Operations or Reference 5. The aircraft performance is highly dependent on this value, requiring different spacing templates for different density ratios. The template selection is made based on the density ratio at the projected time of operations. Templates have been prepared for density ratios of 0.9, 1.0 and 1.1. These templates provide both the repair spacing and the repair quality requirements. The scale factor for these templates must be the same as the airfield map.

**3.3 Rules for Selecting Potential MOS sites.** The following steps outline the process in selecting the potential MOS sites:

- (a) Select a segment with one or less repair ("B" or "C") between the start point and rotation.
- (b) If a segment with only one repair cannot be located, select a segment for which multiple repairs ("B", "C") between the starting point and rotation meet the repair spacing criteria. The procedures and use of the spacing templates are described in paragraph 3.4.
- (c) If spacing criteria cannot reasonably be met, minimize the number of repairs between the starting point and rotation, and upgrade all repairs that do not meet the spacing criteria to category "A".
- (d) All repairs less than 100 feet apart, must be covered with a single AM-2 mat, made into a single crushed stone repair, or upgraded as defined in special requirements of Tables A-1, and B-1. (See Appendices A and B.)
- (e) Landings will be accomplished on the MOS in the same direction as takeoff. The spacing templates, used to define repair categories along the MOS, are based on load limits experienced in takeoffs. They permit multiple "E" repairs 500 feet beyond rotation of the aircraft. For landing aircraft, however, an additional restriction limits aircraft travel over multiple "E" repairs to speeds less than 10 KTS. To accomplish this, a barrier must be used for landing, or multiple "E" repairs disallowed.

If no mobile barrier is available, and more than one "E" repair is indicated by the spacing template, all "E" repairs on the MOS must be upgraded to "D" repairs.

(f) In order to minimize time to repair, crushed stone repairs should be used for the smaller craters. A chart that recommends the type of repair (AM-2 or crushed stone) based on the apparent crater diameter is provided in Appendix D.

(g) It should be anticipated that "A" or "B" AM-2 mat repairs and crushed stone "A" repairs will be difficult and time-consuming (Appendix A, B) and, therefore, avoided during the MOS selection unless the repair team has previously determined that they can successfully perform these repairs.

3.4 Use of Repair Spacing Criteria. A set of templates for the F-4E, C, and D with a 33 percent cg. location, have been prepared to assist in MOS selection. These spacing templates, in conjunction with the plotted damage, are used as a graphic test of whether or not a potential MOS meets spacing requirements. The specific spacing template shown in Figure 6 is for an F-4E, a density ratio of 1.0 and an 1800-foot nose wheel lift-off distance. The shaded region of the template represents the areas where a subsequent repair is not allowed.

After the bomb damage and projected repair area has been plotted on the map, a 5000- by 50-foot strip is picked as a potential MOS. The spacing template is laid over the first section of this potential MOS, matching the origin of the template with the start of the MOS. The template is moved downward in a vertical direction, keeping the start of the MOS co-linear (aligned) with the vertical axis of the template, until the trailing edge of the first repair contacts the equidistant line. If the second repair does not fall in the shaded area, then the spacing is adequate. The next step is to check the spacing between the second and third repair. In the same manner, the template is moved vertically across the MOS to put the second repair on the equidistant line and the spacing of the third crater is checked. This process is repeated until all craters between the start of the MOS and the rotation line (beginning of "D" repair zone) have been checked for satisfactory spacing between them. Throughout the entire process, the vertical axis of the template is matched with the start of the MOS.

Figure 7 shows the case of two repairs located at 1000 and 1500 feet along the MOS. As shown, when the beginning of the MOS is matched with the vertical axis on the template and the trailing edge of the first repair is placed on the equidistant line, the second repair falls inside the shaded unsatisfactory zone. This second repair becomes satisfactory if the MOS start is moved closer to the first repair as shown in Figure 8. It should be noted that this example contradicts the normally accepted technique of starting takeoff roll at the beginning of undamaged pavement. The case of four satisfactory craters is shown in Figures 9, 10, and 11. Repairs are located on the MOS at 0, 500, 1200, and 1850 feet. To check the spacing between the first and second repair, the template and MOS repair plot are set as shown in Figure 9. Since the second repair is not within 400 feet of the first, it is acceptable. Next, as shown in Figure 10, the beginning of the MOS is lined up with the template vertical axis and the trailing edge of the second repair is placed on the 500-foot mark on the equidistant line. Since the third repair does not fall in the shaded area, the spacing is satisfactory.

To check the spacing between the third and last repair, the template is moved vertically, as shown in Figure 11. The beginning of the MOS remains lined up with the template vertical axis. Since the last repair is outside the shaded area, it is satisfactory.

#### 4.0 SELECTION OF ACCESS ROUTES

4.1 Choke Point Identification. As a part of specific base preplanning, the airfield should be analyzed to establish access routes to all possible MOS. In the case of our simple example, only the runway 5/23 is considered acceptable for the MOS. There are two access routes from the ramp area to the runway and these are identified as TW1 and TW2 in Figure 5.

4.2 Runway Transition Routes. From the intersection of each of these taxiway choke points to a potential MOS location, a taxi route must be planned. As an example the access from TW1 to the potential MOS would be called the TW1 transition or abbreviated the TW1-MOS. Similarly, for TW2 there would be a TW2 transition or TW2-MOS. From each of the three aircraft dispersal areas (A, B, C) a taxi route must be planned to each of the taxiways TW1 and TW2. Their transition routes will be called A-TW1, A-TW2, and B-TW1, etc. For clarity only three of these six routes are shown on Figure 5.

4.3 Access Route Selection. For the example in Figure 5, two access routes can be defined to each potential MOS location. Each consists of one of the taxiways and an associated transition to the potential MOS. The MOS selection team must determine what damage must be repaired for each of these access routes, using the taxiway repair criteria (for F-4s only) in Table 1. Normally the Damage Assessment team can advise the MOS selection team if adequate clearance exists for an F-4 to taxi around damage on the taxiway. If clearance is available the Damage Assessment Team should not spend excessive time measuring crater location or size since these craters would not be a high priority for repair. It should be noted that the repairs on TW1, and TW2, A-TW1, A-TW2, B-TW1, etc., only have to be determined once for all potential MOS locations. Also, many of the taxiway to MOS transition routes will be the same or similar for different MOS locations.

TABLE 1. Taxiway Repair Criteria

	<u>Feet</u>	<u>Notes</u>
Repaired Width	25	1,2
Cleared Width	35	1,3
90° Turn Width	30	1
180° Turn Width	50	1

## NOTES:

1. This table is for F-4 aircraft. Wing Walkers may be required for minimum clearances.
2. Category E taxiway repairs should be used to reduce materials and repair time. They must be at least 70 feet apart at 10 knots. Closer spacing requires 5 knot taxi speeds.
3. Debris removed but craters outside repaired width not repaired.

## 5.0 CALCULATION OF TIME TO REPAIR

5.1 A repair time work sheet (Table 2) should be filled out for each potential MOS location, each of the associated "MOS to taxiway transitions" (Table 3) and each of the two taxiways (Table 3). In addition Table 3 should be filled out for two access routes from each dispersal area to the two respective taxiways. The taxiway and dispersal area taxi routes work sheets will be applicable to every MOS location. The transition work sheets will be applicable to a given potential MOS location. An example of completed work sheets is included as Appendix E. The specific repair times listed in Table 2 and Table 3 are fictitious, and should be replaced with values validated for a given base's capabilities.

TABLE 2. MOS Time Sheet

MOS IDENTIFICATION _____							
Apparent Crater Diameter		QUALITY					TIME
		A	B	C	D	E	
10 FT	NO.						
	TIME/REP	136	130	123	121	116	
	SUBTOTAL						
20 FT	NO.						
	TIME/REP.	140	136	127	125	120	
	SUBTOTAL						
30 FT	NO.						
	TIME/REP.	143	141	137	136	130	
	SUBTOTAL						
40 FT	NO.						
	TIME/REP.	150	149	*	144	140	
	SUBTOTAL						
50 FT	NO.						
	TIME/REP.	156	155	*	*	141	
	SUBTOTAL						
60 FT	NO.						
	TIME/REP.	170	166	*	*	143	
	SUBTOTAL						
70 FT	NO.						
	TIME/REP.	182	175	*	*	146	
	SUBTOTAL						
>70 FT	CASE NO.						
	1	TTR =					
	2	TTR =					
	3	TTR =					
	4	TTR =					
	5	TTR =					
ESTIMATED EOD CLEARANCE TIME							
SPALLS	NO.	TIME/SPALL = 1 MIN					
TOTAL REPAIR TIME							

The above TIME/REP values are fictitious and should be replaced with values validated for a given bases capabilities.

\* Upgrade to "B" repairs

TABLE 3. Taxiway Time Sheet

Pavement Identification \_\_\_\_\_

Estimated EOD Clearance Time \_\_\_\_\_

<u>Repair Type/Crater Diameter</u>	<u>Number</u>	<u>Time per Repair</u>	<u>Time per Type</u>
<u>SPALLS</u>	_____	1 min	_____
<u>CRUSHED STONE</u>			
10 feet (1)	_____	116 min	_____
20 feet (2)	_____	120 min	_____
30 feet (3)	_____	130 min	_____
40 feet (4)	_____	140 min	_____
<u>AM-2 MAT</u>			
50 feet (5)	_____	141 min	_____
60 feet (6)	_____	143 min	_____
70 feet (7)	_____	146 min	_____
		Total Time*	_____

Category E repairs are used as the basis for this time per repair estimate since they are the fastest repair. Spall repair time assumes that Silikal® repair are completed before the crater repairs and have sufficient time to cure, (30 minutes).

5.2 Typical damage scenarios will include craters spaced very close together or overlapping. Under such conditions the fastest repair could consist of making a single crushed stone repair by removing the concrete in between them, repairing with a single AM-2 mat, or making two separate high quality stone repairs. No data base exists for field guidance in making repairs of this type. Judgement must be used in selecting the method, and could be dependent on base resources and talents. The times required to repair craters in excess of 70 feet should be estimated and entered at the bottom of Table 2 on a case by case basis.

5.3 Estimates of EOD times must be obtained from the EOD representative in the control center, and included in the time to repair work sheets. The EOD estimate should only include time to dispose of the UXO's that threaten the repair or retention of the potential MOS and the associated access routes.

5.4 Estimate the number of spalls on the MOS that require repair and record in Table 2. The F-4 can be operated over unrepaired spalls that are less than 1.5 inches deep and 2 feet long with no more than two spalls in any 24 foot length along the direction of travel.

5.5 Table 4 should now be completed for each potential MOS location. This table does not include time to repair routes from Dispersal Areas to taxiways.

TABLE 4. MOS Repair Time

MOS ID \_\_\_\_\_

	TIME TO REPAIR			
	MOS	TW	TW - MOS	TOTAL
TW1	_____	_____	_____	_____
TW2	_____	_____	_____	_____
			Minimum Time	

## 6.0 MOS COMPARISON AND SELECTION

6.1 The potential MOS locations are now compared in the format shown in Table 5, and the aircraft dispersal to taxiway routes are compared in Table 6.

TABLE 5. MOS Comparison

MOS ID	TW ID	REPAIR TIME (MOS + ACCESS)
_____	_____	_____
_____	_____	_____
_____	_____	_____
_____	_____	_____

TABLE 6. Dispersal Area Times

Dispersal Area	Taxiway	Time to Repair
A	TW1	_____
	TW2	_____
B	TW1	_____
	TW2	_____
C	TW1	_____
	TW2	_____

6.2 The Base Commander should now be briefed on the team's recommendations. The primary basis for the commander's decision will be the minimum time (from Table 5) to restore a MOS to operations and his highest priority for aircraft dispersal areas, tempered by the time to repair the dispersal area access routes to the taxiways as shown in Table 6. Although these times will be a major factor in the team briefing, they must include other considerations, such as nearby UXO, alternate direction landings, and barrier location as discussed in paragraphs 7 and 8 below.

6.3 After a tentative MOS selection is made, a marking and surveying team should be sent out to mark those repairs that are required, validate coordinates of craters and to determine that the selection appears reasonable. This is an essential step since it is very possible that errors exist in the reported and plotted data. During this marking process, the repair crew should be briefed on the repair locations and quality.

6.4 As repairs are made, the selection team should continually update the data and re-evaluate the MOS selection in light of damage assessment revisions and new damage that may occur. Prior to use of the MOS and access route base operations personnel should be briefed on all details of the repair and provided a sketch of the MOS, access routes, and hazards.

7.0 Repeat the above procedure to select an MOS for an alternate direction. If necessary it may be desirable for a bidirectional MOS to be repaired as shown in Figure 12, but local priorities should be used to determine if the extra time required for a bidirectional repair should be used at this time.

## 8.0 CONSIDERATIONS FOR LANDING AIRCRAFT

8.1 Category "E" Repairs: If more than one category "E" repair is used, the landing aircraft must be stopped before it encounters multiple "E" repairs at speeds above 10 knots. If more than one "E" repair is required all "E" repair must be upgraded to "D" repairs.

8.2 Bidirectional Landings: A properly placed barrier (at 1000 feet from the start of the MOS) would permit barrier landings in either direction with a 1000-foot approach since there will never be an "E" repair within 1000 feet.

8.4 Tail Hook: For a completely safe operation, the barrier should be placed such that the pilot has several seconds to lower the F-4E tail hook without crossing a

repair. Although this restraint might be operationally unrealistic, crossing an expedient repair with the tail hook down could possibly result in engagement of the repair by the tail hook. For each second that the tail hook is extended at a roll out speed of 150 knots, the aircraft will travel approximately 250 feet. Since the F-4E tail hook requires 5 seconds to extend, a fully safe departure end barrier engagement would require 1500 to 2000 feet of runway without repair in front of the barrier. Since the barrier lifts the tail hook upon engagement, only a short clear zone of approximately 50 or 100 feet is required after the barrier.

8.5 Clearance Height: The vertical clearance heights must be checked on both ends of the MOS. Vertical clearances should not be a problem on main runways. However, if the MOS is found on an auxiliary taxiway, terrain or vertical structures could lie in approach or takeoff flight paths. Pre-attack planning should be accomplished for each base to assure vertical clearances (Reference 5) are available on both ends of any pavement where a MOS may be selected. The vertical clearances can be predetermined for all pavements identifying those that qualify for potential MOS sites.

8.6 Icy or Wet Runways: Under icy or wet conditions, the 5000-foot MOS may be of inadequate length for aircraft recovery. The MOS selection team chief should check with base operations prior to MOS selection to determine if the 5000 feet is adequate for recovery under the existing runway conditions.

#### REFERENCES

1. Caldwell, L. R. and Jacobsen, F. J., Interim Guidance for Surface Roughness Criteria, ESL-TR-79-37, dated October 1979.
2. Knox, K. J., Airfield Damage Repair Methods for North Field Tests, May 1980.
3. AFR 93-2, Disaster Preparedness and Base Recovery Planning, Department of the Air Force, Washington DC, July 1974.
4. McNerney, M., Interim Field Procedure for Bomb Damage Repair, ESL-TR-79-01, dated April 1979.
5. T. O. 1F-4E-1, February 1979.
6. Kvammen, A., and Pichumani, R., Pavement Cratering Studies, AFWL-TR-72-61, December 1972.

#### APPENDIX A

##### AM-2 MAT ROUGHNESS CRITERIA

Inspecting for Surface Roughness. After the repair compaction is complete and prior to installation of the AM-2 MAT the repair must be inspected for surface roughness. The interim criteria summarized in Table A-1 should be used. All surface roughness measurements should be made along the centerline of the crater, and halfway between the centerline and the crater edge on either side. These three lines should be parallel with the expedient runway's centerline.

a. The easiest way to evaluate upheaval in the field is to use upheaval markers as shown in Figure A-1. These markers permit a string to be stretched taut at certain heights above the pavement surface; these heights correspond with the maximum upheaval allowed for each repair category as shown in Table A-1.

b. The upheaval marker posts should be located on opposite sides of each crater, outside the limits of pavement upheaval. A string should be stretched between the posts at equal heights above the pavement, corresponding to the allowable maximum upheaval for the applicable repair category. The entire crater repair must lie beneath the string to meet the maximum upheaval criteria.

c. Sag is defined as the vertical distance between the low points of a repair and an "imaginary repair surface." In order to measure sag, the "imaginary repair surface" must be established by stretching the string across the repair so that it contacts the pavement just outside the start of the upheaval, as shown in Figure A-2. Then the vertical distance from the repair surface to the string must be measured. No measured distance may exceed the peak sag shown in Table A-2. Furthermore, the repair surface must rise above the nominal allowable sag shown in Table A-2 at least once within any specified "maximum span of nominal sag."

d. Excessive upheaval shall be removed and excessive sag shall be filled in accordance with the procedures in Reference 2.

e. Periodic inspections after installation of the AM-2 mat should be made to check roughness after use. The marker posts must be located off the MAT surface, and the 1.5 inch thickness of the mat must be included in the allowable upheaval as shown in Table A-1.

TABLE A-1. AM-2 Repair Categories

	A	B	C	D	E
Maximum Upheaval Before Mat Installation Inches, (cm)	0	1.5 (4)	1.5 (4)	1.5 (4)	3 (8)
Maximum Upheaval After Mat Installation Inches, (cm)	1.5 (4)	3.0 (8)	3.0 (8)	3.0 (8)	4.5 (12)
Maximum Sag	See Table A-2				
Maximum Length of Crater	N/A	N/A	70 (20)	70 (20)	N/A
Max. Length of Mat Feet, (m)	>77 (23.5)	>77 (23.5)	77 (23.5)	77 (23.5)	>77 (23.5)
Maximum Change in Slope (Percent)	0	3	3	3	3
Special Requirements	1	2	2,3	1,3	1

#### Special Requirements

1. Any spacing except that if spacing between mats is 100 ft or less, make one long repair.
2. Must meet spacing criteria, or upgrade to "A" repairs.
3. Maximum single "C" or "D" repair length is 77 feet. If a single repair exceeds 70 feet upgrade to a "B" repair.

TABLE A-2. AM-2 Repair Categories

	REPAIR CATEGORY				
	A	B	C	D	E
Peak Sag, inches (cm)	1.0 (2.5)	1.0 (2.5)	2.5 (6.5)	2.5 (6.5)	4.0 (10.0)
Nominal Allowable Sag, Inches (cm)	0.5 (1.5)	0.5 (1.5)	2.0 (5.0)	2.0 (5.0)	3.5 (9.0)
Maximum Span of Sag, Below Nominal Sag, feet (m)	5 (1.5)	5 (1.5)	10 (3.0)	10 (3.0)	20 (6.0)

#### APPENDIX B

##### SURFACE ROUGHNESS REQUIREMENTS FOR CRUSHED STONE REPAIRS

Inspecting for Surface Roughness. After the repair compaction is complete and prior to installation of the FOD cover the repair must be inspected for surface roughness. The interim criteria summarized in Table B-1 should be used. All surface roughness measurements should be made along the centerline of the crater, and halfway between the centerline and the crater edge on either side. These three lines should be parallel with the expedient runway's centerline.

a. The easiest way to evaluate upheaval in the field is to use upheaval markers as shown in Figure A-1. These markers permit a string to be stretched taut at certain heights above the pavement surface; these heights correspond with the maximum upheaval allowed for each repair category as shown in Table B-1.

b. The upheaval marker posts should be located on opposite sides of each crater, outside the limits of pavement upheaval. A string should be stretched between the posts at equal heights above the pavement, corresponding to the allowable maximum upheaval for the applicable repair category. The entire crater repair must lie beneath the string to meet the maximum upheaval criteria.

c. Sag is defined as the vertical distance between the low points of a repair and an "imaginary repair surface". In order to measure sag, the "imaginary repair surface" must be established by stretching the string across the repair so that it contacts the pavement just outside the start of the upheaval, as shown in Figure A-2. Then the vertical distance from the repair surface to the string must be measured. No measured distance may exceed the peak sag shown in Table B-2. Furthermore, the repair surface must rise above the nominal allowable sag shown in Table B-2 at least once within any specified "maximum span of nominal sag."

d. Excessive upheaval shall be removed and excessive sag shall be filled in accordance with the procedures in Reference 2.

TABLE B-1. Crushed Stone Repair Categories

	A	B	C	D	E
Maximum Upheaval, inches (cm)	1.5 (4)	2.5 (6)	2.5 (6)	3.0 (8)	4.5 (11)
Maximum Sag	See Table B-2				
Maximum Length of Crater, feet (m)	N/A	N/A	70 (20)	70 (20)	N/A
Maximum Change in Slope (Percent)	3	3	3	3	3
Special Requirements	(none)	2	2,3	1,3	1

#### Special Requirements

1. Any spacing except that if repairs are closer than 100 feet "D" and "E" repairs must be upgraded, "D" to "A" and "E" to "C" repairs.
2. Must meet spacing criteria, or upgrade to "A" category.
3. Maximum length of a single "C" or "D" repair is 70 feet. If a single repair exceeds 70 feet upgrade to a "B" repair.

TABLE B-2. Crushed Stone Repair Sag Criteria

	REPAIR CATEGORY				
	A	B	C	D	E
Peak Sag, inches (cm)	1.0 (2.5)	1.0 (2.5)	2.5 (6.5)	2.5 (6.5)	4.0 (10.0)
Nominal Allowable Sag, Inches (cm)	0.5 (1.5)	0.5 (1.5)	2.0 (5.0)	2.0 (5.0)	3.5 (9.0)
Maximum Span of Sag Below Nominal Sag, feet (m)	5 (1.5)	5 (1.5)	10 (3.0)	10 (3.0)	20 (6.0)



## APPENDIX C

## MOS SELECTION FLOW CHART

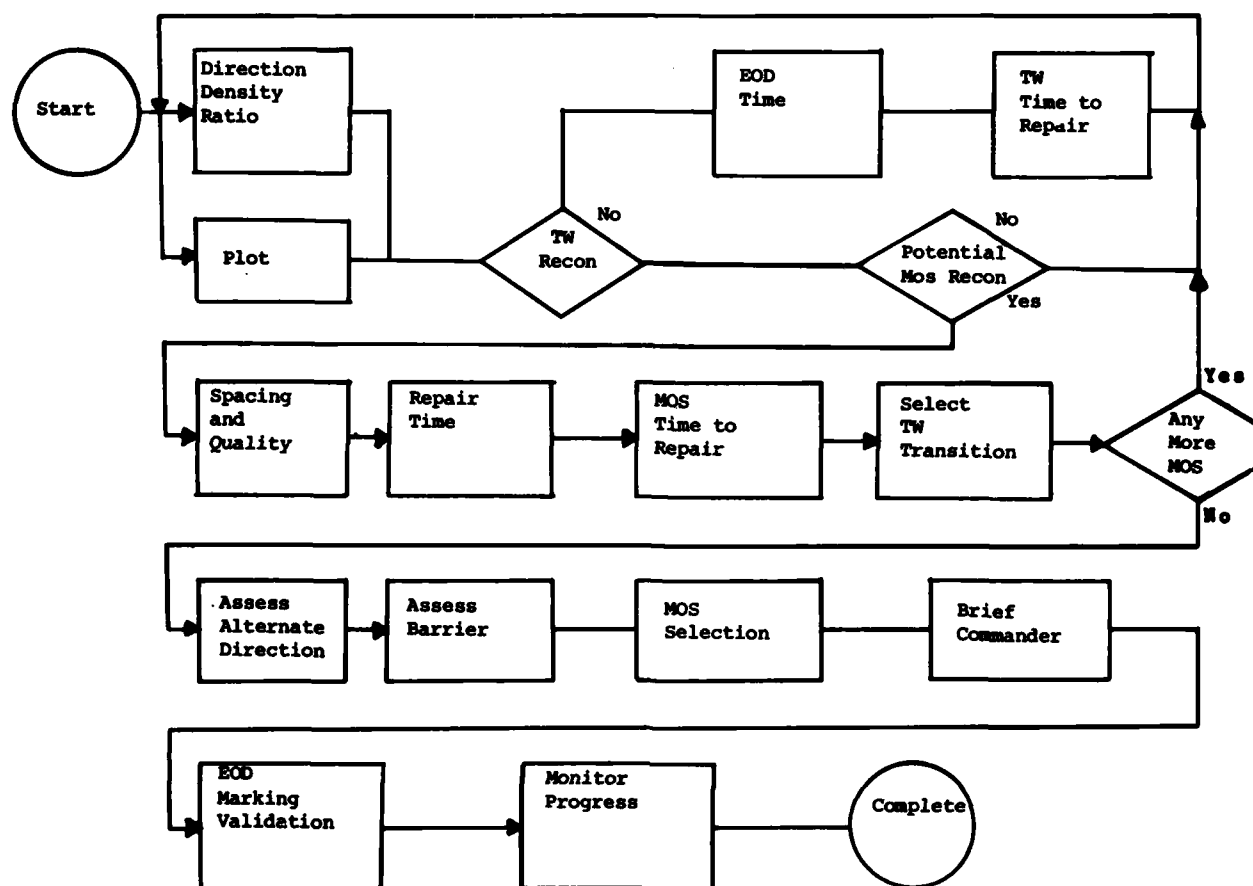


TABLE C-1. MOS Selection Checklist

1. Avoid "A" and "B" AM-2 repairs.
2. Avoid "A" crushed stone repairs.
3. Minimize total number of repairs.
4. Taxiways must be 25 feet wide.
5. F-4E requires 30 feet to turn 90°, 50 feet to turn 180° during taxi.
6. Only 1 "E" repair permitted in MOS if no barrier is present. If more than one repair exists in "E" category, make all repairs "D" or better.
7. If "A", "D" or "E" AM-2 repairs are less than 100 ft apart and do not overlap repair both with single AM-2 mat ("B" and "C" AM-2 repairs must be upgraded to "A"). If separate crushed stone repairs closer than 100 ft are made, upgrade "B", "C" and "D" repairs to "A" repairs. Upgrade "E" repairs to "C" repairs.
8. For overlapping craters, estimate "equivalent" crater diameter, and make single repair.
9. "C" or "D" repairs longer than 70 feet are not permitted. Upgrade to "B" repairs.

## APPENDIX D

## REPAIR TYPE

TABLE D-1. Determining Type of Repair

Apparent Crater Diameter (Up to)	Category Repair Required*				
	A	B	C	D	E
10	CS	CS	CS	CS	CS
20	CS	CS	CS	CS	CS
30	AM-2	CS	CS	CS	CS
40	AM-2	AM-2	AM-2	CS	CS
50	AM-2	AM-2	AM-2	AM-2	AM-2
60	AM-2	AM-2	AM-2	AM-2	AM-2
70	AM-2	AM-2	AM-2	AM-2	AM-2

\* CS - Crushed Stone  
AM-2 - AFR 93-2

## APPENDIX E

## TIME TO REPAIR EXAMPLES

TABLE E-1. Taxiway Repair Time Worksheet

Pavement Identification TW-1Estimated EOD Clearance Time 60 min

Repair Type/ Apparent Crater Diameter	Number	Time per Repair	Time per Type
<u>Spalls</u>		1 min	
<u>Crushed Stone</u>			
10 feet		116 min	
20 feet	1	120 min	120
30 feet		130 min	
40 feet	1	140 min	140
<u>AM-2 Mat</u>			
50 feet		141	
60 feet		143	
70 feet		146	
		Total Time*	320 Min

Category E repairs are used as the basis for this time per repair estimate since they are the fastest repair. Spall repair time assumes that Silikal® repair are completed before the crater repairs and have sufficient time to cure, (30 minutes).

TABLE E-2. Taxiway Repair Time Worksheet

Pavement Identification TW-2Estimated EOD Clearance Time 60 min

<u>Repair Type/ Apparent Crater Diameter</u>	<u>Number</u>	<u>Time per Repair</u>	<u>Time per Type</u>
<u>Spalls</u>		<u>1 min</u>	
<u>Crushed Stone</u>			
10 feet		<u>116 min</u>	
20 feet	<u>1</u>	<u>120 min</u>	<u>120</u>
30 feet	<u>1</u>	<u>130 min</u>	<u>130</u>
40 feet		<u>140 min</u>	
<u>AM-2 Mat</u>			
50 feet		<u>141 min</u>	
60 feet		<u>143 min</u>	
70 feet		<u>146 min</u>	
		<u>Total Time*</u>	<u>310</u>

Category E repairs are used as the basis for this time per repair estimate since they are the fastest repair. Spall repair time assumes that Silikal® repair are completed before the crater repairs and have sufficient time to cure, (30 minutes).

TABLE E-3. Taxiway Repair Time Worksheet

Pavement Identification TW1-MOS(0,-75)Estimated EOD Clearance Time 0

<u>Repair Type/ Apparent Crater Diameter</u>	<u>Number</u>	<u>Time per Repair</u>	<u>Time per Type</u>
<u>Spalls</u>		<u>1 min</u>	<u>0</u>
<u>Crushed Stone</u>			
10 feet		<u>116 min</u>	<u>0</u>
20 feet		<u>120 min</u>	<u>0</u>
30 feet		<u>130 min</u>	<u>0</u>
40 feet		<u>140 min</u>	<u>0</u>
<u>AM-2 Mat</u>			
50 feet		<u>141 min</u>	<u>0</u>
60 feet		<u>143 min</u>	<u>0</u>
70 feet		<u>146 min</u>	<u>0</u>
		<u>Total Time*</u>	<u>0</u>

Category E repairs are used as the basis for this time per repair estimate since they are the fastest repair. Spall repair time assumes that Silikal® repair are completed before the crater repairs and have sufficient time to cure, (30 minutes).

TABLE E-4. Taxiway Repair Time Worksheet

Pavement Identification TW2-MOS(0,-75)Estimated EOD Clearance Time 30

Repair Type/ Apparent Crater Diameter	Number	Time per Repair	Time per Type
<u>Spalls</u>		<u>1 min</u>	
<u>Crushed Stone</u>			
<10 feet	<u>1</u>	<u>116 min</u>	<u>116</u>
10-20 feet		<u>120 min</u>	
20-30 feet		<u>130 min</u>	
40 feet		<u>140 min</u>	
<u>AM-2 Mat</u>			
50 feet		<u>141 min</u>	
60 feet		<u>143 min</u>	
70 feet		<u>146 min</u>	
		<u>Total Time*</u>	<u>146</u>

Category E repairs are used as the basis for this time per repair estimate since they are the fastest repair. Spall repair time assumes that Silikal® repair are completed before the crater repairs and have sufficient time to cure, (30 minutes).

TABLE E-5. MOS Time Sheet

MOS IDENTIFICATION		23(0,-75)		DR = 1.0			
Apparent Crater Diameter		QUALITY					TIME
		A	B	C	D	E	
10 FT	NO.				2		242
	TIME/REP.	136	130	123	121	116	
	SUBTOTAL				242		
20 FT	NO.		1		1		261
	TIME/REP.	140	136	127	125	120	
	SUBTOTAL		136		125		
30 FT	NO.						
	TIME/REP.	143	141	137	136	130	
	SUBTOTAL						
40 FT	NO.						
	TIME/REP.	150	149	*	144	140	
	SUBTOTAL						
50 FT	NO.		1				155
	TIME/REP.	156	155	*	*	141	
	SUBTOTAL		155				
60 FT	NO.						
	TIME/REP.	170	166	*	*	143	
	SUBTOTAL						
70 FT	NO.						
	TIME/REP.	182	175	*	*	146	
	SUBTOTAL						
>70 FT	CASE NO.						
	1	TTR =					
	2	TTR =					
	3	TTR =					
	4	TTR =					
	5	TTR =					
ESTIMATED EOD CLEARANCE TIME							90
SPALLS	NO. 235	TIME/SPALL = 1 MIN					235
TOTAL REPAIR TIME							983

The above TIME/REP values are fictitious and should be replaced with values validated for a given bases capabilities.

TABLE E-6. MOS' Repair Time

MOS ID 23(0,-75)

<u>Time To Repair</u>			
	<u>MOS</u>	<u>TW</u>	<u>Transition</u>
			<u>Total</u>
TW1	983	320	0
TW2	983	310	146
Minimum Time			1303

TABLE E-7. MOS Comparison

<u>MOS ID</u>	<u>TW ID</u>	<u>REPAIR TIME</u> <u>(MOS + ACCESS)</u>
23-(0,-75)	TW1	1303
23-(1200, -75)	TW1	1703
23-(3000, 60)	TW1	1800
23-(5000, 25)	TW2	2100

TABLE E-6. Dispersal Area Times

<u>Dispersal Area</u>	<u>Taxiway</u>	<u>Time to Repair</u>
A	TW1	0
	TW2	0
B	TW1	120
	TW2	120
C	TW1	0
	TW2	0

## APPENDIX F

DAMAGE DIAMETER TEMPLATE (See Figure F1)

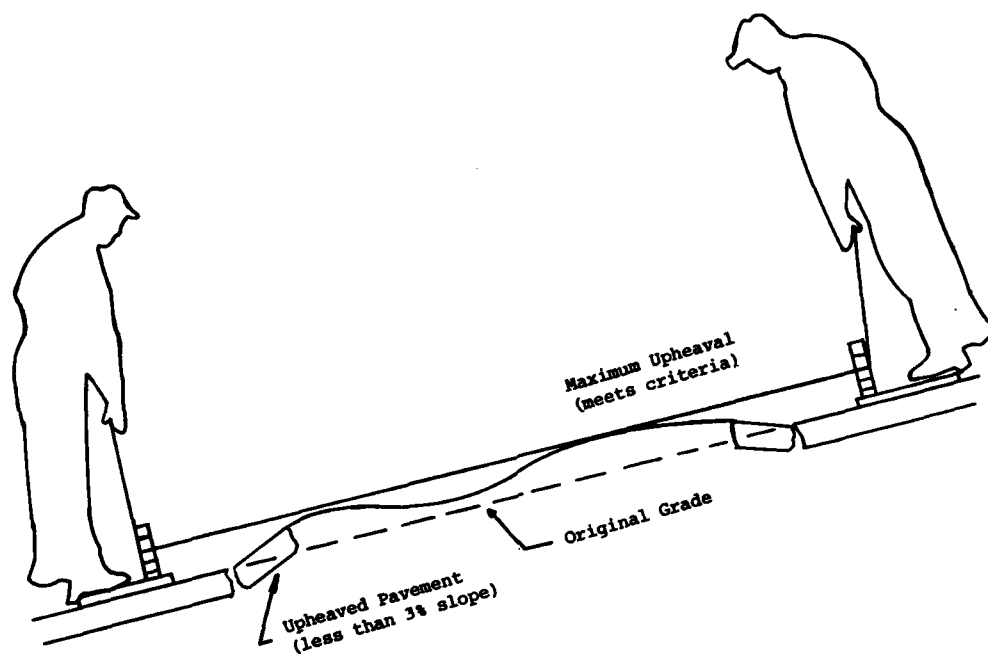


Fig.1 Maximum allowable upheaval

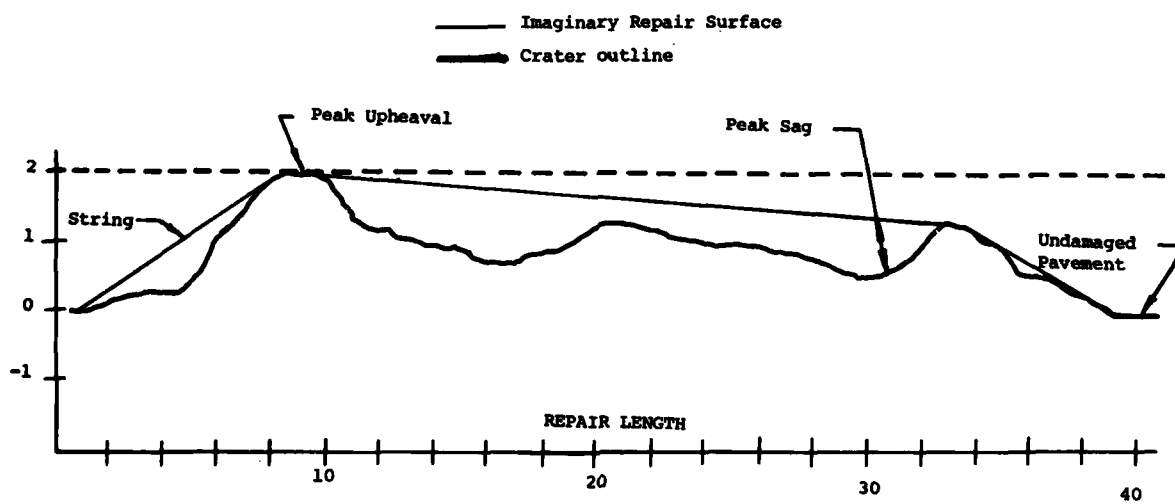


Fig.2 Typical sag

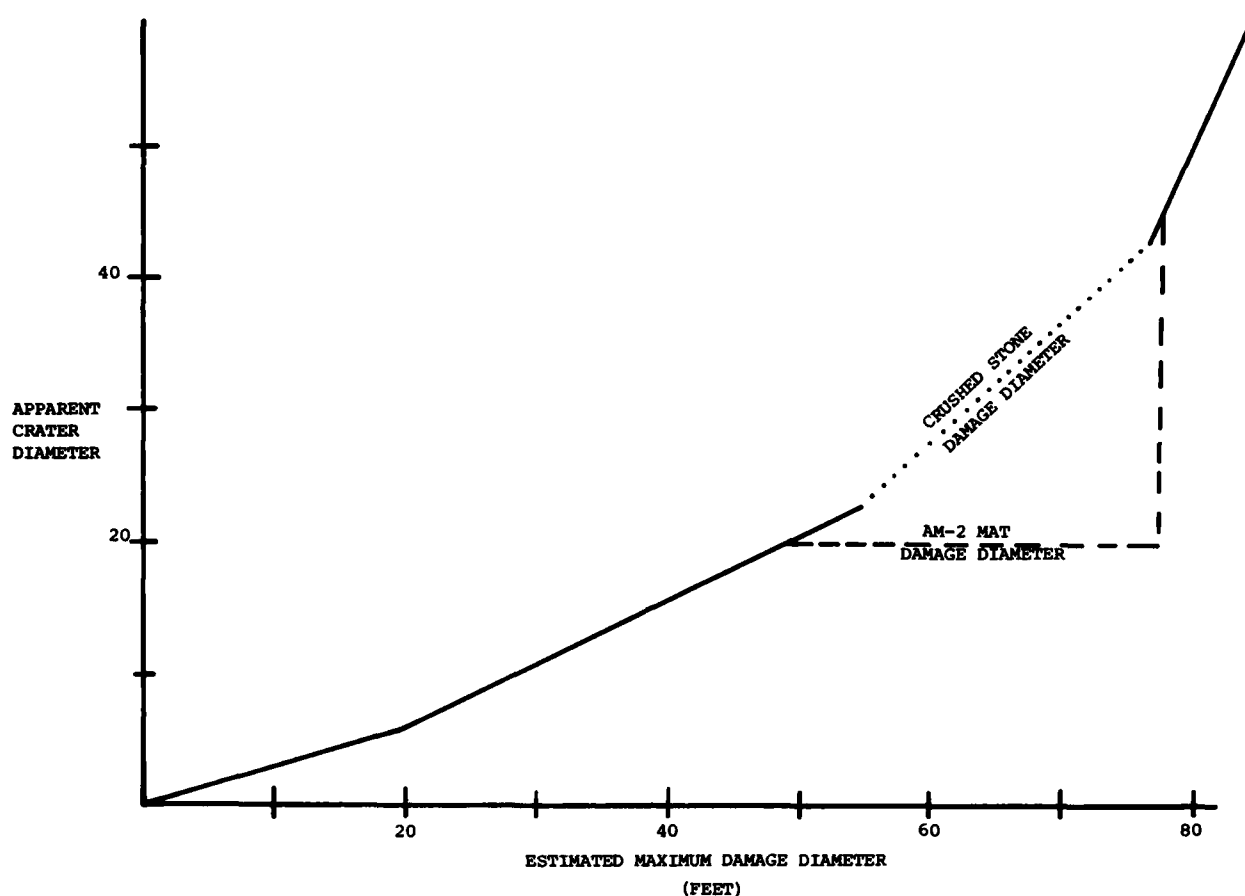


Fig.3 Apparent vs maximum diameter

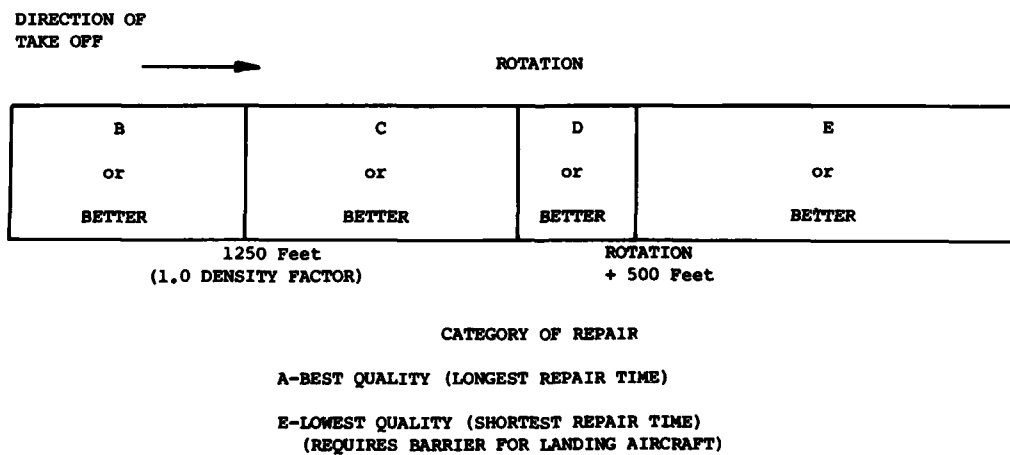


Fig.4 General MOS repair (50 by 5000 feet) (single direction take off)

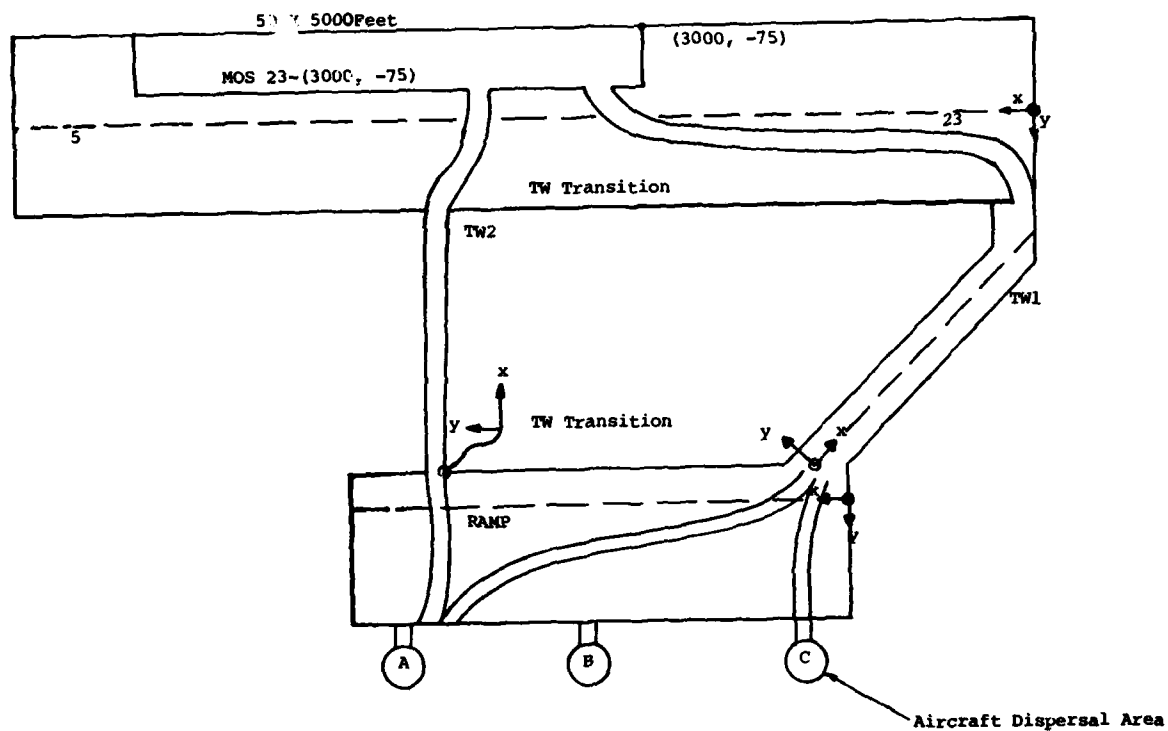


Fig.5 Typical field (not to scale)

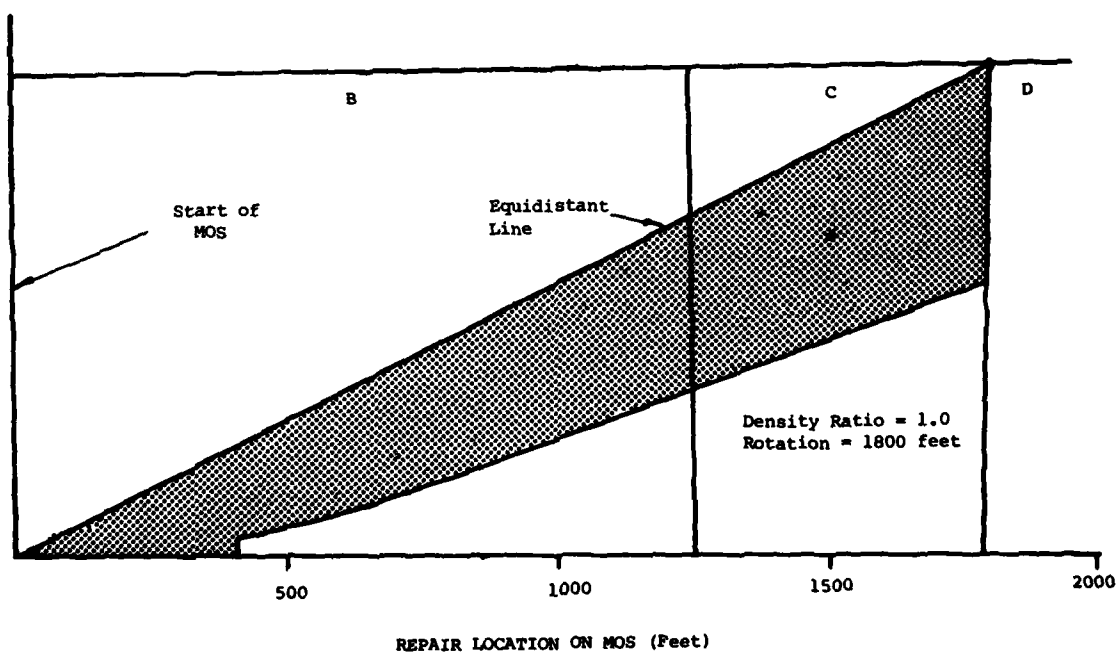


Fig.6 Spacing template



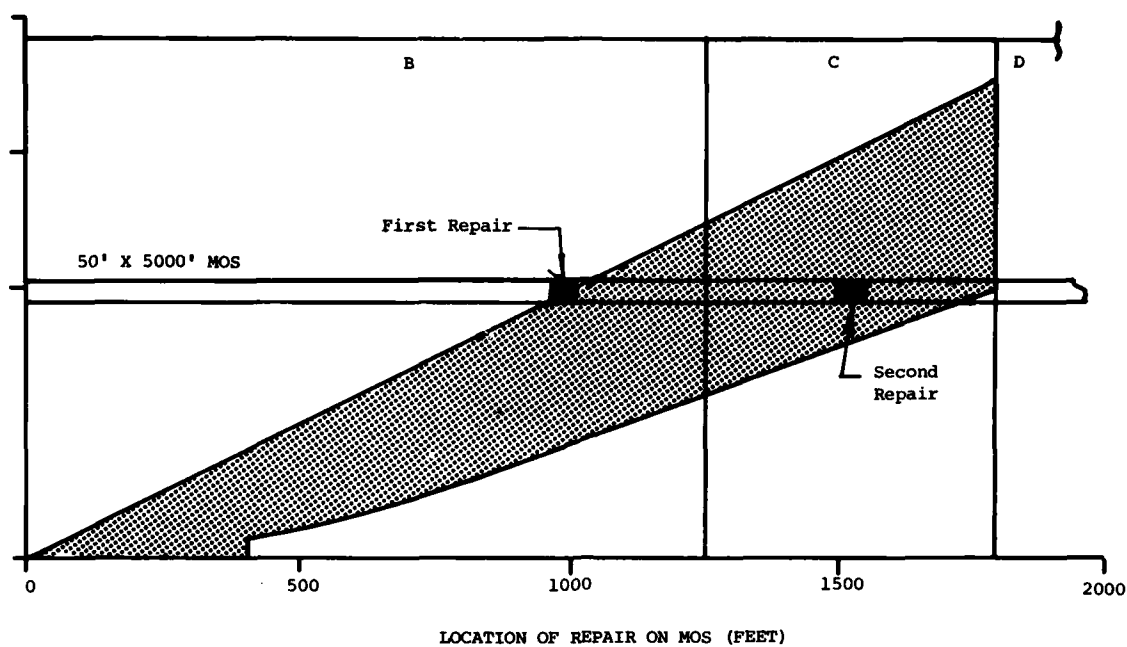


Fig.7 Unsatisfactory case

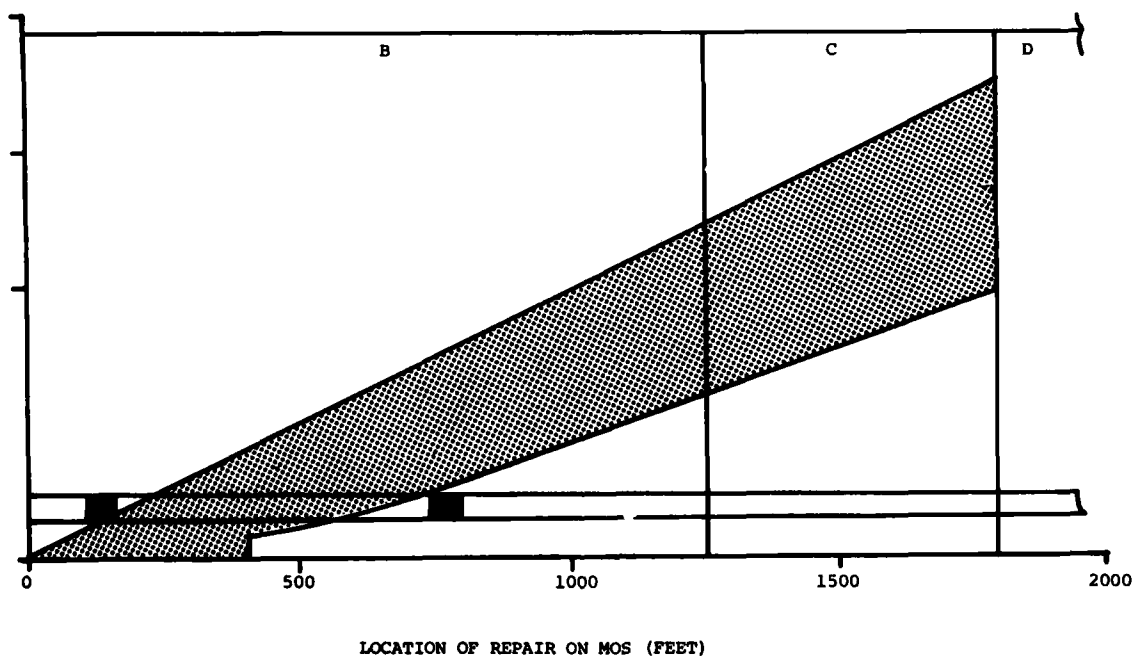


Fig.8 Satisfactory case

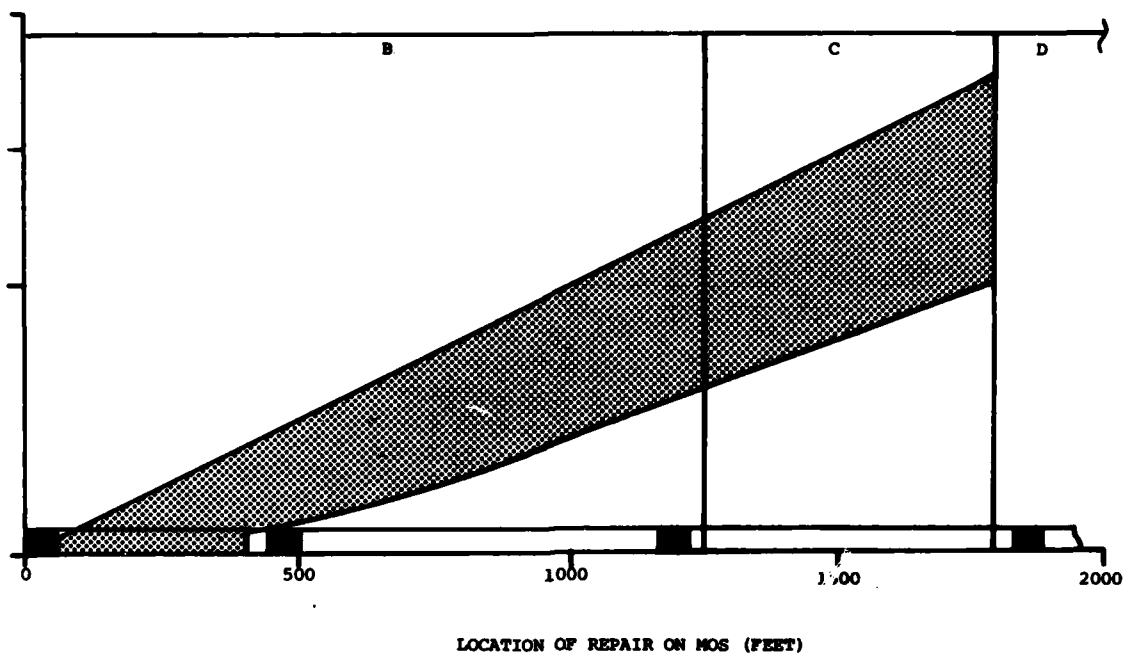


Fig.9 First and second repairs

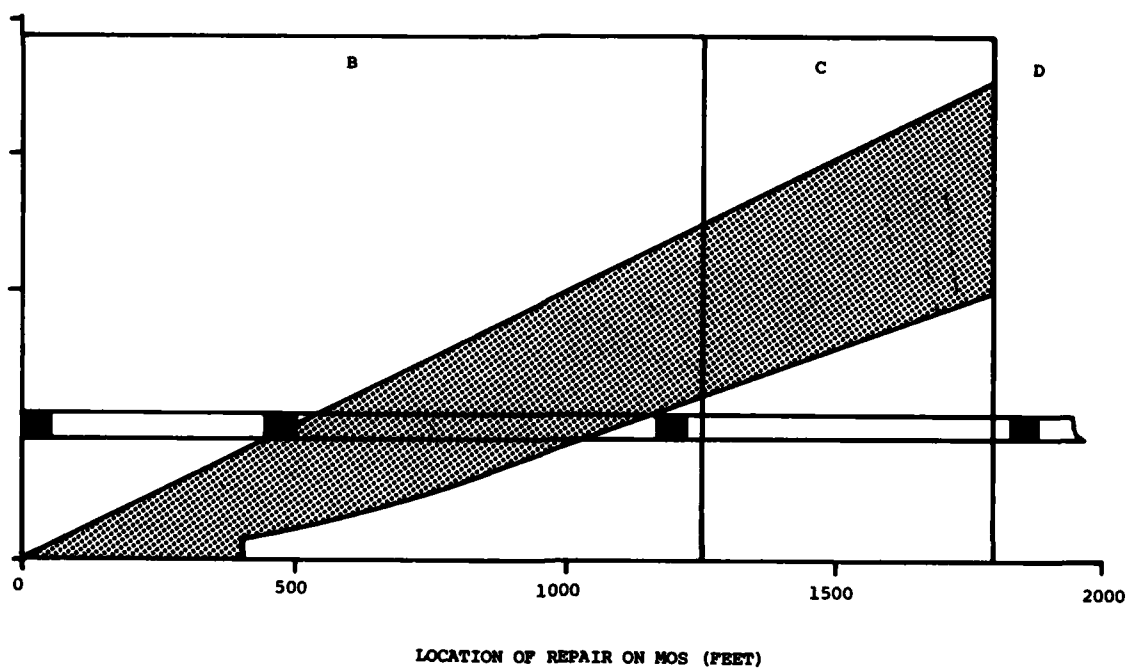


Fig.10 Second and third repairs

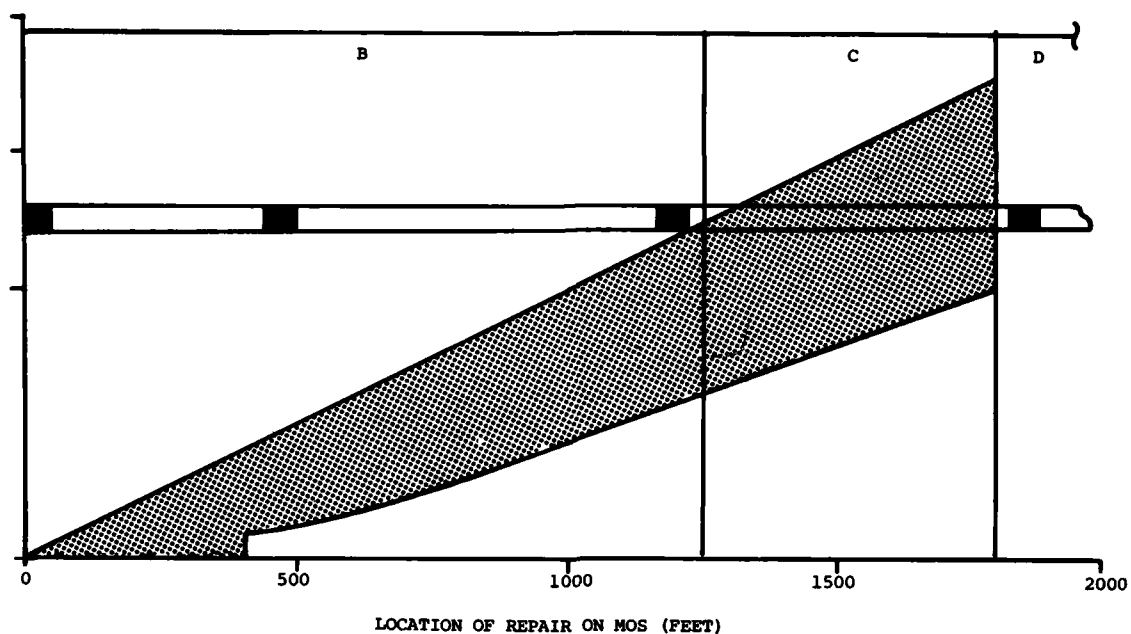
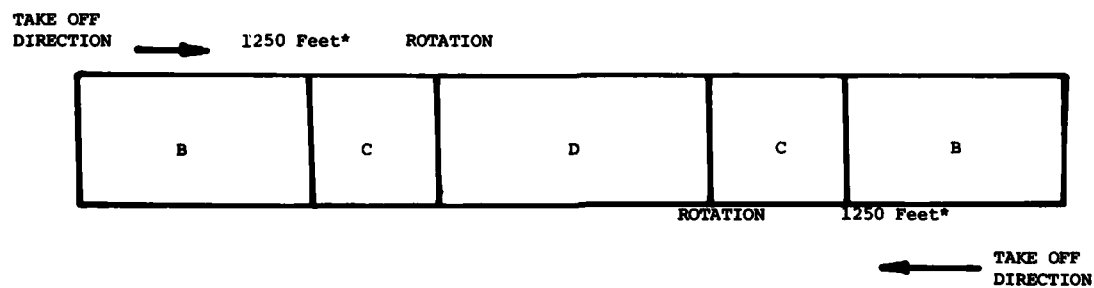


Fig.11 Third and fourth repairs



\*1.0 DENSITY FACTOR

Fig.12 Bi-directional MOS

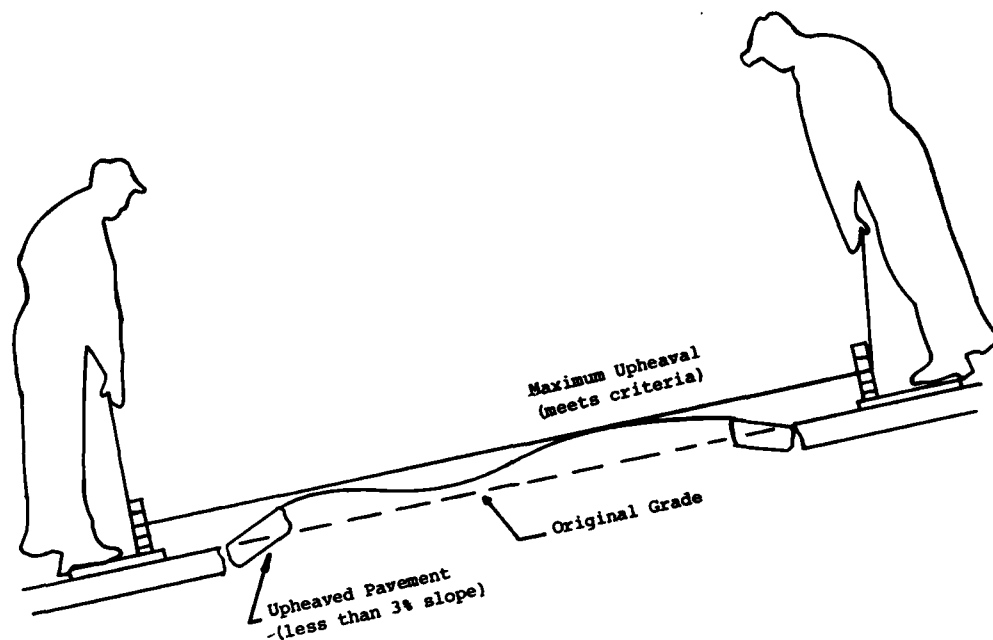


Fig.A-1 Maximum allowable upheaval

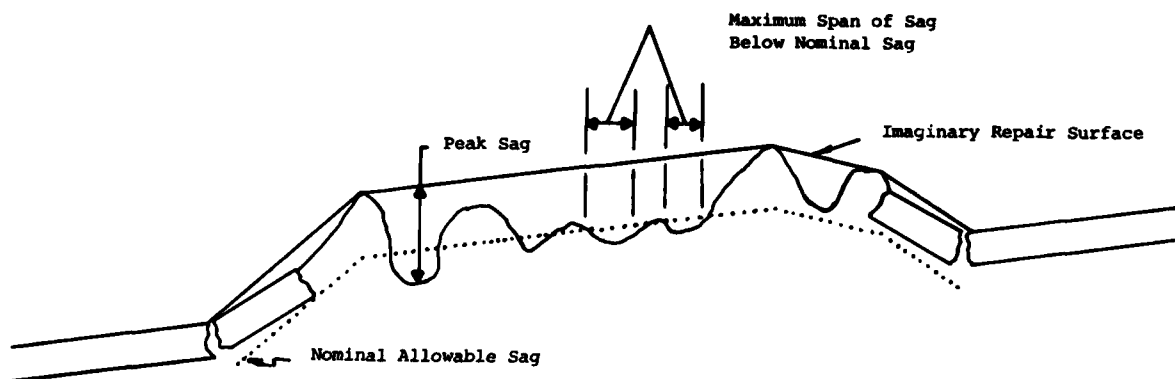
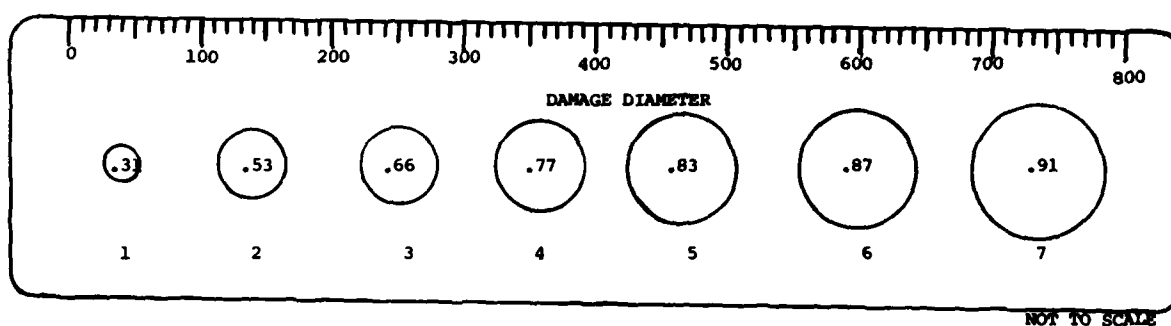


Fig.A-2 Sag measurement



- NOTES: 1. 1-7 represents apparent crater diameters in feet X 10.
2. Hole size (inches) represent crater damage diameter plus .031 inch to allow for pencil width.
3. This templet is for use on maps scaled 1 inch = 100 feet.

Fig.F1 Damage diameter templet

# PROPOSED SPECIFICATIONS FOR INTERNATIONAL INTEROPERABILITY ON REPAIRED BOMB DAMAGED RUNWAYS

Lt Col Lapsley R. Caldwell  
AFESC/RDCR  
Tyndall AFB, FL 32403  
USA

Anthony G. Gerardi  
AFWAL/FIBE  
Wright-Patterson AFB, OH 45433  
USA

## SUMMARY

This paper suggests definitions for data, data formats, and National responsibilities for development of war emergency airfield pavement repair specifications. An airfield manager would use these specifications to make repairs after an enemy attack. Minimum Operating Strip size, repair quality, repair spacing, and other parameters are specified. If the repair specifications for a specific aircraft can not be met, then discrepancies can be identified and the aircraft operator could assess the additional risk. Exchange of these specifications between the nation operating an aircraft and the nation managing an airfield would enhance NATO interoperability.

## I INTRODUCTION

The present scenario for a conventional war in an European environment depicts a fast moving, high intensity engagement. Extensive airfield pavement damage is anticipated and rapid, high rates of launch and recovery of aircraft is required. Some of the launched aircraft may be recovered at an alternate base. Personnel at this alternate base may or may not be familiar with that particular aircraft. When the aircraft is operated by one nation and the alternate airfield managed by another nation, the problem of interoperability on different types of bomb crater repairs arises.

NATO Standardization Agreement (STANAG) 2929 (ADR), Airfield Damage repair (Ref 9) defines the need to repair an airfield after an attack. This report suggests definitions for data, data formats, and National responsibilities for development of war emergency airfield pavement repair specifications. Throughout this report the term Airfield manager is used to mean the Nation or National agency responsible for operating a specific airfield or group of airfields. The term aircraft operator is used to mean the Nation or National agency responsible for operating a particular aircraft, even though that aircraft may be manufactured by some other nations.

An airfield manager would utilize these specifications for one or more aircraft to select a Minimum Operating Strip (MOS) and to make repairs to the airfield's pavement after an enemy attack as shown in Figure 1. MOS size, repair quality, repair spacing, and other parameters must be specified. If repair specifications for a specific aircraft are impracticable, then discrepancies can be identified and the aircraft operator can determine if the risk is acceptable, or a decision may be made to evacuate one or more types of aircraft using an Evacuation Strip. Exchange of these specifications between the nation operating an aircraft and the nation managing an airfield would enhance NATO interoperability.

## II GENERAL DISCUSSION

Several NATO countries have been conducting independent tests to predict the effect of expedient pavement repairs on the structural loads induced in an aircraft operating over these repairs. Testing suggests wide variations in the tolerance of specific types of aircraft to surface roughness. Based upon test results to date it appears that it will be difficult (if not impossible) to extrapolate the effects of surface roughness on one specific type of aircraft, such as a F-4E Phantom to a second type of aircraft such as a F-15 Eagle. It will even be difficult for field personnel to extrapolate the effects of surface roughness on a F-4E to a F-4C.

The purpose of the report is to attempt to "standardize" and minimize the data that will be required to repair a bomb damaged runway for a specific type of aircraft. Since an airfield must be compatible with many different types of aircraft, it is necessary that this data can be combined or merged. Then each airfield can optimize its repairs to accommodate the anticipated mix of aircraft that will use the airfield, even though these aircraft may be designed, manufactured and operated by different nations.

In preparation of this report it has been necessary to adopt several assumptions which are listed below.

(a) War Emergency Only. These airfield repair specifications will be used in time of war for expedient repairs and will not be used under peacetime conditions or for permanent repairs.

(b) Time to Repair. After an enemy attack has occurred, the estimated "time to repair" will be the primary factor used to trade off the selection of various MOS that could be repaired. Lower priority aircraft mission requirements may have to be sacrificed in order to accomplish the high priority mission tasks as expeditiously as possible.

(c) Quality of Repair. "Perfect" repairs, (smoothness), require more time than imperfect repairs. Significant amounts of time and resources can be saved by making poorer quality repairs.

(d) Aborts. In the European conventional war scenario the need to launch and recover aircraft is so high that the loss of aborting aircraft is an acceptable risk. This assumption is necessary to place reasonable limits on MOS size and repair quality.

The determination of acceptable repair specifications is affected by aircraft design, operational techniques, acceptable risk levels, pilot ability and National objectives. The establishment of these specifications should, therefore, be the responsibility of the nation operating the aircraft. The aircraft operator should include in these requirements his assessment of wartime emergency acceptable risk and specify the "worst case" repair that he can tolerate. Over specification could easily result in the inability of the airfield repair crew to meet the stated repair requirements in a timely manner.

The nation managing a specific airfield is responsible to review each specific aircraft's specification and estimate his ability to meet those specifications. It is possible that merging of specifications for several aircraft to create a "worst case" specification will result in inability of the airfield manager to respond rapidly. Mission priorities may therefore dictate that a specific airfield cannot spend the time or resources necessary to meet repair specifications for a specific type of aircraft or a particular mix of aircraft.

In the event that an airfield manager determines repair specifications for a specific type of aircraft cannot be met, the manager must notify the aircraft operator of discrepancies so that the associated risk can be reevaluated, or operational restriction (such as gross weight limitation) imposed if the aircraft must be operated at that field.

Throughout this report examples of interim repair specifications for an F-4E are presented for a density ratio of 1.0. These interim specifications are extracted from Reference 7.

A suggested glossary is included in Appendix B.

### III MINIMUM OPERATING STRIP REQUIREMENTS

The requirements for the MOS for each specific aircraft can be different and urgent mission needs at a particular airfield may dictate a necessity to prioritize repair options. For example, a particular airfield manager may decide (based on time to repair estimates), to first repair a narrow MOS that is only suitable for fighter aircraft, but not adequate for logistic aircraft. Expansion of the MOS for logistic aircraft would normally be accomplished as soon as possible.

Definition of the following MOS parameters will be required to enable the airfield manager to select and repair a MOS that will be adequate for a specific type of aircraft. Typical data for an F-4E is summarized in Table 1.

(a) MOS Size: The aircraft operator will specify the minimum MOS width and length that is required for a specific aircraft's anticipated ground roll and 50 foot obstacle clearance under worst case takeoff or landing conditions to include weather, aircraft loading, performance, etc. The aircraft operator is responsible for making the necessary trade-offs between aircraft safety and acceptable operational risks.

(b) Abort Requirements: Since the anticipated scenario assumes war emergency conditions, it is anticipated that the aircraft operator is willing to accept the loss of aircraft that abort on take-off. The airfield manager will place first priority on achieving the minimum time to repair a MOS and restore the airfield to limited operation. Repairing the airfield to accommodate aborting aircraft will be a secondary priority.

(c) MOS Marking and Lighting: The airfield manager will mark the MOS with a centerline and threshold as required by reference 9. Portable lighting will be provided for use at night and during low visibility operation. The airfield manager will advise the aircraft operator on the details of actual MOS marking and lighting.

(d) MOS Direction: Under some repair conditions the MOS may only be suitable for takeoffs and landings in a single direction, (unidirectional MOS). The airfield manager will notify the aircraft operator if the MOS is unidirectional instead of bidirectional.

(e) **Instrument Approaches:** The airfield manager will notify the aircraft operator of damage to airfield approach instrumentation and any deviations from published approaches that are required.

(f) **Barriers/Arrestors:** If the airfield manager can provide a barrier or arrestor on the MOS, the manager will advise the aircraft operator of the type and location of the barrier.

**Evacuation Strip:** In the event that the airfield is so extensively damaged that is is not practical to repair a MOS the aircraft operator may request that the airfield manager prepare an Evacuation Strip as discussed in section IX.

TABLE 1. F-4E MOS REQUIREMENTS

Length	5000 feet (1524 meters)
Width	50 feet (15.24 meters)
Take-off to clear 50 ft obstacle	5700 feet (1767 meters) (3)(4)(6)
Landing over 50 feet obstacle	5300 feet (1615 meters) (3)(4)(5)(6)
Abort Requirements	NONE
MOS Marking	Centerline and Threshold (1) (7)
Lighting	MOS edge, Threshold (1) (7)
MOS Direction	(1)
Instrument Approaches	(1)
Barriers/Arrestors	(1) (2)

- Notes:
1. Airfield manager will advise of specific details as soon as possible after repairs are complete.
  2. Desired but not required.
  3. "Worst case" density ratio of .9
  4. Dry runway
  5. 38,000 lb Aircraft
  6. Reference 1
  7. Reference 9

#### IV REPAIR QUALITY VERSUS LOCATION

High quality repairs will require more manpower, materials and more repair time than lower quality repairs. A "perfect" repair would require removal of all upheaved concrete and placement of repair material would have to be perfectly flush with the original pavement surface. Considerable time could be saved by leaving some of the upheaved concrete in place, since not only would the removal time be saved, but also the repair area would be smaller, (in some cases by a factor of 2.5). Analyses of effects of the repairs on some aircraft indicate that at very slow (taxi) speeds the aircraft will be able to tolerate relatively rough (low quality) repairs. On the first part of the MOS, while the aircraft is above low taxi speeds but still at moderate speeds where aerodynamic lift is small the repairs will tend to cause high dynamic loads in the aircraft, but as the aircraft builds up lift runway induced aircraft loads will be reduced and additional roughness may be acceptable (Ref 4). The important result of these variations in aircraft tolerance to roughness vs aircraft speed is that the minimum required quality of each pavement repair will vary depending on location.

The aircraft operator will define various levels of repair quality, such as "A," "B," or "C" quality, and identify acceptable quality versus location on the MOS as follows.

(a) **MOS Repair Quality.** The aircraft operator will specify repair quality versus repair location on the MOS for both unidirectional and bidirectional runways, (Figure 2). This specification could include the effects of density ratio or be a combined "worst case" specification at the option of the aircraft operator.



(b) **MOS Repair Spacing.** Since runway repairs will have a reinforcing or cancellation effect, it will also be necessary to specify acceptable repair spacing. This will be provided on a plot that shows location of a repair on the MOS (from start of the MOS) versus the minimum distance to the next repair (Figure 3).

(c) **Touchdown Zone.** The aircraft operator will specify any special requirements for the touchdown zone. As an example some aircraft may require perfect repairs in the touchdown zone, which would greatly restrict flexibility in the selection of an MOS.

(d) **Thrust Effects.** Since jet engine blast can cause damage to temporary repairs the aircraft operator will identify air velocity and temperature effect due to aircraft prop and jet blast, to include the effects of reverse thrust. The operators should minimize these effects on taxiway repairs through operational restrictions if necessary (Figure 4).

## V INDIVIDUAL CRATER REPAIR SPECIFICATIONS

Individual craters will be repaired to the qualities discussed in Section IV and are a function of their particular location on the MOS and taxiway access routes. In the specification an individual crater repair is considered to be a single crater, overlapping craters, or craters that are so close together that the repair procedure results in removal of the pavement between the repair.

The aircraft operator will quantify the following parameters to define quality of repair for each aircraft. This should be done in a manner to insure that operation on any repair that falls within these specifications will be an acceptable operational risk. The aircraft operator will define repair categories of increasing quality. This should be done so that a given quality of repair is an acceptable substitute for repairs of lower quality. The airfield manager will be responsible to insure that the repair quality meets or exceeds these specifications. All repair quality measurements will be made at least along the crater's center and halfway between the center and the crater edge on each side. If a portion of the repaired area falls outside the MOS the quality measurement shall be performed on three equally spaced lines within the MOS. These three lines should be parallel with the MOS's centerline (Figure 5).

(a) **Peak Upheaval:** The peak upheaval is the repair peak highest above a line between the undamaged pavement on each side of the repair. The measurement of the upheaval in the field is performed using upheaval markers as shown in Figure 6. These markers permit a string to be stretched taut at certain heights above the pavement surfaces. These heights correspond with the maximum upheaval allowed for each repair quality as defined by the aircraft operator (Table 2). The upheaval marker posts should be located on opposite sides of each crater, outside the limits of pavement upheaval. A string should be stretched between the posts at equal heights above the pavement, corresponding to the allowable maximum upheaval for the applicable repair category. The entire crater repair must lie beneath the string to meet the maximum upheaval criteria. One of the current repair techniques uses an aluminum mat on top of select fill in the crater. The upheaval, as specified in Table 2, must include the thickness of this repair mat.

(b) **Percent Change in Slope.** This parameter establishes the maximum rate of change of the repair height, and is applicable to both the upheaved pavement and the repair surface. For example, if the damaged pavement is heaved up 1.5 inches in 5 feet, then this represents a  $[1.5/(5 \times 12) = 0.025]$  2.5 percent change in slope from the adjacent undamaged pavement. Typically, change in slope would be measured with a template as shown in Figure 7.

(c) **Sag:** Sag is the vertical distance between the low points of a repair and an "imaginary repair surface." The "imaginary repair surface" is established by stretching a string across the repair so that it contacts the pavement just outside the start of the upheaval as shown in Figure 8. Then the vertical distance (sag) from the repair surface to the string can be measured from the string. The parameters peak sag, nominal sag, and maximum span below nominal sag are defined in the following paragraphs. The span width is a factor because relatively short sags will tend to stimulate the aircraft above its response frequencies and hence will not tend to reinforce aircraft dynamic loads (Table 3).

(d) **Repair Length:** Minimum or maximum limits, if any, on repair length shall be specified. It is probable that repairs with significant upheaval and sag will have a maximum allowable length, and if this length is exceeded then the repair must be upgraded to have less sag or upheaval as is shown for F-4E "C" repairs in Table 3.

(e) **Load Bearing Forces:** The aircraft operator will specify the tire pressure, tire footprint, wheel pattern/ spacing, and equivalent single wheel load (Figure 9).

(f) **Braking Force:** The aircraft braking forces that must be absorbed by the repair cover will be specified by specific wheel location (Figure 9). Variation in braking forces for different locations on the MOS will be specified. The operator will prohibit braking operations on taxiway repairs.

TABLE 2. F-4E REPAIR QUALITY CATEGORIES

	A	B	C	D	E
Maximum Upheaval, inches (cm)	1.5 (4)	2.5 (6)	2.5 (6)	3.0 (8)	4.5 (11)
Sag (See Table 3)					
Maximum Length of Crater, feet (meter)	N/A	N/A	70 (20)	70 (20)	N/A
Maximum Change in Slope (percent)	3	3	3	3	3
Special Requirements	1	2	2,3	1,3	1

Special Requirements

1. Any spacing except that if repairs are closer than 100 feet "D" and "E" repairs must be upgraded, "D" to "A" and "E" to "C" repairs.
2. Must meet spacing criteria, or upgrade to "A" category.
3. Maximum length of a single "C" or "D" repair is 70 feet. If a single repair exceeds 70 feet upgrade to a "B" repair.

TABLE 3. F-4E REPAIR SAG CRITERIA

	REPAIR CATEGORY				
	A	B	C	D	E
Peak Sag Inches (cm)	1.0 (2.5)	1.0 (2.5)	2.5 (6.5)	2.5 (6.5)	4.0 (10.0)
Nominal Allowable Sag, Inches (cm)	0.5 (1.5)	0.5 (1.5)	2.0 (5.0)	2.0 (5.0)	3.5 (9.0)
Maximum Span of Sag Below Nominal Sag, feet (m)	5 (1.5)	5 (1.5)	10 (3.0)	10 (3.0)	20 (6.0)

(1) Peak Sag: The peak distance below the string is the peak sag. This peak sag will be specified by the aircraft operator and must be associated with a "maximum span below nominal sag" as discussed below.

(2) Nominal Sag: This sag is the maximum allowable sag that is acceptable without consideration for sag length. There is no associated sag span with the nominal sag.

(3) Maximum Span below Nominal Sag: This parameter defines how wide (how long down the MOS) that sag can exceed the nominal sag towards the peak sag limit. The repair surface must return to a point above the nominal sag at least once in each maximum span. This parameter allows sag to approach the peak allowable sag as long as the effective frequency does not stimulate reinforcement of aircraft dynamic loads.

(g) Asymmetric Repair. At this time, it appears that most aircraft critical loads will not be higher due to asymmetric repairs than they are due to symmetric repairs. Since attempting to make very symmetric repairs may be difficult and time consuming, the aircraft operator should assume that the aircraft may travel asymmetrically across the repairs.

**Tolerance:** The airfield manager will insure measurement of repair quality is such that the actual parameters meet or exceed the required specification.

**Quality Control:** The airfield manager is responsible for quality control of the repairs and will make periodic inspections for degradation of repair quality.

## VI SCAB (SPALL) REPAIR REQUIREMENTS

Straffing, defective ordinance, ricochets, explosion debris, etc., may cause extensive scabs (spalls) that could range from slight pavement chipping to almost 5 foot holes that do not penetrate through the pavement (the base course is not exposed).

This section defines the types of scabs that must be repaired, scab spacing and scab repair parameters.

(a) **Unrepaired Scabs.** Some pavement damage will be so slight that repair will not be required. The aircraft operator will define the following parameters to establish the maximum size of unrepaired scabs (Figure 10).

(1) **Scab Depth.** The peak depth of the scab from a line across the undamaged edges (scabs do not have upheaval since the pavement is not penetrated).

(2) **Scab Width.** The maximum distance across the scab parallel to the MOS centerline.

(3) **Slope of Scab Sides.** The slope of a straight line that approximates the side of the scab.

(4) **Unrepaired Scab Spacing:** Since multiple scabs could reinforce, it is necessary for the aircraft operator to either specify a scab spacing criteria, or to account for the effects of reinforcement in the maximum unrepaired scab specification.

(b) **Repaired Scabs.** Scabs that exceed the specification for unrepaired scabs must be repaired. It is anticipated that a tolerance of  $\pm 3/4$ -inch from the original surface can be readily met on scab repairs.

TABLE 4. F-4E UNREPAIRED SCABS

Maximum Depth	1 1/2 inches (3.8 cm)
Maximum Length Parallel to MOS centerline	2 feet (62 cm)
Maximum Slope of Scab Sides	25%
Spacing Parallel to MOS centerline	No more than 2 scabs per 24 feet (7.3 meters)

## VII TAXIWAY REPAIR REQUIREMENTS

In general taxiway repairs are considered to be less critical than runway repairs. It is anticipated that aircraft will taxi slowly and use brakes sparingly. Therefore, repair quality requirements, repair spacing, and braking resistance requirements may be relaxed in order to permit taxiway repairs to be made faster.

Definition of the following taxiway repair parameters by the aircraft operator will be required to insure that specific aircraft can operate on taxiways that have been repaired at a specific airfield after an attack (Table 5).

(a) **Quality of Repair:** The repair quality will be defined in the same manner as Section IV. If possible, only one level of quality will be specified for taxiway repairs.

(b) **Taxiway Repair Spacing.** The specified repair quality shall be such that any repair spacing will be acceptable at the approved taxi speeds for the specific aircraft. The aircraft operator will establish and specify aircraft taxi speeds to insure that aircraft loads are compatible with multiple repairs on any spacing on taxiways.

(c) **Taxiway Repaired Width:** The minimum acceptable load bearing width for the specific aircraft to taxi on a meandering path between unrepaired craters or non-load bearing surfaces. This path would be swept as best as possible to minimize Foreign Object Damage (FOD) damage.

(d) **Cleared Width:** The minimum acceptable width centered on the repaired taxiway from which debris must be removed to the height of the repaired taxiway. This would be required for wing tip, pylon, armament, or propeller obstruction clearance. It is anticipated that only occasional points on the taxiway will be as narrow as the minimum cleared width.

(e) **Swept Width:** That desirable width which should be swept to prevent debris from being blown and scattered by propeller and jet blast from the taxiing aircraft.

(f) **90° Turn Width:** The minimum distance required on a taxiway for the aircraft to make a 90° turn onto an intersecting taxiway or runway. This width should include tolerance to compensate for the pilot's inability to see the actual tire position on the runway. An example is shown in Figure 11.

(g) **180° Turn Width:** The minimum width required for the specific aircraft to make a 180° turn, including tolerance to compensate for the pilots inability to see the actual tire position on the runway.

TABLE 5. F-4E TAXIWAY REPAIR CRITERIA

Taxi Speeds	10 knots
Repair Quality	"E" or better
Repair Spacing	Greater than 70 feet (21 meters) (any spacing at 5 knots)
Repaired Width Feet (m)	25 (7.6 )
Cleared Width Feet (m)	35 (10.7)
Swept Width Feet (m)	35 (10.7)
90° Turn Width Feet (m)	30 (9.1 )
180° Turn Width Feet (m)	50 (15.2 )

## VIII FOD CONSIDERATIONS

Of the many techniques under consideration for use in runway repair one technique is crushed stone with or without a FOD cover. Debris from an uncovered repair or other debris from attack damage could potentially cause FOD damage to aircraft operating on the airfield. Some aircraft are very susceptible to FOD damage while others are more tolerant, and some aircraft are certified to operate on gravel runways and should be able to operate successfully on crushed stone repair without a FOD cover. The removal of all potential FOD and use of FOD covers on repairs could substantially increase repair time.

The aircraft operator will provide as much guidance as possible on the ability of a specific aircraft to tolerate FOD. It must be recognized that evaluation of FOD tolerance of an aircraft involves estimates of acceptable operational risk and that FOD removal from a damaged airfield will, of necessity, be incomplete.

## IX EVACUATION CONSIDERATIONS

One possible scenario is that the airbase is damaged to the extent where base closure and evacuation is a necessity. Certain things can be done to most aircraft to improve and speed up evacuation procedures. The MOS repair requirements will be decreased to be an Evacuation Strip (ES).

The following action can be taken to decrease F-4 MOS length and load bearing requirements.

(a) Reduce Gross Weight: The aircraft operator can reduce gross weight to shorten the takeoff distance required.

(b) Reduce Tire Pressure: Aircraft tires are designed to operate at a specific percent deflection under static load. When the gross weight is reduced, the tire pressure can also be reduced, thus reducing the aircraft's flotation requirements, and, consequently the load bearing requirements for a repair.

(c) Evacuation Strip Size and Strength: Using the reduced weight and reduced tire pressures, the Evacuation Strip and load bearing requirements should be specified. This may provide the airfield manager with the option of using a perimeter road, sod surface, or other surface. An example for the F-4E is included as Table 6.

Special Servicing or Operating Techniques: The aircraft operator should specify any other action that can improve an aircraft's surface roughness capability. For evacuation these special servicing procedures and/or operational techniques should be identified and the subsequent Evacuation Strip runway repair requirements specified. Appendix A contains a sample F-4E evacuation procedure using special servicing of the main gear struts that results in increased roughness tolerance, (High Pressure Struts).

TABLE 6

## F-4E EVACUATION STRIP DATA

Gross Weight lbs	44,563 lbs
Center of Gravity	31.1%
Main Gear Tire Pressure, PSI	200
Nose Gear Tire Pressure, PSI	120
Evacuation Strip Length, feet (m)	
1.1 Density Ratio	1,600 (488)
1.0 Density Ratio	2,000 (607)
0.9 Density Ratio	2,400 (732)

- NOTES: 1. Full Internal Fuel
2. No External Stores (639 rounds of 20 mm)
3. Repair Load Bearing Capability in accordance with reduced Gross Weight and Main Tire Pressure
4. Roughness Specification should be the same as a standard MOS (section IV or V) except that the Evacuation Strip length may be much shorter.

## X CONCLUSIONS AND RECOMMENDATIONS

**Conclusions:** The data, data formats and responsibilities defined in this report can be used to exchange data between nations for the purpose of defining requirements for rapid repair of bomb damaged runways after an enemy attack. The exchange of data is essential for NATO interoperability.

**Recommendations.** This report only represents a first attempt to quantify and document these parameters that establish Rapid Runway Repair specifications. Other individuals or nations may have better techniques for presenting, documenting and measuring the essential parameters. NATO nations should be encouraged to review this report and comment upon its usefulness.

## XI REFERENCES

1. USAF T.O. 1F-4E-1, February 1979. Unclassified.
2. Caldwell, L.; Borowski, R.; McCracken, J.; and Riechers, J., F-4K HAVE BOUNCE Tests, March-April 79, ESL-TR-79-13, Engineering Services Laboratory, Air Force Engineering and Services Center, Tyndall AFB, FL. CONFIDENTIAL.
3. Redd, Tracy L. and Borowski, F., HAVE BOUNCE Phase I Test Results, AFFTC-TR-79-1, Air Force Flight Test Center, Edwards AFB, CA, April 1979. Declassified.
4. Caldwell, L. R.; and Jacobson, R., Interim Guidance for Surface Roughness Criteria, ESL-TR-79-37, Engineering and Services Laboratory, Air Force Engineering Service Center, Tyndall AFB, FL, October 1979. Unclassified.
5. Lenzi, D.; and Borowski, R. A., HAVE BOUNCE Phase II Test Results, AFFTC-TR-80-4, Air Force Flight Test Center, Edwards AFB, CA, June 1980. Unclassified.
6. Redd, Tracy L., Addendum I, HAVE BOUNCE Phase II Test Results (Spall Tests), AFFTC-TR-80-4, Air Force Flight Test Center Edwards AFB, CA, September 1980. Unclassified.
7. Caldwell, L. R.; and Strickland, W. S., Minimum Operating Strip Selection Criteria for North Field Test, ESL-TR-80-52, Engineering and Services Laboratory, Air Force Engineering Services Center, Tyndall AFB, FL, October 1980. Unclassified.
8. Hag, Delynn R., Aircraft Characteristics For Airfield Pavement Design and Evaluation, AFWL-TR-69-54, Air Force Weapons Laboratory, Kirtland AFB, NM, October 1969.
9. NATO Standardization Agreement 2929 (ADR) Airfield Damage Repair. CONFIDENTIAL.
10. Caldwell, L.; and Gerardi, A., Proposed Specifications for International Interoperability on Repaired Bomb Damaged Runways, ESL-TR-81-03, Engineering and Services Laboratory, Air Force Engineering Services Center, Tyndall AFB, FL, January 1981. Unclassified.

## APPENDIX A

## Proposed Special Servicing Procedures for F-4E Evacuations (High Pressure Strut)

In the event that the airfield is damaged to the extent that evacuation is required and it is necessary to make extremely rough repairs special servicing of the F-4E main gear struts can significantly increase the ability of the F-4E to tolerate roughness.

The aircraft gross weight and tire pressure should be reduced as discussed in Section IX of this report. These changes will decrease the Evacuation Strip length and load bearing requirements as shown in Table A-1.

The main landing gear upper chamber strut pressure should be increased as outlined in Reference 10. This will increase the roughness capability of the F-4E to allow "D" quality repairs with no spacing restriction. "E" quality repair may be used after the first 1000 feet without spacing restriction.

In this configuration the F-4E must fly with the Main Landing Gear lock pin installed and therefore with the Main Landing Gear down. This results in a substantially reduced range.

TABLE A-1

F-4E EVACUATION STRIP FOR VERY ROUGH SURFACE  
USING HIGH PRESSURE STRUT

Gross Weight lbs	44,563
Center of Gravity	31.1%
Main Gear Tire Pressure, PSI	200
Nose Gear Tire Pressure, PSI	120
Main Gear Upper Chamber Strut Pressure	See Table C-2
Evacuation Strip Length, feet (m)	
0.9 Density Ratio	1,600 (488)
1.0 Density Ratio	2,000 (607)
1.1 Density Ratio	2,400 (732)
Repair Quality (any spacing)	
Any location	"D"
After first 1,000 ft (304 m)	"E"

- NOTES:
1. Full Internal Fuel
  2. No External Stores (639 pounds of 20 mm)
  3. Load bearing capability in accordance with reduced tire pressure and gross weight
  4. Main Gear must be Extended. Use drag index of 30 for main gear down range. Gear down airspeed limit is 250 knots calibrated airspeed.

## APPENDIX B

## GLOSSARY

Access Route. The route aircraft must take from the parking area/shelter to the MOS. Typically the route will meander on or off existing pavement. The time to repair the access route and distance covered is a consideration in MOS selection.

Craters/Pavement Damage Categories.

Camouflet. Pavement damage caused by a deep penetrator which creates a void in the base course or subbase and an uplift of the pavement. Collapse or partial collapse of the void is likely. Camouflets are considered to be a form of small craters.

Large Crater. Large craters are pavement damage from conventional weapons that penetrates the subgrade and has an apparent crater diameter greater than 15 feet (Figure B-1).

Small Crater. Small craters are pavement damage from conventional weapons that penetrate/disturb the subgrade and result in possible pavement upheaval around the crater edge, and an apparent crater diameter of less than 15 feet. (Reference Figure B-1).

Scab. Pavement damage that does not penetrate the pavement base course and which results in a damage area that could typically be up to 5 feet (1.5 m) in diameter.

Damage Length. The length, parallel to the MOS centerline, including upheaved pavement, of the damaged pavement. If the repair has an FOD cover or a mat with a significant thickness then the damage length includes the cover or mat (Reference Figure B-2). The measurement includes all material including upheaved pavement, repair mats, etc., that may not be at the original pavement level and would result in surface roughness.

Debris. Material ejected from the crater including broken pavement and soil. Debris is sometimes useable as backfill material particularly for large crater repair but for small crater or scab repair it is generally not adviseable.

#### Diameters.

Apparent Crater Diameter. The apparent crater diameter is the visible diameter of the crater, inside edge to inside edge at the original surface level, prior to debris being removed. In actual practice this can be measured from pavement edge to pavement edge. (Reference Figure B-3)

Actual Damage Diameter. The damage diameter is the diameter across the upheaved pavement from the start of upheaval on one side of the crater to the end of upheaval on the far side of the crater. (Reference Figure B-3)

Repair Diameter. The repair diameter is the maximum distance across the repair, not necessarily parallel to the MOS centerline. The repair diameter is measured from the unrecovered pavement on one side of the repair to the unrecovered pavement on the other side and represents the portion of the repair that has a significantly different load bearing capability than the original pavement. (Reference Figure B-2)

Evacuation Strip (ES). The minimum size and reduced load bearing capability operating strip required to launch but not recover a specific aircraft under restricted conditions such as reduced gross weights and reduced tire pressure.

Fallback. Crater material which is ejected at such a high angle that it falls back into the crater. This material is characteristically loose. Its compaction or removal to a depth of 2 feet (0.61 m) is required for small crater repair.

Foreign Object Damage (FOD). Damage to aircraft caused by small loose objects--usually debris on the runway--being ingested in the engine, damaging the tires, or being thrust into other parts of the aircraft.

Minimum Operating Strip (MOS). The minimum operating strip is the smallest amount of area that an airfield manager must repair in order to launch and recover aircraft after an attack. Selection of this MOS will depend upon mission requirements, taxi access, resources available and estimated time to repair. The current NATO standard for an MOS is 50 feet wide by 5000 feet long.

Repair Quality. The repair quality is identified by a series of progressively less restrictive specifications identified as A, B, C, D, etc., such that a higher quality level is always better than a lower quality level and can be used in place of the lower quality level. For example, a B level meets or exceeds the C level specification and can be used in place of a C repair, but does not meet or exceed the A level repair requirements.

Sag. Sag is the vertical distance between the low points of a repair and an "imaginary repair surface." In order to measure sag, the "imaginary repair surface" must be established by stretching a string across the repair so that it contacts the pavement just outside the start of the upheaval as shown in Figure B-5. Then the vertical distance from the repair surface to the string must be measured. Sag will probably increase with aircraft traffic as the fill settles.

Peak Sag. The peak distance below the string is the peak sag. This peak sag must be associated with a "maximum span below nominal sag" as discussed below.

Nominal Sag. This sag is the maximum allowable sag that is acceptable without consideration for sag length. There is no associated sag span with the nominal sag.

Maximum Span below Nominal Sag. This parameter defines how wide (how long down the MOS) that sag can exceed the nominal sag towards the peak sag limit. The repair surface must return to a point above the nominal sag at least once in each maximum span. This parameter allows sag to approach the peak allowable sag as long as the effective frequency does not stimulate reinforcement of aircraft dynamic loads.

#### Upheaval.

Pavement Upheaval. The vertical displacement of the airfield pavement around the edge of an explosion produced crater. (See Figure B-3.) The pavement upheaval is within the crater damage diameter, but is outside the apparent crater diameter. The upheaved pavement may be completely removed, partly removed or not removed during the repair process depending upon the repair quality level.

Peak Upheaval. The peak upheaval is the repair peak highest above a line between the undamaged pavement on each side of the repair. The measurement of the upheaval in the field is performed using upheaval markers as shown in Figure B-4. These markers permit a string to be stretched taut at certain heights above the pavement surfaces. The upheaval marker posts should be located on opposite sides of each crater, outside the limits of pavement upheaval. A string should be stretched between the posts at equal heights above the pavement, corresponding to the allowable maximum repair upheaval for the applicable repair category. The entire crater repair must lie beneath the string to meet the maximum upheaval criteria. One of the current repair techniques uses an aluminum mat on top of select fill in the crater. The peak upheaval, includes the thickness of this repair mat.

Repair Upheaval. Repair upheaval is the height of the repair above the original pavement elevation. It occurs where the pavement has been raised by the explosion around the edge of the crater or by overfill in the crater during the repair operation. Repair upheaval includes the height of an FOD cover or a repair mat such as the US AM-2 mat or the UK Class 60 mat if it is used for a particular repair. (Reference Figure B-4)

Percent Change in Slope. This parameter establishes the maximum rate of change of the repair height, and is applicable to both the upheaved pavement and the repair surface. For example, if the damaged pavement is heaved up 1.5 inches in 5 feet, then this represents a  $[1.5/5 \times 100] = 3.0$  percent change in slope from the adjacent undamaged pavement. Typically, change in slope would be measured with a template.



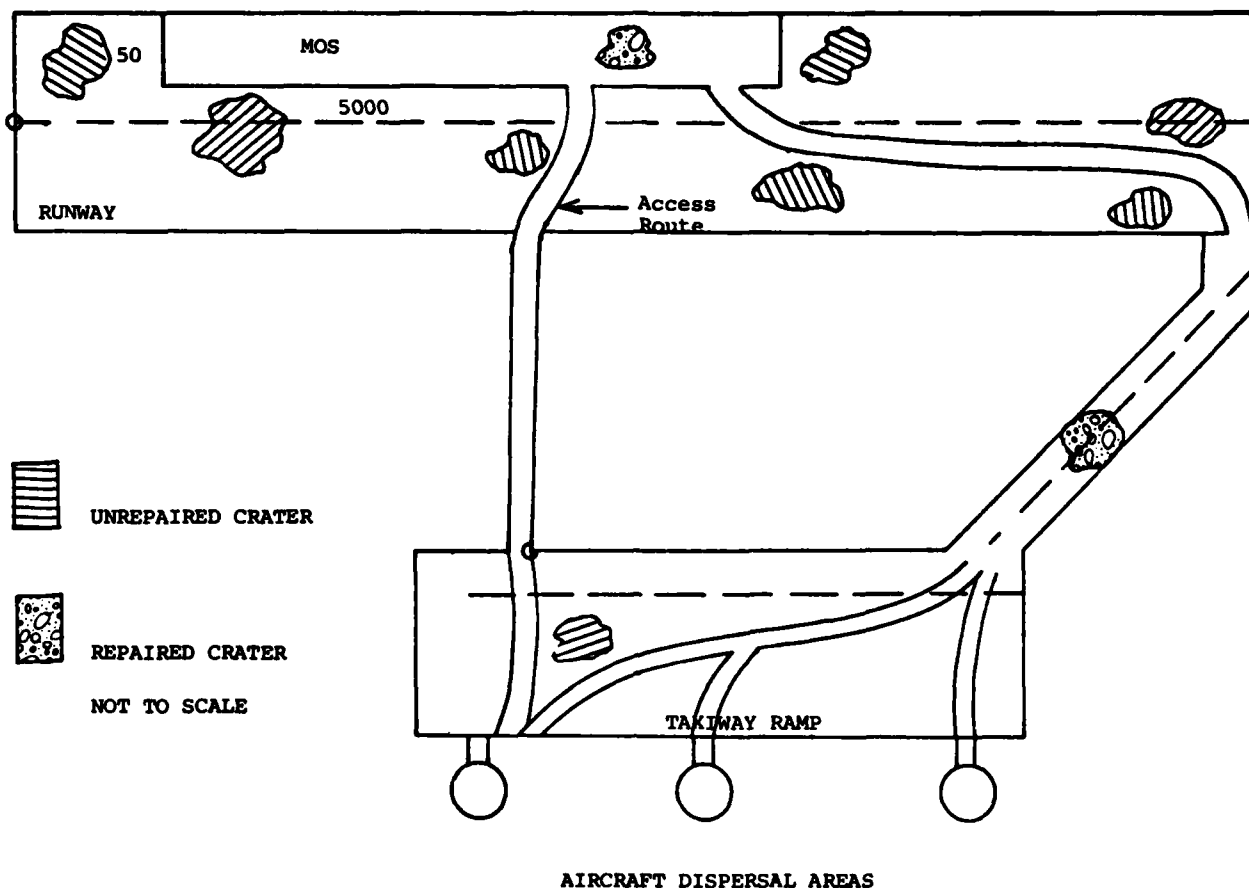
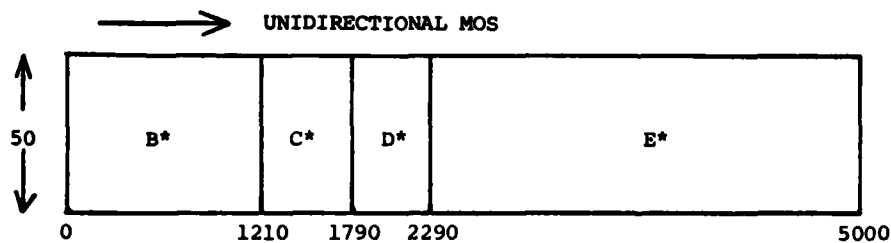
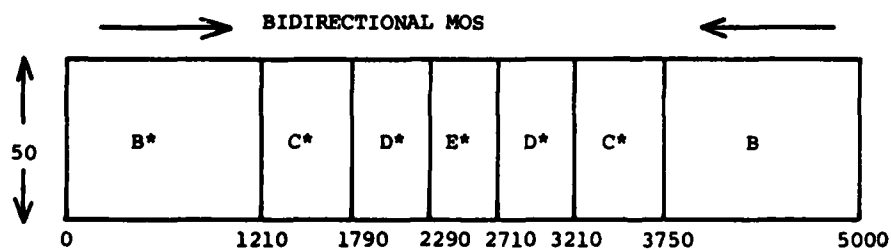


Fig.1 Typical MOS



- NOTES: 1. \* or better  
 2. Density Ratio=1.0  
 3. Repair Quality is defined in Section V



FEET

Fig.2 F-4E MOS repair quality vs locations

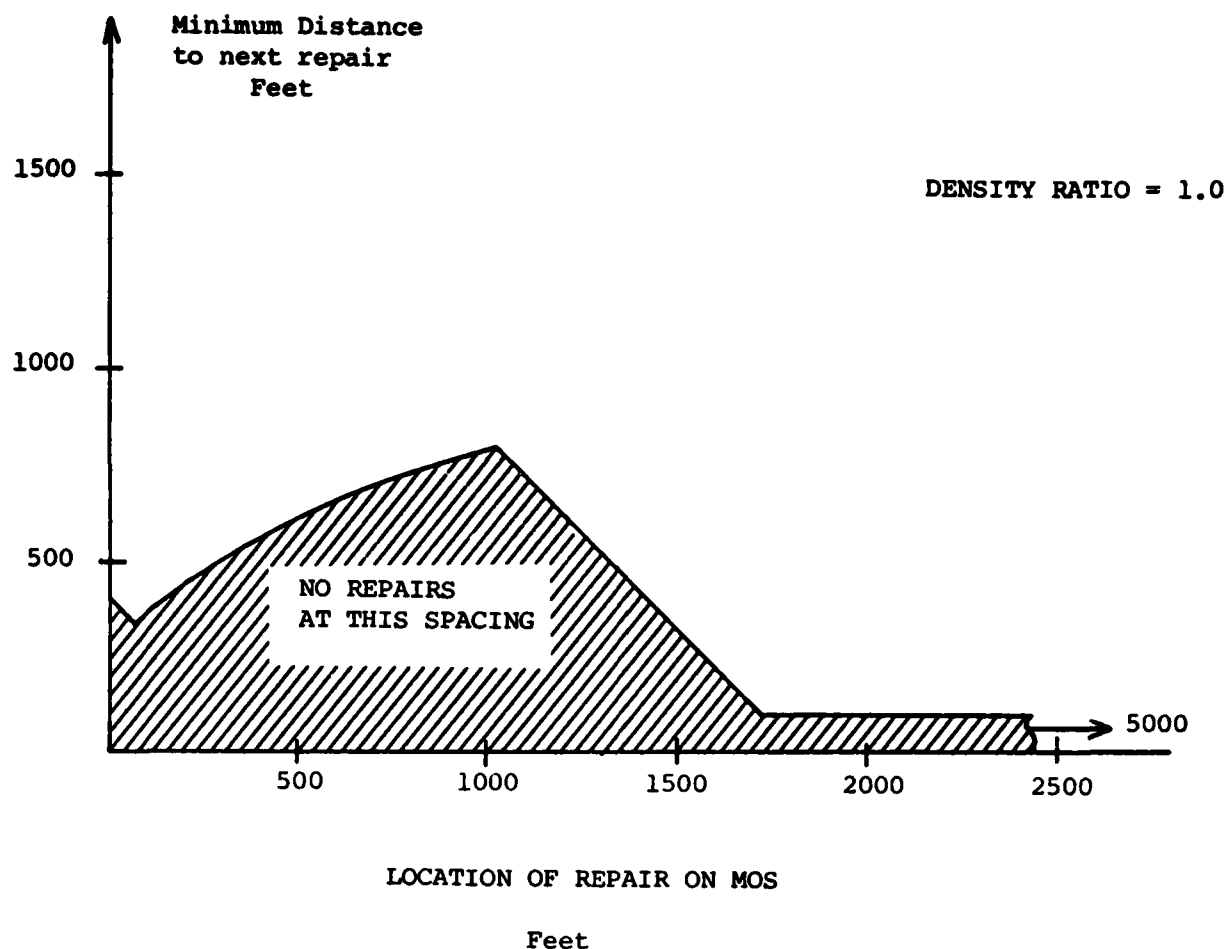


Fig.3 F-4E MOS spacing

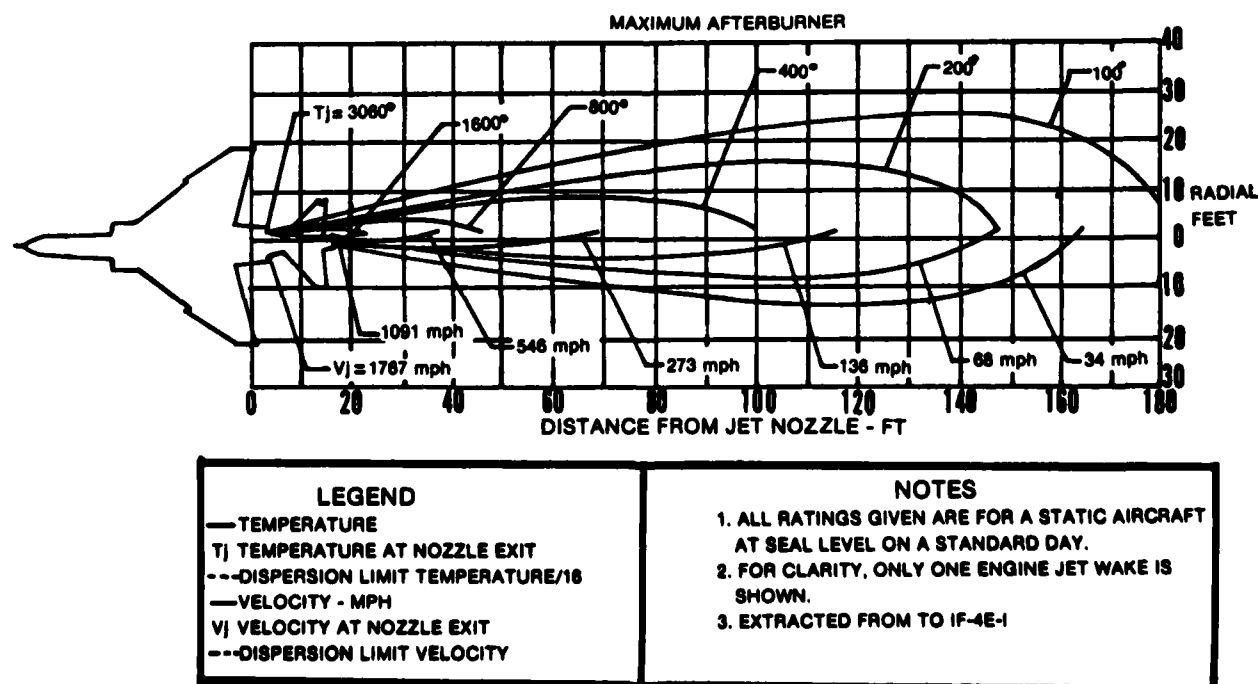


Fig.4 F-4E thrust effects

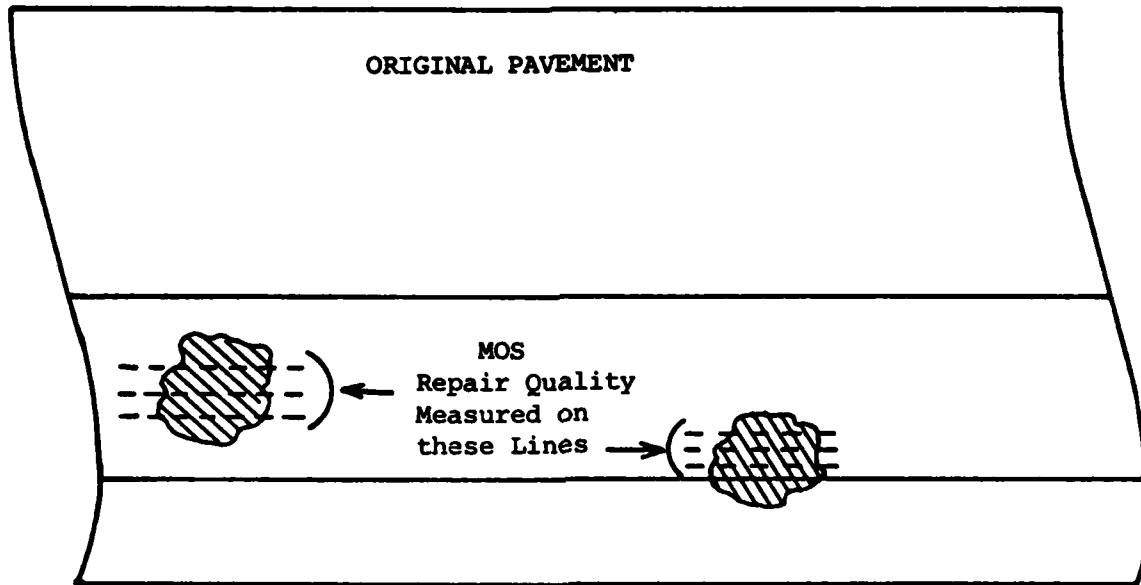


Fig.5 Repair quality measurements

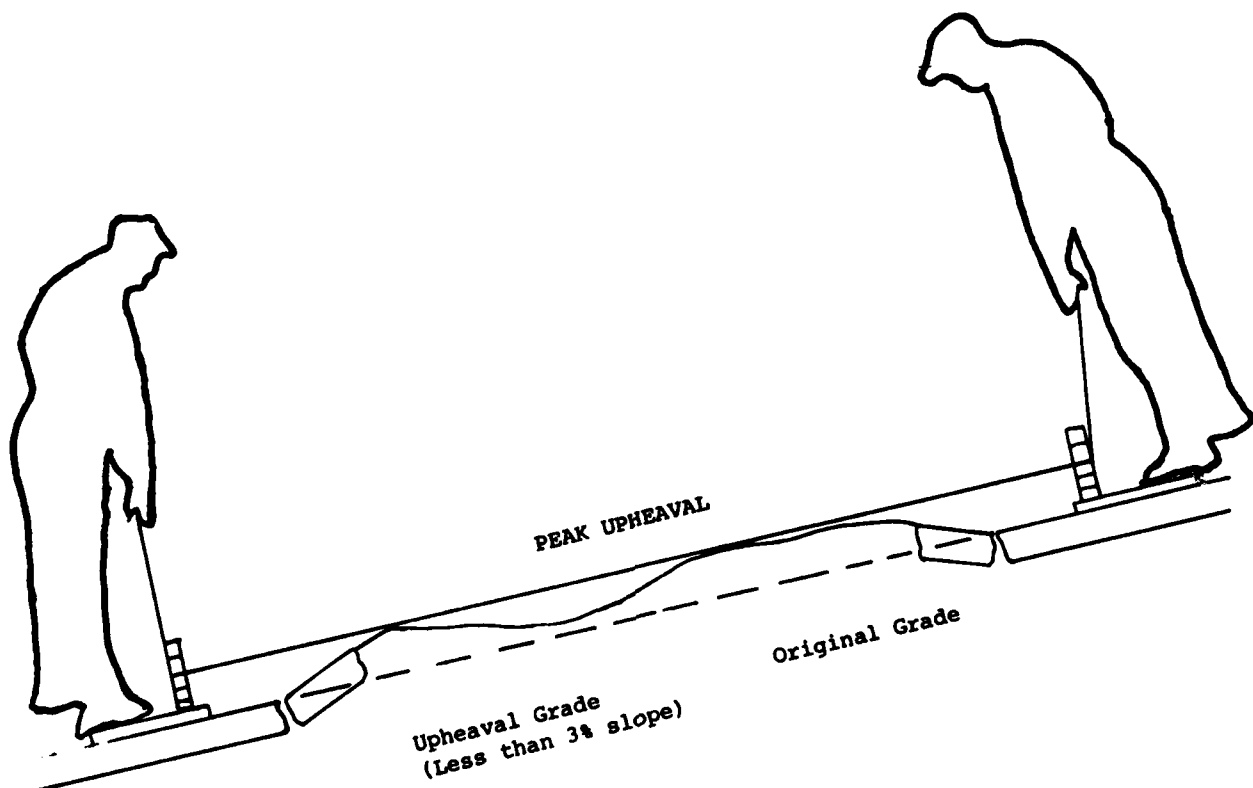


Fig.6 Peak upheaval measurement

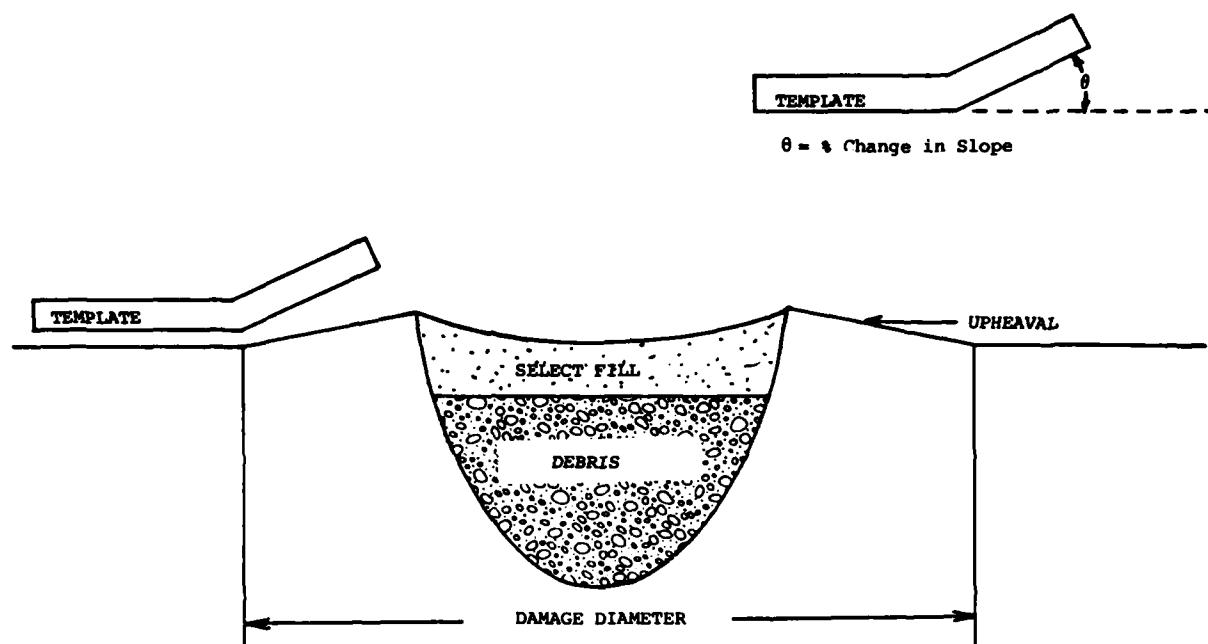


Fig.7 Slope template

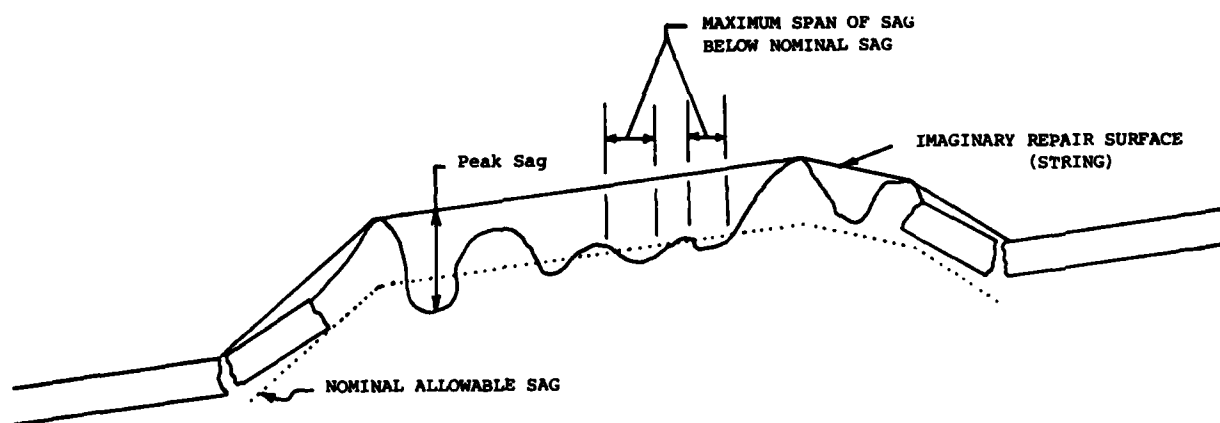


Fig.8 Sag measurement

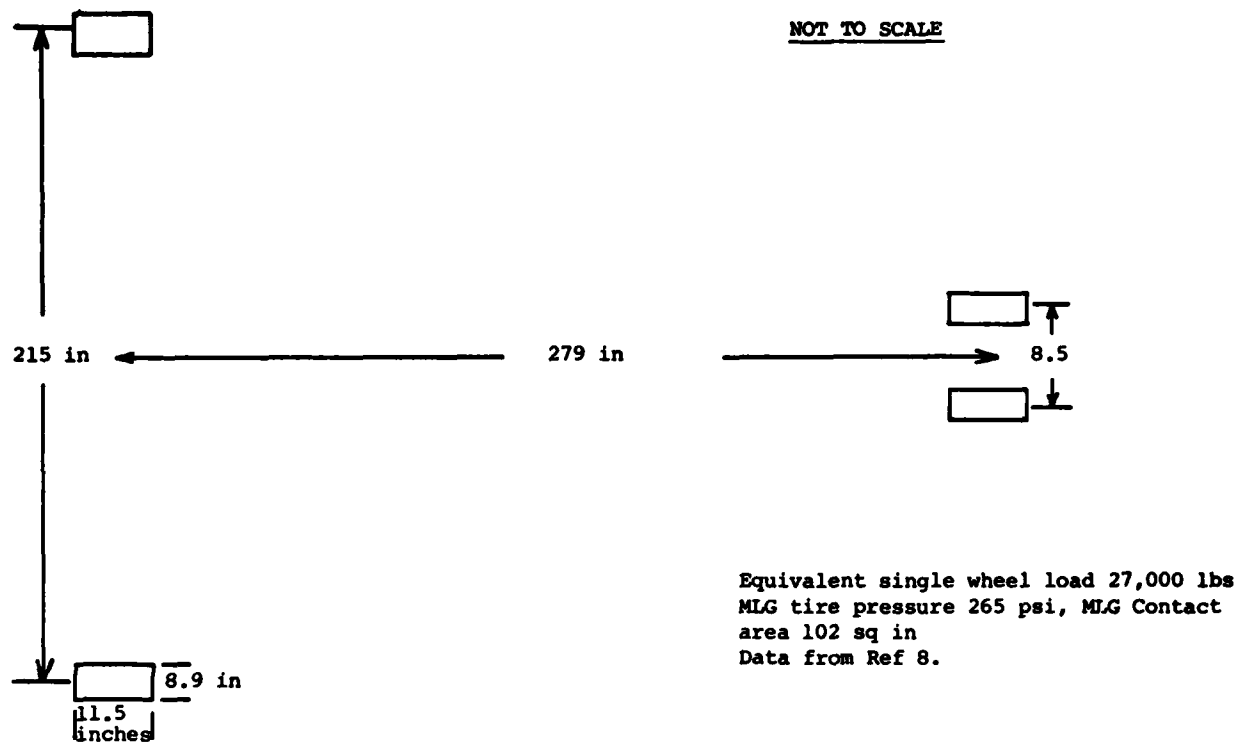


Fig.9 F-4E wheel pattern

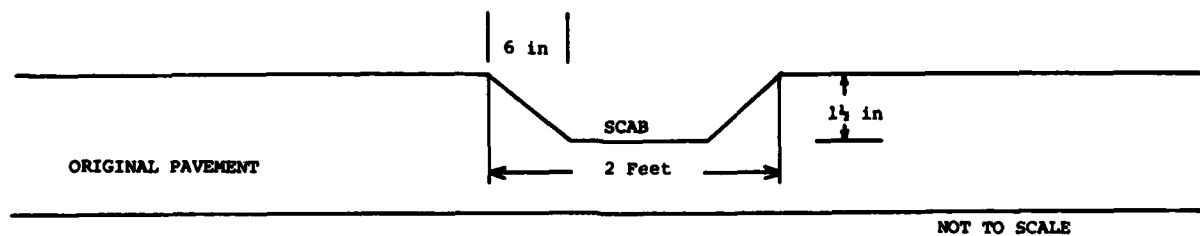


Fig.10 F-4E unrepaired scabs

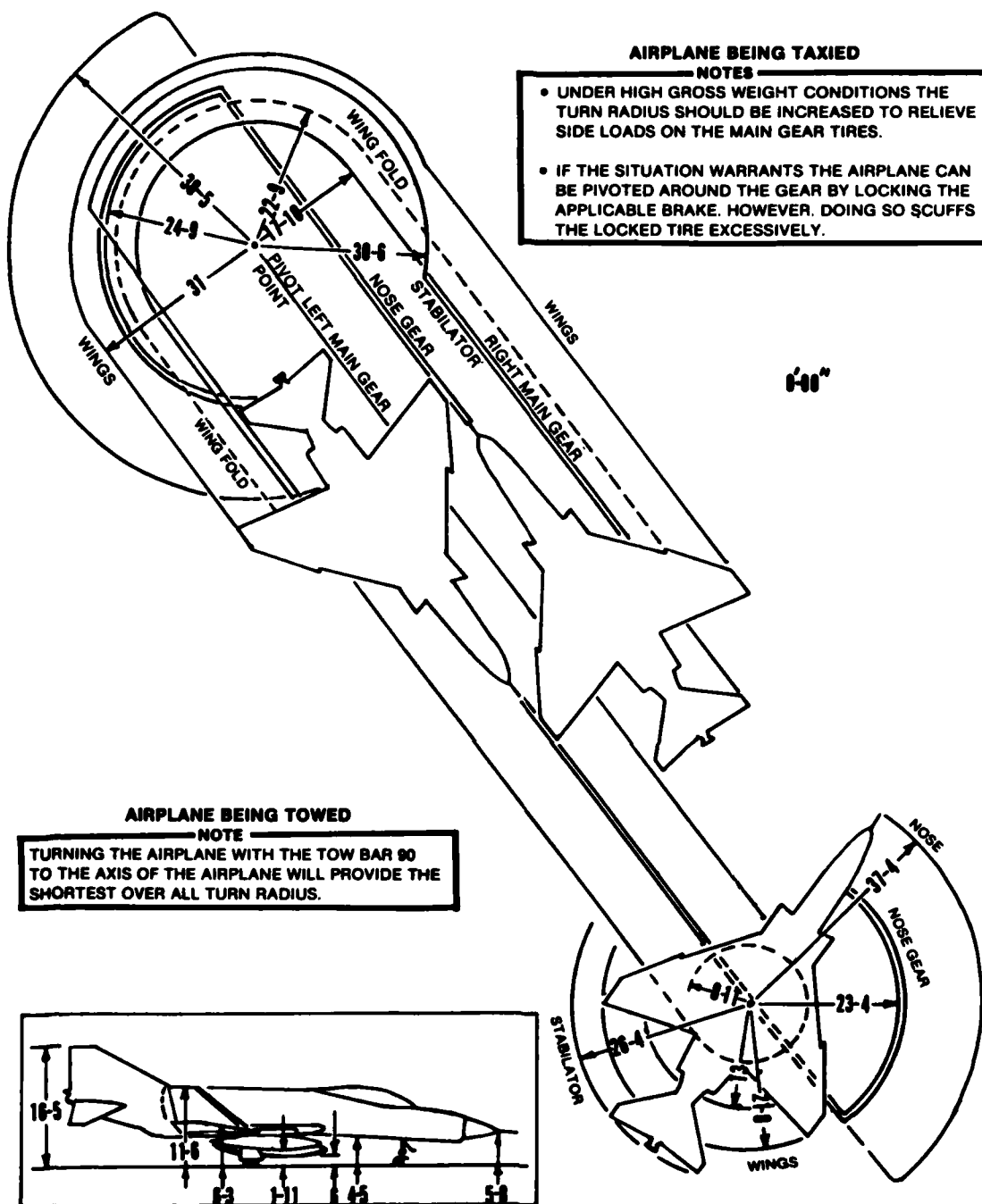


Fig.11 F-4E turning radius and ground clearance

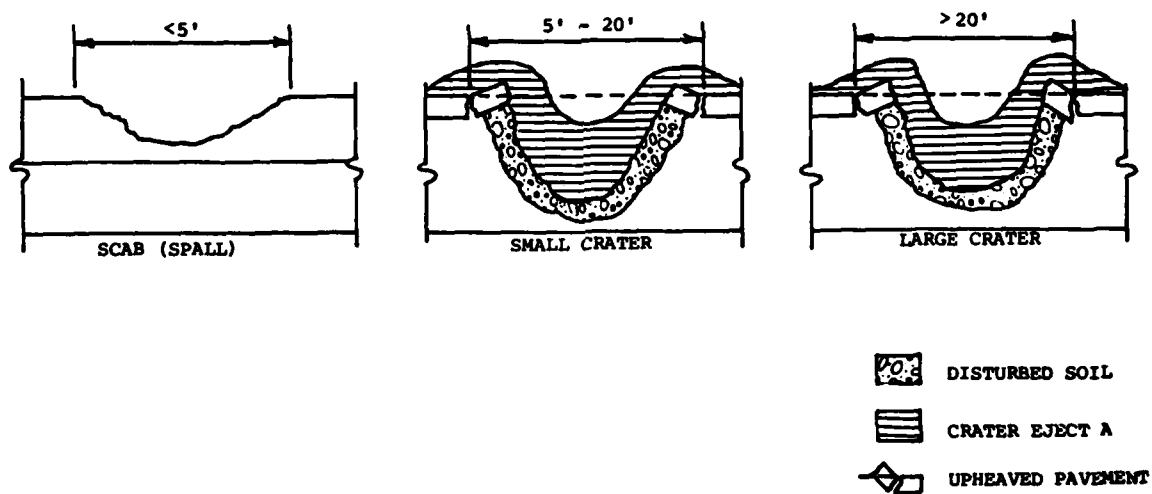


Fig.B-1 Pavement damage categories

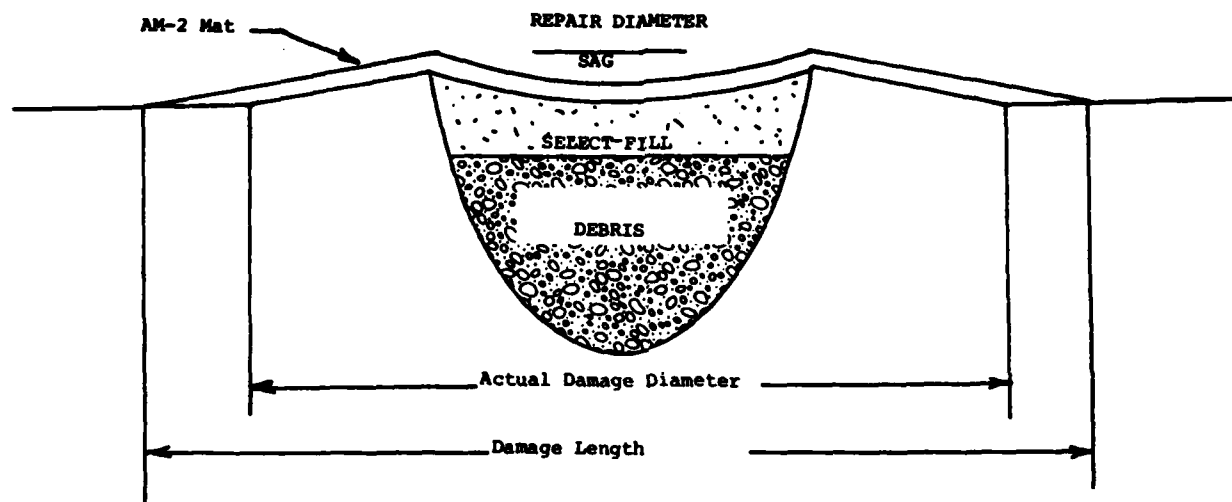


Fig.B-2 Repair using AM-2 mat

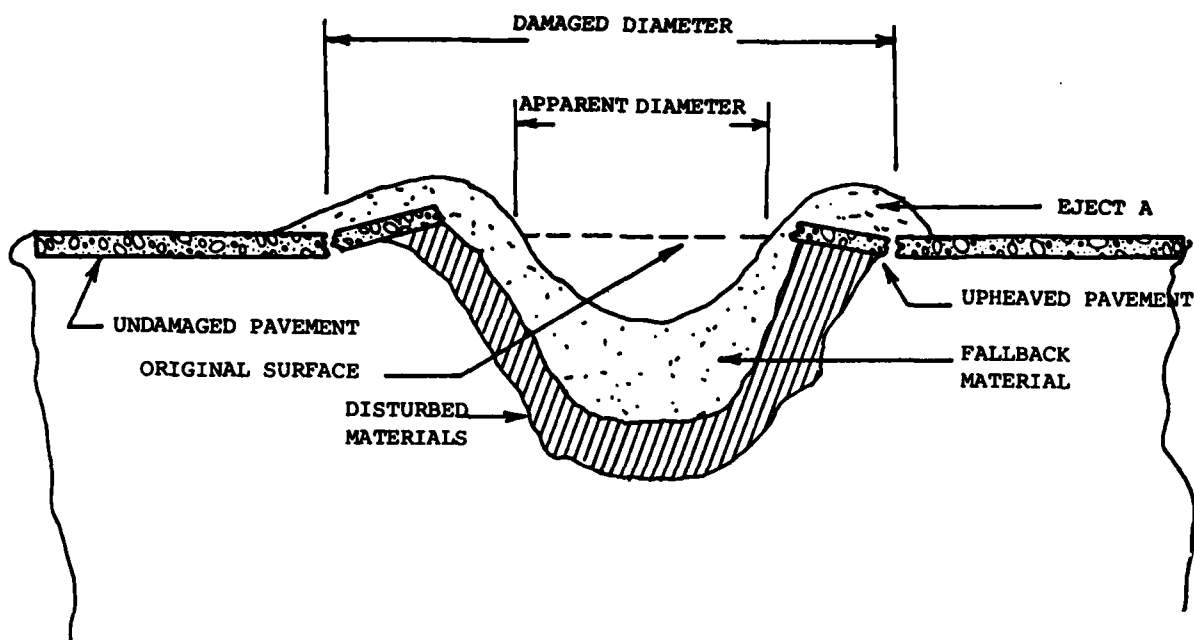


Fig.B-3 Apparent crater nomenclature

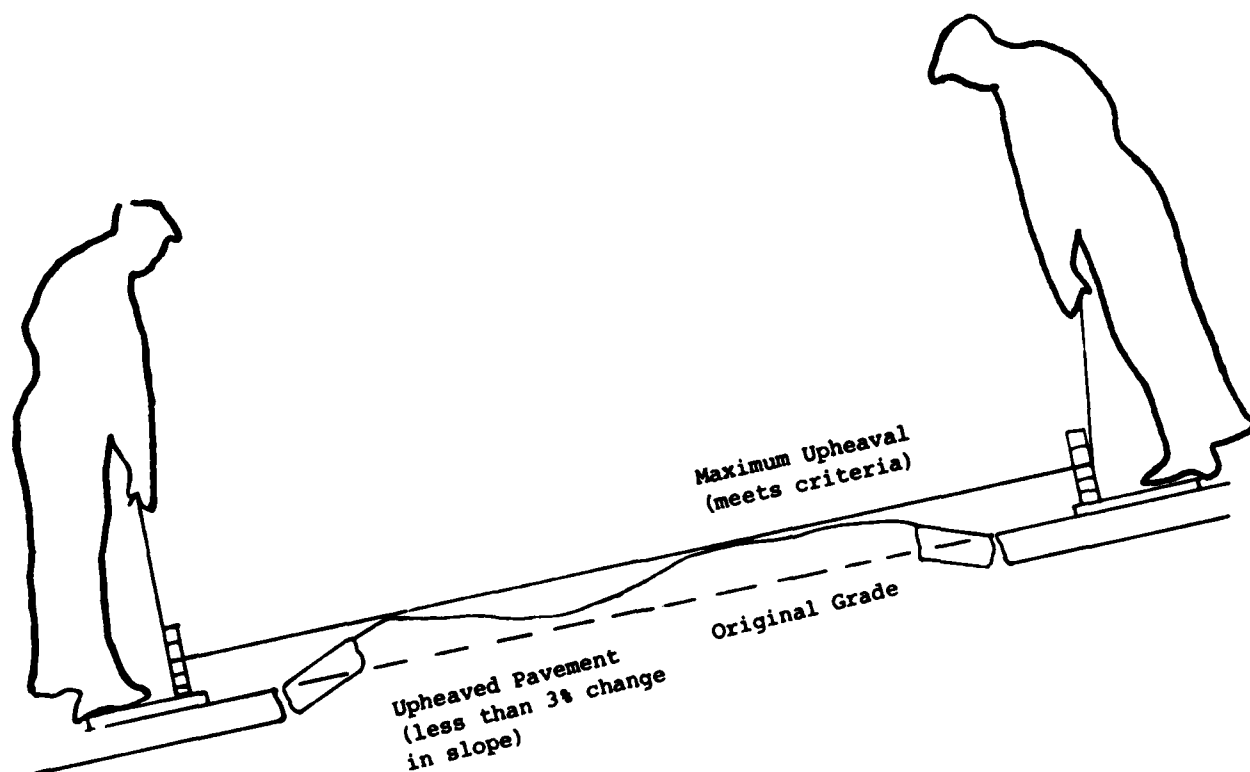


Fig.B-4 Maximum allowable upheaval



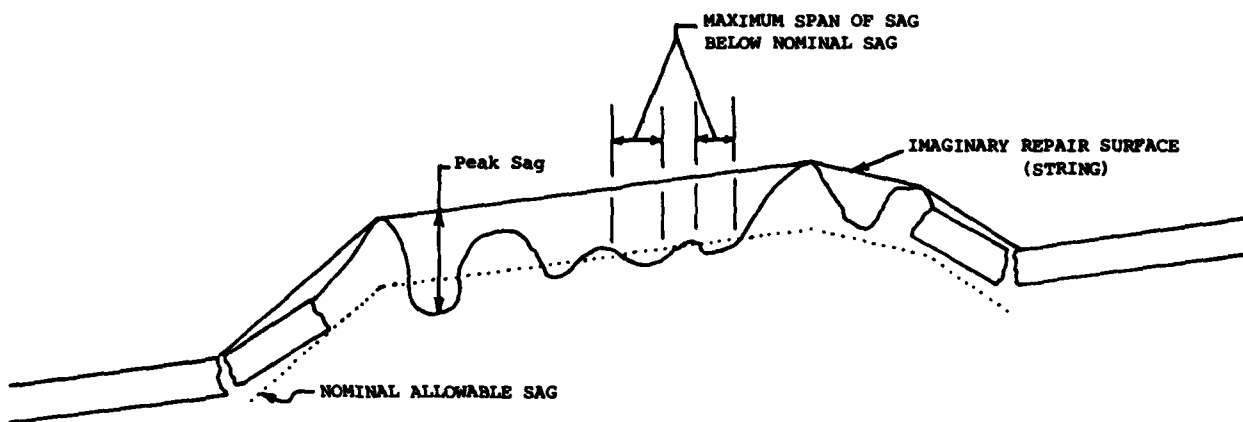


Fig.B-5 Sag measurement

**PART 2**

**SPECIALISTS' MEETING**

**SPRING 1982**

ADVANCED RAPID RUNWAY REPAIR  
A STABLE AND FLUSH REPAIRED RUNWAY SURFACE

RICHARD J. BERGHOLZ, LT COL, USAF  
CHIEF, FORCE DEVELOPMENT DIVISION  
UNITED STATES AIR FORCES EUROPE  
EUROPEAN AIR COMBAT OPERATIONS  
STAFF-ENGINEERING AND SERVICES  
APO NEW YORK 09012



SUMMARY

Aircraft operations are limited by rough runway pavement resulting from conventional Rapid Runway Repair (RRR) of cratered aircraft launch surfaces. Rapid Runway Repair methods can be improved to provide rapidly repaired flush pavement surfaces to support high dynamic aircraft loading.

This paper examines the nature of damage to aircraft launch surfaces that may reasonably be expected to occur during a conflict, suggests the need to develop rapid large area and deep trenched runway repair, proposes new civil engineering methods to deal with rapid repair of that damage, and postulates effects on aircraft landing gear shock absorbers. It further describes currently ongoing field investigative efforts to adapt commercially available materials and equipment to provide flush repaired runway surfaces for this expected damage, lessening vertical and horizontal shock forces on aircraft landing gear systems.

This paper represents the views of the author and does not necessarily reflect the official views of HQ US Air Forces Europe or the Department of the Air Force.

## I. INTRODUCTION - BACKGROUND

Surface roughness characteristics resulting from bomb damage repaired runways have been measured for several types of repair processes. Two such processes are: 1) 3/8-inch thick fiberglass reinforced polyester covers bolted to the surrounding pavement over single craters refilled with crushed limestone; and 2) AM-2 aluminum matting covers over single craters refilled with debris. Both repair systems have been tested with fighter and transport aircraft under a project called HAVE BC'NCE. These tests have shown repair problems, as well as aircraft operation limitations, with both repair systems.

Repairs using crushed limestone as repair surface backfill require heavy and extensive compaction and cannot successfully be performed during precipitation or in areas with high ground water levels. Further, soft surface repairs consisting of polyester or similar covers are not recommended for wide-body aircraft operations other than for slow speed taxiing. On the other hand, repairs with AM-2 aluminum matting are restricted to spacing distance limitations between repaired surfaces which vary for each aircraft type and aircraft rolling speed. These distances between repairs are critical to avoid sympathetic oscillations induced into aircraft shock absorbing systems as aircraft roll over consecutive repairs. These limitations call for alternate solutions to Rapid Runway Repair (RRR) which will minimize forces exerted against aircraft landing gears for both light and heavy aircraft. At the same time, these solutions must provide a flush repaired surface of sufficient mass to withstand the horizontally induced dynamic forces of heavy aircraft rolling at high speeds. Finally, these solutions must be independent of climatic influences. This paper addresses such an alternative; the use of pre-manufactured, reinforced concrete block. Flush-surface concrete block repairs lend themselves not only for individual crater repair, but for large-scale area damage and deep trenched runway area repair as well.

## II. THREAT EFFECT ASSESSMENT

The current conventional air-to-surface warfare threat to airfields, be they forward tactical or rearward aerial ports of debarkation, will severely tax our ability to place them quickly back into operation in such a manner that normal aircraft sortie generation can resume. To more thoroughly understand the problems facing us, it is important to simulate as accurately as possible the nature of this threat by:

- Assessing the magnitude of the potential threat.
- Evaluating the nature of the effect of the threat; i.e., assessment of expected damage.
- Evaluating the damage repair methodologies.

Two automated simulation models performing these functions are currently in operation: the Attack Assessment Program (AAP), and the Airfield Interdiction Damage Assessment (AIDA) Program.

The AAP permits simulations of conventional air-to-surface battle damage prediction and assessment to a degree not possible before. The simulation methodology requires as input, or data base, variable information regarding three basic elements:

- Definition of an attack combination.
- Description of target elements.
- Description of weapons effects.

Through the use of random number generators, such as the Monte Carlo Technique, probabilistic events affecting the attack effectiveness can be predicted with a reasonable degree of mathematical reliability.

In the AAP, the distribution of certain probabilistic events, used as input variables, are assumed known and are approximated with a Monte Carlo sample. These events are:

- Aiming error in range.
- Aiming error in deflection and dispersion.
- Ballistic error in range and deflection.
- Weapon fuse reliability.

Based on these samples, computed over several hypothesized attacks, the probable damage is calculated. An analyst may choose any one of the samples and have the results displayed graphically on a high speed computer plotter. The results of such a sample for a hypothetical series of low level tactical fighter bomber attacks on a hypothetical airfield are shown in Figure 1.

The AAP activates a search subroutine between each set of theoretical attacks to determine whether a Minimum Operating Strip (MOS) for aircraft operations (50 x 5,000 ft nominal), clear of damage and with a clear access path, can be found. If such an MOS with access path cannot be found, the MOS area with the minimum craters is identified

and the amount of repair work is computed and recorded. These strips are then automatically chosen by the computer logic as an aim point for the next attack. In this manner, a reasonably realistic picture of most likely threat effects will emerge.

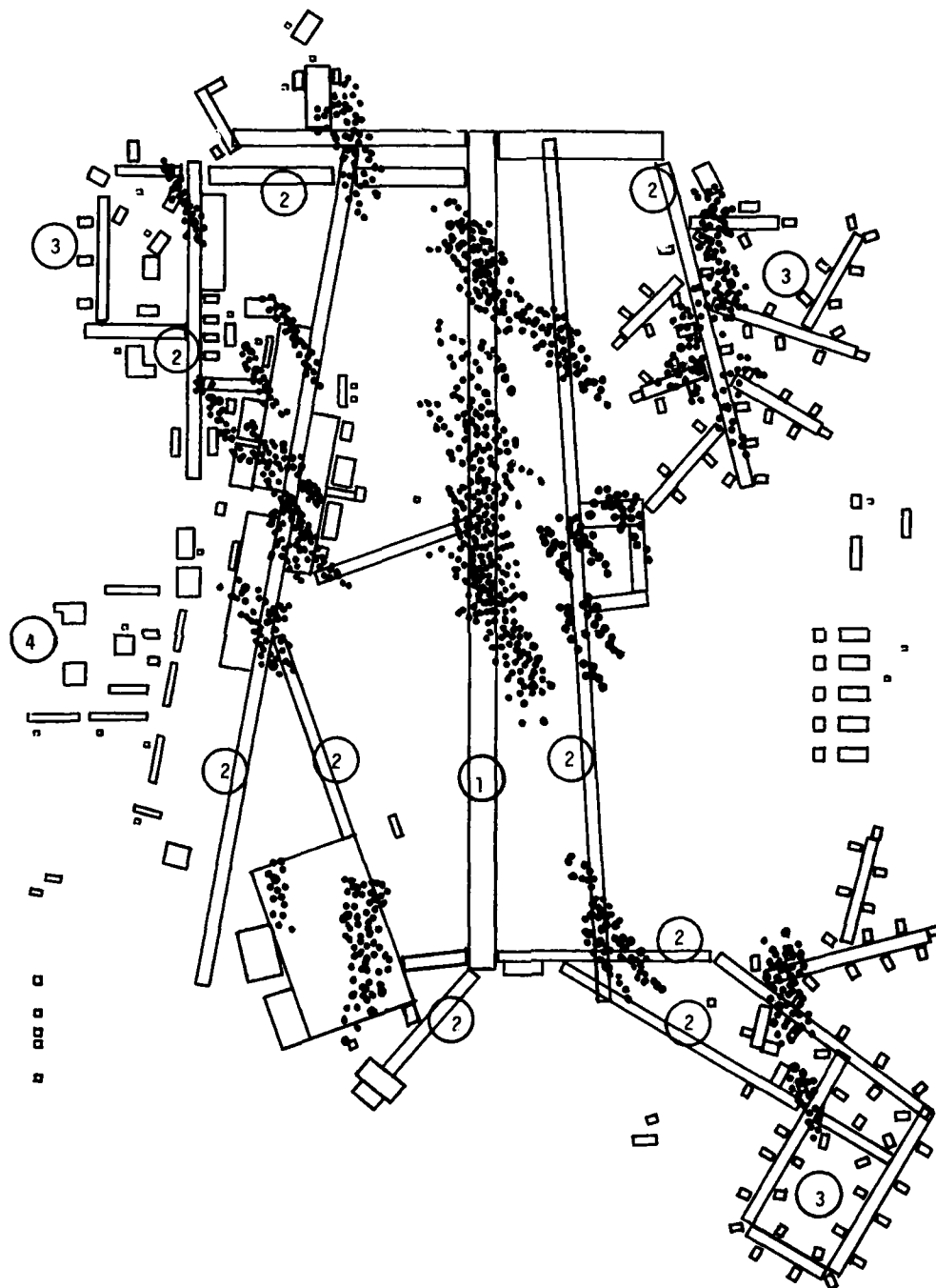


FIGURE 1. THEORETICAL DAMAGE IMPACT POINTS

1. Runway
2. Taxiways
3. Dispersed Aircraft Shelters
4. Operations Facilities

While the analysis of quantitative information is of value to planners, it is probably worthwhile analyzing the picture of the theoretically attacked airfield (Figure 1) as well, since it provides a means for a better appreciation for the nature of the

problem. Several key elements then become apparent:

1. It is easier for an attacker to keep aircraft from taking off by cutting the runway than by any other choice of aim points. Admittedly, attacking runways is not a permanent neutralization of aerodrome operations, but it can be sufficient to keep the runways closed until subsequent attacks can be generated. This conclusion is reached for the following reasons:

a. A greater number of errors (aiming/ballistic) and higher levels of weapon unreliability can be tolerated without reducing the overall attack effectiveness; i.e., keeping aircraft from taking off.

b. Given runway redundancy in terms of parallel runway/taxiways--that is, take-off surfaces--several aircraft launch surfaces can be cut by only one pass of an attacker. Aircraft launch surface redundancy, therefore, becomes a viable concept only if redundant launch surfaces exist in an accessible vicinity of the aerodrome but not on the aerodrome--and only if such redundant surfaces are not parallel to primary runways or taxiways.

c. Aiming points consisting of specific point targets such as aircraft shelters, command posts, communication centers, weapon storage points, taxiway choke points, etc. require extensive saturation weapon delivery patterns since point target neutralization is not as tolerant of probabilistic weapon delivery events as is area (launch surface) targeting.

2. Damage to runways or taxiways is not random, as often is assumed to be the case. Randomness occurs only in the distribution of impacts around aim points and then only in terms of deflection and range.

3. Damage to launch surfaces should not be expected to consist of only single impact points that can be repaired as discrete bomb craters. As a result of aiming errors, it can be expected that several bomb sticks released by a flight of attacking aircraft will be delivered adjacent to or on top of each other. Therefore, engineers responsible for repair of aircraft launch surfaces must be prepared to deal with:

- Large area launch surface repair.
- Trenched launch surface repair.

Rapid Runway Repair (RRR) techniques developed to date do not encompass these possibilities.

4. The quantity of launch surface repair work is crucial and warrants attention.

5. Expected damage to taxiway choke points leading from dispersed aircraft shelters to launch surfaces is not crucial; repairing surfaces for slow taxiing or towed aircraft is simple and can be carried out expeditiously. In addition, targeting choke points requires precision or saturation weapon delivery to compensate for difficulty in point target acquisition. Therefore, it may be expected that taxiway choke points may not be chosen as aim points since they do not present as lucrative a target as is generally thought.

A conclusion can be reached from the above that emphasis should be placed on developing Advanced Rapid Runway Repair (ARRR) techniques specifically addressing rapid large surface area repair and deep trench repair of runways. These repairs should result in flush repaired surfaces, rather than surface covers, that will accept the dynamic force loading of both fighter and heavy (wide body) aircraft without exacting aircraft design penalties in terms of increasing wheel design strength, weight, configuration, shock absorbant systems, or aircraft body structural strength. Off-the-shelf pavement substitute systems are available commercially today that will satisfy the above criteria. However, adaptation of these available systems to ARRR technology has not been fully exploited, nor has it been introduced as a standard ARRR system.

### III. CONCRETE SLAB SYSTEMS

The key element in meeting the above-stated criteria is the rapid emplacement of a massive and stable, yet flexible, pavement surface that can be aligned smoothly with surrounding original pavement; i.e., is flush and is easily replaceable in case of subsequent damage or sub-surface induced instability. Such surfaces can be provided through the use of premanufactured concrete elements or slabs.

A typical concrete slab is a prefabricated unit of dense, double-reinforced, high-early-strength concrete, bound by a steel angle frame protecting the surface edge as shown in Figure 2. The frame is strongly anchored into the mass of the concrete. The wedge-shaped void between adjacent concrete elements is particularly noteworthy. This space, when filled with fine gravel (or sand), acts mechanically on the similar principle as a keystone in a Roman arch. That is, the vertical forces exerted on the slabs tend to compress (wedge) the gravel (sand) between the slabs causing high resistance to vertical movement of concrete element edges. This resistance or wedge effect provides the basic stability between slabs without having to resort to load transfer systems using mechanical locking devices. In fact, locking devices would tend to be counter-effective in that such devices would cause weakness in the concrete element structure resulting from heavy vibrating transfer loads.

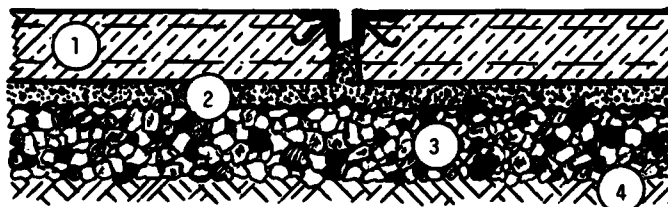


FIGURE 2. CONCRETE SLAB INSTALLATION CROSS SECTION

1. Concrete element.
2. Sand or fine gravel bed.
3. Crushed stone.
4. Sub-grade.

Two holes in the slab provide a means to insert special keys with which the slab can be lifted and transported. Should sub-surface weakness occur, then the elements can be easily lifted for readjustment of the sub-grade, as shown in Figure 3.

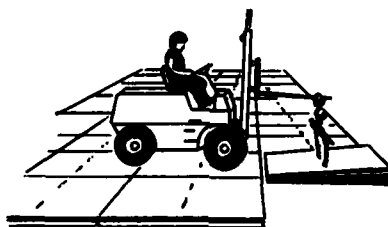


FIGURE 3. CONCRETE ELEMENT INSTALLATION

The concrete element can be produced in several configurations, although the most effective dimensions appear to be 2 x 2 meters and 14 or 16 cm in thickness. Concrete elements have been developed that will withstand single wheel loading of up to 15 tons, therefore lending themselves even for use in support of tracked vehicles, especially combat tanks. The ratio of surface load bearing or load impact area to thickness and weight of the slab is such that heavy loads on the surface are evenly distributed over the sub-surface, thus providing a stable bridging effect without load transfer between slabs.

Simulated and actual HAVE BOUNCE tests with aircraft high speed taxiing conducted over AM-2 aluminum matting repairs have produced oscillations in aircraft shock absorbers of the kind shown in Figure 4.

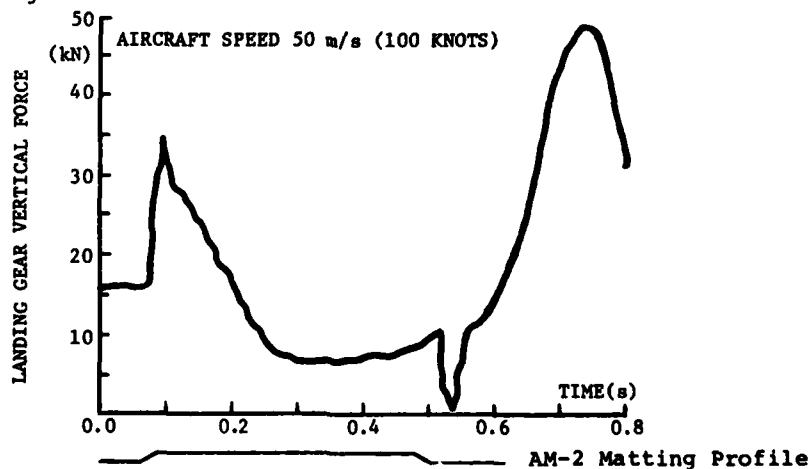


FIGURE 4. APPROXIMATE LANDING GEAR ABSORBED FORCE GENERATED BY AM-2 MATTING AT 50 METERS PER SECOND.

On the other hand, the vertical force displacing landing gear shock absorbers over concrete element systems can be expected to be similar to that shown on Figure 5, although this theoretical displacement has to be verified. However, it is reasonable to expect significant reduction in vertical aircraft oscillations.



FIGURE 5. EXPECTED FORCE GENERATION

#### IV. CONCRETE ELEMENT TESTING

The German Air Force Engineer Training Company at Fuerstenfeldbruck Air Base, Germany, conducted a series of tests in March 1980 to determine horizontal and vertical displacement characteristics of the concrete slabs when subjected to heavy loading immediately after emplacement. For this test, 2 x 2 meter concrete blocks, 14 cm thick, were placed on top of a refilled crater with 15 mm spacing between blocks. The blocks were not interconnected. However, a rubber grommet (Trixolit B415) was placed into the space between blocks. Loaded trucks (total weight 22 to 25 tons or an equivalent single wheel load of approximately four tons) approached the concrete block area at speeds of 25 to 30 km per hour and were braked to a full stop on top of the concrete plates, roughly simulating aircraft landings. The truck travel approach on the plates was always from the same direction. The vertical and horizontal displacement of each plate was measured after 20 and 50 rolls.

The results of this test revealed that settling of single concrete slabs after 20 rolls only varied between 1 and 3 mm. Measurements after 50 passes did not reveal any further vertical displacement. On the other hand, a total horizontal displacement of 16 mm was noticeable. In other words, vertical displacement under the same dynamic loads was relatively small and stopped altogether at some point before the 20th roll, presenting relatively small wheel roll-over interference; i.e., bump.

While these test results are limited--far greater dynamic loading occurs on active runways supporting fighter and wide-body aircraft--they nevertheless support the conclusion that the use of concrete slabs in support of aircraft operations is feasible and should be further investigated to determine the precise range of limitations, if any.

#### V. CURRENT USE OF CONCRETE ELEMENTS

The use of concrete element systems for aircraft parking aprons and taxiways is not new. The system has been in use for approximately ten years at Enschede, East Netherlands, as shown in Figure 6.

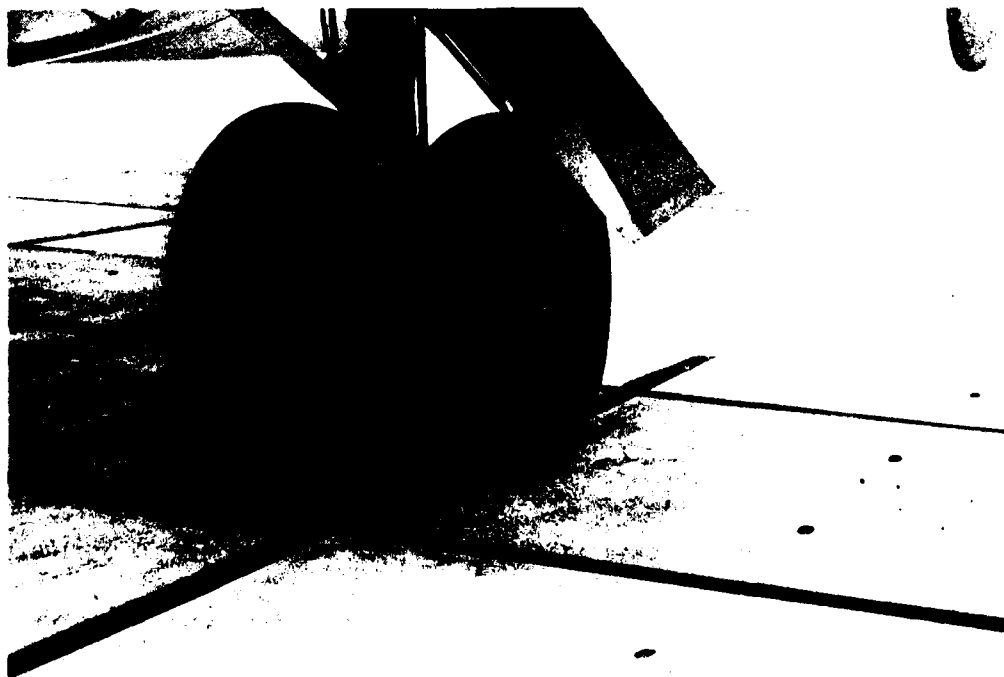


FIGURE 6. APRON AND TAXIWAY ON THE AIRPORT TWENTE (3 MILES NORTH OF ENSCHEDE, EAST NETHERLANDS).



The Swiss Air Force has been experimenting with the use of concrete slabs recently and has adapted them for their standard RRR system. Mirage aircraft have successfully performed high speed taxi operations over craters repaired with concrete elements.

Concrete element installations for permanent parking areas can also be found at Rotterdam as can be seen in Figure 7.



FIGURE 7. APRON ON THE AIRPORT ROTTERDAM.

#### VI. USAFE FIELD INVESTIGATION

Encouraged by these experiments and the current commercial use of concrete slabs at airports, Headquarters, United States Air Forces in Europe, has undertaken field investigations examining methods to improve runway repair capabilities for U.S. air bases in Europe. Three major investigative efforts, essential elements to ARRR, are underway.

- Overlaying an 8,000 m<sup>2</sup> aircraft parking apron area with pre-fabricated concrete slabs.
- Investigating high speed concrete saw characteristics.
- Developing high speed sequences for the Advanced Rapid Runway Repair procedures using concrete slabs.

The aircraft parking apron project, called "D-Ramp," will begin in October 1982. The parking ramp will be adjoining an existing main taxiway. The purpose of this project is to investigate heavy fighter and transport aircraft low speed taxi characteristics over free-floating concrete slabs supported by a conventional sub-base, as well as one consisting of only crushed rock. Fighter aircraft of the F-4, F-15, F-16, and F-111 series will be taxiing at various controlled speeds and loads over this surface. Additionally, heavier aircraft of the VC-135/707/C-130 and C-141 series can be taxied over this surface as well. Sufficient space for C-5 aircraft operations is, unfortunately, not available at this location. The subsurface of this parking area will consist of two parts: one part will be a conventional sub-base, while the other part will consist of a simulated repaired crater, 14 meters in diameter, backfilled with uncompacted crushed stone to a depth of 3 meters. The crushed stone is of the kind used as railroad ballast and used in lieu of conventional select fill to avoid the need for compaction as well as to determine if water accumulations inside the crater and between the crushed rock can be tolerated by the concrete slabs on the surface.

The purpose of the high speed concrete saw investigations is to determine maximum cutting speeds that can be achieved in different kinds of concrete or asphalt/concrete combinations. This investigation is an integral part of the ARRR process in that damaged concrete must be removed in such a manner as to leave squared, straight edges along the

undamaged runway portions (Figure 8). These straight edges are necessary to provide a smooth transition surface between the undamaged pavement and the concrete slabs, thereby avoiding any lifting or roll-up of aircraft.



FIGURE 8. PRECISION CUT CONCRETE TO 15 CM DEPTH.

High speed concrete cutting is feasible with heavy 45 to 50 HP diesel engines to provide the necessary force and specially designed diamond tipped steel cutting blades. To date, cutting speeds of 3.5 meters per minute at 15 cm depth of cut in 35-year-old, high-strength concrete have been achieved. Investigations programmed to take place in September 1982 will determine if speeds of 5 to 6 meters per minute are achievable at the same depth of cut. Greater depths of cut are not necessary since the concrete slabs have only a thickness of 14 cm. Should a runway surface have a greater thickness than 14 cm, then the cut portions can be broken away mechanically or explosively with shaped charges.

Developing a complete ARRR procedure with the use of concrete blocks is, of course, the ultimate goal. Testing of high speed sequences will take place during the November to December 1982 time frame so as to take advantage of the adverse European weather conditions. Included in this investigation will be the use of a newly designed wheeled steel beam system, called "screed beam," to be towed or pushed across a backfilled surface to scrape it smooth. This smooth sub-base is necessary to provide accurate alignment of the concrete elements. The beam is 16 meters long to permit surface screeding between 2 and 14 meters wide with one single pass. It possesses an adjustable vertical blade that permits leveling of the backfill material from 25 cm below and 10 cm above the undamaged pavement surface. This adjustable blade permits the use of this beam for other RRR methods.

The combination of revised procedures, new methods, new materials, and new prototype equipment is expected to provide us a means to perform ARRR of large damaged runway areas, of deep trenching damage to runways as well as single craters, and yet provide a flush surface repair that will support a greater variety of aircraft at all rolling speeds without subjecting landing gears to the kind of uplift/downroll experienced with aluminum matting. These procedures are less complicated and therefore will not require high troop training costs. Finally, these procedures provide for cost effective investments in that the concrete slabs can be used in peacetime for the construction of aircraft or vehicle parking ramps, taxiways, roadways, or sidewalks. In time of emergencies, these slabs can be lifted and carried quickly to emergency repair sites. The dual use of this material, peacetime in-use storage/wartime application, provides the basis for economic investments.

## VII. CONCLUSION

The use of pre-manufactured concrete elements (slabs) for aircraft taxi/parking surfaces is feasible. The use of high speed diamond tipped concrete saws as part of the ARRR techniques is equally feasible. A combination of these methodologies may result in ARRR technology which will result in greatly reduced horizontal and vertical dynamic forces exerted against aircraft wheel assemblies. Therefore, it is feasible to conduct further field investigations to determine the exact range of concrete slab uses in support of aircraft operations. As these repair methods may influence aircraft wheel assembly design considerations, aircraft industries may be interested in conducting field investigations of their own and suggest improvements to those currently ongoing at Headquarters, USAFE.

## EVALUATION OF THE PILOT PAPERS FROM THE SPRING 1981 SMP MEETING

ARNULF KRAUSS  
MESSERSCHMITT-BÜLKOW-BLOHM GMBH  
Unternehmensbereich Flugzeuge  
Postfach 801160  
D-8000 München 80, W-Germany

### 1. INTRODUCTION

Three papers were presented at the Spring 1981 SMP Meeting:

- [1] Minimum Operating Strip Selection Procedure
- [2] Proposed Specifications for International Interoperability on Repaired Bomb-Damaged Runways
- [3] Damage Control on German Airfields with Particular Regard to "Rapid Runway Repair".

References 1 and 2 are closely interrelated and are based on the same data and experience. [1] and [2] are therefore mostly treated together in the following.

[1] provides Minimum Operating Strip (MOS) selection procedures for use in post attack launch and recovery operations. The specific details and examples are given for an F-4 aircraft, yet the general procedures can be applied to MOS selection for any aircraft at any particular airfield. [2] supplements the ground roughness data from [1] and expands the scope to the problems to be solved in an environment where a nation managing an airfield is to accommodate other nations operating a variety of aircraft types.

[3] presents data on manpower and equipment for Rapid Runway Repair and describes two runway repair procedures developed and tested in Germany.

### 2. EVALUATION

#### 2.1 Runway Damage

Essentially there are two different types of damage, viz. regular craters and scabs (spalls), see Fig. 1. A scab may be caused by strafing, defective ordnance, explosion debris etc., and does not penetrate through the pavement. A crater (Fig. 2) penetrates through the pavement and consists of disturbed materials, fallback material, and ejecta covering upheaved pavement.

#### 2.2 Repair Methods

##### 2.2.1 Scab

Depending on the magnitude of certain parameters scabs will or will not have to be repaired. The following table shows unrepaired scab criteria for the F-4E from [2].

F-4E Unrepaired Scabs	
Maximum Depth	1 1/2 inches (3.8 cm)
Maximum Length Parallel to MOS centerline	2 feet (62 cm)
Maximum Slope of Scab Sides	25 %
Spacing Parallel to MOS centerline	No more than 2 scabs per 24 feet (7.3 meters)

All three papers assume that scabs needing repair will be repaired by a process employing fast-curing Silikal<sup>®</sup>. It is assumed that these repairs are completed before the crater repairs and have sufficient time to cure (30 minutes). There is, however, no hint how fresh repaired scabs will be protected from moving crater repair equipment.

### 2.2.2 Craters

There is a variety of crater repair methods. Great differences exist between the methods with respect to

- o the extent to which upheaved pavement is to be removed around the crater edge,
- o the material which forms the upper layer of the repair proper,
- o the type of cover or mat (if any) which is installed upon the repair.

References [1] and [2] deal with two types of crater repair, viz. "AM-2 Mat Repair" and "Crushed Stone Repair". Depending on the repair quality required (to be discussed later) both repair methods yield a choice to which extent upheaved pavement must be removed.

"AM-2 Mat Repair" (Fig. 3) means that an AM-2 mat is installed covering both upheaved pavement and compacted select fill of the crater. Due to the height of the AM-2 mat even a "perfect" repair cannot be flush with the original pavement.

"Crushed Stone Repair" means that the upper layer of the repair is formed from compacted crushed stone. Depending on the susceptibility to FOD (foreign object damage) of the aircraft to be operated an FOD cover is installed on the repair. Though a "perfect" Crushed Stone Repair could be flush with the original pavement surface, this case has not been treated in the Crushed Stone Repair Categories of Ref. [1].

Ref. [3] describes two types of runway repair procedures which were developed and tested with GAF, viz. the "Vacuum Concrete Procedure" and the "Variable Concrete Slab System (VP-1)".

The "Vacuum Concrete Procedure" in its first steps resembles closely the US "AM-2 Mat Repair" except that normally all upheaved pavement is cut off with especially designed concreté saws. After having filled up and compacted up to 20 cm ( $\approx 8$ ") below the upper edge of the runway surface there is a choice of completing the repair to an "AM-2 Mat Repair" or of applying Vacuum Concrete.

The problem of applying freshly cast concrete in RRR is that for orderly mixing and casting concrete a much higher water/cement factor (between .5 and .7) is required than the cement actually needs to cure (approximately .3). Evaporation of excess water takes up to 28 days. This problem is overcome by vacuum treatment of the concrete, i.e. reduction of the water/cement factor, by applying commercially available equipment (vacuum unit, filter mats, vacuum dewatering mats and suction hoses). Immediately following the vacuum treatment the concrete may be walked on and is trafficable for light vehicles. In order to operate aircraft an AM-2 mat is installed on the repair surface. This AM-2 mat can be removed after 12 to 24 hours, when vacuum treated concrete exhibits about the same strength as normal concrete after 5 to 7 days (see Fig. 4).

The "Variable Concrete Slab System (VP-1)" uses prefabricated concrete slabs to form a surface which is flush with the undamaged pavement and has immediate full load bearing capacity. The upheaved pavement at the crater edge must be cut off to form straight edges which fit the grating of the slabs. Any settlements which could occur after extended use of the repair can be easily corrected by temporarily removing the slab affected and fixing the foundation. Ref. [3] states that the price per unit area of prefab slab is only about 15 percent of that of AM-2 mats.

### 2.3 Repair Quality

References [1] and [2] describe the quality of the "AM-2 Mat Repair" and of the "Crushed Stone Repair". The quality is described by essentially 6 parameters which are characteristic for the final form of the repaired surface (Fig. 5). Numerical values of these parameters are combined to form five repair categories with decreasing quality from "A" to "E". Ref. [1] shows some differences in numerical values of the parameters between the same quality categories for "AM-2 Mat Repair" and "Crushed Stone Repair", while Ref. [2] shows the "Crushed Stone Repair Categories" of Ref. [1] as unified "F-4E Repair Quality Categories". The latter are reproduced here as Tables 1 and 2.

TABLE 1. F-4E REPAIR QUALITY CATEGORIES

	A	B	C	D	E
Maximum Upheaval, inches (cm)	1.5 (4)	2.5 (6)	2.5 (6)	3.0 (8)	4.5 (11)
Sag (See Table 2)					
Maximum Length of Crater, feet (meter)	N/A	N/A	70 (20)	70 (20)	N/A
Maximum Change in Slope (percent)	3	3	3	3	3
Special Requirements	1	2	2,3	1,3	1

Special Requirements

1. Any spacing except that if repairs are closer than 100 feet "D" and "E" repairs must be upgraded, "D" to "A" and "E" to "C" repairs.
2. Must meet spacing criteria, or upgrade to "A" category.
3. Maximum length of a single "C" or "D" repair is 70 feet.  
If a single repair exceeds 70 feet upgrade to a "B" repair.

TABLE 2. F-4E REPAIR SAG CRITERIA

	Repair Category				
	A	B	C	D	E
Peak Sag Inches (cm)	1.0 (2.5)	1.0 (2.5)	2.5 (6.5)	2.5 (6.5)	4.0 (10.0)
Nominal Allowable Sag, Inches (cm)	0.5 (1.5)	0.5 (1.5)	2.0 (5.0)	2.0 (5.0)	3.5 (9.0)
Maximum Span of Sag Below Nominal Sag, Feet (m)	5 (1.5)	5 (1.5)	10 (3.0)	10 (3.0)	20 (6.0)

These tables are very useful for the aircraft designer and for the dynamicist, because they yield a realistic picture of the obstacles which their airplanes will have to surmount on repaired runways and taxiways. However, in the evaluator's opinion there should be a clearcut separation between the form parameters proper of the repair and the dynamic properties of the F-4E which latter make themselves felt in "Maximum Length of Crater" and in "Special Requirements" of Table 1.

Unfortunately no list of descriptors, much less repair quality categories, was presented for other repair methods. Yet there is a need for further information e.g. about step heights to be expected with different repair methods as for instance the "VP-1". Besides a repair employing UK Class 60 mats would also not fit into the repair categories of Refs. [1] and [2], because the ramp of this mat is much shorter than that of the AM-2 mat and has a much steeper slope. These examples show that there is still a long way to a unified repair categorization within NATO.

#### 2.4 Repair Spacing

Any single repair on a runway excites not only the structural modes of the airplane, but also rigid body modes (mainly heave and pitch). Therefore the conditions with respect to undercarriage strut and tyre compression at a second repair can be quite different (less as well as more severe) from those at the first repair. This holds true for any other consecutive repair.

Critical distances between consecutive repairs are dependent on aircraft rolling speed. On the other hand increasing speed, especially after nose wheel lift-off, lessens the load to be carried by the undercarriage.

These influences were evaluated and combined into repair spacing criteria for the F-4E as shown in Fig. 6 (from [2]). Fig. 6 can be transformed into the spacing template of Fig. 7 (from [1]) which is proposed as one of several graphical aids for MOS selection in [1].

Ref. [2] in a thorough description of the respective responsibilities of aircraft operators and airfield managers in an international interoperations environment states that amongst others repair quality and spacing required must be specified to the airfield manager by the aircraft operators.

However, in the light of the very stringent requirements for the F-4E the evaluator foresees that quality and spacing criteria will be needed for a choice of masses for every airplane type and for a variety or even a mix of repair types. Very likely this will result in a MOS selection task to the airfield manager which is not to be performed "by hand" anymore or will result in non-optimal effectiveness of operations.

### 3. CONCLUSIONS AND RECOMMENDATIONS

There exists a need for repair quality parameter definitions for all repair procedures in NATO use.

The repair quality categories approach of Refs. [1] and [2] appears promising. However, efforts should be made to remove all aircraft type related data from category descriptions.

Repair time is the only measure which can be applied to all repair methods regardless of their typical parameters. Therefore it is proposed here to develop a unified repair time index for all interesting repair methods. Repair quality categories could then be formed by giving numerical values for the repair-typical parameters at equal repair time index values.

Quantitative information about repair time vs repair quality is also needed by aircraft operators and engineers. In my opinion this is the only way to prepare optimum decisions on aircraft configurations to be operated and on possible permanent or temporary aircraft adaptation to the damaged and repaired runway environment.

In order to enhance international interoperability it appears necessary to simplify MOS selection criteria. Repair spacing is a complicating factor in MOS selection, because it could prove virtually impossible for the airfield manager to merge the different spacing criteria thus that the needs of the different operators can be fairly met. Probably, a good way to get over those difficulties could be the following: Once that the repair categories for a certain repair method are defined, the aircraft operator defines not only one or more "favorite" aircraft configurations but also that repair quality distribution along the MOS which each configuration can take without restrictions of repair length and spacing. After on this basis having selected a MOS which promises maximum operational effectivity within a specified total time to operability, the airfield manager can check whether and where he can perform one or more lower quality repairs, yet still meeting the combined spacing criteria of his aircraft mix.

Superior flight performance is void when you cannot get it airborne. Therefore AGARD should continue, even intensify, their effort to gain and spread experience on runway damage, runway repair, and airplane ground performance on damaged and repaired runways.

### REFERENCES:

- [1] Strickland, William S., Caldwell, Lapsley R.:  
Minimum Operating Strip Selection Procedure
- [2] Caldwell, Lapsley R., Gerardi, Anthony G.:  
Proposed Specifications for International Interoperability  
on Repaired Bomb-Damaged Runways
- [3] Kempf, D.:  
Damage Control on German Airfields with Particular Regard  
to "Rapid Runway Repair".

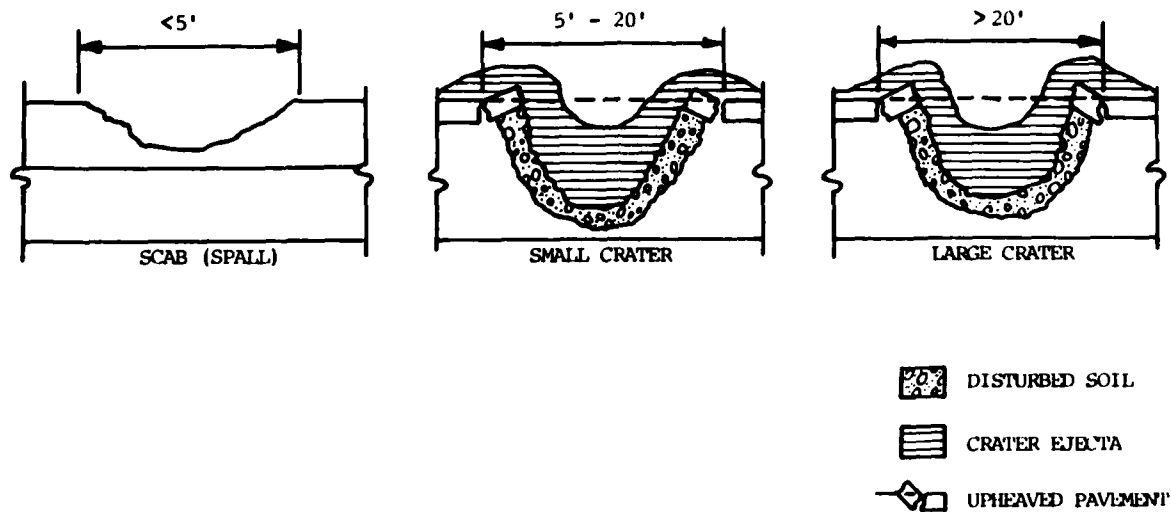


Fig. 1 Pavement Damage Categories

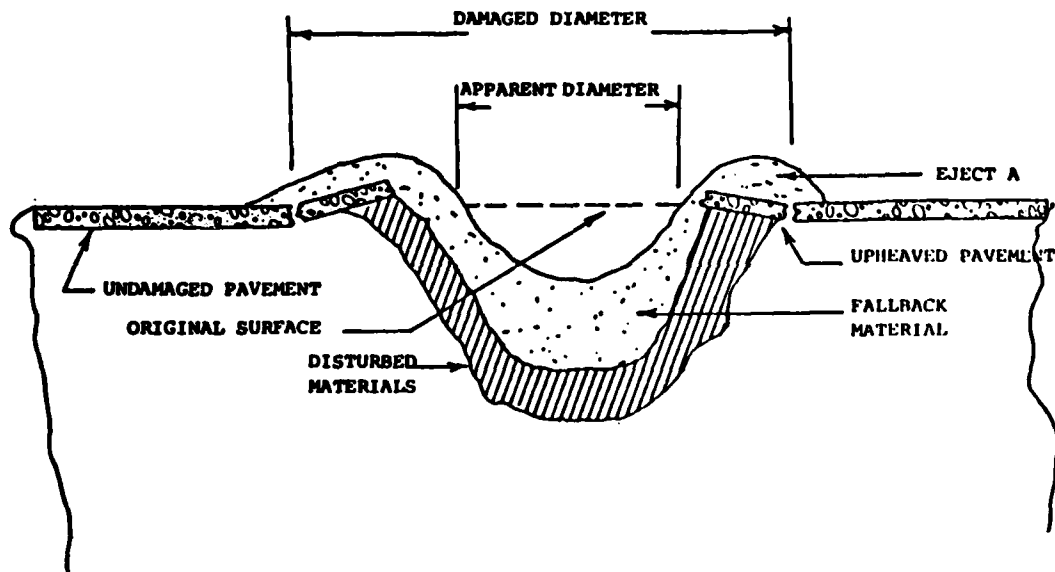


Figure 2 Apparent Crater Nomenclature

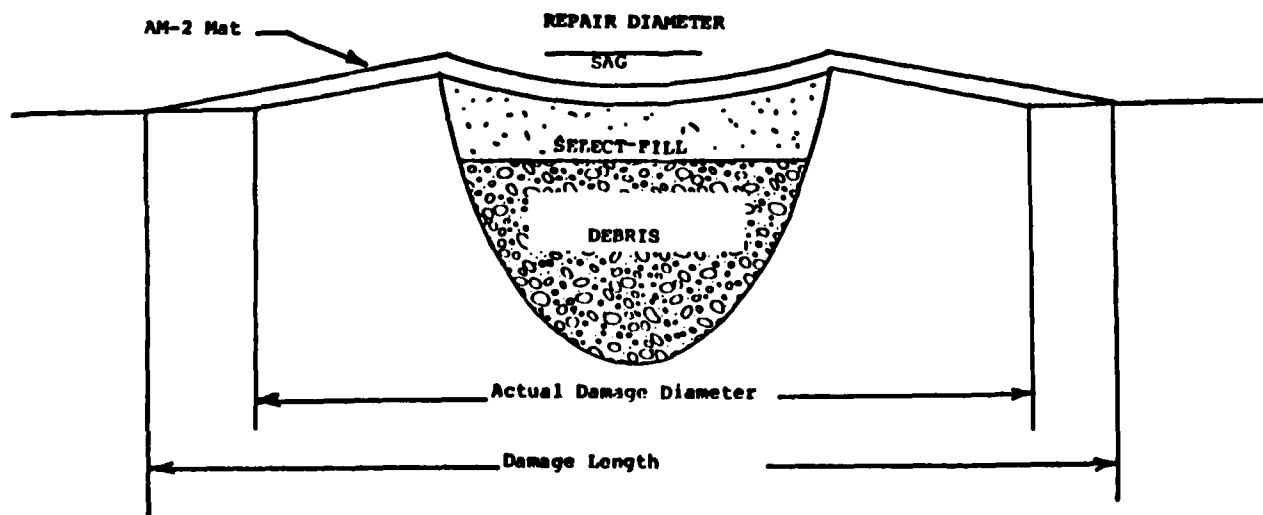


Figure 3 Repair using AM-2 Mat

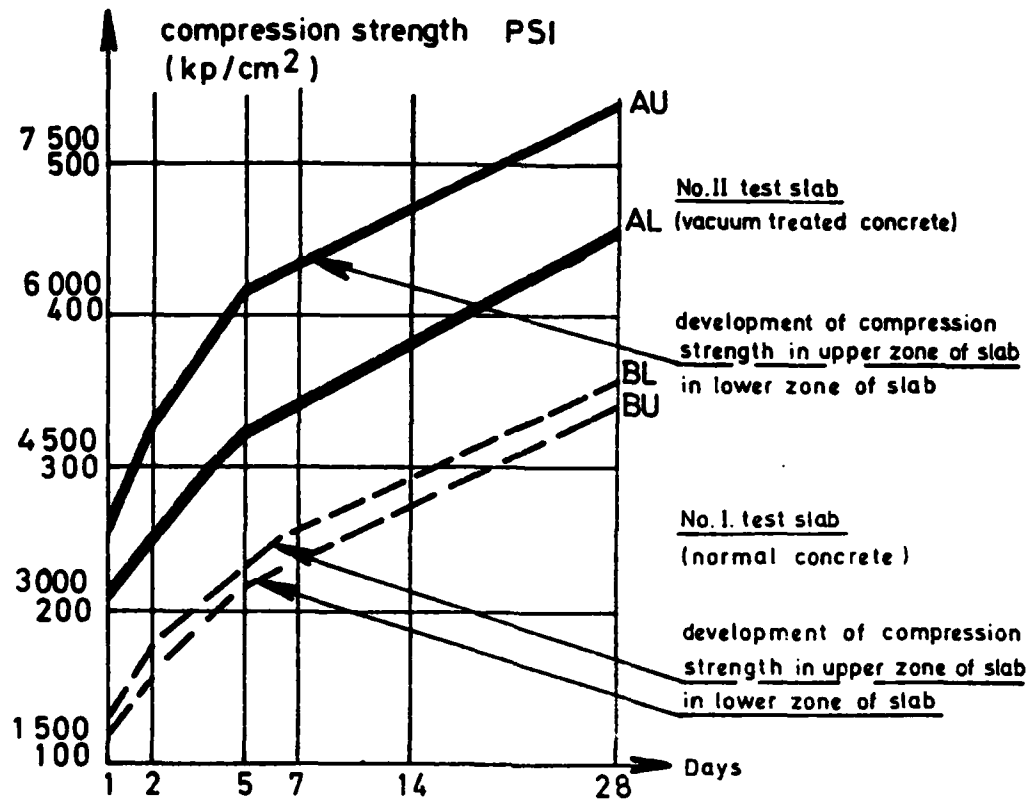


Fig. 4 Development of Compression Strength in the Upper and Lower Zone of the Test Slabs

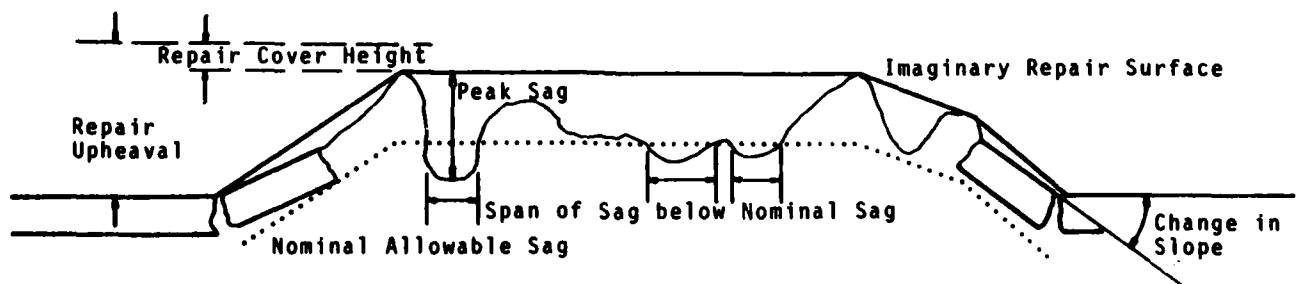


Fig. 5 Repair Parameters



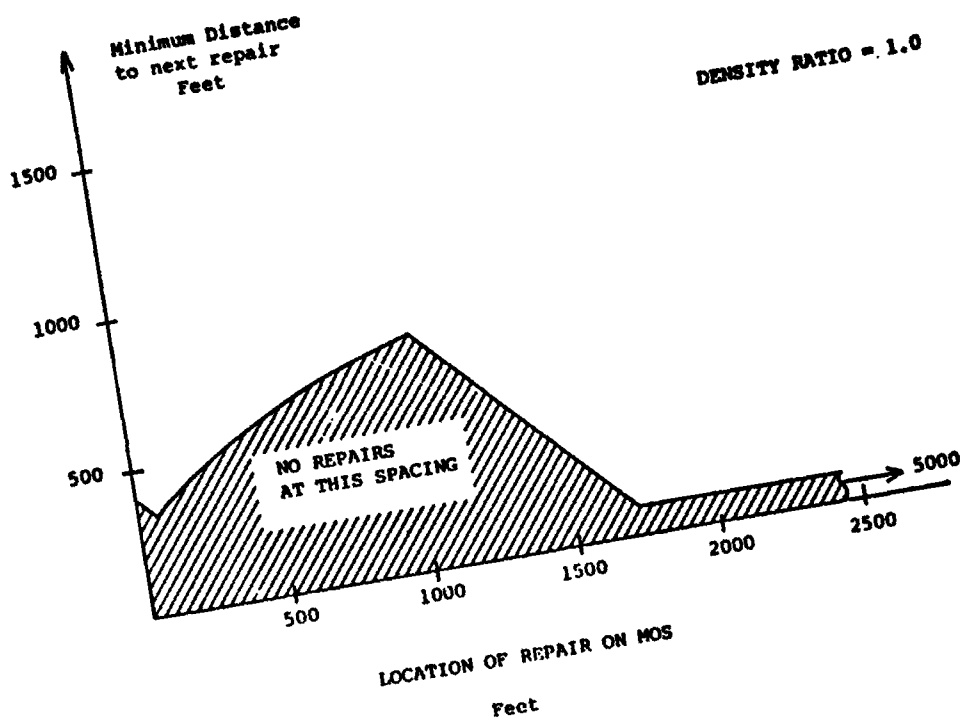


Figure 6 F-4E MOS Spacing

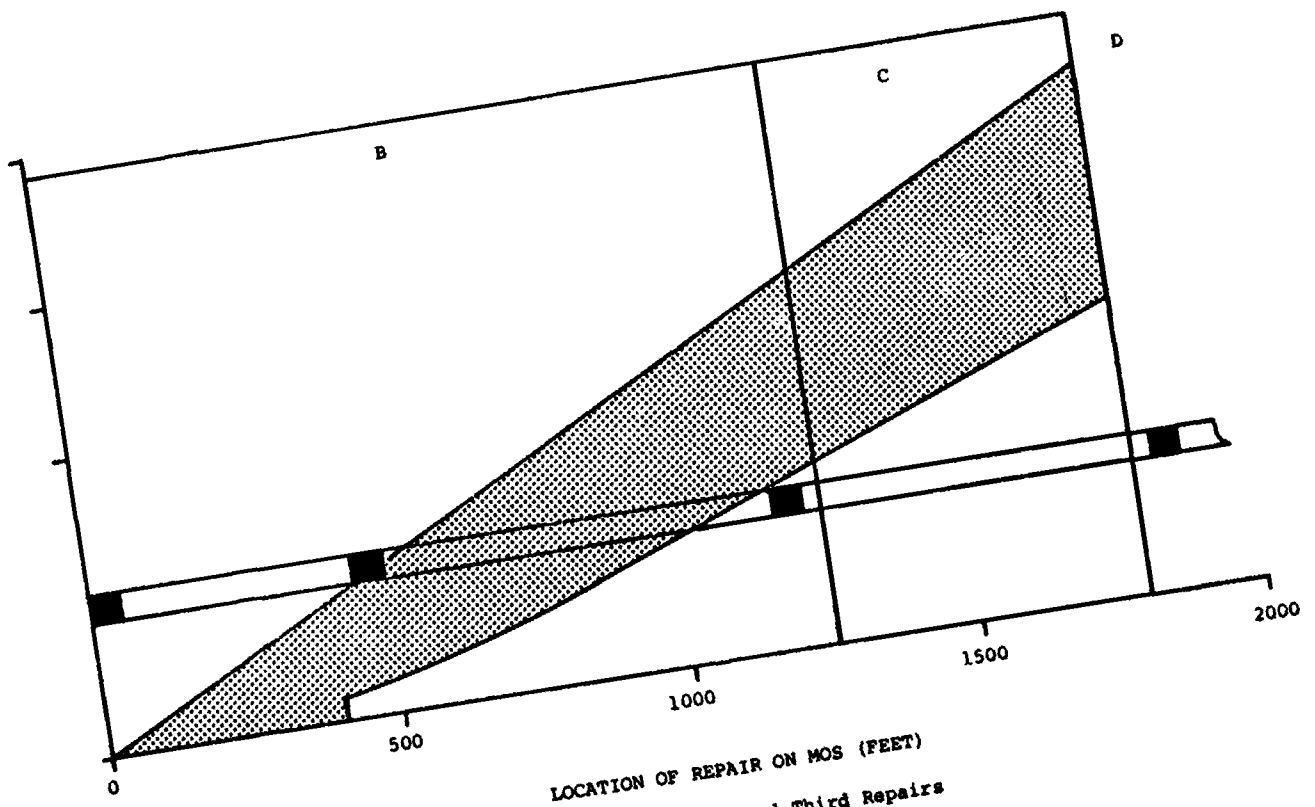
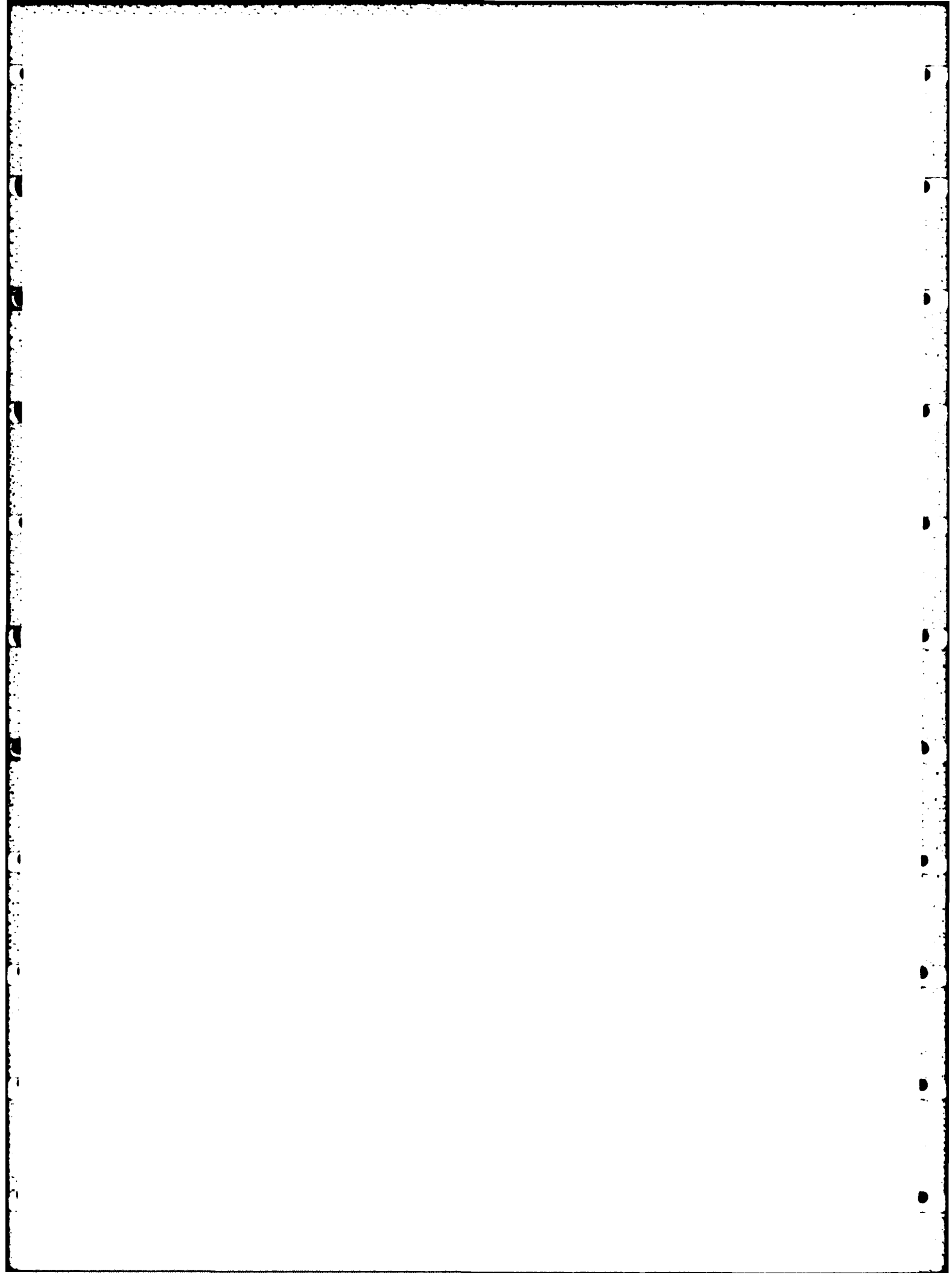


Figure 7 Second and Third Repairs



## APPLICATION OF SEMI-RIGID PAVEMENTS IN RAPID RUNWAY REPAIR

by

A.F. Tovar de Lemos

Associate Professor/Head Thermomechanics Section  
 Instituto Superior Técnico/Centro de Mecânica e Engenharia Estruturais (CMEST)  
 1096 Lisboa Codex  
 Portugal

## SUMMARY

A general description of the so called semi-rigid pavements is given, when compared with the traditional types: rigid pavements made of cement concrete and flexible pavements made of bituminous concrete. Some information about the design and process of application is furnished, as far as aeronautic pavements are concerned.

The Portuguese experience on the application of semi-rigid pavements in Europe and in Africa is described. It is emphasized that normally in Portugal this type of pavement has been used in new runways, chiefly thresholds, but there is also some experience about pavement repairs, though not due to bombs.

Finally a discussion of the merits and disadvantages of the semi-rigid type pavements against the traditional ones is made.

## INTRODUCTION

Damage repair in airfields is a routine activity in peace time. However Airfield Damage Repair (ADR) expresses in military language the need of repairing the destroyed or damaged areas in an airfield after an attack. The operational capability of the airfield and of the flying combat units imposes that the repair work is made as fast as possible. That is the reason why tactically ADR means all the techniques which should be used to obtain the rapid repair of the runways and all paved operational areas. These techniques define the procedures of the so-called Rapid Runway Repair (RRR).

It is evident that not all the repairing procedures are adequate for RRR. This is normally the case of the cement concrete rigid pavements, due to the relatively long time of setting, unless that very special techniques are used. That is why bituminous concrete flexible pavements would then be preferred. However, these last ones are unsuitable in given sites and circumstances, such the areas like thresholds and turning cycles where it may there be the action of heat and blast or the spillage of oil or fuel. In all these cases, concrete pavements exhibit a very good behaviour.

The so called semi-rigid pavements<sup>(\*)</sup> exhibit the advantages of both the rigid and flexible ones and so they may perhaps be used in RRR. Although the Portuguese experience about this type of pavement has been only in circumstances where bomb damage was not involved, it was considered interesting to give in this meeting the description of the procedure, so that its use in RRR may be explored, weighing conveniently its merits and disadvantages in this case. Other two characteristics to be considered under very low temperatures are the resistance to anti-gel products (for instance the isopropyl + glycol mixture) and the behaviour in the frost-defrost cycles.

## 1. SYSTEM DESCRIPTION

Briefly speaking, semi-rigid pavements are characterized by a surfacing process combining the flexible characteristics of bituminous materials with the rigid properties of cement concrete. In Portugal, either in Europe or in Africa (Angola, Moçambique, Guiné, Cabo-Verde) the Company INTERAL applied some years ago a special type of semi-rigid treatment called SALVIACIM, a Registered Trade Mark of Société SALVIAM - Paris, whose first applications in airfields started in France in 1955, in the military base of Cognac-Chateaubriand.

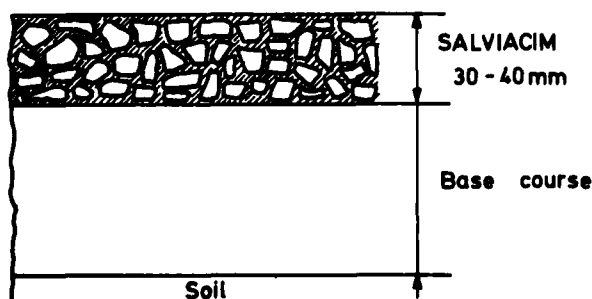


FIG. 1

The product is laid in two operations and the process comprises a bituminous surface, called the support coat (thickness of 30-40 mm) followed by the application of a special grout. The support coat is applied on the base course, whose thickness depends on the specifications, nature of soil and applied loads (Fig.1).

(\*) We are using this term, though it may have some other meanings, as for instance the soil-cement. This is not the case, as it will be described.

The normal flexible pavements have always a binder (tar or bitumen) whose plasticity makes possible that they exhibit strains without cracking. However they don't carry usual metal tired vehicles, heavy static loads, punching, impacts, etc. Besides that they are not completely impermeable.

On the other hand, rigid pavements use an hydraulic binder and have a hard and impermeable surface. But under the combined action of the underlying layers and of the successive dilatations and shrinkage of the hydraulic binder it is well known that these pavements tend to present cracks, sooner or later. Besides that, the presence of construction joints between the slabs is always unsuitable.

The aim of the Salviacim is to make penetrate a special cold mixture of cement, mineral filler and chemical additives at the bituminous surface layer. This is how may be obtained some stiffness in the surface layer for the thickness of 1 or 2 cm, though maintaining the flexibility of the bituminous pavement. It may be said that the essential feature of the Salviacim mixture is to produce artificial aggregates (Fig.2).

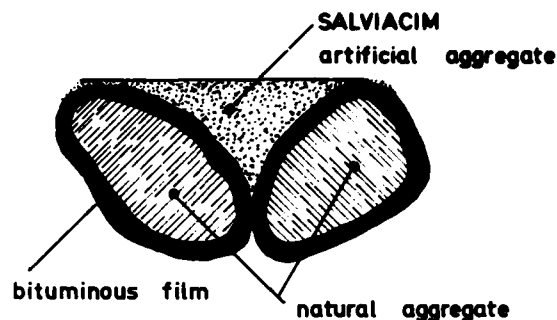


FIG. 2

The binder films which combine natural and artificial aggregates act as plastic joints to assure the flexibility of the pavement.

It must be emphasized that this process is not intended to confer any additional bearing capacity to the pavement and so this one must be designed accordingly to the usual standard specifications, as far as the thickness of sub-base, base and surfacing is concerned. Of course this procedure disregards any additional contribution assigned by the stiffness of the support coat with Salviacim.

## 2. PROCESS OF APPLICATION

A layer of bituminous material (support coat) produced from a selected bitumen binder and a suitable carefully graded aggregate to produce a controlled percentage of voids is laid to a thickness usually between 30 and 40 mm. A moderate compaction is applied, we mean a compaction to be carried out just till the moment the roller does not leave any marks. Then the support coat temperature may go down till it becomes completely cold. Afterwards, even a few days later, the voids are filled with the grout. Application of brush or other spreading devices together with a vibrating roller if necessary ensures a complete penetration. That is why a previous heavy rolling may not be used. Of course voids must be perfectly clean at the moment of spreading, in particular exempt of dust.

The grout, which contains a special binding agent, sets in the voids producing then a synthetic aggregate. At the same time a solid surface is formed resisting to damage. The bitumen coating of aggregates keeps the basic properties of flexibility while the grout imparts rigidity when set.

The support coat is made and applied as any other black top. The grout is prepared with any concrete or mortar mixer or mixer transporter. The penetration of the grout is achieved normally by gravity or by any mechanical spreading device or manual brushing followed by a small vibratory roller, if necessary.

Salviacim can be laid as quickly as a black top and it does not need expansion or construction joints. Its surface is easy to maintain and quick to repair in the event of any damage occurring in the pavement.

## 3. THE PORTUGUESE EXPERIENCE

The Portuguese experience on application of Salviacim started in civilian airports in 1959 - Lisboa, Porto, Faro, Sal-Cabo Verde, Luanda and Beira. However we think that it will be more interesting for the purposes of this meeting to have a description of some military typical applications. Three examples will be referred.

The first example relates to the surfacing of the ends of a runway in the Air Force

Academy airfield of Sintra near Lisbon, in 1962. It became necessary to apply this procedure in that airfield when the training T-37 aircraft was introduced there since jets became to be intensively used, with consequent heating and blasting on the pavement.

As it was mentioned above, the aggregates to be used in the base course must be conveniently chosen. In Appendix A, it may be found the grading curve we have used. In fact two curves are shown (A and B) both acceptable. Actually it will be necessary to make a previous study for each site accordingly to the local conditions and any curve satisfying standard specifications given by the producers may be used.

On the other hand, the composition of the grout depends on the weather conditions during application. In Europe, a typical composition like the following may be used, with the highest rate of water in winter:

SALVIACIM MIXTURE (parts in weight)

Water	55-60
Product PROSALVIA 1	6
Filler	25
Sand (passing 0,5 mm)	15
Portland cement	60
Product PROSALVIA 2	2

For the preparation of the mixture it is essential that the components are introduced in the mixer accordingly to the order above described. It must be explained that if Salviacim is laid under low temperature conditions, some precautions about transportation and storing of the mixture must be taken.

The other example relates to the repair of an apron in the military airfield of Montijo, which is a NATO military base. In this case the concrete pavement was very damaged due to an insufficient previous compaction of the foundation soil. It was necessary to apply a bituminous pavement and again Salviacim was used.

The last example we mention of the Portuguese experience in this field is the application of Salviacim in 1972 in the airfield of Serpa Pinto (nowadays Menongue) - Angola. It is impossible to give now the composition of the mixture used there, but we may say that it was rather different from those in Europe, even in Summer.

It is interesting to compare this last application with another one of Salviacim which was made for use in quite different weather conditions. We mean the runway of the Copenhagen airfield (1) where Salviacim was used in 1972 in the most part of the runway (length 3600 m), half of the surface of taxiways, and aprons. It is interesting to point out that the pilots since the beginning of the new airfield design had said that the runway should be light-coloured which is the normal aspect of the cement concrete. This claim was met by Salviacim.

#### 4. EVALUATION

The use in Rapid Runway Repair of the semi-rigid pavements like Salviacim has of course merits and disadvantages, which must be weighed by the RRR experts, comparing them with other procedures like AM-2 topping, vacuum treated concrete, precast concrete (VP-1), etc. or combined with them.

As a result of the above considerations, we think that the essential merits of the described semi-rigid pavements are:

- a) A high resistance to heat, blast and spillage of oil or fuel and to the impact loads due to take-off and landing of heavy and rapid aircrafts. So these pavements offer a special suitability for VTOL and STOL needs.
- b) A practical process of repairing damaged cement concrete pavements, but without construction or dilatation joints, which is favourable to landing gears and instruments of control in the aircrafts.
- c) No dust, which is usually the case of the concrete slabs.
- d) A great impermeability of the pavement, preventing ingress of water in soil.
- e) A rapid time of application. This is a quality to be perhaps improved for the needs of RRR.
- f) Pavement elasticity which allows the adaptability of the pavement to a slight movement of the foundation layers, without crackings.
- g) No special training and equipment or application problems like in some other procedures (for instance the polymer concrete, toxic and aggressive for the eyes).
- h) A much more antiskid surface than the concrete ones.

However, application of treatments like Salviacim exhibits some disadvantages like the following ones:

- a) Dependence on the availability of resources about products PROSALVIA in mobilization environment.
- b) Influence of the time of setting on the operational readiness (walking or rolling in 1 or 2 days, braking in 4 or 5 days, turning in 10 or 15 days, final setting in 28 days). To solve this problem, perhaps the process may be combined with the AM-2.
- c) Probably the problem of the cost, when compared with concrete pavements.

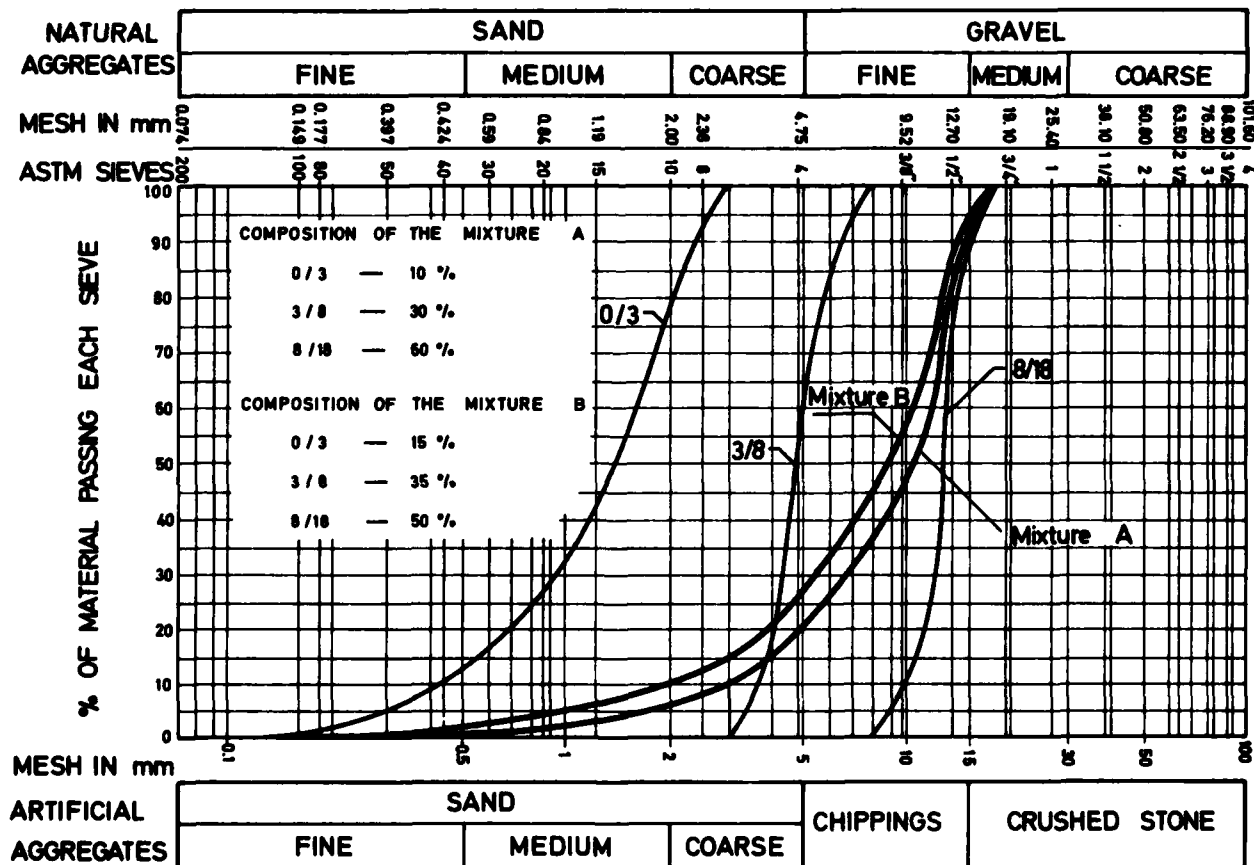
#### ACKNOWLEDGEMENTS

We should acknowledge the Portuguese Air Force authorities for allowance to refer the Portuguese experience on the application of Salviacim in military airfields which was partly assisted by the author and the INTERAL Company for the technical support during the preparation of this paper

#### REFERENCES

- (1) HVIDBERG, E. ; POULSEN, O. - Une nouvelle piste à l'Aéroport de Copenhague - Revue Générale des Routes et des Aérodrômes, n° 473, Fev. 1972, pgs. 78-84.

### APPENDIX A - GRADING CURVE FOR THE SUPPORT COAT



# THE REPAIRED RUNWAY CLEARANCE ENVIRONMENT

Colin Brain  
Aeroplane and Armament Experimental Establishment  
Procurement Executive, Ministry of Defence  
Boscombe Down  
Salisbury  
Wiltshire SP4 0JF

## SUMMARY

This paper looks at aspects of the repaired runway operational environment which influence considerations of aircraft dynamic response. These aspects include: the roughness of repaired and unrepaired operating surfaces; operational factors which give rise to variability of aircraft response and pilot techniques which influence the loads on undercarriages. The paper also looks at how aircraft can be cleared to operate from repaired runways; the safety margins required for this type of operation and the need to transfer data between NATO nations on the roughness tolerance of individual aircraft types if there is to be genuine inter-operability.

## 1 INTRODUCTION

For the past 7 years we at A&AEE have been involved with testing aircraft operation on repaired, damaged and natural runway surfaces. The aim of this programme of work is to define the operational penalties, for each aircraft type, which are attendant on the use of these sub-standard runways and the corresponding techniques which are required to minimise these penalties. In common with most other agencies in this field, these trials programmes centre on the use of digital computer simulation models. The tests themselves then serve principally to validate the simulations, and are planned to progressively extend the neighbourhood of validity of the simulator to cover the whole of the required operating envelope. This approach is necessary since aircraft traditionally have been designed to operate from smooth, hard surfaces and in most cases obtaining a realistic operating envelope from damaged, natural or repaired surfaces involves testing and clearing aircraft right to their limits. This process must be carried out cautiously because of the obvious risks involved, but there is no room for the use of blanket safety-factors to conveniently cover unknowns, if the results are to be of more than academic interest. Hopefully at the end of the test and simulation development phase, for each aircraft type, the differences between the tests and the results from the simulation model, for the same input conditions, are within acceptable limits. The validated model is then available for use in calculating the capabilities of the aircraft: this paper looks at some of the considerations affecting the way these calculations are undertaken to produce the information required by those who might have to repair or use bomb damaged runways. In particular the nature of the inputs to the aircraft system; the influence of variability on the response of this system; the parameters which govern the acceptability of the resultant response and the problems of conveying the output of the calculations, in the most useful form to the people who might need them will be discussed in order. Any views expressed are those of the author and do not necessarily represent those of the Procurement Executive, Ministry of Defence. All items quoted are from unpublished MOD(PE) data.

## 2 INPUTS

The aircraft traversing a repaired runway will respond to time-varying undercarriage forces, aerodynamic forces and propulsive forces. The engineer repairing the runway is however concerned with the spacial distribution of features; particularly in choosing the optimum minimum operating strip to repair out of all the damaged pavement areas. For him the strip is then characterised by crater size and distribution, which in turn become repair mat lengths, repair mat spacing and crater fill profiles under the mats. Obviously none of these items can be known in advance, hence information must be provided to aid in the execution of the repairs. This for the United Kingdom takes the form of setting standards for the quality of the crater repair profile, checking this against the quality achieved during realistic exercises and publishing guidance on the acceptable spacing of repairs covered by various lengths of mat. Figure 1 shows a comparison between some achieved crater fill profiles and the standard set in terms of peak fill height. For various reasons this figure overestimates the likely deviations from the standard, but it serves to illustrate the wide spread of achieved profiles which could well be encountered. This problem is fairly widely acknowledged and efforts are in hand to improve the situation. What is not so well appreciated however, is the influence that the basic runway profile has on the response due to repair mats. Figure 2 illustrates the calculated spacing envelopes of a pair of mats to give a specified limit load for one aircraft type. The calculations were carried out for the mats positioned on a flat profile and then for 2 arbitrarily chosen positions on the Boscombe Down runway 35. Although this is a good quality runway surface it can be seen that it makes a considerable difference to the spacings which can be allowed.

Surface roughness effects are naturally apparent over the whole range of ground speeds, but the aerodynamic effects are normally confined to the higher speed ranges, say above half the take-off or landing speeds. However, since this speed regime accounts for 75% of the landing or take-off distance, they are still very important. The main sources of variation here are wind effects and pilot inputs. Although the former is perhaps less important, it is worth noting that at 55 knots the difference between a 5 knot tailwind and a 15 knot headwind amounts to a doubling of the aerodynamic forces, and a 15 knot crosswind can change the main undercarriage static loads by  $\pm 20\%$  at high speeds. Figure 3 illustrates the measured effect that pilot inputs can have on the critical loads caused by repair mat crossings. In this case the 2 runs illustrated were under almost identical conditions except for the pilot elevator input and a light wheel braking input. The enormous difference between the 2 curves illustrates the importance that developing the correct pilot technique can have on operation over repair mats, but it is vital to ensure that the techniques assumed in calculations are communicated to, and are acceptable to the pilots, since there are often excellent reasons why they might choose quite the opposite philosophy. It must also be remembered that any recommendations of pilot technique are interpreted subjectively. For instance, Figure 4 shows the result of a test to determine how 5 pilots interpreted 'light' wheel braking, during measured decelerations with and without reverse thrust compared with the values achieved by one pilot on different occasions. For this test the pilots were briefed that 'for real' excessive braking would lead to nose undercarriage failure and insufficient braking would lead to the aircraft over-running the repaired minimum operating strip into an unrepaired crater!

This introduces the other side of input variability which is due to aircraft speed. Earlier it was indicated that the aircraft response is time dependent, hence the response to a given spacial profile will be dependent on the aircraft's achieved speed at any distance. The variables affecting an aircraft's take-off performance are well documented, but it is perhaps worth pointing out that a variation of  $15^{\circ}\text{C}$  in temperature and 15 knots in headwind plus engine tolerances etc can give a 10% change in speed at a given distance even if aircraft weight, airfield altitude, and runway slope are all kept constant. Speed variation at a given point on a landing run however is likely to be considerably greater than this, since it is dependent on touchdown speed, touchdown position and deceleration after touchdown. The last point has already been discussed, but the accuracy of the first 2 will also be affected by the use of minimum operating strips instead of normal runways, where the laterally and longitudinally displaced thresholds, and possible lack of visual approach indication will degrade pilot abilities. Perhaps the most relevant data here is that from 74 measured landings carried out on a 1000 metre long aluminium strip at a dispersed site, which gave a spread of 240 metres between extreme touchdown points.

### 3 SYSTEM RESPONSE

Compared with the list of unknowns existing in the inputs, it might be thought that the response of the aircraft system is relatively well defined. Unfortunately this does not appear to be the case. Of the aircraft we have tested or have been associated with the testing, none of the undercarriages have behaved entirely as the designers intended and rarely if ever have the correct oleo charging pressures been maintained. Notably we believe we have encountered: mild detonation of the air/oil mixture, gas solution in the oil, damping degradation due to leakage past the damping piston, due to air bubbles, due to oil compressibility and due to cavitation, and excessive friction due to structural deformation.

In terms of system response, the most important parameter is probably undercarriage stiffness. This is split into oleo stiffness and tyre stiffness. Apart from the problem of the gas dissolving in the oil, which appears to be exhibited in varying degrees by all undercarriages where there is no physical separation between the two, the main sources of variability in oleo stiffness are due to charging pressure variation and temperature effects. In order to establish the magnitude of the charging pressure problem, a check was carried out along a flight line of 32 aircraft; the measured pressures and extensions from this survey are shown in Figure 5, compared with specified limits for the aircraft. Looking at this it is easy to say that the standards of servicing should be improved, but in practice under ideal conditions, we have found it surprisingly difficult to maintain anything like the correct charging pressures and there seems little hope that even if peace-time standard were improved, that under war-time conditions things would be better.

In terms of tyre stiffness the most important feature is definitely temperature. Here variations can be due to ambient temperature, tyre heating due to rolling flexure, and heat transferred from wheel brakes or from aerodynamic heating in the undercarriage bays. For the kind of operation which would be anticipated from repaired runways, temperature induced pressure rises of 30 to 40% above nominal might be typical and this will give rise to a similar increase in tyre stiffness. Tyre stiffness is also dependent on the rate of loading and in some tyre types only, appears to be dependent on tyre rotational speed. Measured load deflection characteristics at typical rates of loading for the same tyre at 2 different forward speeds are shown in Figure 6.

Figure 7 shows the measured degradation in damping characteristics of one shock absorber with repeated operations. This is thought to be due to aeration of the oil and amounts to something like a 95% drop in damping. This is the worst example encountered due to this cause, but in another leg the permitted range of tolerances allow a 3:1 variation in the damping coefficient.



#### 4 RESPONSE LIMITATIONS

There are a number of different levels against which the results of excessive aircraft response may be measured, ranging from the inability of the aircraft to fulfil its complete mission, to the loss of the aircraft, the personnel and equipment on-board and temporary blockage of the minimum operating strip. However, there are no absolute values which can be used here. The mechanical integrity of systems, such as inertial navigation equipment, vary between individual aircraft, structural strength will vary due to fatigue and battle damage effects and pilot tolerance to the vibration levels will vary between individuals. Whilst loss of mission effectiveness may occur due to system failures or loss of external stores, aircraft loss is likely to be due to structural failure or loss of control by the pilot. These are probably best categorised by mean levels, the exceedance of which will cause either sufficient deformation or sufficient aircraft response that there is a 50% probability of aircraft loss. However, these levels of response are only usable if the undercarriage units continue functioning. Since the primary cause of the loading is deflection of the undercarriage due to the combined effects of surface profile and aircraft response, load levels become meaningless if the unit stiffness becomes very high following tyre and shock absorber bottoming. From this comes the concept of maximum usable load or response, which is dependent on the functional limits of the undercarriage as well as the points mentioned above. Unfortunately these undercarriage limits are dependent on many of the factors discussed above. One point which may be quite critical is the damage done to an oleo if it is allowed to bottom; if this is serious then this may become a limitation in its own right. Figure 8 shows the effect of temperature on the load deflection curve for an undercarriage. If this were combined with the kind of charging pressure variations shown in Figure 5 it can be appreciated that there would be vast spread in the load at which bottoming could occur. An example of the nominal overall load-deflection curve for a shock absorber/tyre combination is shown in Figure 9. It can be seen that even though in this case the tyre pressure had been increased to improve the capability of the unit, it still bottomed completely some way below the ultimate strength of the unit and little residual travel remained at the nominal limit strength.

A failure will occur if the load or response level reached by an aircraft exceeds the structural or functional capability of that particular sample, or the vibration acceleration capability of that particular pilot. Earlier the concept of maximum usable load/response was introduced as being the mean value for the type at which such failures will occur. If then simulation model calculations are carried out using mean data for the crater fill profiles, a flat runway surface, nominal speeds and mean component characteristics, it is possible to arrive at mean predicted simulation maxima for a particular aircraft configuration/repair mat combination. Use of information derived from the model validation against test results then allows this to be transferred to mean predicted maxima. Should these values be used directly in conjunction with the maximum usable load or response to define 'allowable' conditions there will be about a 50% failure probability. As the allowable mean predicted maxima are reduced below the maximum usable load, the probability of failure will progressively reduce, as the overlap between the high load and low strength envelopes diminishes. If one were fortunate enough to know the shape and variance of the load and strength distributions picking a suitable factor would merely depend on the choice of the desired failure probability.

In practice I see little prospect of knowing the load distribution, the strength distribution or the acceptable probability of failure. The only way out of this situation is, I believe, to carry out the calculations using 2 sets of limits for the mean predicted maxima, based on relatively arbitrarily derived factors and notionally associated with high risk and low risk operation. Although I never anticipate being in a position to define what the risks actually are, which are associated with the selected levels, it will at least allow the risk producing elements to be clearly identified and will mean that the complex trade-offs can be made 'there and then' rather than 'here and now'.

#### 5 OUTPUT FROM THE CALCULATIONS

The digital simulation model has the capability to produce a vast amount of data for each aircraft type. The engineer who needs the data as a basis for decisions affecting many aircraft types has a much lower information handling capability, even given computer assistance, so considerable simplifications must be made. For any aircraft type there are potential trade-offs, for take-off runs, between aircraft weight, repair quality, repair lengths and spacings and risk levels. For landing runs the amount of braking/reverse thrust normally replaces aircraft weight as a parameter. Operationally these translate into mission effectiveness, time and resources required to effect the runway repairs and probable loss rates. Depending on the relevant national operational philosophies in this area, some of these may be fixed, for instance the ability to operate maximum weight aircraft to obtain full mission effectiveness may be paramount. Another plan might however call for the operating surfaces to be re-opened in the minimum possible time, even if the aircraft's capabilities when launched from it were strictly limited. Any decisions must also be based on a mix of aircraft types, not just one. It is quite conceivable that decisions would have to be taken to repair a minimum operating strip for say 2 aircraft types, which was totally unsuitable for a third type.

Within one nation the mission effectiveness, loss rate and time to repair 'operator' considerations can be balanced against the resource considerations of the repairer, but when this is viewed in the context of interoperability between nations the problem must become more complex. The only basis which I can see for carrying out this process is for the aircraft operating nation to provide a complete set of data to each nation from whom interoperability is sought, so that they can decide which of the trade-offs are appropriate to their philosophies and resources and communicate this back to the aircraft operating nation.

One of the major problems in deriving any data at all, is how to treat the multiple mat situation. With one or two mats the position is simple and data can easily be presented in a form such as that shown in Figure 2, or in spacing vs distance plot derived from it. However, as the number of mats considered increases to 3 or 4, the problem of defining acceptable conditions explicitly rapidly becomes impossible. The only way of overcoming this appears to be to develop an approach which looks at the acceptability of each pair of mats in turn, but even this appears in a general case to be quite difficult, both conceptually and numerically. In certain specific cases however, simplification can be made which allows reasonable solutions to be achieved.

## 6 CONCLUSION

In the discussions some of the causes of variability of input conditions and of the system response have been highlighted, together with some of the uncertainties concerning the failure limitations. The clearance problem thus becomes a matter of judging the response of a system with an ill-defined transfer function and with unknown input, against an uncertain standard. However, the information on aircraft capabilities is required by both the operators and those tasked with repairing the runways and it is required to the best possible standard. Overconfidence could mean loss of aircraft at the worst possible time, excessive conservatism could mean loss of operational flexibility - which may be worse, excessive delay could mean no information at all - which would be worse still. But in order to gain the required repaired runway operational capabilities from the current generation of aircraft, their abilities must be fully exploited. This necessarily implies acceptance of risk levels which would be unacceptable in peace-time. If there is to be genuine management of these risks then future effort must be concentrated on some of the problems of applying simulation models which have been highlighted in this paper.

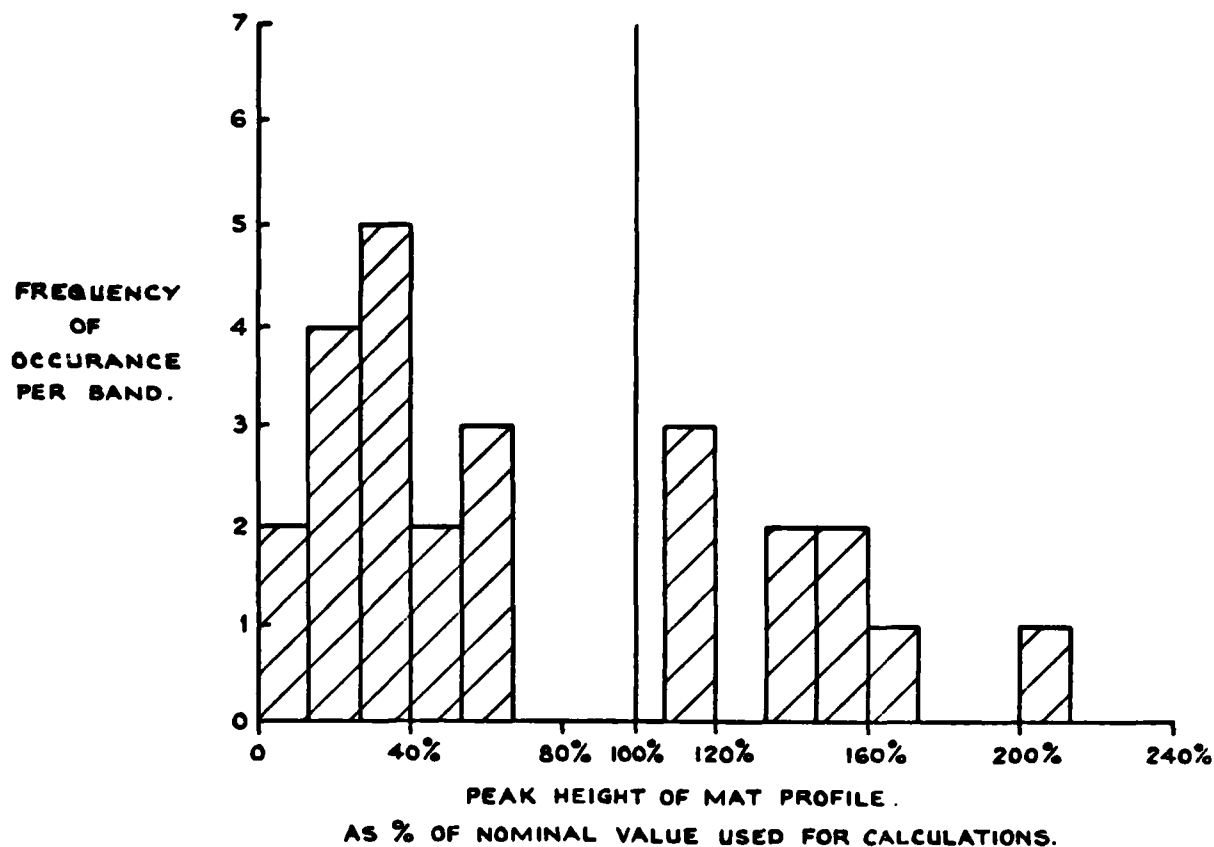


FIG. 1 HISTOGRAM OF PEAK HEIGHTS OF 25 RRR MAT PROFILES.

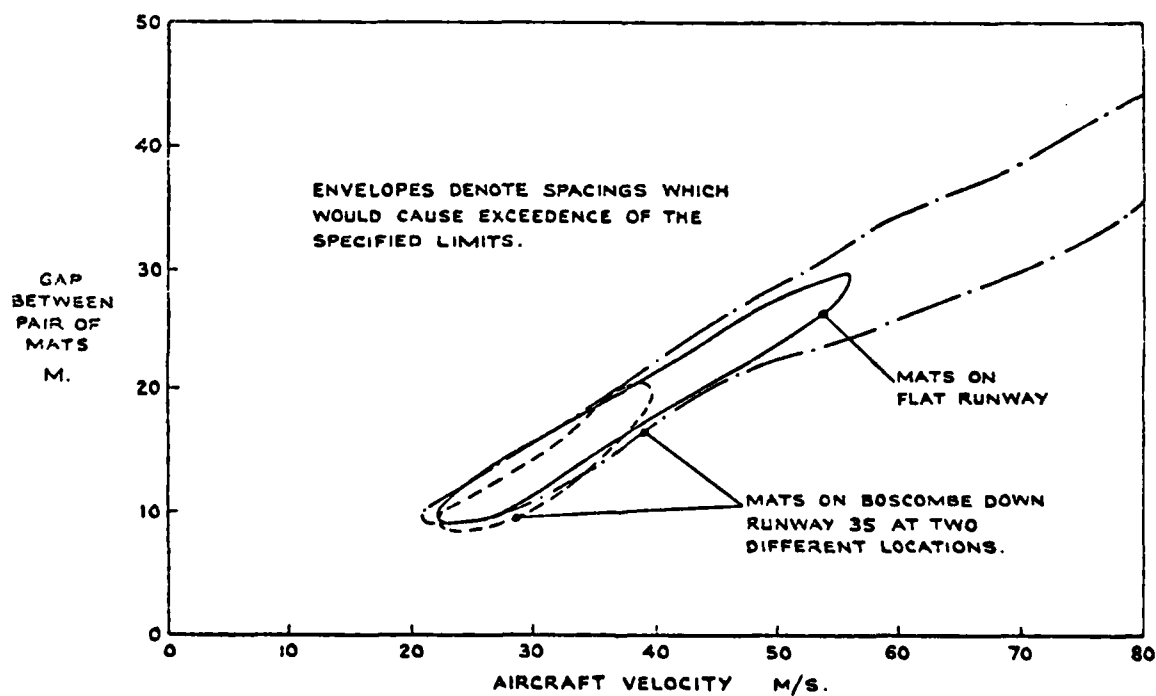


FIG. 2 GRAPH SHOWING THE CALCULATED EFFECTS OF UNDERLYING RUNWAY PROFILE ON THE SPACINGS OF MATS REQUIRED TO GIVE CRITICAL PEAK LOADS.

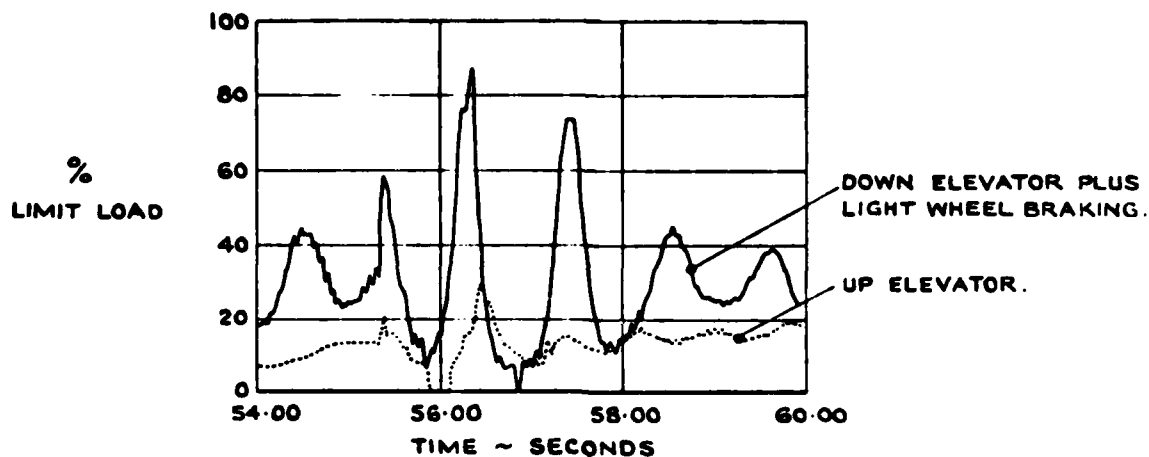


FIG.3 GRAPH SHOWING THE EFFECT OF PILOT INPUTS ON LOADS CAUSED BY REPAIR MAT CROSSINGS AT SIMILAR WEIGHTS AND SPEEDS.

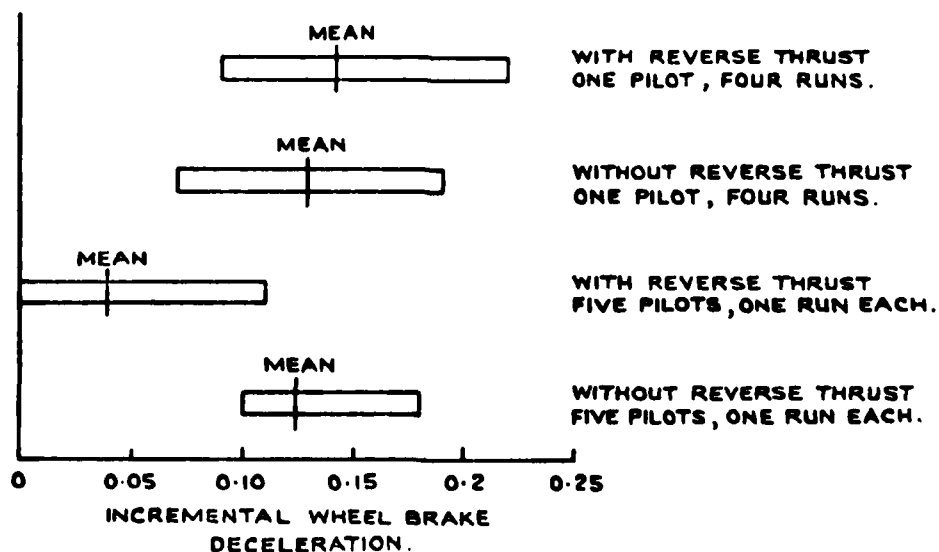


FIG.4 DISTRIBUTION OF INCREMENTAL AIRCRAFT DECELERATIONS DUE TO WHEEL BRAKING.

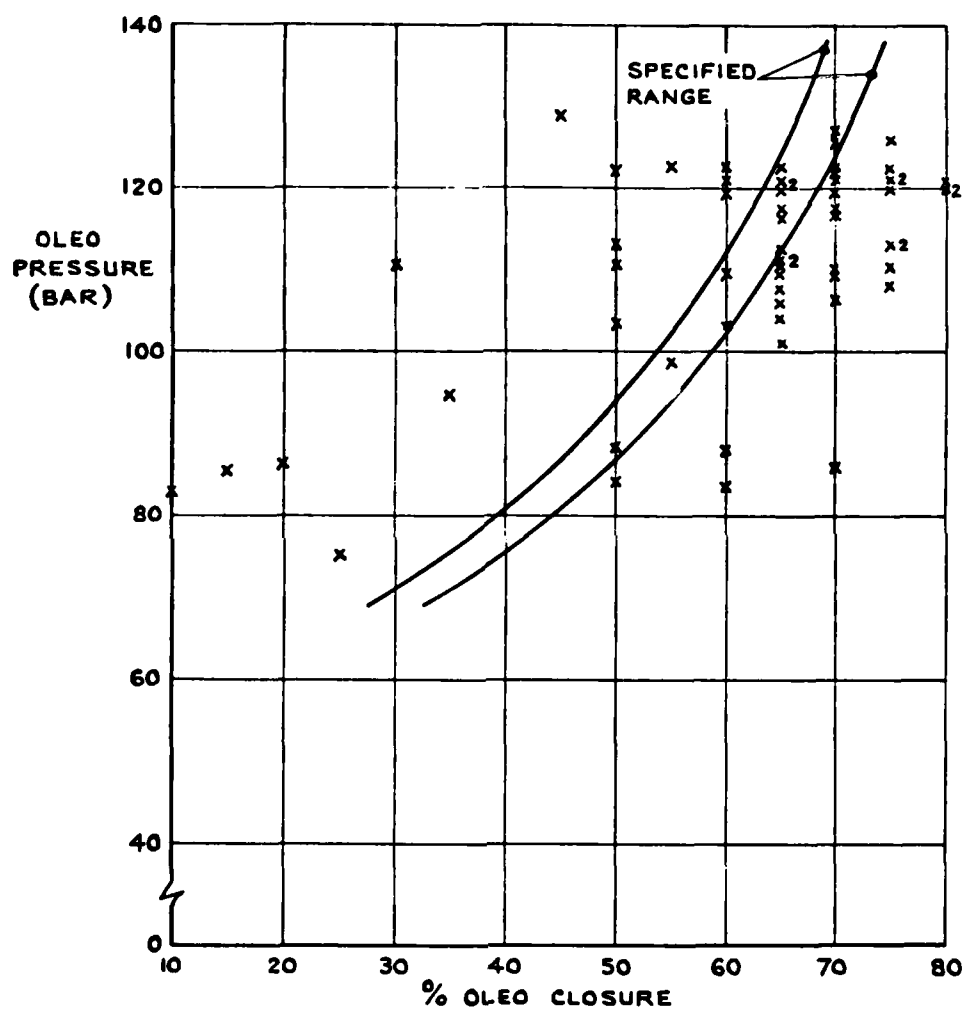


FIG.5 GRAPH SHOWING MEASURED AND SPECIFIED MAIN OLEO PRESSURES AGAINST CLOSURE FOR 32 AIRCRAFT.

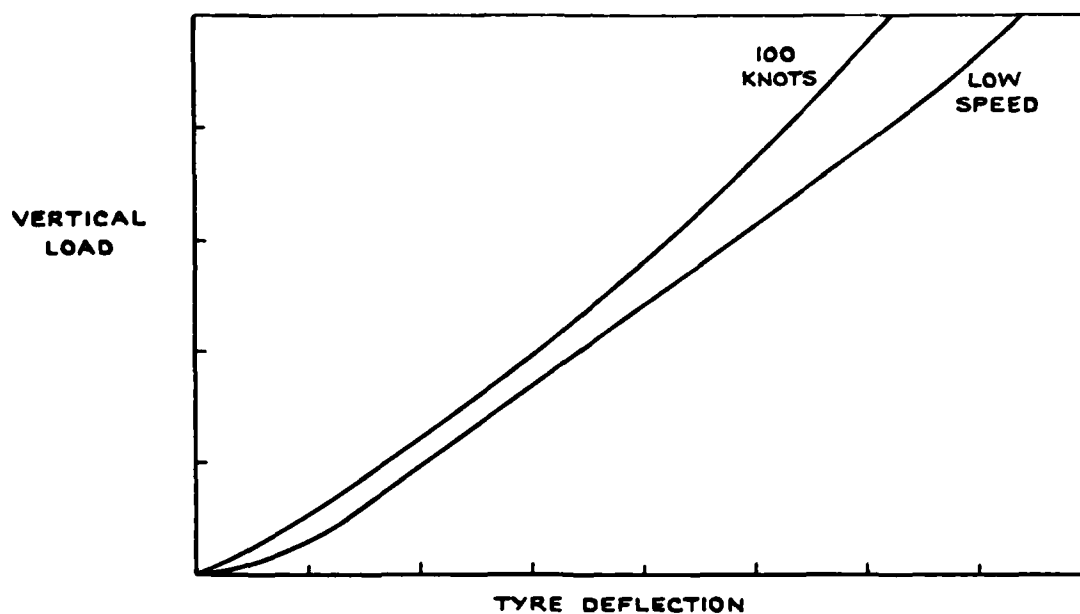


FIG. 6 GRAPH SHOWING THE EFFECT OF FORWARD SPEED ON THE LOAD DEFLECTION CHARACTERISTICS OF A NOSEWHEEL TYRE.

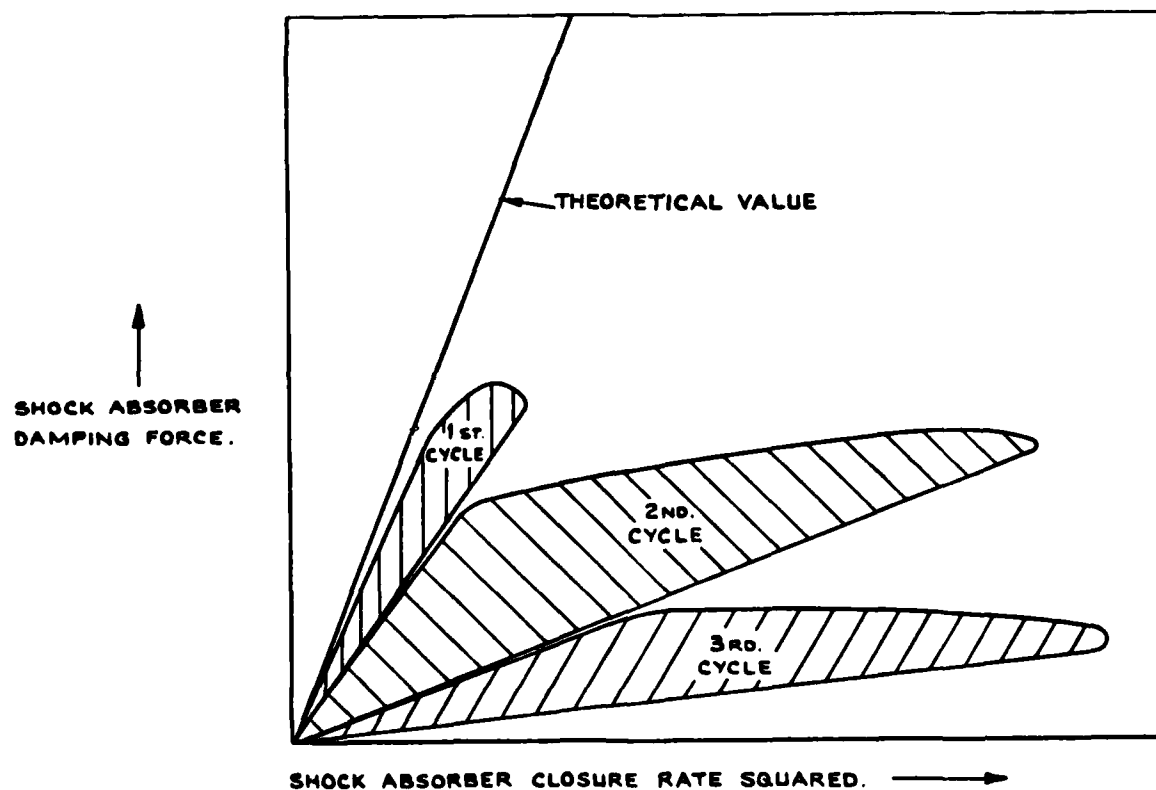


FIG. 7 GRAPH SHOWING DEGRADATION OF DAMPING IN SHOCK ABSORBER DUE TO REPEATED OPERATION.

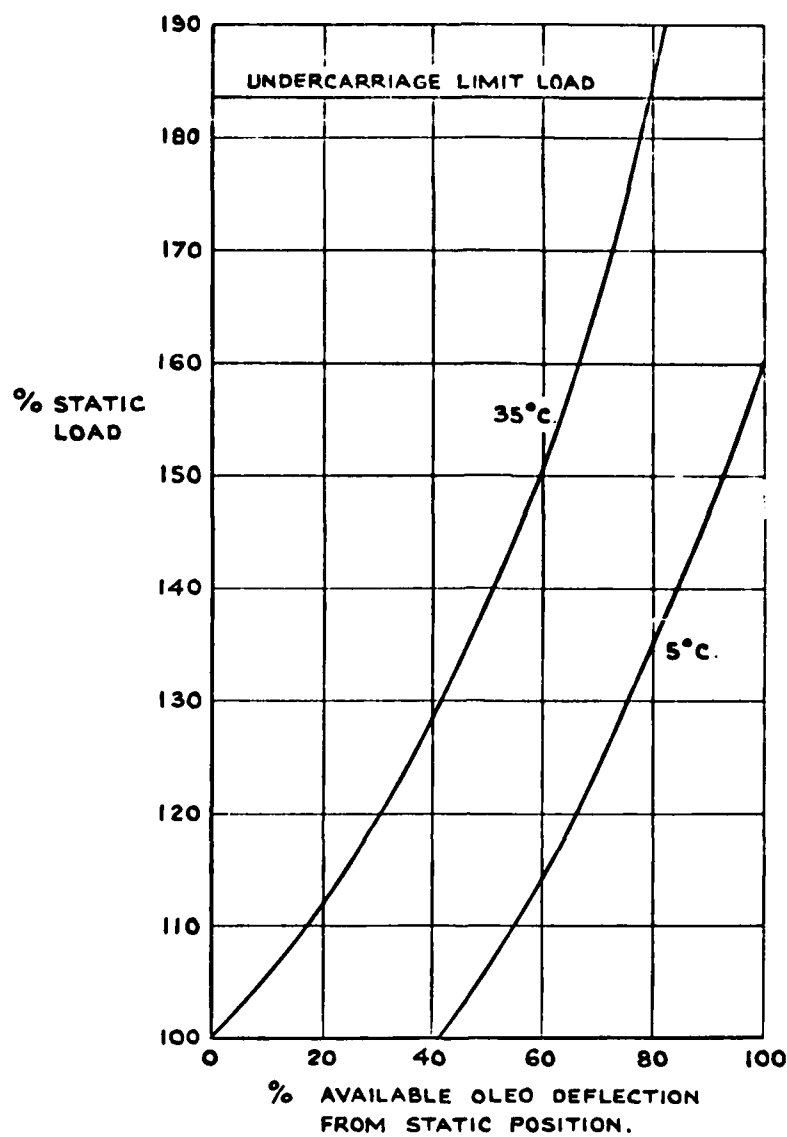


FIG. 8 GRAPH SHOWING EFFECT OF TEMPERATURE  
ON THE LOAD DEFLECTION CURVE OF A  
MAIN OLEO.

CORRECT PRESSURE AT 20°C.

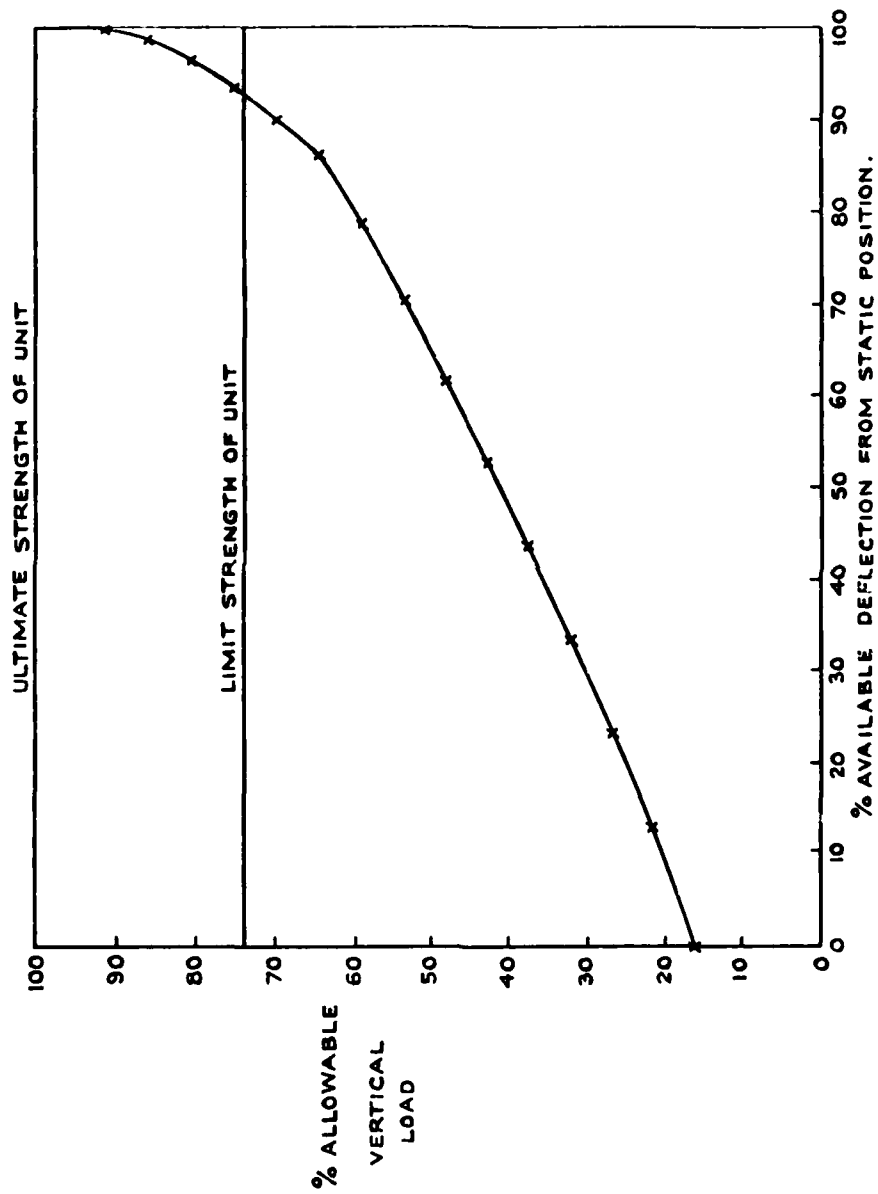


FIG. 9 LOAD-TOTAL DEFLECTION CURVE FOR A NOSE UNDERCARRIAGE.  
NOMINAL PRESSURES AND TEMPERATURES.



## The HAVE BOUNCE Program

James E. Holpp, Program Engineer  
Aeronautical Systems Division, TAEF  
Wright-Patterson AFB Ohio 45433

### SUMMARY

The purpose of the HAVE BOUNCE Program is to define aircraft response to runway repair in a military conflict environment. This is done by developing computer programs that model the dynamic and structural response of aircraft and then by testing aircraft over simulated repaired runways to gather data for use in validating these computer programs. HAVE BOUNCE has two objectives; (a) a computer program which models the dynamic response of an aircraft operating over repaired bomb damaged runways, and (b) aircraft operating limitations and guidelines for operation over these repair surfaces. This paper discusses how the program is being conducted, progress to date, and planned future efforts.

### INTRODUCTION

The tactics of modern warfare include the early destruction of the opposition's airfield. Runways by their nature, represent a relatively easy target for an attacking aircraft, being located at a known, fixed position, easily seen and destroyed either by traditional weapons or by the modern specially designed penetration bombs. Because of this threat, the U.S. Air Force has required an improved Rapid Runway Repair (RRR) capability. A RRR program (in which the HAVE BOUNCE program is a subtask) was established and is managed by the Air Force Engineering and Service Center (AFESC) located at Tyndall Air Force Base, Florida. Due to the complexity of the problem, this program was divided into the following four technical areas:

1. Alternate Launch and Recovery Surfaces - These surfaces are defined as runway surfaces other than conventional concrete and asphalt that will support a limited number of aircraft operations. The objectives of studies in this area are: (a) develop economical aircraft launch and recovery surfaces capable of supporting a limited number of aircraft passes that are independent of, and redundant to, the primary airfield pavements (runway, taxiway); and (b) develop a surface or system that would limit the damage from conventional weapons.
2. Post-Attack Environment - The objectives of studies in this area are: (a) develop techniques and systems/equipment to rapidly assess damage after an attack and, (b) develop a post-attack action plan which states the timely actions that should take place following an attack.
3. Bomb Damage Repair (BDR) - The objectives of studies in this area are to develop methods to rapidly repair pavements damaged by the full range of conventional (non-nuclear) weapons (i.e., from aircraft cannon fire to large iron bombs). Various backfill and capping materials, equipment and techniques will be developed, tested, evaluated and validated.
4. Surface Roughness - The objective of studies in this area is to determine how rough the aircraft launch and recovery surface can be without creating structural damage to the aircraft or causing it to lose its external stores, or causing the pilot to lose control. The rougher the allowable aircraft operational surface, however, the less time it takes to repair the surface and the quicker that surface can be used by aircraft. The major output of studies in this technical area is surface roughness repair criteria to be used in the field by those personnel repairing the damaged runways.

As a subtask of the Surface Roughness technical area, the HAVE BOUNCE program was established to support and furnish a major evaluation tool for use in determining surface roughness repair criteria. HAVE BOUNCE efforts are managed by the Aeronautical Systems Division (ASD), Wright-Patterson Air Force Base (WPAFB), Ohio. The objectives of the program are to: (a) develop a computer program which models the dynamic response at the aircraft operating over repaired bomb damaged runways. This computer program is validated by data measured during tests of an instrumented aircraft over simulated repaired runways, and (b) develop aircraft operating limitations and guidelines for operating over repaired bomb damaged runways. The computer program and operating limitations are aircraft dependent and are, therefore, developed separately for each aircraft included in the HAVE BOUNCE program. As the validated computer programs are acquired by ASD, they are forwarded to AFESC to be used in the surface roughness technical area for determining and specifying the surface roughness repair criteria for each aircraft. As the operating limitations are acquired, they are included (by ASD) in the respective aircraft flight manuals.

### THE HAVE BOUNCE PROGRAM

The objectives of the HAVE BOUNCE program are obtained by contracted effort performed by the manufacturers of the aircraft being evaluated. As previously stated, the HAVE BOUNCE program is managed by the Fighter-Attack System Program Office (SPO) at ASD, WPAFB, Ohio. The SPO responsibilities include contracting with the various aircraft manufacturers, establishing baseline schedule and budget requirements, conducting periodic program reviews, coordinating the effort of other Air Force organizations who support the program (these other organizations will be identified later) and, insuring the end products of the HAVE BOUNCE program are acceptable to and useable by AFESC. The aircraft evaluated in this program are; F-15, F-16, A-10, F-111, C-141, C-5A, DC-10, and 747. A program similar to the HAVE BOUNCE program was also conducted for the F-4 and C-130 aircraft and was managed by the AFESC. The contracted HAVE BOUNCE effort performed by the aircraft manufacturers is divided into four major tasks. These tasks plus a brief description of the technical efforts involved follow.

**TASK I: DEVELOP DYNAMIC LANDING AND TAXI LOAD  
SIMULATION COMPUTER PROGRAMS**

A. The dynamic mathematical model is developed to analytically describe the aircraft and incorporates, as a minimum, these characteristics: (Additional characteristics may be included, as required, to obtain reasonable accuracy for the predicted responses.)

1. Rigid body plunge, pitch, roll, and horizontal translation degrees of freedom.
2. Strut bearing friction forces.
3. Strut hydro-pneumatic forces.
4. Ground friction forces.
5. Aircraft aerodynamic forces (lift, drag, pitching moment).
6. Sufficient number of flexible modes to accurately define internal structural loads for critical components.
7. Airplane structural damping.
8. Runway roughness description, providing for all critical or suspected critical symmetric and asymmetric encounters of the repair mat or mats with the aircraft landing gear.
9. Tire pneumatic force to include tire imprint model, if necessary.

B. The dynamic simulations conducted using this model will monitor the time histories of the loads and responses listed below and will plot these time histories upon operator request.

1. Vertical acceleration at aircraft c.g.
2. Vertical acceleration at pilot station.
3. Vertical and drag loads at main landing gear.
4. Vertical and drag loads at nose landing gear.
5. Loads and/or bending moments at other components suspected to be critical (critical components).

C. The dynamic simulations tabulate the maximum and minimum extremes of these loads and responses (Task I.B.) and, upon operator request, will plot the data for any selected variable versus aircraft velocity or landing sink rate for a particular aircraft configuration and runway configuration. Velocity increments between 2 and 20 knots may be selected by the operator, and the velocity range is 0 to takeoff velocity. Sink rate increments are 1 foot per second (FPS) and the sink rate range is 1 to 10 FPS.

D. Input Parameters. The bomb damaged runway repair roughness profile is used as the forcing function in the aircraft response simulation models to supply symmetrical and asymmetrical input forces at all the aircraft landing gear. The computer simulation programs have the capability of inputting the roughness parameters and aircraft parameters as variables. Roughness parameters include runway survey, repair size, repair spacing, repair upheaval, repair deflection, and repair location. The parameters for each repair are independently variable. The aircraft parameters include weight, center of gravity, sink rate, velocity, acceleration, reverse thrust, and braking. These aircraft parameters are also independently variable. The runway profile between repaired areas may be smooth or as specified on the undamaged runway survey profile.

**TASK II: CONDUCT DYNAMIC LOAD SIMULATIONS**

A. A specified data bank of pertinent literature is reviewed to become familiar with bomb damaged runway repair procedures and operational criteria.

B. Studies are conducted to select aircraft components/systems that may be vulnerable to operations on repaired bomb damaged runways. Overload criteria based on design limit loads are established for these components. Overload occurrences in the fuselage, wing, pylons, empennage, landing gear, and tires are considered in evaluating potential vulnerable components. Load factor limits at the pilot station are also considered as possible overload criteria.

C. Using the dynamic landing and taxi simulation computer programs, various combination of aircraft taxi velocities or landing sink rates are analyzed in conjunction with the aircraft configurations listed in Figure 1, and the repair mat and spall configurations in Figure 2, to determine what loading conditions produce the maximum load or response in the aircraft components defined in Task II.B. above. For each critical response condition, simulations are conducted at two additional speeds, both above and below the critical speed, so as to bracket the maximum response velocity. The significance of simultaneously occurring landing gear vertical and drag loads are assessed for the critical landing gear cases.

D. Upon completion of Tasks I and II, the results are detailed in an interim report and reviewed by the cognizant Air Force organizations for approval before proceeding further.

### TASK III: VALIDATION OF DYNAMIC LOAD SIMULATION COMPUTER PROGRAMS

A. With assistance from the Air Force Flight Test Center (AFFTC), that aircraft instrumentation and calibration necessary to obtain sufficient test data to validate the dynamic load simulation computer programs is specified.

B. The test conditions (e.g., aircraft configuration, taxi speed, repair patch configuration, repair patch spacing, etc.) required to obtain the necessary validation data are then determined.

C. Upon completion of the Tasks III.A. and III.B. effort, the results plus corresponding rationale are presented in an interim report. This report is reviewed by the cognizant Air Force organizations for approval before proceeding further.

D. Upon approval to proceed, a detailed flight test plan is prepared.

E. The individual flight tests are planned, conducted, and monitored with assistance from the AFFTC test engineers who also record and process the test data.

F. Based upon the test results, the simulation programs are validated. This is accomplished by comparing the test results with the analytically predicted results and then making any necessary corrections/refinements to the simulation programs. When this is completed, the computer programs (in the suitable FORTRAN V language) are documented in two volumes. The first volume provides a general description and source listings of the program. The second volume is a user's manual completely detailing the definitions of all variables, listing all input data, etc., and any instructions required to operate the computer program.

### TASK IV: DEVELOPMENT OF AIRCRAFT OPERATING LIMITATIONS

The technical efforts included in this final task are:

A. Performing parametric studies of aircraft configurations (Figure 1), landing sink rates, taxi speeds, repair patch configurations (Figure 2), repair patch spacing, etc., to determine the conditions that excite the various critical aircraft components.

B. Recommending operating techniques, aircraft configuration variations, etc., which may be useful in reducing the detrimental aircraft responses. Selected simulation studies may be required to evaluate the structural integrity and aircraft performance resulting from these recommendations.

C. Developing preliminary runway repair guidelines for the aircraft in terms of gross weight, center-of-gravity location, repair patch configuration, repair patch spacing, taxi speeds, and any other parameters deemed pertinent.

D. The aircraft operational limitations and preliminary runway repair guidelines are documented (with the corresponding supporting rationale) in a final report. The aircraft operating limitations are presented in a format suitable for direct incorporation into the aircraft flight manual.

These four tasks (I, II, III, IV) constitute the normal HAVE BOUNCE program. However, due to the high costs associated with instrumenting and calibrating certain aircraft, Task III (as stated) may not be completed for each aircraft evaluated. When this decision is made, a revised Task III effort is contracted for. The revised Task III technical efforts are:

### TASK III: VALIDATION OF DYNAMIC LOAD SIMULATION COMPUTER PROGRAM (REVISED)

A. The dynamic load simulation computer program is validated using any applicable data from previous aircraft tests (taxi, landing, performance, drop test, etc.). The validation includes using the simulation program to analytically predict the results of these tests and comparing the predicted results to the actual test data. If comparison is not favorable, corrections and/or refinements shall be made to the simulation program as necessary.

B. When Task III.A is completed, an interim report is prepared detailing the results. This report contains the final comparisons of the actual test data with the analytically predicted results calculated after the corrections and/or refinements were made to the total program. Other substantiations or rationale that would add to the verification of the program's validity is included in the report. This report is reviewed by cognizant Air Force organizations for approval before proceeding further.

C. After approval of the Task III B. interim report, and when the dynamic response computer model is recognized as acceptable for HAVE BOUNCE purposes, the computer program (in the suitable FORTRAN V language) is documented in two volumes. The first volume provides a general description and source listings of the program. The second volume is a user's manual completely detailing definitions of all variables, listing all input data, etc., and any instructions required to operate the computer program.

### OTHER ORGANIZATIONS ASSOCIATED WITH THE HAVE BOUNCE PROGRAM

Three other Air Force organizations are associated with the HAVE BOUNCE program and the major areas of support provided are:

A. Air Force Engineering Services Center, Tyndall AFB, Florida.

○ Provides funds.

○ Monitors budgets.

○ Acts as the focal point for all civil engineering technical exchange and resource support.

- B. Air Force Wright Aeronautical Laboratories/Flight Dynamics Laboratory, Wright-Patterson AFB, Ohio.
- Provides technical support for monitoring the development of the contractor's dynamic response computer program.
  - Assists in developing the various aircraft test plans and in validating the computer programs with the resulting data.
  - Develops a version of TAXI for each aircraft being evaluated (TAXI is a Flight Dynamics Laboratory in-house dynamic response computer program that is less sophisticated and uses less computer time than the contractor developed program).
  - Serves as technical consultant to the HAVE BOUNCE SPO.
- C. Air Force Flight Test Center, Edwards AFB, California.
- Manages the HAVE BOUNCE test programs.
  - Formulates the test plan with inputs from the airframe contractor.
  - Provides and manages test support resources.
  - Insures compliance with appropriate flight, safety, and maintenance directives during the testing.
  - Conducts the test, records and reduces the data, and provides the data to the aircraft contractor for use in validating their computer program.

#### HAVE BOUNCE SCHEDULE

The schedule for the completion of the four tasks for each aircraft being evaluated are shown in Figure 3.

#### HAVE BOUNCE RESULTS

All tasks of the HAVE BOUNCE program have been completed for one aircraft, the C-141B. The final results are summarized below in the form of CRITICAL COMPONENTS, PRELIMINARY SURFACE ROUGHNESS CRITERIA, and OPERATING LIMITATIONS AND PROCEDURES.

Tasks I and II have been completed on three aircraft, the F-15, C-5, DC-10. Pertinent results contained in the interim report are summarized in Table I.

Final results (completion of Tasks I, II, III, and IV), C-141B:

#### CRITICAL COMPONENTS

Nose landing gear.  
Main landing gear  
Outer engine pylon.

#### PRELIMINARY SURFACE ROUGHNESS CRITERIA.

CASE	REPAIRS		
	DOUBLE BUMP	SINGLE BUMP	SINGLE MAT
Runway:			
Configuration			
Maximum Takeoff	May Not Traverse	200 Ft. Min. Spacing	No Spacing Restriction
Medium Takeoff	No Spacing Restriction	No Spacing Restriction	No Spacing Restriction
Design Landing	160 Ft. Min. Spacing	160 Ft. Min. Spacing	No Spacing Restriction
Light Takeoff	No Spacing Restriction	No Spacing Restriction	No Spacing Restriction
Light Landing	No Spacing Restriction	No Spacing Restriction	No Spacing Restriction
Emergency Takeoff	Smooth Runway Operation Only		
Taxiway	No Spacing Restriction	No Spacing Restriction	No Spacing Restriction
Landing Zone	No Repairs in Landing Zone		
Spalls	No Restriction		

## OPERATING LIMITATIONS AND PROCEDURES

### 1. BRAKING PROCEDURES

There is no restriction on using steady braking, however abrupt braking or varied braking should not be used in the vicinity of the repairs because of the effect on nose gear loads. Braking should be applied smoothly and held constant while near repairs. Parameter studies indicate that transient braking induces aircraft pitch oscillations that can increase nose gear load when operating on a repair.

### 2. ELEVATOR POSITION

Parameter studies indicate that static elevator position has little effect on loads so there is no restriction on elevator position. However, the elevator should be held steady prior to and on repairs as not to induce aircraft oscillations that could increase nose gear loads.

TABLE 1

INTERIM RESULTS F-15, C-5, DC-10  
(completion of Tasks I and II)

Aircraft	Critical components	Capability to operate on profiles in Figure 2 (multiple profiles not considered)	Status of computer program.
F-15	Nose landing gear Main landing gear Inboard store pylon	Can land on all profiles. Can taxi on all profiles.	Program needs to be validated.
C-5	Engine pylons  Nose landing gear	No landing conditions considered Can taxi on all profiles.	Program needs to be validated.
DC-10	Forward fuselage Outer wing Center main gear	Can land on 1-1/2 inch profiles. Cannot land on 3 inch profiles. Can taxi on all profiles.	Program needs to be validated.

**FIGURE 1**

### AIRCRAFT CONFIGURATIONS

<u>Type</u>	<u>Aircraft Basic</u>	<u>Payload</u>	<u>Fuel</u>	<u>Aircraft Operating Weight</u>	<u>Center of Gravity</u>
Max Takeoff					Forward
Max Takeoff					Aft
Max Landing					Forward
Max Landing					Aft
Light Landing					Normal

Aircraft configurations are specified to the contractor in the above format. These typical operational aircraft configurations are defined by the Air Force using command. The contractor uses these configurations for simulation purposes, although familiarity with the aircraft allows the contractor to propose a configuration they feel is more appropriate or will cause a maximum response.

FIGURE 2

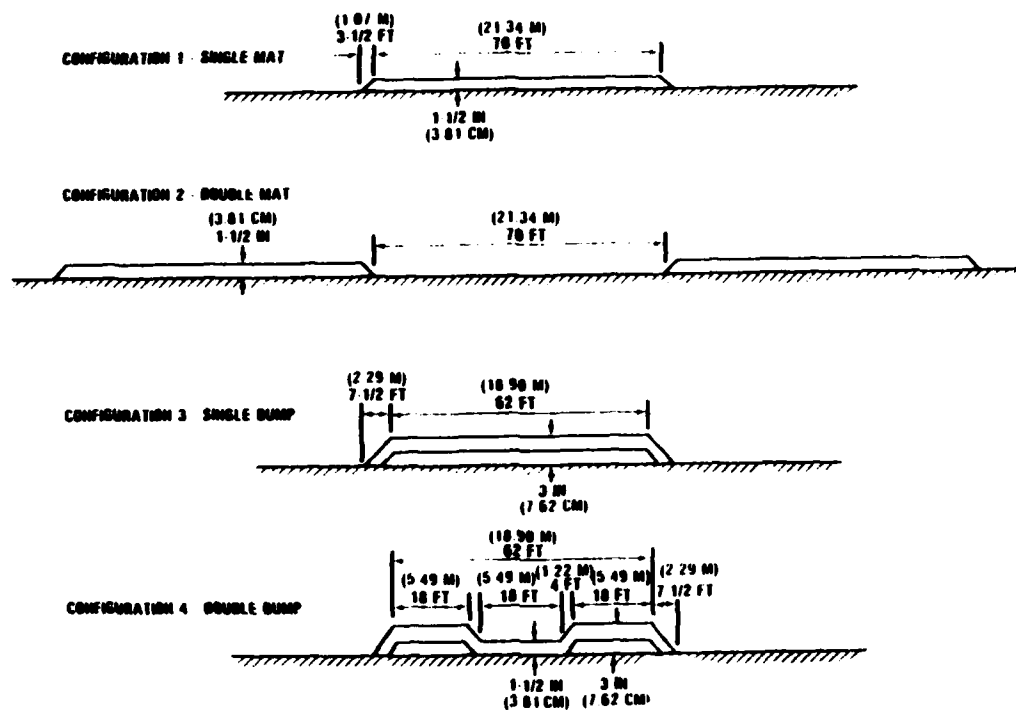
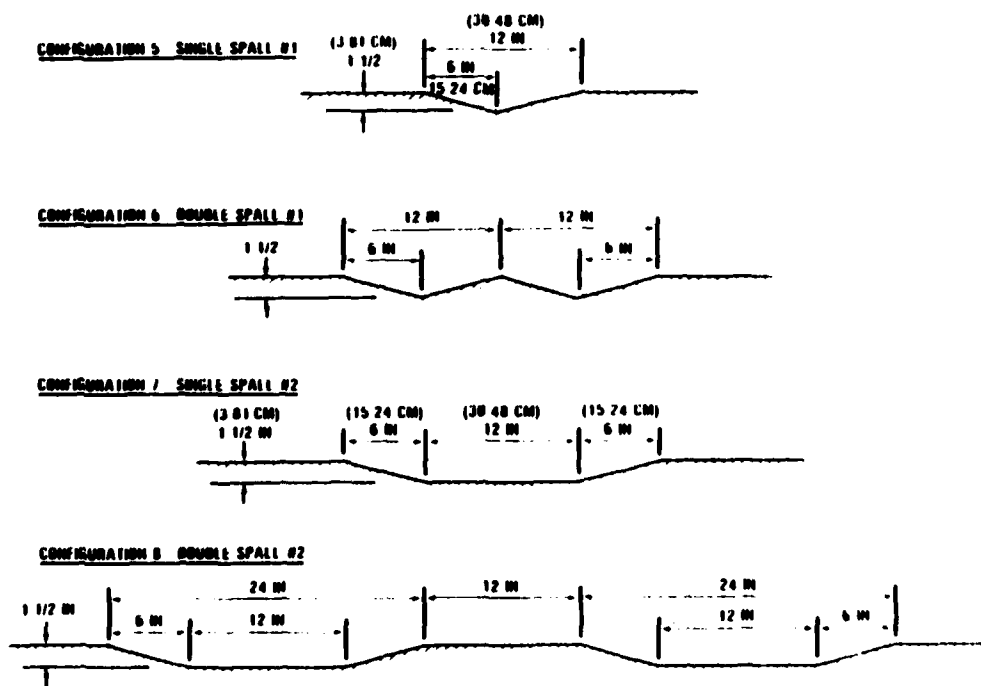
**REPAIR MAT CONFIGURATIONS****SPALL CONFIGURATIONS**

FIGURE 3

**HAVE BOUNCE SCHEDULE**

	CY 82				CY 83				CY84	
	FY 82				FY 83				FY84	
F-15	Δ III		IV	Δ						
F-16	II		III			IV			Δ	
A-10	I	Δ	II	Δ	III		Δ	IV	Δ	
F-111			I		II	Δ				
C-141	COMPLETED									
C-5	Δ III	Δ IV		Δ						
DC-10	II	Δ	III	Δ	IV		Δ			
747	II	Δ	III	Δ	IV		Δ			

# INFLUENCE OF MATHEMATICAL MODELLING OF UNDERCARRIAGES ON THE PREDICTION OF AIRCRAFT LOADS DUE TO DAMAGED AND REPAIRED RUNWAYS

Arnulf Krauss, Otto Bartsch, Gunther Kempf

MESSERSCHMITT-BÖLKOW-BLOHM GMBH  
Unternehmensbereich Flugzeuge  
Postfach 801160  
D-8000 München 80, W-Germany

## SUMMARY

Aircraft dynamic response to damaged and repaired runways is difficult, expensive and risky to test. Simulation models therefore are indispensable tools to calculate dynamic response beforehand and to extrapolate test results to extreme conditions.

The peculiarities of the response-on-damaged-runway-simulation are described and their influence on the loads assessed. Specific reference is taken to the requirements of digital simulation. It is shown that simulating an oleo-pneumatic shock strut as a parallel combination of gas-spring and hydraulic damper by far overestimates undercarriage load and hence structural response on short-wave obstacles. Rather, physically existing additional flexibility of the undercarriage in series to the oleo strut must be included in the model.

## 1. INTRODUCTION

There are some publications which describe mathematical models of undercarriages. Not the first one, but probably the most widely known of those is NACA Rep. 1154 [1] published back in 1953. According to that report the force along an oleo-pneumatic strut is composed of the pneumatic spring force, the hydraulic damping force, and the bearing friction force. The mathematical formulations of these physical phenomena have proven their value in innumerable undercarriage design load calculations.

Continuous increase in capacity and speed of digital computers has enhanced the development of large simulation models which comprise coupled undercarriage/airframe dynamics. However, there are essentially two problem areas induced by digital simulation. One is that some of the mathematical models of physical phenomena which were readily adaptable for analog computer networks are unwieldy for digital simulation. The other problem is that in spite of large models not all the physics can be simulated and that just because of large models it is hard to decide whether incorrect physical modelization or incorrect data are to be blamed for eventual discrepancies between simulation and test.

Some minor physical effects beyond the scope of ref. [1], such as compressibility of hydraulic fluid, volume dilatation of the strut, and structural flexibility of the strut in stroking direction have been taken into account in investigations mostly involving single legs and aiming at improvement of the correlation between analysis and test results (e.g. [9], p.89). However, no evidence is given in [3], [5], [6], [7] that this was done for undercarriages forming part of a complex undercarriage/airframe coupled dynamic system. Yet there are clues that better correlation between analysis and test results is also required with regard to dynamic response of the airframe in such coupled systems:

- o "Cockpit, wing and tailplane tip vertical oscillations were not well predicted..." ([11], para 4.4).
- o Fig. 1 of this paper is a quotation from [10] (Fig. 11 there) and shows a considerable difference between simulation and test.
- o Our own (unpublished) experience with those difficulties dates from 1966/67 and is reflected in the comments of para 4 of [12].

There is a lot of potential sources for those discrepancies between simulation and test and it is virtually impossible to treat all of them at once and simultaneously. When the problem of aircraft dynamic response to damaged and repaired runways came up again, we therefore decided to proceed from a general analysis of this special simulation task to studies of the physical details. The following paper to a certain degree reflects this proceeding.

With regard to the physical detail we concentrated on the undercarriage. It is shown that velocity-squared hydraulic damping force in the model without due consideration of undercarriage structural flexibility and hydraulic fluid compressibility may lead to very conservative load predictions.



## 2. PECULIARITIES OF THE REPAIRED RUNWAY/AIRPLANE SIMULATION

### 2.1 Modal Representation of the Airframe

In a comprehensive study of structural loads due to damaged and repaired runways structural flexibility of the airframe must be included. In order to assess the range of eigenfrequencies to be included in an analysis it is useful to have a look on the frequencies contained in the excitation.

The most prominent obstacles with significant height on a repaired runway are ramps of repair mats:

The ramps of AM 2 mats are 1.14m deep, the peak amplitude contained in a Fourier-series representation of an ongoing/offgoing ramp combination therefore lies at a spatial frequency of 0.44 cycles/meter. Assuming a lift-off speed of approx. 80 m/s results in a frequency of 35 Hz.

The ramp of the UK Class 60 mat is considerably shorter (0.1524 m or 6 in.) which leads into the vicinity of the footprint length of an 18 inch tyre. Since the vertical force of the tyre governs the dynamic behaviour of the undercarriage/airframe system, in a first approximation the length of the tyre footprint may be added to the basic wavelength of the ongoing/offgoing ramp combination in order to arrive at the critical wavelength. Therefore an assumed 80 m/s lift-off speed yields a frequency of around 160 Hz for an 18" tyre, and a frequency of around 100 Hz for a 30" tyre.

From these figures it appears desirable to include many natural modes and high eigenfrequencies in the modal representation of the elastic airframe. Since proper selection of relevant modes requires a good amount of engineering judgement, and since in many areas the ratio of saved computer cost to engineer cost has fallen below one, there is an inherent trend to simply use the full capacity of a computer program by including the maximum possible number of modes in rising sequence of eigenfrequencies.

This may however introduce considerable problems with respect to other features of the model, as for instance aerodynamic damping of the modes and simulation of the undercarriage.

### 2.2 Proper Comparison of Simulation and Test Results

Validation of a computer model is tied to proper comparison of simulation and test results. Though this is not strictly subject of this paper some remarks must be made:

Whether or not elastic modes are contained in the simulation, the integration step size of a digital simulation should be orientated at three points:

- o The distance traveled during one time step should not be greater than 1/10 to 1/5 of the footprint length of that tyre which is crossing an obstacle or is bearing more than 80 percent of its bottoming load.
- o At least ten time steps should fall into one period of the heave motion of the aircraft mass on the tyres.
- o At least ten time steps should fall into one period of that natural mode with the highest eigenfrequency.

This appears to be rather expensive, yet it is worth the money because it helps to avoid errors induced by numerical instabilities and it provides resolution good enough to register all peak loads.

Time resolution plays also a very important rôle for test measurements. If the resolution of the measurement record is not fine enough there is a good chance that load peaks of short duration (e.g. while crossing a step) will not be recorded with their true peak value, thus rendering the comparison of simulation and test a matter of fortune-telling rather than of science.

However, even if the sampling rate for the output of the test instrumentation should be perfectly adequate there is still another stumblingblock on the way to a meaningful comparison of simulation and test. The frequency band of the sensor/sensor attachment/wiring/amplifier/data transmission-chain is a crucial point. Besides limitations set by the physical means of measurement this chain usually contains filters in order to separate the "useful" signal from "noise" in the upper frequency range and from quasi-steady values in the lower frequency range.

In the light of the frequency assessment for tyre loads on repaired runways (para 2.1) it is advisable to have a frequency band of 0 to approximately 200 Hz for the loads related instrumentation. If this cannot be achieved part of the information about the loads occurring during the test can get lost and eventually the load results of the simulation will be more "true" than those of the test. This again can mean considerable difficulties when trying to perform a comparison simulation/test. Probably the most straightforward method to cope with this situation is to extend the simulation by a section which simulates the behaviour of the test instrumentation, i.e. to perform a comparison based on calculated vs. actual output of the test instrumentation.

### 3. PROBLEMS OF SIMULATION

From section 2. above it is apparent that not in all cases theory is to be blamed for discrepancies between analysis and test results. Yet it cannot be detrimental to examine even well-established and familiar models whether they still hold in the damaged and repaired runway environment.

#### 3.1 Model Set-Up

Essentially there are two ways to establish a coupled dynamic model of undercarriage and airframe for ground roll loads investigations.

One is to describe the airframe by a set of linear equations employing natural modes, to describe the undercarriage by a separate set of nonlinear equations, and to couple both systems at some suitable points.

Another one is to treat airframe and undercarriage as one linear dynamic system from the outset and to determine a set of natural modes for the complete system. A model of this kind is shown in Fig. 2. With regard to calculating loads from a ground roll this method is most straight-forward because it yields a rather simple set of equations of motion. However, this relative simplicity can be achieved only by linearization of the undercarriage. Thus there is a shift of difficulties in the two methods. Whilst in the first case the difficulty lies in proper mathematical description of the nonlinearities of the undercarriage the second method has its problems in defining the quantities and the range of validity of the linearization.

Since simulation of an aircraft rolling on a damaged and repaired runway will inter alia have to comprise the whole stroking range of the undercarriage legs from almost fully compressed to fully extended with tyres off the ground, the second method is not very likely to yield correct loads for these extreme conditions. Therefore the first method is considered superior to the second for the purpose of loads simulation on damaged runways. However, in the context of the present paper the linearized case may serve as an aid to identify features of the nonlinear model which deserve reconsideration:

The abbreviated notation for the equations of motion of a linear system is

$$[M] \{\ddot{q}\} + [D] \{\dot{q}\} + [K] \{q\} = \{F\} \quad (1)$$

where

- $\{q\}$  Vector of displacements in the generalized coordinates of the system,
- $[M]$  Matrix of generalized masses,
- $[D]$  Matrix of generalized (viscous) damping,
- $[K]$  Matrix of generalized stiffness,
- $\{F\}$  Vector of generalized forces acting on the system,
- $\dot{\phantom{x}}$  denotes differentiation with respect to time.

If eigenmodes are chosen as generalized degrees of freedom the generalized mass matrix and the generalized stiffness matrix become diagonal matrices. If damping is assumed to be distributed proportionally to the mass distribution, matrix  $[D]$  becomes diagonal, too [14]. This means that after removal of the external forces the motions in the generalized coordinates were completely independent of one another. However, the assumption of damping being distributed proportionally to mass does certainly not hold true for a system containing concentrated directional damping as produced by an undercarriage. As a consequence, off-diagonal terms appear in the damping matrix, i.e. coupling between the modes takes place even if the external forces are removed from the system. The magnitude of these off-diagonal damping terms depends amongst others on the magnitude of the damping coefficients attributed to the different undercarriage legs as a result of the linearization. Though objective criteria exist for this type of linearization (e.g. equality of energy dissipated in one stroking cycle of the damper) success of the simulation depends heavily on proper prediction of the results of the simulation, viz. frequencies and amplitudes of the system's response.

Considering the range of frequencies and amplitudes involved in simulating aircraft dynamic response on damaged and repaired runways it appears reasonable to dispense with linearization of the undercarriage and to accept the consequential increase in complexity of the simulation. This means in the first place that the elastomechanic system is split into several components, viz. the airframe and the different undercarriage legs.

If the modelization of the airframe contains the same number of natural modes as before the system of equations for the airframe alone will be of the same size as for the linearized unified airframe/undercarriage system. Mode shapes and frequencies will be different due to missing undercarriage, and that part of the vector of the generalized forces  $F$  attributable to the undercarriage will be formed from forces and moments acting at the undercarriage/airframe interface rather than at the wheels.

This linear system of equations for the airframe must be supplemented by a system of equations describing the dynamics of the different undercarriage legs. These undercarriage equations now may contain all nonlinearities which are considered relevant to the problem. However, there are certain practical aspects of performing a simulation on a computer which make one type of nonlinearity more suitable for simulation than another. This statement is explained by the following (Fig. 3):

Let M be a point on the undercarriage leg, the position of which is described in a Cartesian coordinate system  $u, v, w$ . This  $u, v, w$ -system shall be fixed to the airframe at point A which represents the undercarriage leg/airframe interface point. In the undeformed state of the airframe the  $u, v, w$ -system coincides with another coordinate system  $\bar{u}, \bar{v}, \bar{w}$  which is fixed at point A of the undeformed airframe. The displacement of the  $u, v, w$ -frame from the  $\bar{u}, \bar{v}, \bar{w}$ -frame is completely described by three coordinates  $\bar{u}_A, \bar{v}_A, \bar{w}_A$  and three orientation angles  $\varphi, \vartheta, \psi$ . Finally  $\bar{u}, \bar{v}, \bar{w}$  shall be fixed to an inertial system  $x, y, z$ .

Orientation angles  $\varphi, \vartheta, \psi$  are not shown in Fig. 3. With the assumption of small angles  $\varphi, \vartheta, \psi$  represent clockwise rotations about the positive  $u, v, w$ -axes.

The coordinates of undercarriage point M in the  $x, y, z$ -system can be written as

$$\begin{Bmatrix} x_M \\ y_M \\ z_M \end{Bmatrix} = \begin{Bmatrix} x_A \\ y_A \\ z_A \end{Bmatrix} + [TR] \cdot \left\{ \begin{Bmatrix} \bar{u}_A \\ \bar{v}_A \\ \bar{w}_A \end{Bmatrix} + \begin{bmatrix} 1 & -\psi & \vartheta \\ \psi & 1 & -\varphi \\ -\vartheta & \varphi & 1 \end{bmatrix} \begin{Bmatrix} u_M \\ v_M \\ w_M \end{Bmatrix} \right\} \quad (2)$$

[TR] being the transformation matrix from  $\bar{u}, \bar{v}, \bar{w}$  into  $x, y, z$ .

The velocity of point M in the  $x, y, z$ -system is composed of the velocity of point M in the  $u, v, w$ -system and the velocity of the  $u, v, w$ -system with respect to the  $\bar{u}, \bar{v}, \bar{w}$ -system.

Since  $\bar{u}, \bar{v}, \bar{w}$  is fixed in the inertial system, the appropriate time derivatives vanish:

$$\begin{Bmatrix} \dot{x}_M \\ \dot{y}_M \\ \dot{z}_M \end{Bmatrix} = [TR] \left\{ \begin{Bmatrix} \dot{\bar{u}}_A \\ \dot{\bar{v}}_A \\ \dot{\bar{w}}_A \end{Bmatrix} + \begin{bmatrix} 0 & -\dot{\psi} & \dot{\vartheta} \\ \dot{\psi} & 0 & -\dot{\varphi} \\ -\dot{\vartheta} & \dot{\varphi} & 0 \end{bmatrix} \begin{Bmatrix} u_M \\ v_M \\ w_M \end{Bmatrix} + \begin{bmatrix} 1 & -\psi & \vartheta \\ \psi & 1 & -\varphi \\ -\vartheta & \varphi & 1 \end{bmatrix} \begin{Bmatrix} \dot{u}_M \\ \dot{v}_M \\ \dot{w}_M \end{Bmatrix} \right\} \quad (3)$$

Consequently, the acceleration of point M in the inertial system is

$$\begin{Bmatrix} \ddot{x}_M \\ \ddot{y}_M \\ \ddot{z}_M \end{Bmatrix} = [TR] \left\{ \begin{Bmatrix} \ddot{\bar{u}}_A \\ \ddot{\bar{v}}_A \\ \ddot{\bar{w}}_A \end{Bmatrix} + \begin{bmatrix} 0 & -\ddot{\psi} & \ddot{\vartheta} \\ \ddot{\psi} & 0 & -\ddot{\varphi} \\ -\ddot{\vartheta} & \ddot{\varphi} & 0 \end{bmatrix} \begin{Bmatrix} u_M \\ v_M \\ w_M \end{Bmatrix} + 2 \cdot \begin{bmatrix} 0 & -\dot{\psi} & \dot{\vartheta} \\ \dot{\psi} & 0 & -\dot{\varphi} \\ -\dot{\vartheta} & \dot{\varphi} & 0 \end{bmatrix} \begin{Bmatrix} \dot{u}_M \\ \dot{v}_M \\ \dot{w}_M \end{Bmatrix} + \begin{bmatrix} 1 & -\psi & \vartheta \\ \psi & 1 & -\varphi \\ -\vartheta & \varphi & 1 \end{bmatrix} \begin{Bmatrix} \ddot{u}_M \\ \ddot{v}_M \\ \ddot{w}_M \end{Bmatrix} \right\} \quad (4)$$

Now,

$$\begin{bmatrix} 0 & -\ddot{\psi} & \ddot{\vartheta} \\ \ddot{\psi} & 0 & -\ddot{\varphi} \\ -\ddot{\vartheta} & \ddot{\varphi} & 0 \end{bmatrix} \begin{Bmatrix} u_M \\ v_M \\ w_M \end{Bmatrix} = \begin{bmatrix} 0 & w_M & -v_M \\ -w_M & 0 & u_M \\ v_M & -u_M & 0 \end{bmatrix} \begin{Bmatrix} \ddot{\varphi} \\ \ddot{\vartheta} \\ \ddot{\psi} \end{Bmatrix} \quad (5)$$

and

$$\begin{Bmatrix} \ddot{x}_M \\ \ddot{y}_M \\ \ddot{z}_M \end{Bmatrix} = [TR] \left\{ \begin{Bmatrix} \ddot{\bar{u}}_A \\ \ddot{\bar{v}}_A \\ \ddot{\bar{w}}_A \end{Bmatrix} + \begin{bmatrix} 0 & w_M & -v_M \\ -w_M & 0 & u_M \\ v_M & -u_M & 0 \end{bmatrix} \begin{Bmatrix} \ddot{\varphi} \\ \ddot{\vartheta} \\ \ddot{\psi} \end{Bmatrix} + \begin{bmatrix} 1 & \psi & \vartheta \\ \psi & 1 & -\varphi \\ -\vartheta & \varphi & 1 \end{bmatrix} \begin{Bmatrix} \ddot{u}_M \\ \ddot{v}_M \\ \ddot{w}_M \end{Bmatrix} + 2 \cdot \begin{bmatrix} 0 & -\dot{\psi} & \dot{\vartheta} \\ \dot{\psi} & 0 & -\dot{\varphi} \\ -\dot{\vartheta} & \dot{\varphi} & 0 \end{bmatrix} \begin{Bmatrix} \dot{u}_M \\ \dot{v}_M \\ \dot{w}_M \end{Bmatrix} \right\} \quad (6)$$

If a mass value  $m$  is assigned to point M, the acceleration from equation 6 can be used in the pertinent equation of motion:

$$m \cdot \begin{Bmatrix} \ddot{x}_M \\ \ddot{y}_M \\ \ddot{z}_M \end{Bmatrix} = \begin{Bmatrix} F_x \\ F_y \\ F_z \end{Bmatrix} \quad (7)$$

with the vector of forces acting on the point mass  $m$  being composed of the forces acting as "external" forces (i.e. on the section lying towards the free end of the leg) and of the forces acting as "internal" forces.

Hence,

$$\begin{Bmatrix} F_x \\ F_y \\ F_z \end{Bmatrix}_{\text{ext}} + \begin{Bmatrix} F_x \\ F_y \\ F_z \end{Bmatrix}_{\text{int}} = m \left[ \text{TR} \right] \begin{Bmatrix} \ddot{u}_A \\ \ddot{v}_A \\ \ddot{w}_A \end{Bmatrix} + [\text{OF}] \begin{Bmatrix} \ddot{\phi} \\ \ddot{\theta} \\ \ddot{\psi} \end{Bmatrix} + [\text{OR}] \begin{Bmatrix} \ddot{u}_M \\ \ddot{v}_M \\ \ddot{w}_M \end{Bmatrix} + \{\text{CR}\} \quad (8)$$

with abbreviations  $[\text{OF}]$  for offset influence matrix,  $[\text{OR}]$  for orientation influence matrix, and  $\{\text{CR}\}$  for Coriolis acceleration vector.

Usually numerical integration routines require the highest derivative of the dependent variables to be isolated on one side of the equations. Now, the displacement of the  $u, v, w$ -system from the  $\bar{u}, \bar{v}, \bar{w}$ -system can be expressed as the sum of modal values pertinent to point A multiplied by the displacements of the respective modes. Modal values are independent of time, therefore

$$\begin{Bmatrix} \ddot{u}_A \\ \ddot{v}_A \\ \ddot{w}_A \\ \ddot{\phi} \\ \ddot{\theta} \\ \ddot{\psi} \end{Bmatrix} = \begin{bmatrix} \Lambda_{u_1} & \dots & \Lambda_{u_n} \\ \Lambda_{v_1} & & \vdots \\ \Lambda_{w_1} & & \vdots \\ \Lambda_{\phi_1} & & \vdots \\ \Lambda_{\theta_1} & & \vdots \\ \Lambda_{\psi_1} & & \Lambda_{\psi_n} \end{bmatrix}_A \begin{Bmatrix} \ddot{q}_1 \\ \vdots \\ \ddot{q}_n \end{Bmatrix} = \begin{bmatrix} \Lambda_{u,v,w}^A \\ \Lambda_{\phi,\theta,\psi}^A \end{bmatrix} \begin{Bmatrix} \ddot{q} \end{Bmatrix} \quad (9)$$

Equation 8 is rewritten:

$$\begin{Bmatrix} F_x \\ F_y \\ F_z \end{Bmatrix}_{\text{ext}} + \begin{Bmatrix} F_x \\ F_y \\ F_z \end{Bmatrix}_{\text{int}} = m [\text{TR}] \left\{ \left[ \Lambda_{u,v,w}^A \right] + [\text{OF}] \left[ \Lambda_{\phi,\theta,\psi}^A \right] \right\} \begin{Bmatrix} \ddot{q} \end{Bmatrix} + [\text{OR}] \begin{Bmatrix} \ddot{u}_M \\ \ddot{v}_M \\ \ddot{w}_M \end{Bmatrix} + \{\text{CR}\} \quad (10)$$

Equation 1 yields the vector of accelerations in the generalized coordinates of the airframe

$$\{\ddot{q}\} = [M]^{-1} \{ \{F\} - [K] \{q\} - [D] \{\dot{q}\} \} \quad (11)$$

Rearranging equation 10 yields the vector of accelerations of mass point M in the local undercarriage reference system

$$\begin{Bmatrix} \ddot{u}_M \\ \ddot{v}_M \\ \ddot{w}_M \end{Bmatrix} = \frac{1}{m} [\text{OR}]^{-1} [\text{TR}]^{-1} \left\{ \begin{Bmatrix} F_x \\ F_y \\ F_z \end{Bmatrix}_{\text{ext}} + \begin{Bmatrix} F_x \\ F_y \\ F_z \end{Bmatrix}_{\text{int}} \right\} - [\text{OR}]^{-1} \{\text{CR}\} - [\text{OR}]^{-1} \left[ \Lambda_{u,v,w}^A + [\text{OF}] \left[ \Lambda_{\phi,\theta,\psi}^A \right] \right] \{\ddot{q}\} \quad (12)$$

Substituting equation 11 into equation 12 and radically abbreviating all terms which are not needed for the following considerations, yields

$$\begin{Bmatrix} \ddot{u}_M \\ \ddot{v}_M \\ \ddot{w}_M \end{Bmatrix} = \frac{1}{m} [A_1] \begin{Bmatrix} F_x \\ F_y \\ F_z \end{Bmatrix}_{\text{int}} + [A_2] [M]^{-1} \{F\} + \{F\}_{\text{rem.}} \quad (13)$$

Equations 11 and 13 now appear in a form which makes them suitable for numerical integration, provided that the vectors  $\{F\}$ ,  $\{F\}_{\text{int}}$ , and  $\{F\}_{\text{rem}}$  do not implicitly contain functions of any of the accelerations. These vectors are studied in this respect.

- o The vector of generalized forces,  $\{F\}$ , contains contributions from all forces and moments acting on the airframe, including forces and moments acting at the undercarriage/airframe interface. Since these interface forces are a function of the vector  $\{F\}_{\text{int}}$ , the problems will be considered there.

- o The vector  $\{F\}_{rem}$ , the subscript rem standing for remaining, amongst others contains contributions from forces and moments acting at the ground/tyre interface. Usually, vertical, circumferential, and lateral tyre forces can be expressed as (nonlinear) functions of wheel positions and velocities relative to ground, thus presenting no essential difficulties in the equations of motion. One constituent of the lateral tyre force, however, is dependent on the curvature of the wheel path in the horizontal plane. Though this force is small and usually negligible in the context of dynamic response to repaired runways it may serve as an example for a troublemaker in the mathematical model.

The basic mechanism for sideforce due to curvature of the wheel path in the x-y-plane is sketched in Fig. 4 : A point on the tyre tread which enters the contact patch at point 1 can be considered fixed to the ground, thus experiencing a lateral displacement relative to the wheel plane while moving through the patch (e.g. at point 2). This displacement leads to elastic forces in the tyre which act to the outside of the wheel path curve. The curvature of the wheel path

$$k = \frac{\ddot{y} \dot{x} - \ddot{x} \dot{y}}{(\dot{x}^2 + \dot{y}^2)^{3/2}} \quad (14)$$

Thus part of the side force becomes in turn dependent on the accelerations it produces. Therefore, in order to suit the needs of the numerical integration procedure a tedious elimination process is required for isolating the accelerations on the left hand side of the equations before programming the model. In an ill-conditioned case (e.g. side force being not a linear function of k) iterative solution for the accelerations could be required at each time-step in executing the program, which might result in a dramatic increase of computer time required for the simulation.

- o The vector  $\{F\}_{int}$  is the most interesting with respect to structural loads as well as to modelling difficulties. If the mass point M of Fig. is considered the last one on the undercarriage before the interface to the airframe, the forces and moments at this interface are exclusively composed from  $\{F\}_{int}$ . Therefore this vector appears to be most important with regard to aircraft dynamic response to repaired runways.

There are several features of undercarriage physics and/or modelization which render  $\{F\}_{int}$  a function of the accelerations of the elastomechanic system. Possibilities to avoid or at least to reduce the consequential difficulties in setting up the simulation model are discussed in the following sections.

### 3.2 Kinematic Constraints

If the mass point M (Fig. 3) is subjected to any kinematic constraint with respect to the u,v,w-system, the motion of the mass point in the inertial system becomes tied to the motion of the interface point A, hence to the motions of the airframe.

Considering first the most simple case, that is mass point M being fixed in the u,v,w-system, equation 13 by virtue of

$$\begin{Bmatrix} \ddot{u}_M \\ \ddot{v}_M \\ \ddot{w}_M \end{Bmatrix} = \begin{Bmatrix} 0 \\ 0 \\ 0 \end{Bmatrix}$$

yields

$$\begin{Bmatrix} 0 \\ 0 \\ 0 \end{Bmatrix} = \frac{1}{m} [A_1] \begin{Bmatrix} F_x \\ F_y \\ F_z \end{Bmatrix}_{int} + [A_2][M]^{-1} \{F\} + \{F\}_{rem} \quad (15)$$

Since the contribution of the vector  $\{F\}_{int}$  to the vector of generalized forces  $\{F\}$  can be expressed as a transformation matrix times the vector  $\{F\}_{int}$ , equation 15 actually represents a linear equation in the unknown vector  $\{F\}_{int}$ . However, taking into account that usual systems contain three undercarriage legs and that all undercarriage legs contribute to the vector of generalized forces  $\{F\}$ , a whole system of vector equations has to be algebraically solved (some matrices containing time-varying coefficients) to arrive at expressions for the different forces which then are suitable for inclusion in the simulation programme. Effectively the result is the same as if the mass point M pertaining to the undercarriage but rigidly connected to the airframe had been included in the vibration analysis of the airframe, thereby avoiding a lot of error-prone work in formulating the simulation programme.

However, a usual case of kinematic constraint is that the mass point M has only one degree of freedom in the  $u, v, w$ -system like the stroking motion of an oleo-pneumatic strut. This problem can be tackled in three ways:

First, a system of equations can be set up and algebraically solved for the unknown acceleration and forces. However, this is a tremendous effort for perfectly simulating a physically unrealistic model.

Second, a relatively straightforward approach is to assign nonzero mass values to the "mass point" only in its independent degree(s) of freedom, thereby putting the unknown "internal" forces equal to the known "external" forces in the dependent d.o.f.'s. The error which thereby is introduced to simulation of aircraft dynamic response to repaired runways is small.

The third way to solve the problems of kinematic constraints is to replace the kinematic constraints by elastic constraints. This is certainly the model which is closest to physical reality, though acquisition of undercarriage stiffness data sometimes can be a cumbersome task. Yet the data is anyway required for landing loads calculations in which undercarriage leg bending and torsion play an important rôle. In general no peculiar trick is required to establish a model which lends itself to numerical integration. Therefore we prefer this type of approach for simulations which are performed for prediction or recalculation of full scale aircraft tests.

### 3.3 Bearing Friction

Depending on the design of an oleo-pneumatic undercarriage leg some 20 % of the longitudinal force in the strut can be introduced by friction at the sliding bearings between piston and cylinder, the other 80 % being made up by the gas-spring force, the hydraulic damping force, and the sealing friction force. Average magnitude of the effect alone would already justify the inclusion of friction in the simulation model, notwithstanding the fact that a poor undercarriage design in combination with adverse loading conditions can lead to transient self-locking of the strut. This and static friction at reversal of the strut stroking motion contribute discontinuous undercarriage load fluctuations which may excite higher eigenfrequencies of the airframe.

The friction of undercarriage bearings can be considered to be dry friction [17], therefore friction force is proportional to the normal force on the bearings. Normal forces on upper and lower bearing depend on magnitude of forces and moments acting on a suitably chosen reference point on the piston longitudinal axis (see Fig. 5a), on momentary distances from this reference point to the lower piston bearing and from lower to upper bearing, and on torque link geometry. Torque link geometry is quite important, because torque around piston longitudinal axis acting at the reference point is taken out from the piston by a force couple acting at points A and B (Fig. 5a) normal to the torque link plane, thus introducing an additional shear force normal to the piston at point A.

This shear force with the geometry of Fig. 5b is

$$F_{NT} = \frac{M_{ZR}}{l_T} \quad (16)$$

$l_T$  being nonlinearly dependent on the stroke  $s$ .

Hence

$$F_{NxT} = F_{NT} \cdot \sin \varphi \quad (17.a)$$

$$F_{NyT} = F_{NT} \cdot \cos \varphi \quad (17.b)$$

where the angle  $\varphi$  gives the orientation of the torque link plane with respect to the positive x-axis. Now the normal force x-component at the upper bearing (Fig. 5c)

$$F_{1x} = \frac{F_{NxT}(l_3-s) + F_{NxR}(l_2-s) + M_{YR}}{(l_1+s)} \quad (18.a)$$

The y-component is

$$F_{1y} = \frac{F_{NyT}(l_3-s) + F_{NyR}(l_2-s) - M_{xR}}{(l_1+s)} \quad (18.b)$$

For the lower bearing the components read

$$F_{2x} = -\frac{F_{NxT}(l_1+l_3) + F_{NxR}(l_1+l_2) + M_{YR}}{(l_1+s)}$$

$$F_{2y} = -\frac{F_{NyT}(l_1+l_3) + F_{NyR}(l_1+l_2) - M_{xR}}{(l_1+s)}$$

AD-A122 061

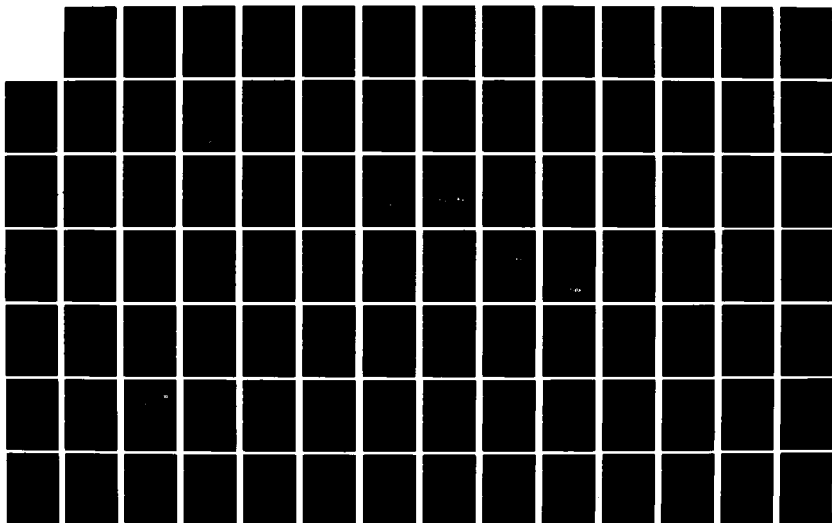
AIRCRAFT DYNAMIC RESPONSE TO DAMAGED AND REPAIRED  
RUNWAYS(U) ADVISORY GROUP FOR AEROSPACE RESEARCH AND  
DEVELOPMENT NEUILLY-SUR-SEINE (FRANCE) AUG 82  
AGARD-CP-326

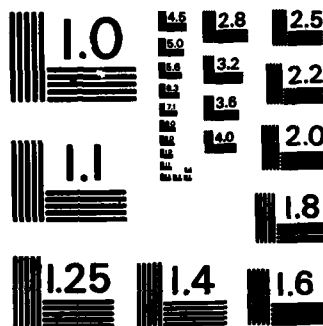
2/3

UNCLASSIFIED

F/G 1/5

NL





MICROCOPY RESOLUTION TEST CHART  
NATIONAL BUREAU OF STANDARDS-1963-A



The resultant normal forces at the upper and lower bearings are

$$F_1 = + \sqrt{F_{1x}^2 + F_{1y}^2} \quad (19.a)$$

$$F_2 = + \sqrt{F_{2x}^2 + F_{2y}^2} \quad (19.b)$$

The kinetic friction force

$$F_{Fk} = \pm (\mu_{1k} \cdot F_1 + \mu_{2k} \cdot F_2) \quad (20.a)$$

where the sign (viz. the direction) is determined by the fact that the kinetic friction force is always opposing the actual motion of the piston.

The static friction force can attain any value between

$$-(\mu_{1s} \cdot F_1 + \mu_{2s} \cdot F_2) \leq F_{Fs} \leq + (\mu_{1s} \cdot F_1 + \mu_{2s} \cdot F_2) \quad (20.b)$$

The actual value balances the sum of  $F_{ZR}$  and gas-spring force  $F_g$ , thus keeping the piston at rest unless the breakout force is exceeded.

As a consequence, a kinematic constraint is added to the system with accompanying difficulties as discussed in para 3.2 above. However, these difficulties should not seduce the analyst to drop strut internal friction from the model, rather he should look for a reasonable approximation. Even if this approximation has a deviation of say 20 % from the true value, the remaining error in the total force is cut to 4 % from an assumed 20 % error when omitting friction force on the whole.

A practical way to avoid the additional kinematic constraint from static friction is to approximate the static friction coefficient by

$$\mu_s = \mu_{s0} \cdot \frac{2}{\pi} \arctan (SF_s \cdot \dot{s}) \quad (21)$$

This leads to "static friction" being zero at rest, but depending on the magnitude of the scaling factor  $SF_s$  the gradient of  $\mu_s$  versus  $\dot{s}$  can be made very steep around  $\dot{s} = 0$ , thus approximating the true rest of the piston by a very slow creeping motion.

If deemed necessary the kinetic friction coefficient can also be defined as a function of the stroking velocity  $\dot{s}$ , and switching between the functions can be performed based on the actual value of  $\dot{s}$ . A practical approximation for the kinetic friction providing an uncritical (stepless) transition from the static friction is

$$\mu_k = \frac{\dot{s}}{|\dot{s}|} \cdot \mu_{k0} \cdot \left(1 + \frac{1}{SF_k \cdot \dot{s}^2}\right) \quad (22)$$

An example for a resulting friction coefficient function is shown in Fig. 6 .

However, the coefficient of friction is only part of the picture because the friction force is calculated from  $\mu$  times normal force on the bearing. Tracing back the normal forces  $F_1$  and  $F_2$  from equations 20 to equation 16 it is realized that the friction force is a nonlinear conglomeration of all forces and moments (except  $F_{ZR}$ ) acting at point R of Fig. 5a . That means that any kinematic constraint between points R and W of the undercarriage leg gives rise to trouble in the model. If the forces and moments at R cannot be determined from elastic deformation, it is therefore advisable to replace in the friction force equations the true values of the unknown forces and moments by estimated values. A very practical and straightforward method to obtain a good estimate is to calculate forces and moments at one point in time and to substitute them to calculate the friction force of the next time step. Obviously the estimate is the better the shorter the integration time step is.

### 3.4 Hydraulic Damping

#### 3.4.1 Derivation of Damping Force

One of the salient features of an oleo-pneumatic shock strut is hydraulic damping. In contrast to the non-controllable and therefore undesirable bearing friction hydraulic damping provides a very efficient and controllable means to dissipate energy from the stroking motion of the strut. Basically, energy is dissipated by displacing hydraulic fluid from one chamber of the strut into another (see Fig. 7 ) the energy dissipated being the integral

$$E_d = \int_0^t (p_1 - p_2) \dot{V} dt \quad (23)$$

where

$$\begin{aligned} p_1 [N/m^2] & \text{ pressure in chamber 1} \\ p_2 [N/m^2] & \text{ pressure in chamber 2} \\ \dot{V} [m^3/s] & \text{ rate of volume displacement} \end{aligned}$$

The momentary power of dissipation is

$$P_d = (p_1 - p_2) \cdot \dot{V} \quad (24)$$

and the damping force acting on the piston is

$$F_d = P_d / \dot{s} = (p_1 - p_2) \cdot \dot{V} / \dot{s} \quad (25)$$

Neglecting compressibility effects  $\dot{V}/\dot{s}$  can be assumed to be constant and is commonly called the hydraulic area  $A_h$  of the piston. Thus the damping force is directly proportional to the pressure drop across the damping diaphragm. The magnitude of this pressure drop depends on the nature of the flow through the damping orifices. Since in usual oleo-pneumatic shock strut design the damping orifices are very small compared with the hydraulic area of the piston and since they are short the flow can be considered to be turbulent except at very low stroking velocities. However, for simulation purposes the flow can be assumed to be turbulent for all stroking velocities, because the damping force at low stroking velocity is negligibly small in any case.

Assuming turbulent flow through the orifices the differential pressure and hence the damping force can be deduced from the physics of efflux out of a pressurized vessel and is proportional to the square of the stroke velocity and opposing the stroking motion:

$$F_d = C_d \cdot \dot{s} \cdot |\dot{s}| \quad (26)$$

Thus the damping force does not pose any modelling problems, even if the damping force coefficient  $C_d$  is made a function of stroke (e.g. orifice being influenced by a metering pin) and/or direction of motion (e.g. due to a rebound snubber valve).

### 3.4.2 Frequency Analysis of a Forced Stroking Motion

As already mentioned in para 3.1 undercarriage damping causes coupling between the structural modes. An experience similar to that appearing in Fig. 1 brought us to thinking over the effects of undercarriage damping in general and specifically of velocity-squared damping. Our experience was that supposedly improving the simulation by addition of higher structural modes resulted in increasing structural peak loads with no distinct trend to leveling off as would have been expected. We concentrated our search for possible causes of this unexpected "improvement" on the hydraulic damping force. Some of these considerations and results are presented in the following.

Consider a model of an oleo-pneumatic shock strut as outlined in Fig. 8. The strut end-load  $F_e$  is composed of the hydraulic damping force  $F_d$  and the gas-spring force  $F_g$ . For sake of simplicity the latter is assumed to result from isothermal compression of a gas volume  $V_0$  prepressurized to yield an  $F_{g0}$  preload in the strut fully extended position ( $s = 0$ ):

$$F_g = F_{g0} \cdot \frac{V_0}{V_0 - A_h \cdot s} - F_{atmos} \quad (27)$$

Substituting  $F_d$  from equation 26 yields

$$F_e = F_d + F_g = C_d \cdot \dot{s} \cdot |\dot{s}| + F_{g0} \cdot \frac{V_0}{V_0 - A_h \cdot s} - F_{atmos} \quad (28)$$

Equation 28 was used to perform some numerical calculations.

In order to obtain illustrative results, the constants of equation 28 were chosen in the vicinity of a real oleo-pneumatic shock strut:

$$\begin{aligned} C_d &= 13000 \text{ Nm}^{-2} \text{ s}^2 \\ F_{g0} &= 23126 \text{ N} \\ F_{atmos} &= 900 \text{ N} \\ V_0/A_h &= 0.3953 \text{ m} \end{aligned}$$

It was assumed that the stroke of the oleo should vary with time according to

$$s = s_0 + \epsilon_1 \cdot \sin(\omega_f t) \quad (29)$$

$$\dot{s} = \epsilon_1 \cdot \omega_f \cdot \cos(\omega_f t) \quad (30)$$

with numerical values

$$s_0 = 0.2953 \text{ m}$$

$$\epsilon_1 = 0.04 \text{ m}$$

$$\omega_f = 6\pi, 12\pi, 18\pi, 24\pi, 30\pi, 36\pi \text{ rad}\cdot\text{s}^{-1}$$

The resulting periodic function for  $F$  was subjected to a numerical Fourier analysis, the result of which is shown in Fig. 11. This figure shows the magnitude of the Fourier coefficients as a function of frequency for the fundamental and the first and second harmonic frequency. The horizontal lines represent the contribution of the gas-spring force, which is (mathematically) independent of frequency. With the present numerical data the magnitude of the gas-spring contribution at the first harmonic is approximately 20 % of that at the fundamental, the contribution at the second harmonic is about 3 %. The velocity-squared nature of the hydraulic damping force is reflected in the parabolic rise of the damping contribution with frequency. Damping does not contribute to the magnitude of the coefficient at the first harmonic (which fact can also be derived analytically). However, there is a contribution of considerable magnitude to the coefficient at the second harmonic. This can be considered a candidate source for excitation of higher structural modes via intermodal coupling.

In a real environment the stroking motion of an oleo-pneumatic strut can be composed of oscillations of different frequencies and amplitudes. We therefore superimposed a stroking oscillation with double frequency and  $1/8$  the amplitude of the fundamental motion, thus that

$$s = s_0 + \epsilon_1 \cdot \sin(\omega_f t) + \frac{\epsilon_1}{8} \cdot \sin(2\omega_f t + \frac{\pi}{2}) \quad (31)$$

$$\dot{s} = \epsilon_1 \cdot \omega_f \cdot \cos(\omega_f t) + \frac{1}{4} \cdot \omega_f \cos(2\omega_f t + \frac{\pi}{2}) \quad (32)$$

Compared with the case of Fig. 11, Fig. 12 shows an increase of about 8 % in damping force coefficient at the fundamental frequency and a damping force contribution at the first harmonic, as expected. However, this contribution is about seven times larger than it would have been for a stand-alone stroking oscillation of  $\epsilon_1/8$  amplitude.

Figs. 11 and 12 demonstrate two inconvenient features of the velocity-squared damping force:

- o The force function produced by a forced stroking oscillation contains considerable components at even harmonics of the fundamental frequency.
- o Superposition of oscillations yields mutual augmentation of the components.

Fig. 13 includes an additional stroking oscillation with frequency  $3\omega_f$  and amplitude  $\epsilon_1/64$ .

$$s = s_0 + \epsilon_1 \sin(\omega_f t) + \frac{\epsilon_1}{8} \sin(2\omega_f t + \frac{\pi}{2}) + \frac{\epsilon_1}{64} \sin(3\omega_f t) \quad (33)$$

Though this additional amplitude is very small ( $0.625 \text{ mm} \approx 0.0246 \text{ in}$ ) it effects a 45 % increase over Fig. 12 of the damping force magnitude at  $3\omega_f$ . The case shown in Fig. 13 was used as a basis for further considerations.

### 3.4.3 Compressibility and Flexibility Effects

Compressibility of the hydraulic fluid, dilatation of the cylinder, and structural flexibilities such as wheel axle bending and local flexibility of the undercarriage attachments reduce the stiffness of the gear in stroking direction. This additional flexibility can amount to about 10 % of the nominal gas-spring flexibility. We evaluated this figure from measurements on an undercarriage attached to an airframe-like structure.

Looking to the amplitudes of the forced stroking motion analyzed in Fig. 13 it is not hard to realize that additional flexibility should have a sensible influence on the force response of our small simulation model. Usually additional flexibility provided by hydraulic compressibility and vessel dilatation is added to the flexibility of the gas-spring [16], [17]. Therefore the basic oleo model of Fig. 8 was "redesigned" to contain an additional flexibility of approximately  $1.5 \cdot 10^{-7} \text{ m/N}$  in series to the gas-spring (Fig. 9). Fig. 14 was obtained by applying the same forced stroking motion (Equation 33) as for Fig. 13, except that  $s_0$  was adjusted to yield identical static load. Fig. 14 therefore is directly comparable to Fig. 13.

The softer spring characteristic shows up at the reduced gas-spring contribution at the fundamental frequencies (dotted lines from Fig. 13 for comparison), however, it is compensated by the damping force contribution at higher fundamental frequencies. Fig. 14 and Fig. 13 are practically identical for the harmonics.

It is concluded that lumping the additional flexibilities into the gas-spring is acceptable for landing loads calculations with appropriately low frequencies. In this case, however, not much of a difference should result from lumping the additional flexibility into the tyre, which yields a more convenient mathematical formulation.

Physically, only a small fraction of the additional flexibility combines with the gas-spring flexibility, namely the compressibility of that part of the hydraulic fluid which is on the gas-spring side of the damping diaphragm, and the dilatation of this part of the shock strut. All the rest of the additional flexibility lies in series to both gas-spring and hydraulic damper. Therefore an oleo model as sketched in Fig.10 is considered more realistic than those of Figs. 8 and 9.

Neither the deflection of the gas-spring nor the stroking velocity of the damper is rigidly connected to the forced stroking motion of the foot point anymore. Rather, the condition that the force produced by deflection of the "additional flexibility" spring must equal the sum of gas-spring force and hydraulic damping force yields a second order differential equation for the displacement  $s_p$  of the piston in the cylinder:

$$\ddot{s}_p = \pm \left[ C_{af} \left( \frac{\dot{s}_p}{s_p} - 1 \right) - F_{go} \frac{V_o A_h}{(V_o - s_p A_h)^2} \right] / (2 \cdot C_d) \quad (34)$$

positive sign for  $\dot{s}_p \geq 0$

negative sign for  $\dot{s}_p < 0$

where

$C_{af}$  [N/m] stiffness of the additional spring,

$s_p$  [m] displacement of the piston in shock strut.

This differential equation was integrated numerically and the resulting endload  $F$  was Fourier-analyzed after the transients has ceased. The magnitude of the coefficients is shown in Fig. 15 a~c, the comparable coefficients from Figs.11, 12, 13 (no additional flexibility) being shown as dotted lines. There is no doubt that neglecting in the model those longitudinal flexibilities of an undercarriage which lie in series to the hydraulic damping will produce an overly conservative prediction of dynamic response to repaired runways for basic excitation as well as for coupling effects between structural modes of the airframe.

### 3.4.4 Further Considerations

With respect to dynamic response of the airframe hydraulic damping becomes a really crucial point in the model only when an "unsprung mass" exists at the lower end of the undercarriage leg, because otherwise the tyre more or less takes on the function of the additional flexibility. Nevertheless, we recommend to model unsprung masses because vertical acceleration of unsprung mass can be high in a damaged runway environment and can lead to significant transient differences between tyre and shock strut forces.

Actual "additional flexibilities", in particular the structure around undercarriage attachments exhibit structural damping which slightly lessens the load-alleviating effect of the additional flexibility. Though the correct value for this damping would be "nice to have", it is much less important than the correct value for the flexibility itself and for the hydraulic damping coefficient.

The magnitude of generalized undercarriage forces acting on the natural modes of the airframe model is dependent on modal values of the assumed undercarriage leg attachment point A (Fig. 3). Usually this point is considered to be rigidly connected to a suitable reference point on the flexible beam representation of the airframe (see for instance Fig. 2). Consider now the case that this reference point misses the physically true proper reference point by an error distance "e". This basic error does not at all affect modal values at point A for rigid body modes. For flexible modes, however an error is introduced to the modal values at point A. The sign and magnitude of the errors relative to the physically true values depend on the change of modal values along the beam at distance "e" from the "true" reference point. Since modal values change more rapidly with increasing order of the mode, relative error in the modal values at point A and hence relative error in the generalized undercarriage forces increases with increasing order of the mode involved.

Therefore the inclusion of high order modes in a simulation model for aircraft dynamic response on repaired runways could require a revised (e.g. three point) method of undercarriage attachment modelling. However, this would entail another sharp increase of model complexity. At present we are looking for a practical method to define an "optimum complexity" model, i.e. a model which is of lowest possible complexity for a specified tolerance bandwidth between simulation and reality.

#### 4. CONCLUSIONS

It has been shown that comprehensive treatment of aircraft dynamic response to damaged and repaired runways requires comprehensive treatment of the undercarriage. In particular a model which is used to predict or recalculate full scale aircraft tests must cope for nonlinearities of the undercarriage.

Bearing friction is one of these nonlinear features which due to its magnitude must not be ignored. Due to peculiar requirements of digital simulation programs, however, bearing friction is hard to treat in a rigorous way. Yet practical methods exist to approximate bearing friction force with sufficient accuracy.

The frequency spectrum of repaired runways may exhibit significant excitation at any of the natural modes which might be included in a structural response analysis. However, already at relatively low frequencies velocity-squared hydraulic damping yields a significant contribution to the force acting along the oleo strut. By parametric studies on a simplified oleo model it has been demonstrated in this paper that besides gas-spring flexibility other undercarriage flexibilities must be included in a realistic simulation model. Otherwise a coupled flexible airframe/undercarriage simulation model will by far overestimate aircraft dynamic loads response on damaged and repaired runways.

## REFERENCES

- [1] Milwitzky, Benjamin, and Cook, Francis E.: Analysis of Landing Gear Behaviour. NACA Rep. 1154, 1953
- [2] Sellers, William H., and Caulkins, Roger E.: Dynamics of Landing Gear Impact, Rebound, and Runout. WADD-TR-60-483, 1962
- [3] Ijff, Jacob: Analysis of Dynamic Aircraft Landing Loads, and a Proposal for Rational Design Landing Load Requirements. Doctoral Thesis, Technische Hogeschool te Delft (Netherlands), 1972.
- [4] Abraham, B.\*: A Dynamic Analysis of Landing Impact. In 20th Israel annual conference on aviation and astronautics. Collection of papers; Ministry of Transport, Tel Aviv (Israel), 1978.
- [5] McGehee, John R., and Carden, Huey D.: A Mathematical Model of an Active Control Landing Gear for Load Control during Impact and Roll-out. NASA TN D-8080, 1976.
- [6] Carden, Huey D., and McGehee, John R.: Validation of a Flexible Aircraft Take-off and Landing Analysis (FATOLA). NASA TP-1025, 1977.
- [7] Gerardi, Anthony G.: Digital Simulation of Flexible Aircraft Response to Symmetrical and Asymmetrical Runway Roughness. AFFDL-TR-77-37, 1977.
- [8] Cox, Joseph J., Henghold, William M., and Russell, John J.: A Literature Search & Review of the Dynamics of Aircraft-Surface Interaction. CEEDO-TR-78-39, 1979.
- [9] Ferguson, T.R., Mollick J., and Kitts, W.W.: A Rational Method for Predicting Alighting Gear Dynamic Loads. Volume I, General Methods. ASD-TDR-62-555, 1963.
- [10] Caldwell, Lapsley R.: Runway Surface Roughness. In "Aircraft Dynamic Response to Damaged Runways", AGARD Report No. 685, 1980.
- [11] Payne, B.W., Dudman, A.E., Morris, B.R., Ormerod, M., Brain, C.: U.K. Approach to Aircraft Dynamic Response on Damaged and Repaired Runways. In AGARD Report No 685, 1980.
- [12] Krauss, Arnulf, Bartsch, Otto, and Kempf, Gunther: Parameters Affecting Aircraft Performance on Runways in Bad Condition. in AGARD Report No. 685, 1980.
- [13] Anon.: Luftfahrttechnisches Handbuch, Handbuch Belastungsmechanik.
- [14] Freymann, R.: Über das aeroelastische Verhalten von Flugzeugen mit aktiven Servo-Kontrollsystemen. Deutsche Forschungs- und Versuchsanstalt für Luft- und Raumfahrt, DFVLR-FB81-05, 1981.
- [15] Guillon, M.: Hydraulische Regelkreise und Servosteuerungen. Carl Hanser Verlag, München, 1968.
- [16] O'Massey, R.C.: Introduction to Landing Gear Design. Douglas Paper 5767, presented to American Society for Metals WESTEC Meeting, Los Angeles, March 1970.
- [17] Wahi, Mahinder K.: Oil Compressibility and Polytropic Air Compression Analysis for Oleopneumatic Shock Struts. J. Aircraft, Vol.13, No.7, July 1976.

---

\* The author's correct name probably is Brot, A.

# HAVE BOUNCE F-4E

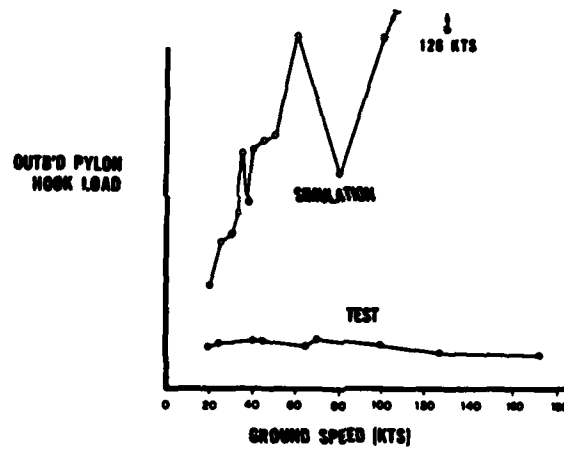


Fig.1 Pylon Loads (from [10])

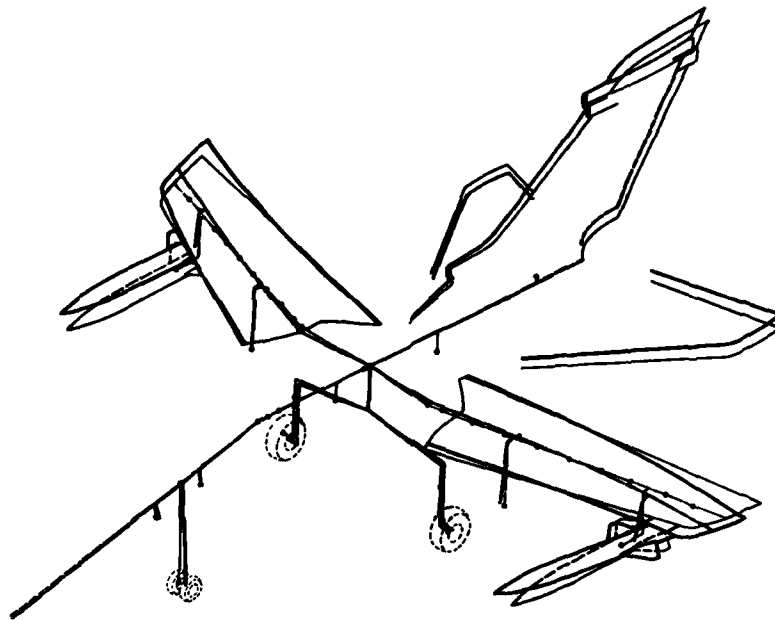


Fig.2 Dynamic Model (superimposed for illustration: 8th natural mode, aircraft yawing and yawing, wing 2nd bending)

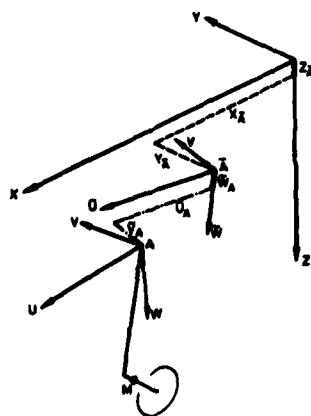


Fig.3 Undercarriage Coordinate Systems

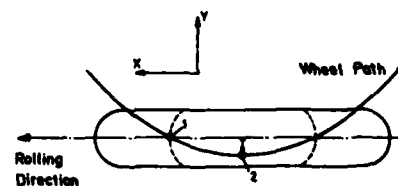


Fig.4 Tyre Sideforce due to Wheel Path Curvature

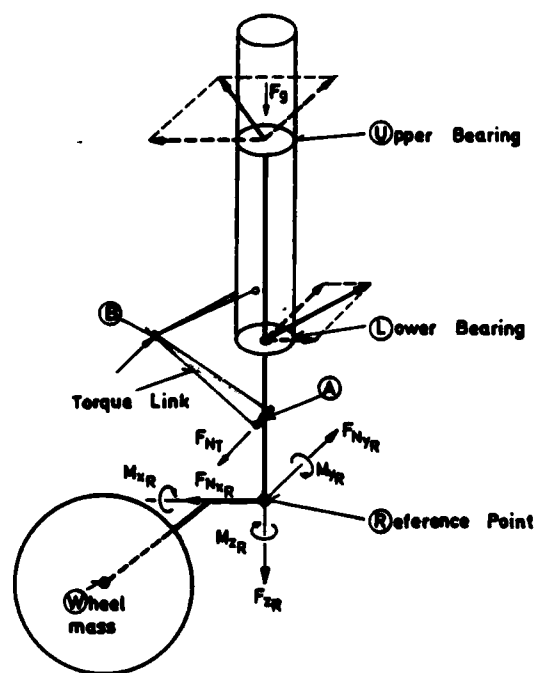


Fig.5a Normal Loads on Sliding Bearings

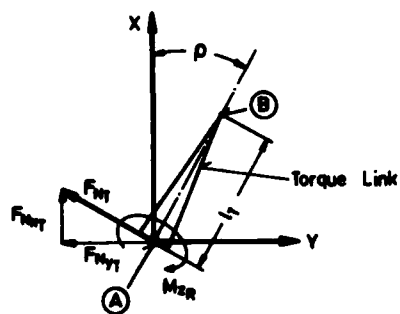


Fig.5b Torque Link Geometry

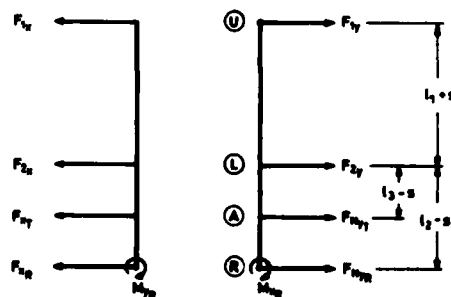


Fig.5c Load Components

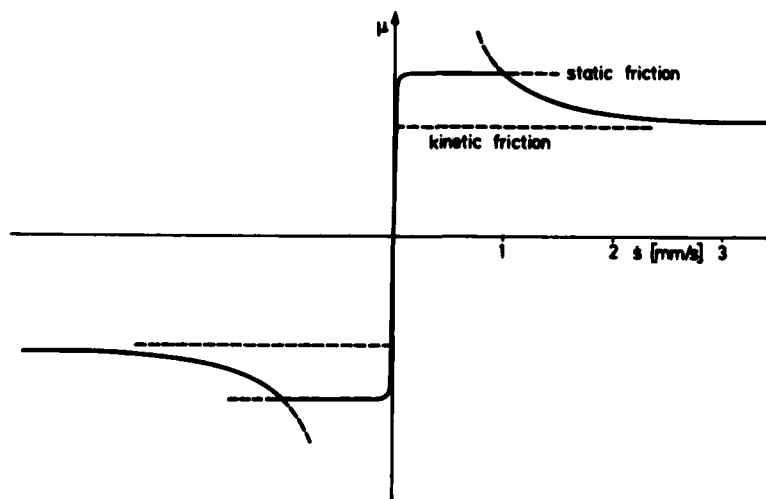


Fig.6 Simulation of Bearing Friction Coefficient



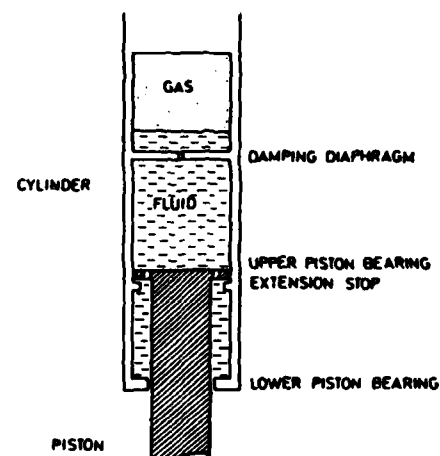
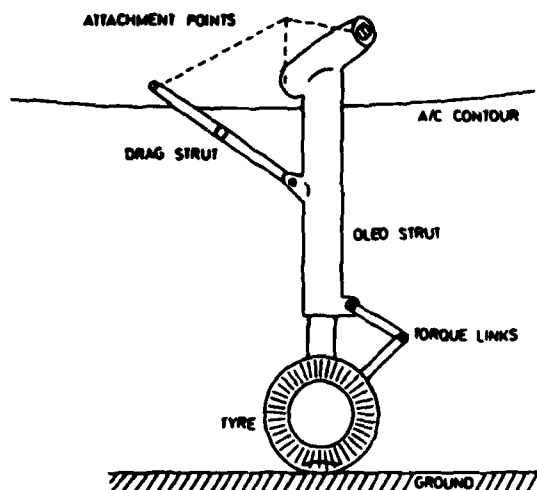


Fig.7 Undercarriage Leg with Oleo-pneumatic Shock Strut

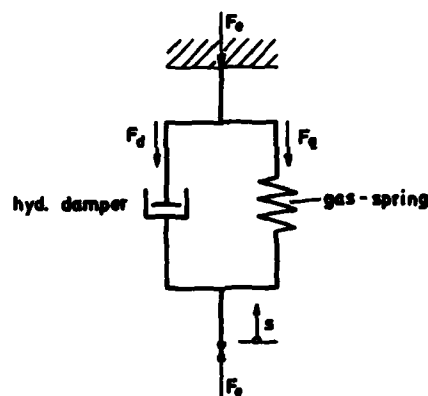


Fig.8 Basic Oleo Model

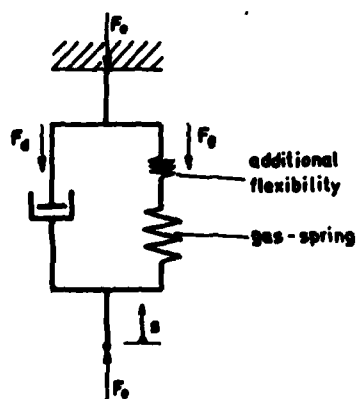


Fig.9 Additional Flexibility in Series to Gas-Spring

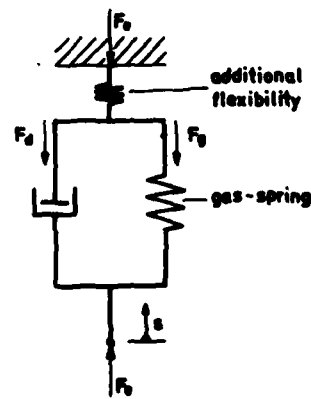


Fig.10 Additional Flexibility in Series to Basic Oleo

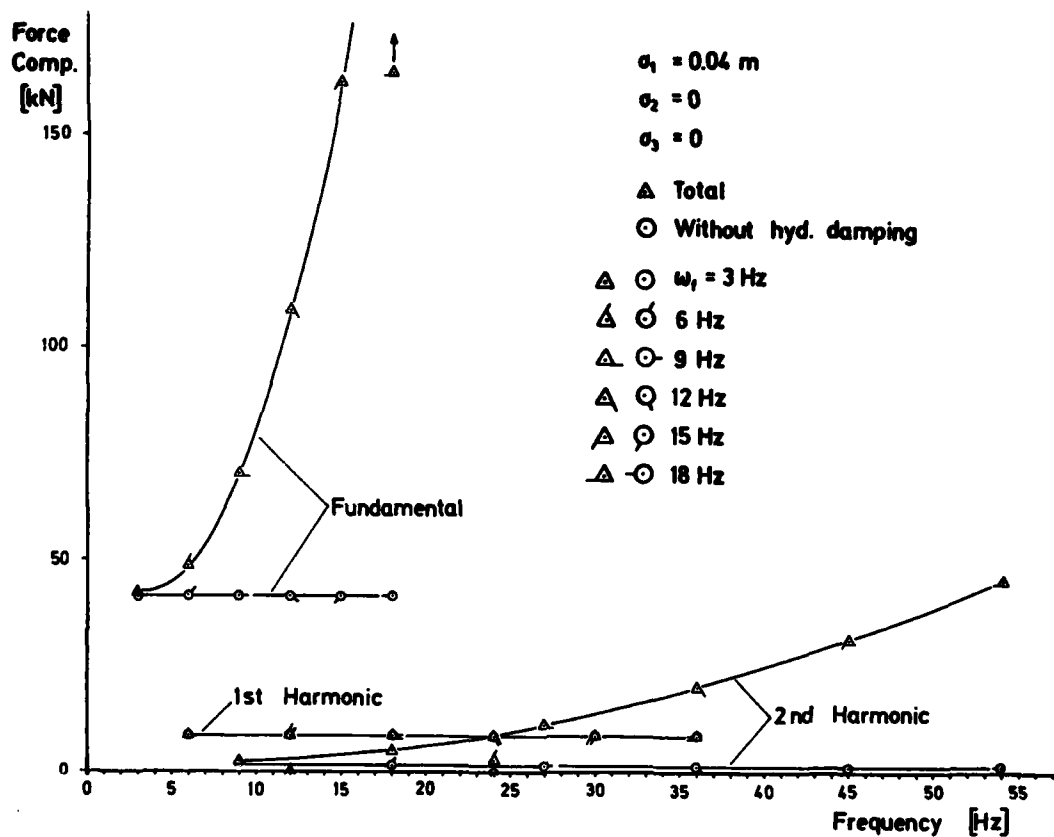


Fig. 11 Fourier Components of Endload (Model from Fig. 8, Excitation at Fundamental Frequency only)

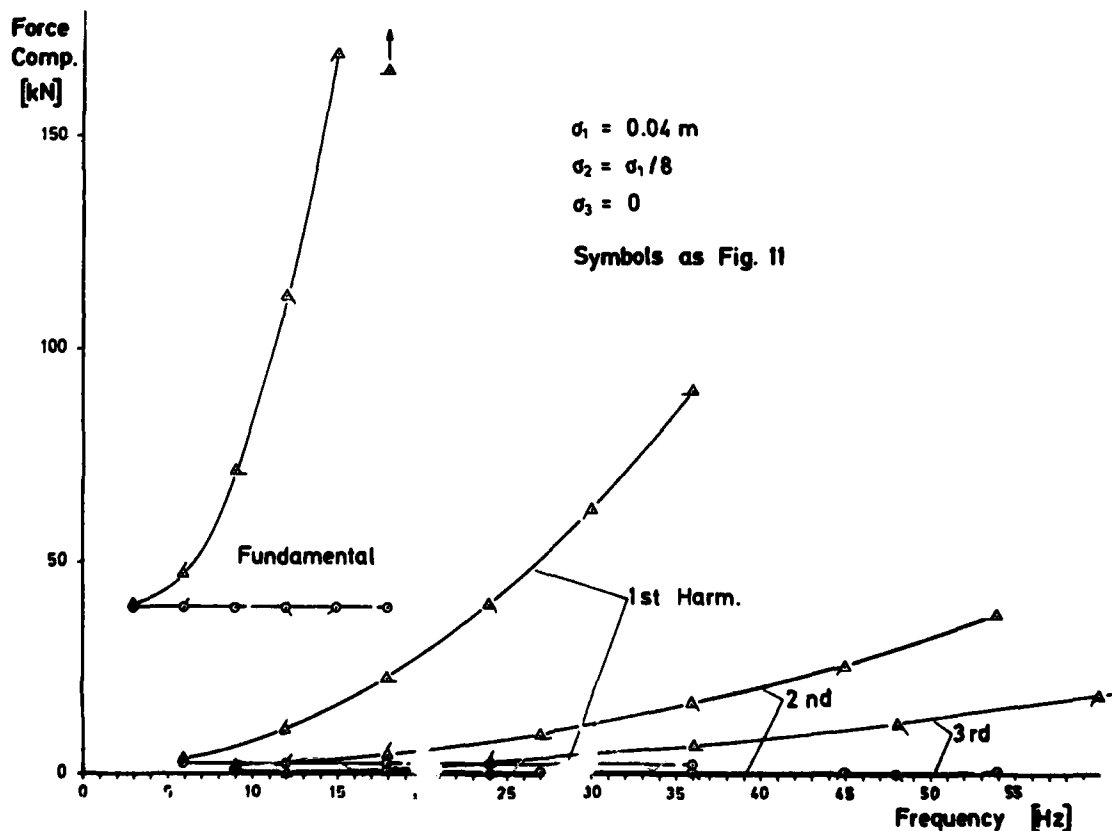


Fig. 12 Fourier Components of Endload (Model from Fig. 8, Excit. at Fundamental and 1st Harmonic)

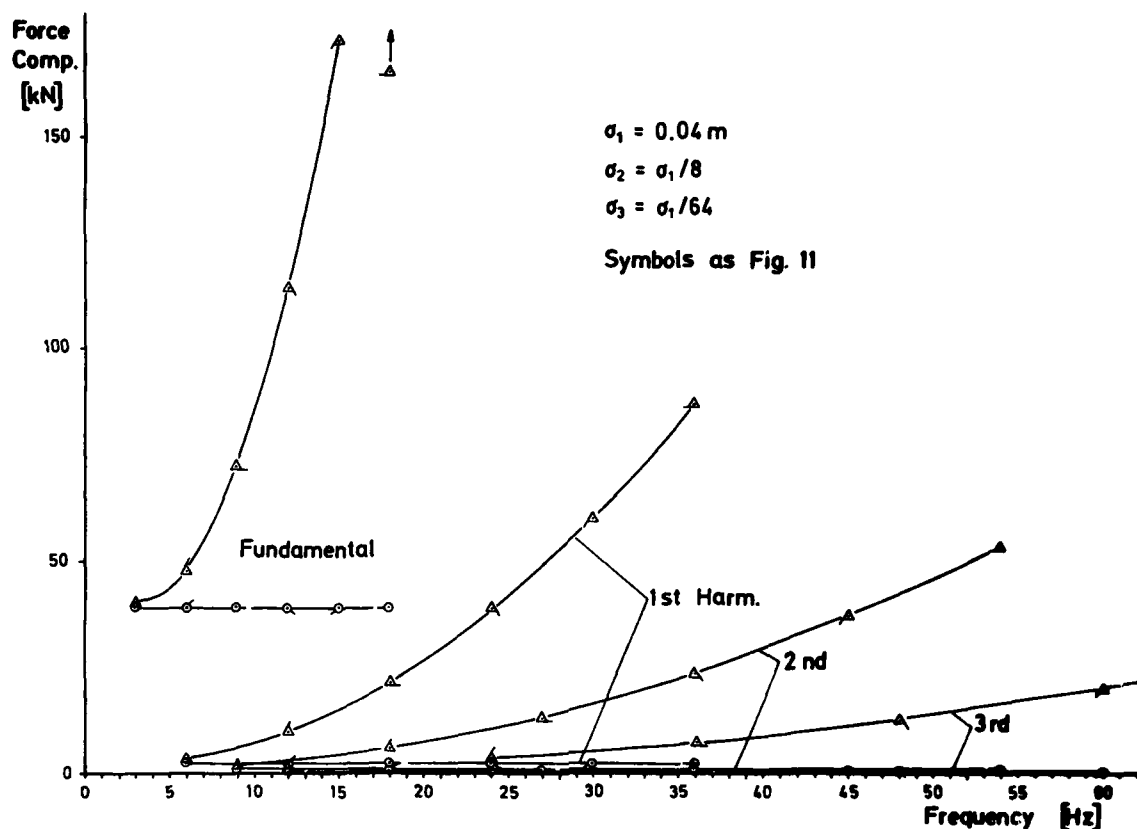


Fig.13 Excitation at Fundamental, 1st, and 2nd Harmonic (Model from Fig.8)

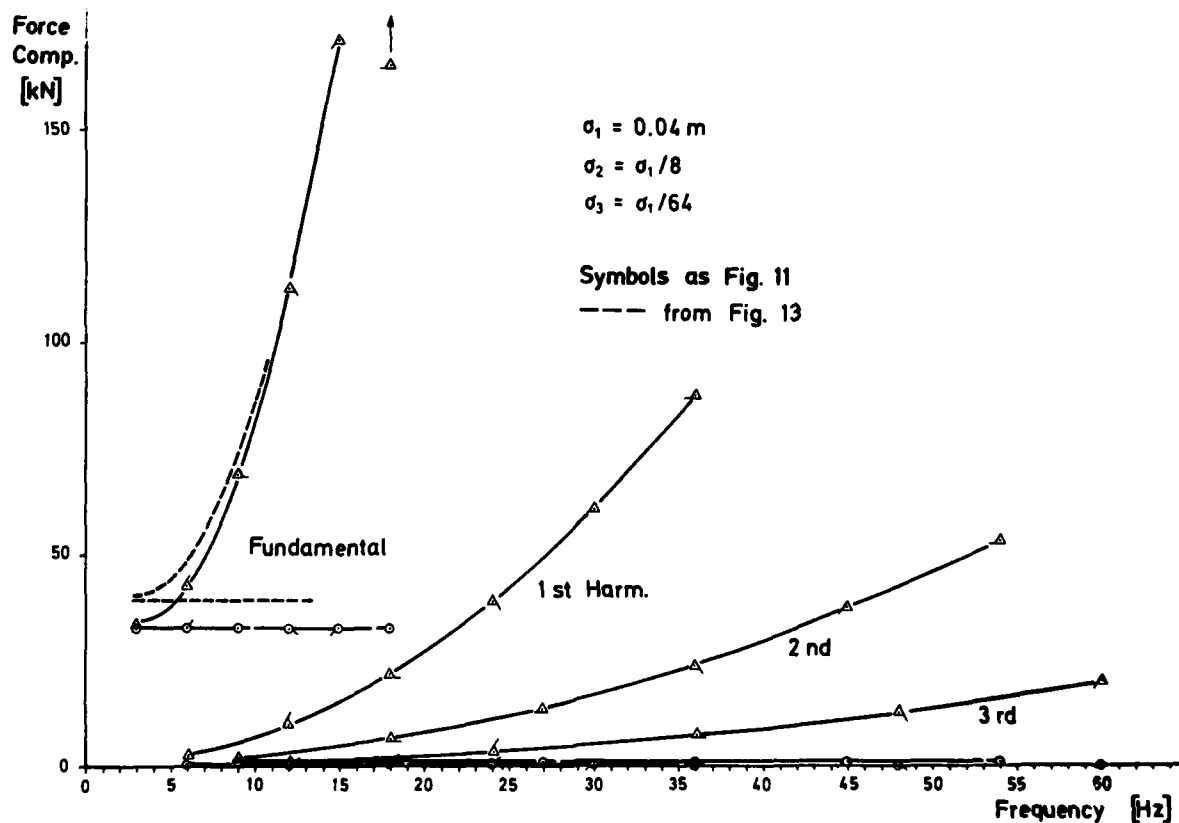


Fig.14 Effect of Additional Flexibility in Series to Gas-Spring (Model from Fig.9)

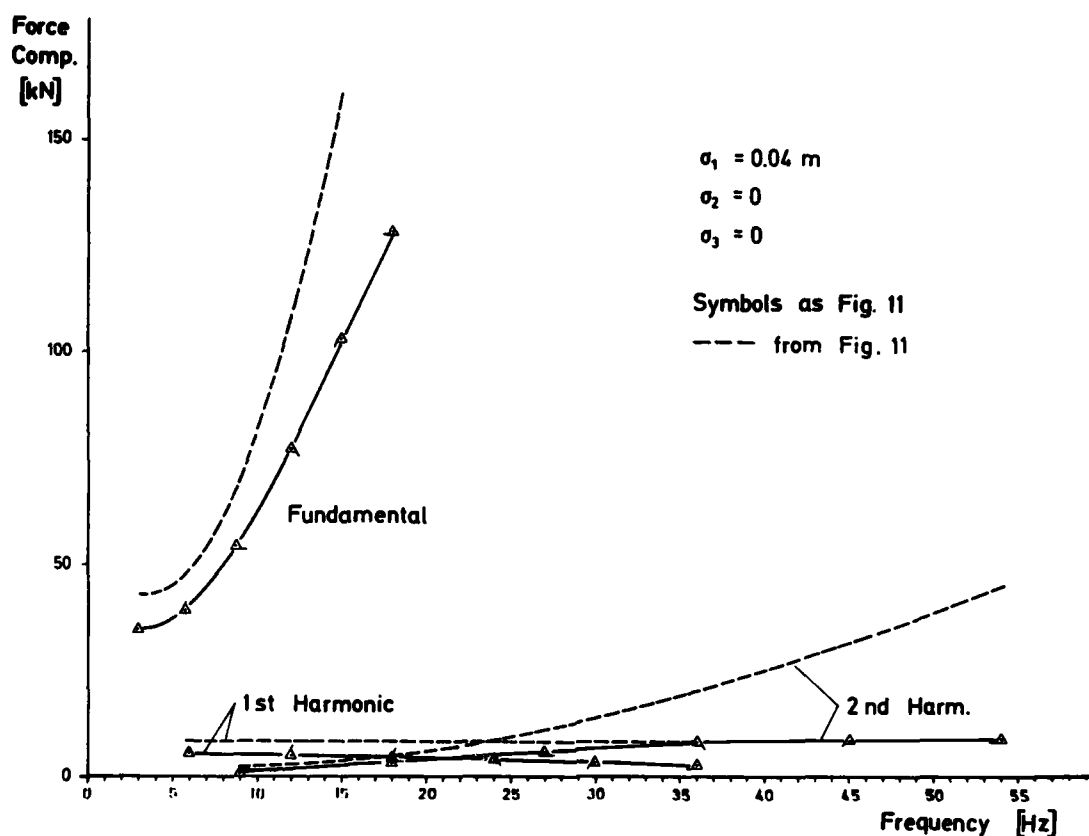


Fig.15a Effects of Additional Flexibility in Series to Basic Oleo (Model from Fig.10). Comparison with Fig.11

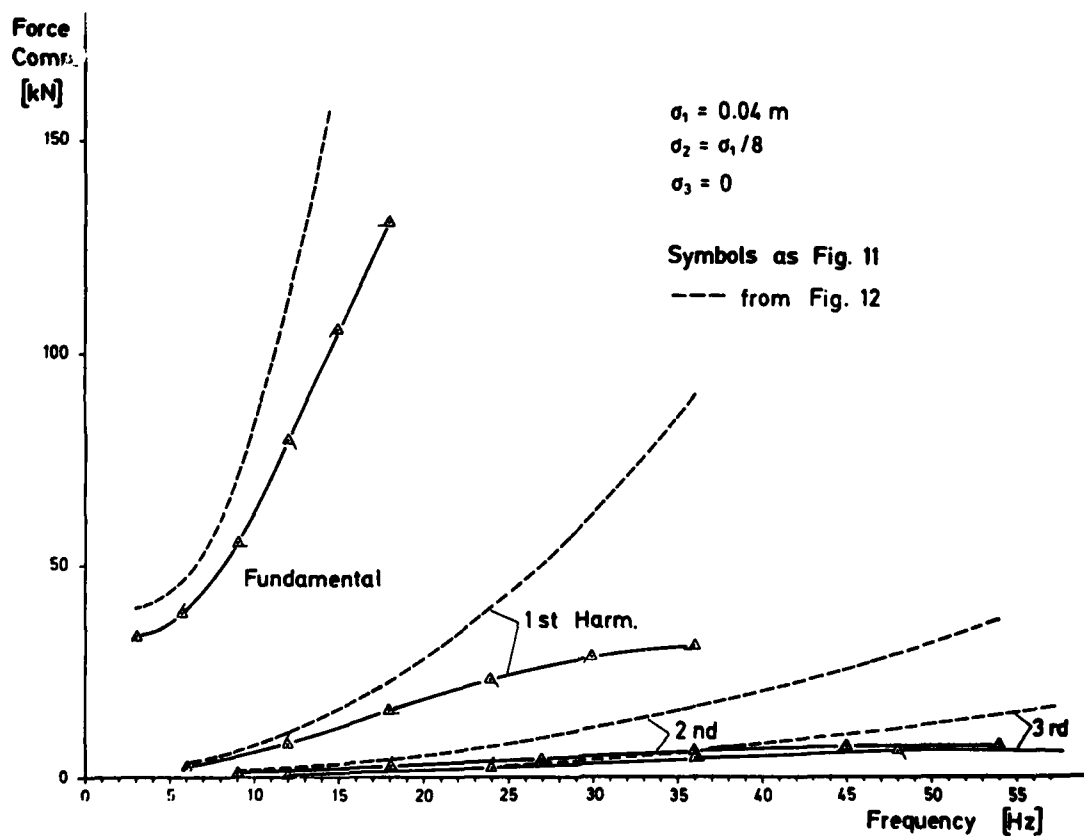


Fig.15b Effects of Additional Flexibility in Series to Basic Oleo (Model from Fig.10). Comparison with Fig.12

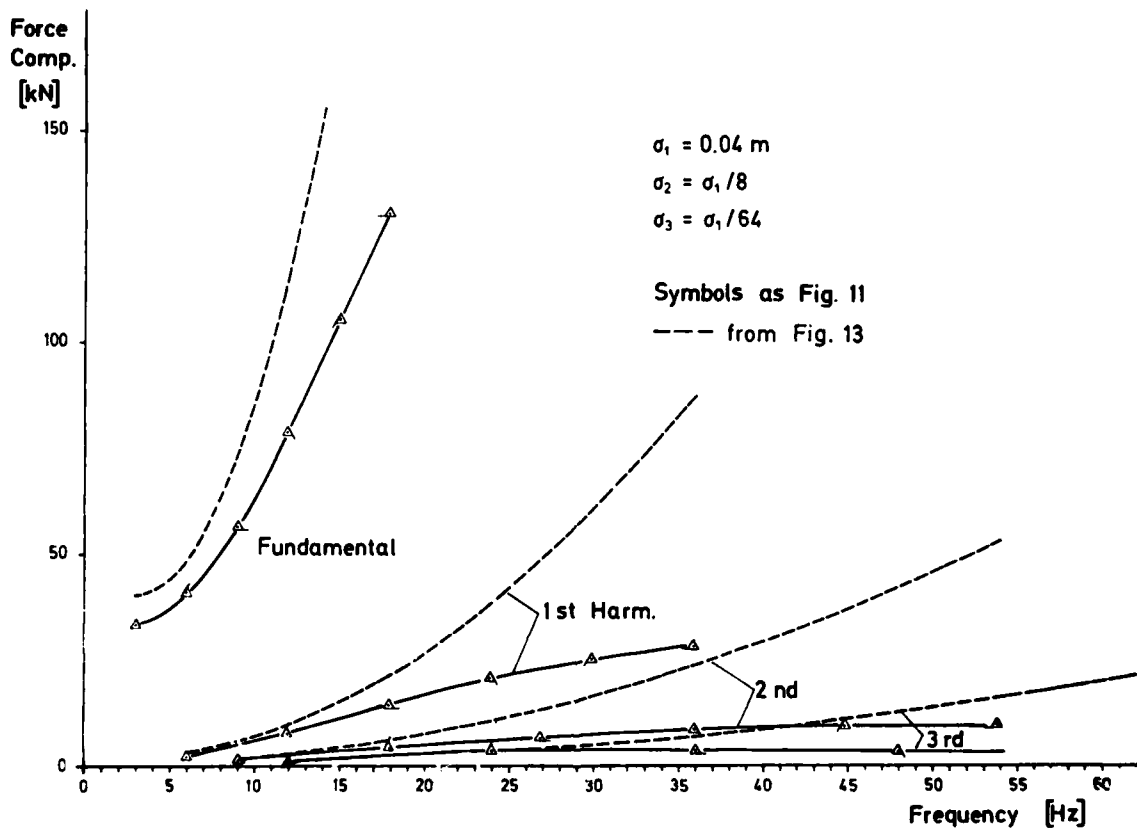


Fig.15c Effects of Additional Flexibility in Series to Basic Oleo  
 (Model from Fig.10). Comparison with Fig.13

# DEVELOPMENT OF A COST EFFECTIVE APPROACH TO MODELLING AIRCRAFT RESPONSE TO REPAIRED RUNWAYS

B.W.PAYNE, A.E.DUDMAN, B.R.MORRIS, M.HOCKENHULL

British Aerospace  
Aircraft Group  
Weybridge-Bristol Division  
Brooklands Road  
Weybridge  
Surrey KT13 0SF U.K.

## SUMMARY

The capability of an aircraft to operate from Repaired Runways concerns the problem of aircraft dynamic response, which in turn gives rise to critical conditions involving aircraft loads and aircraft control.

Present procedures involve mathematically modelling the aircraft, predicting response and validating the theory with the test results, usually without a clear definition of what constitute the limitations in the operational procedures. In order to match the test results accurately, the theoretical computer model may become large, complex and expensive to use and develop, which, because of the limits of resources and time, restricts its operational use.

This paper describes a cost effective approach to this problem, based on development of a simplified model, adapted to each aircraft type, which gives similar results to the fully validated model for the important set of critical loads or accelerations. The simplified model may be used to carry out the operational analyses with the full matrix of variables at minimum cost and time, and use of the more accurate model restricted to the minimum necessary to confirm results.

The final result has been shown to produce an approach which is both adequate and cost effective.

## 1.0 INTRODUCTION

B.Ae (Weybridge) Dynamics Department have been studying mathematical modelling techniques for simulating the response of an aircraft on take-off, landing and during taxiing, for some twenty years, with the basic aim of evaluating structural design loads and accelerations in the aircraft. These theoretical results supported by test measurements have formed the basis of the design clearance.

In recent times there has arisen a need to establish an operational capability for military aircraft on damaged and repaired runways. With this need there has been a fundamental change in test and modelling philosophy. Rather than using test results directly as the basis for specification of the clearance, mathematical modelling is used initially to simulate the response in order to determine the trials requirements, and, once validated, to evaluate the overall operational clearance envelope. Critical loads trials results are now used as a datum against which to validate and improve the mathematical model, and to confirm initial critical modelling predictions. Over the last decade a number of military aircraft, including fighters, bombers and transport aircraft, have been studied in detail regarding their response to repaired runways, and it has been noted that each aircraft has individual and often unique response characteristics critical for the operational clearance.

A consistent and cost-effective approach has been developed to the mathematical modelling of aircraft response to damage repaired runways for three fundamental stages of development

- o a feasibility study leading to trials requirements
- o production of trials results and validation of mathematical model
- o predictions for the operational envelope to define capability

In order to judge the trials requirement for each aircraft, feasibility study results can be obtained quickly using what is basically a relatively simple general purpose computer programme. This allows for subsequent modification of the programme to improve the representation of the critical response areas, and to suit characteristics of the particular aircraft.

In the validation phase, to match the test results accurately, the mathematical model may become large, complex and expensive to use - which, because of limited resources, may restrict its use on the operational envelope. In such cases a need also exists for a simplified model to carry out operational calculations for the full matrix of variables at minimum cost and time. The complex model may then be used to analyse the critical areas shown up by the simplified approach. In some cases it may prove possible to make such simplifications without significant deterioration in the critical response validation - in such an instance minimum reference need be made back to the complex model.

Many of the advantages that accrue from this approach have been made realizable at Weybridge by the use of a dedicated interactive mini-computer system.

This report describes a modelling philosophy which is cost effective and which minimises the requirements on computer resources. Mathematical models of the C-130K Hercules and the VC10 are presented as examples of the overall approach.

## 2.0 MODELLING PHILOSOPHY

### 2.1 General Development

Mathematical modelling of aircraft take-off, landing and taxi response carried out in the Dynamics Department (Weybridge) has been founded on digital computer simulation programmes first directed at fighter and transport aircraft in the late 1950's and early 1960's. Landing gear mathematical modelling of other Weybridge aircraft pre-dates this.

Subsequent development work on Concorde taxi response consolidated the previous programmes into a general purpose take-off, landing and taxi response programme with the following principal features:

- o telescopic nose and main undercarriage with polytropic gas spring, velocity-squared hydraulic damping, and limit friction/stiction.
- o stylus tyre model with single main undercarriage tyre.
- o three symmetric rigid body freedoms with up to eight flexible aircraft modes.

### 2.2 Modelling Philosophy

Diversification of aircraft types, including civil transports such as Concorde and VC.10, and fighters such as Jaguar, accompanied by changing modelling requirements resulted in the need for more detailed modelling capability. This requirement arose partly from the objectives of the task and partly from the characteristics of the aircraft and its undercarriage, and resulted in the establishment of the current overall modelling philosophy. This philosophy is one of "fitness of the model to the task". A consequence is that the area in which modelling detail is concentrated reflects the critical characteristics of the aircraft. Less critical areas need only be represented in reduced detail. For example, if nose undercarriage loads were of principal concern, then a full bogie representation of a main undercarriage may well prove to be unnecessary, but fine detail of a nose oleo gas spring hysteresis and bottoming characteristics may be essential. The fundamental approach to implementing detail improvements is to retain the relatively simple general purpose programme as a basic framework on which to append more detailed subroutines as and when required.

### 2.3 Examples of Approach

Some examples of particular detail modelling requirements follow:

#### 2.3.1 Concorde Taxi Response

Mathematical modelling of Concorde taxi response was directed towards prediction of vertical cockpit accelerations on rough runways and investigations of mechanisms by which they could be reduced. The Concorde fundamental fuselage bending mode was such that the original design of main undercarriage oleo caused it to be excessively excited, causing high cockpit accelerations. The eventual solution was a modification to incorporate a second high pressure oleo gas chamber. Naturally modelling detail was concentrated in this area for investigation and assessment of the benefits of the change. Figure 2.1 shows the 50% reduction in oleo stiffness that was achieved in this way. The oleo gas spring model used for short duration runs allowed polytropic perturbations from a static position on the isothermal curve shown.

#### 2.3.2 Jaguar Taxi Response

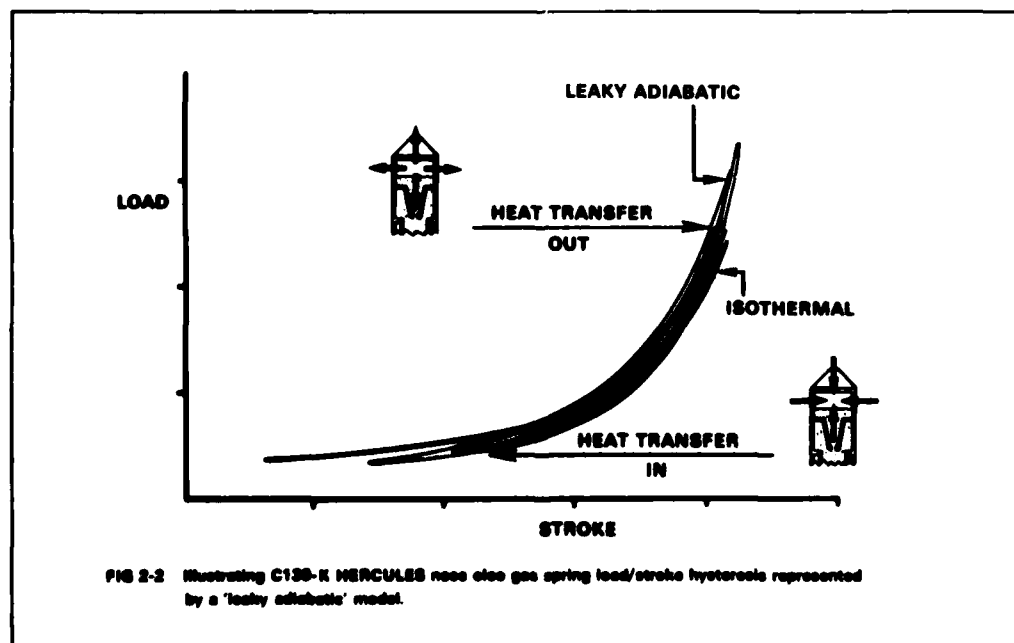
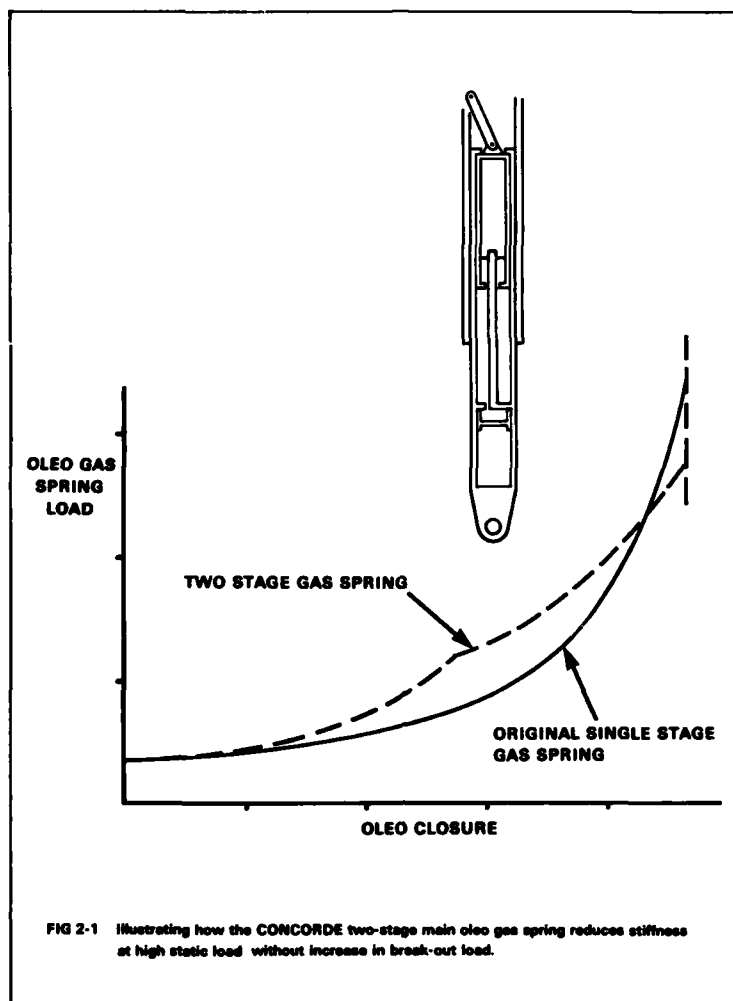
Jaguar taxi response modelling involved response to both runway obstacles and to grass strips. For this aircraft the undercarriage representation was recast with the lever angles as the undercarriage degrees of freedom. A two stage main oleo representation with oil compression as an independent degree of freedom was required to model detail response to 'sharp-edged' runway inputs. Similarly, this situation required a 'footprint' tyre model in place of the usually adequate 'stylus' representation. This model was developed in some detail in order to evaluate undercarriage lever arm loads and to apply additional input forces such as those resulting from parachute deployment on landing.

#### 2.3.3 VC10 Landing and Taxi Response

The VC.10 main undercarriage is unusual in the arrangement of torque links which are connected to a bogie hop-damper in such a way that it significantly augments the main shock absorber during the landing impact. The geometry is quite non-linear and this, together with the hop damper characteristics, require accurate representation for modelling the landing. The non-linearity is much less severe, and the hop damper is almost uncoupled from main strut telescoping motion, in the taxiing situation. A much simpler model, therefore, suffices for taxi work than for landing work. This is discussed in more detail in Section 4.

#### 2.3.4 Hercules Taxi Response

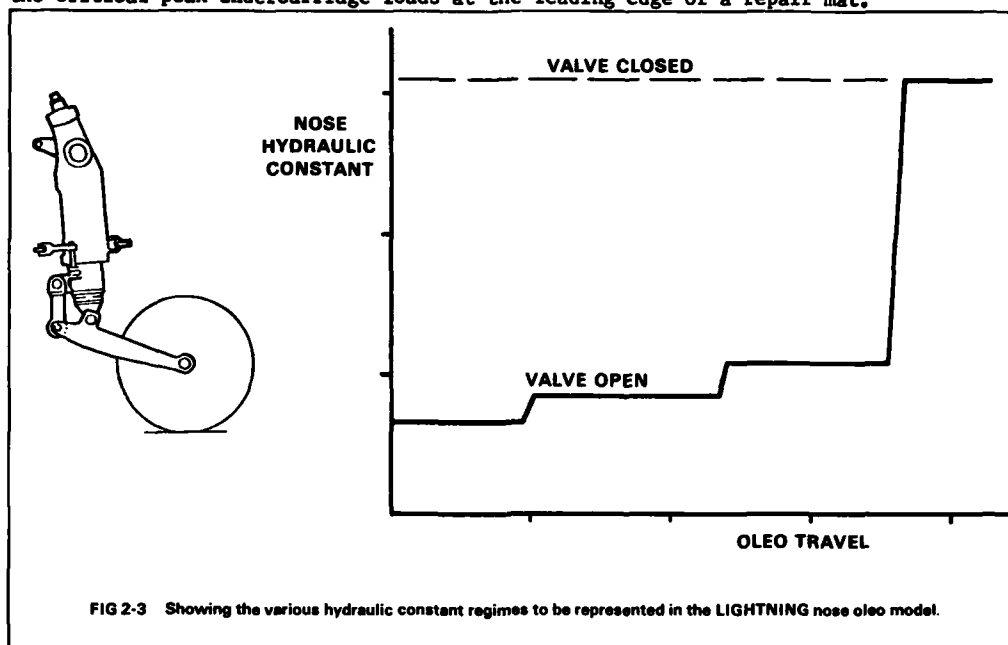
As will be discussed in section 5, the modelling of Hercules response to damage repaired runways was concentrated on nose undercarriage load and wing mid-span bending. Correct simulation of the bottoming characteristics of the nose oleo was found to be important. A 'leaky adiabatic' gas spring representation with oil compressibility was employed to give both appropriate gas spring characteristics at high load and a bottoming load to match trials results. See figure 2.2.





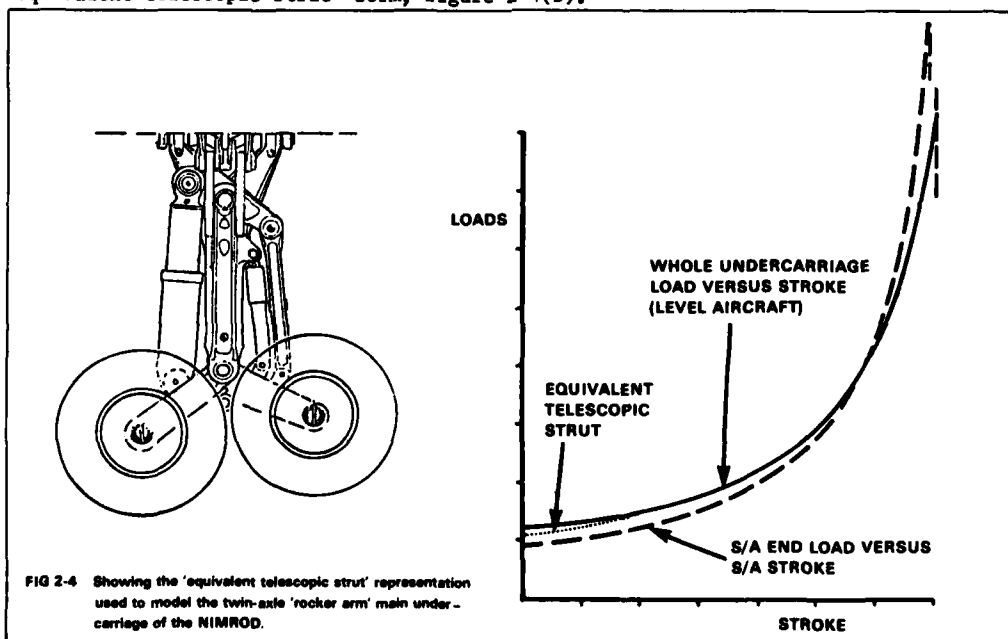
### 2.3.5 Lightning Taxi Response

Lightning required a lever representation for the nose undercarriage. Mathematical modelling detail was applied to the representation of nose and main hydraulic loads. The nose oleo hydraulics coefficients in compression are metered by stroke - but subject to addition control by a restrictor valve, see figure 2-3. Main oleo hydraulics are also metered by stroke. Detail representation of such features is of great importance to the simulation of the critical peak undercarriage loads at the leading edge of a repair mat.



### 2.3.6 Nimrod Taxi Response

The largest representational problem for a Nimrod mathematical model was the unusual 'rocker' type main undercarriage, see figure 2-4(a). For initial studies involving local perturbations from the 'static' datum the load/stroke characteristic could be reduced to an 'equivalent telescopic strut' form, figure 2-4(b).



### 2.4 Validation of Model

Validation of the mathematical model is necessary in order to refine the representation of the aircraft and undercarriage, to ensure that it may be applied with confidence as the basis for predicting the critical loads and accelerations throughout the whole operational envelope.

The effort put into validating any particular aspect of the mathematical model must reflect the importance of that item on the critical responses. The ability to do this successfully is conditional on adequate trials instrumentation in the areas eventually found to be influential on these critical responses. This in turn may reflect the adequacy of the feasibility study modelling investigations. In most aircraft the important items to validate usually include the nose and main undercarriage oleos.

#### 2.4 - continued -

The mechanics of the process of validating the mathematical model against trials results has evolved in parallel with the modelling capability. Much use is currently made of sub-system mathematical models to refine modelling detail. In situations where test results are available for fully instrumented undercarriage legs then a mathematical model of the undercarriage oleo alone, driven by recorded stroke provides a fast and effective way of determining model coefficients prior to incorporation in the full aircraft model. This process improves the scope for ensuring that the mathematical representation is physically realizable.

The requirement for matching the whole aircraft model with trials results remains - but the effort involved is likely to be much reduced.

Trials results from partially, or inappropriately, instrumented aircraft are often not sufficiently comprehensive to be used directly in this way, and early use of the mathematical model employing the theoretical design coefficients established for the feasibility study is inevitable.

Assessment of mathematical modelling is frequently obscured by differences between trials results and predictions that arise, not from shortcomings in the basic aircraft model, but from inadequate representation of the input forces. To obtain a match it has been found necessary to ensure that the following are adequately represented:-

- o pilot inputs, for example elevator, aerodynamic trim, thrust and braking
- o external input, for example the underlying runway profile, and wind
- o initial states, i.e. the residual motion of the aircraft due to unmodelled earlier inputs
- o the overall balance of loads on nose and main undercarriages

Once validation of the mathematical model has been achieved, a number of these items may be removed from the mathematical model to be used for undertaking the majority of 'production' runs extending the operational envelope.

#### 2.5 Techniques

The concept of 'fitness of the model to the task' has application throughout the stages of mathematical model development. As an investigative tool at the feasibility study stage the mathematical model may initially be fairly simple but must soon represent the potential critical areas in sufficient detail to identify where increased modelling and trials effort is required, without there being a danger of overlooking a significant problem.

For the purposes of validating the mathematical model there must also be an emphasis on representing inputs which affect the important aspects of the response of the aircraft.

Production operational clearance calculations, however, should be undertaken using a model which is of minimum complexity necessary to evaluate the critical loads cases. It may prove to be most cost-effective to extend such simplifications beyond the point where critical loads are evaluated precisely, provided that the general trends predicted are sufficient to allow only minimal study of the worst cases using a more detailed model.

### 3.0 COST EFFECTIVENESS

#### 3.1 General

The overall cost-effectiveness of mathematical modelling is very dependent on the balance that has to be struck for a particular task between:

- o costs associated with the development of the mathematical model and computer programme
- o costs associated with the use of the mathematical model in a 'production run' sense

These costs comprise of:

- o manhours (development, data preparation and results processing)
- o computer terminal time (development, data processing)
- o computer central processor time cost (cost per run)
- o computer input/output costs (results listings, plotting etc.)

#### 3.2 Computing

As the digital computer simulation response programmes originated on 'mainframe' computers there has been a tendency for programme complexity to expand without any computer imposed limitations. In recent years the advent of very large and expensive mainframe computers has brought a tendency to concentrate on 'batch' processing, with little improvement in on-line computing functions. In parallel computing costs have risen in such a way that they can now dominate the overall costs of the 'production' clearance calculation task. In addition, the development task can be unduly delayed by the difficulties involved in interactive use of a mainframe computer, and slow job turn round time (in many cases over night). In such a situation the time and cost penalties involved in further developing a specialised, broadly simpler, mathematical model and computer programme results in the eventual acceptance of an unnecessarily complex model for clearance calculations.

For use of a basic configuration mini-computer the cost emphasis is considerably altered. Mathematical model and programme development can be enormously speeded up as a result of the dedicated interactive nature of the mini-computer. As a result development can also concentrate on optimising programme size and efficiency, off-setting the limitations inherent in a mini-computer based system. Computer running costs are almost completely replaced by the first cost, and development manhours can be reduced. It has been the experience at Weybridge that these benefits can carry over from the Feasibility Study, and Validation stages into the Clearance Calculations where the interactive post processing capability of a dedicated computer outweighs the significant run-time benefits that would arise from the use of the mainframe computer.

### 3.3 Minimising Computer Resources

Computer costs, and, in particular, central processor unit costs are directly related to the complexity of the simulation model, and the required accuracy of the time response integration.

Integration accuracy is closely related to the frequency of response, and to the conditioning of the equations of motion. In order to minimise run time a Kutta-Merson variable - step integration method is generally used at Weybridge. It has been found that detail assessment of the accuracy requirements of each individual degree-of-freedom enables the average number of integration steps per run to be reduced by up to 20:1 without significant deterioration of results, as will be illustrated in Section 5. A contributory factor in increasing the average integration step size is the elimination of any higher frequency degrees of freedom found not to be making a significant contribution to the critical parameters under study. For example, for the prediction of Nimrod undercarriage loads the fundamental wing bending mode was the only flexible aircraft mode required. The Hercules study also allowed a reduction in flexible aircraft modes from eight to one for calculation of both the critical nose undercarriage load and the critical wing mid-span bending moment.

Simplification of the undercarriage arrangement in the model may also be usefully employed to reduce modelling complexity and to reduce the numbers of degrees of freedom. Representation of the Hercules twin main undercarriages, which are non-critical items, by a single 'equivalent' oleo strut provides an example of this. The effect of this simplification on the critical loads was small.

For computation of many 'production' runs, for example to establish the operational clearance capability, it has been found efficient to prepare all time dependent input, including forward speed and distance travelled in a pre-processor programme external to the dynamic simulation programme. Many simulation runs may then refer to this data store, ensuring consistency of data preparation and minimising repetitive calculations. In this environment there would also be minimal requirement for expensive auxiliary peripherals (plotter, printer etc.).

### 3.4 Reduction of Results

For the cost effective use of a mathematical model, the application of comprehensive post-processing functions to the reduction of results can play a major role. By maximising the use of the results obtained for the qualification of general trends, and for the estimation of the whereabouts of potential limit conditions, the number of full simulation cases required may be significantly reduced. This is particularly so for operational clearance calculations where many hundreds or thousands of runs may be involved. For programme and model development, interactive graphical display of results is particularly beneficial in giving the engineer a fast understanding of problems encountered. This can extend, if required, to computer animation of the aircraft response.

Post-processing functions found to be particularly useful are:

- o comprehensive plotting of time history results as required
- o coalescence of many sets of results into envelopes of maximum and minimum values, for example
  - wing bending moment trend with speed
  - decay of pitch response following a repair for a selection of 'critical' initial states
- o animation of time history responses
- o routines, for the multiple repair situation, to estimate an 'interface window'. That is, the maximum allowable initial states consistent with the response to the repair remaining within critical load or acceleration limits
- o the interpretation of response results in terms of the 'interface window' in order to define operational clearance limits

As in the case of development of the mathematical model itself, the use of a mini-computer system makes the implementation of such post processing functions increasingly attractive. The rigid framework under which a mainframe computer system is operated does not usually lend itself to the flexible and interactive accessing of results files necessary for most of these operations. The limitations imposed by the mini-computer system have been found to be relatively minor. The most severe limitation has been one of space for the results files, imposed by the use of flexible diskettes as the direct access storage medium. The problem has been tackled by allowing detailed specification of the exact form in which results are to be saved to suit each individual run - it is rarely necessary for 'production' runs to report results as comprehensively as is required for mathematical model development and feasibility studies, although the ability to do so is necessary.

## 4.0 APPLICATION TO VC.10

The concept of 'fitness of the model to the task' in contributing to cost effective modelling can be usefully illustrated by reference to the VC.10. For this aircraft type the forces in the main undercarriage are of considerable interest both during landing and taxiing over runway repairs.

The VC.10 main undercarriage is shown schematically in Fig.4-1. This undercarriage is unusual in that the lower torque link is pivoted to the front end of the bogie rather than to the main strut ram directly, and it extends below this pivot to form a lever which supports one end of a hop-damper, the other end of which is pivoted inside the bogie tube.

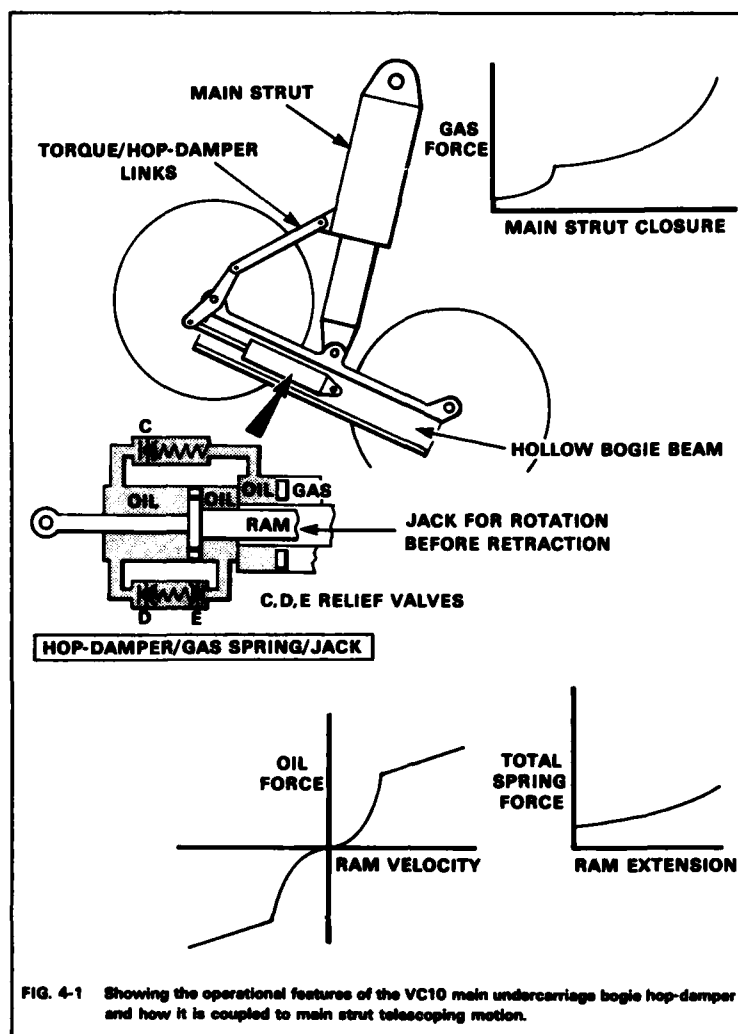


FIG. 4-1 Showing the operational features of the VC10 main undercarriage bogie hop-damper and how it is coupled to main strut telescoping motion.

#### 4.0 - continued -

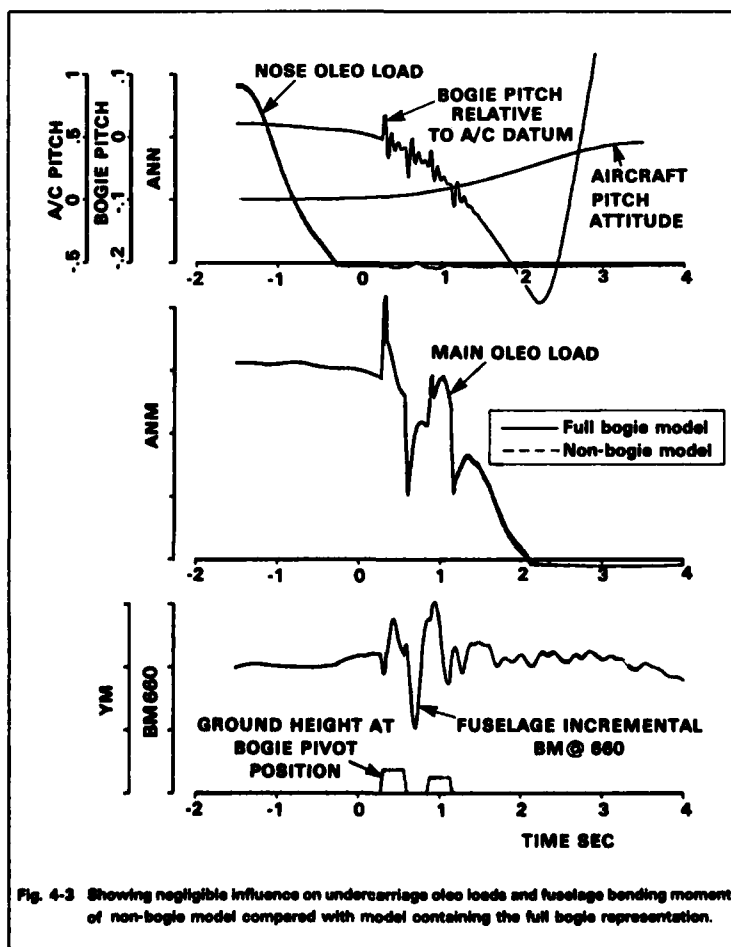
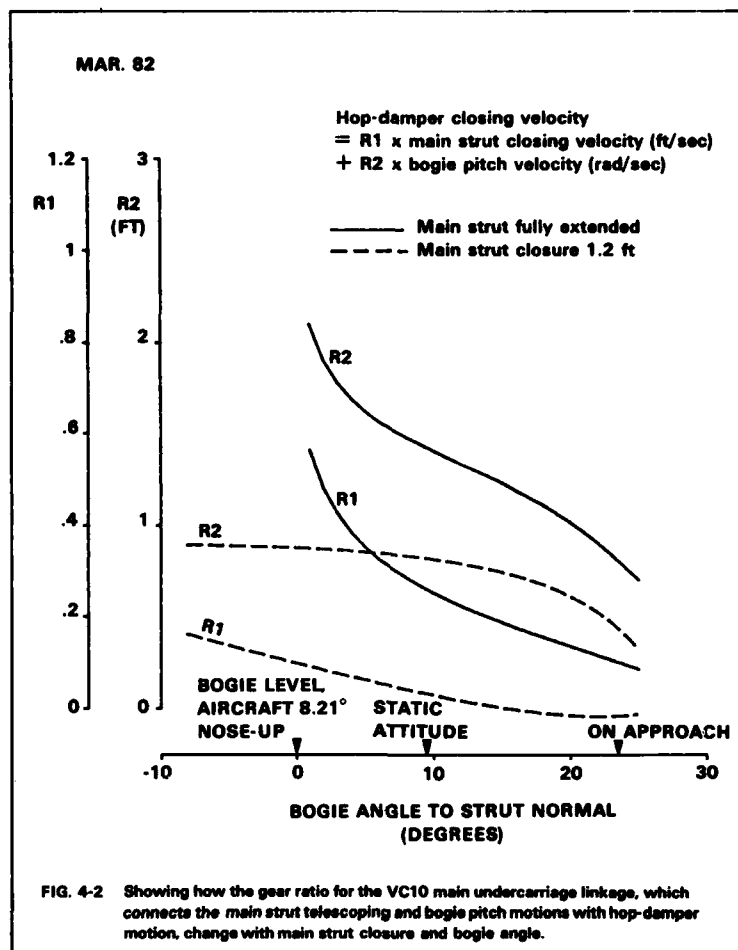
Because of the geometry of this arrangement the hop damper is exercised both by bogie pitching and by main strut telescoping. The effective arm of the hop damper varies with bogie pitch angle in a highly non-linear way when the strut is fully extended, but varies only slightly when the strut is at normal static stroke, at least for bogie angles in the range  $\pm 10^\circ$ . The gear ratio between hop-damper and strut telescoping also varies drastically at full main strut extension but in the static ground attitude the motions are almost uncoupled. This is shown in Fig.4-2.

The hop damper is a combined gas spring and hydraulic damper with relief valves and physical bottoming spring plus jack for bogie positioning prior to retraction. It acts as a significant additional shock absorber during landings and for modelling the landing a fairly detailed description of its force and kinematics are necessary. However, for taxi work a much simpler representation suffices.

A further simplification is possible for the taxi work regarding the main strut gas curve. The oleo is a two-stage one with the high pressure chamber working for strut closure greater than about 4 inches, and the low pressure chamber for closures from zero to about 14 inches. For taxi work where closure remains greater than 4 inches the gas compression can be closely approximated by a single stage.

Going a major step further in the simplification of the model by deleting the bogie but leaving the ground inputs at the correct wheel positions gives a programme which is 1.4 times faster for taxi work than the full model.

The effect of these simplifications is seen in Fig.4-3 which shows time-histories of main undercarriage strut force and front fuselage bending moment at a typical station when crossing a runway repair. Although there are differences of detail between the results for the two models, the critical features are not degraded by using the simpler model.



## 5.0 APPLICATION TO C-130K 'HERCULES'

5.1 The development of a cost effective mathematical model of the Hercules C-130K, initially for validation against trials but leading to operational clearance calculations, provides a useful illustration of the approach adopted. Prior to the runway repair mat trials it was prudent to establish a mathematical model that gave a representation of the aircraft that was comprehensive, including -

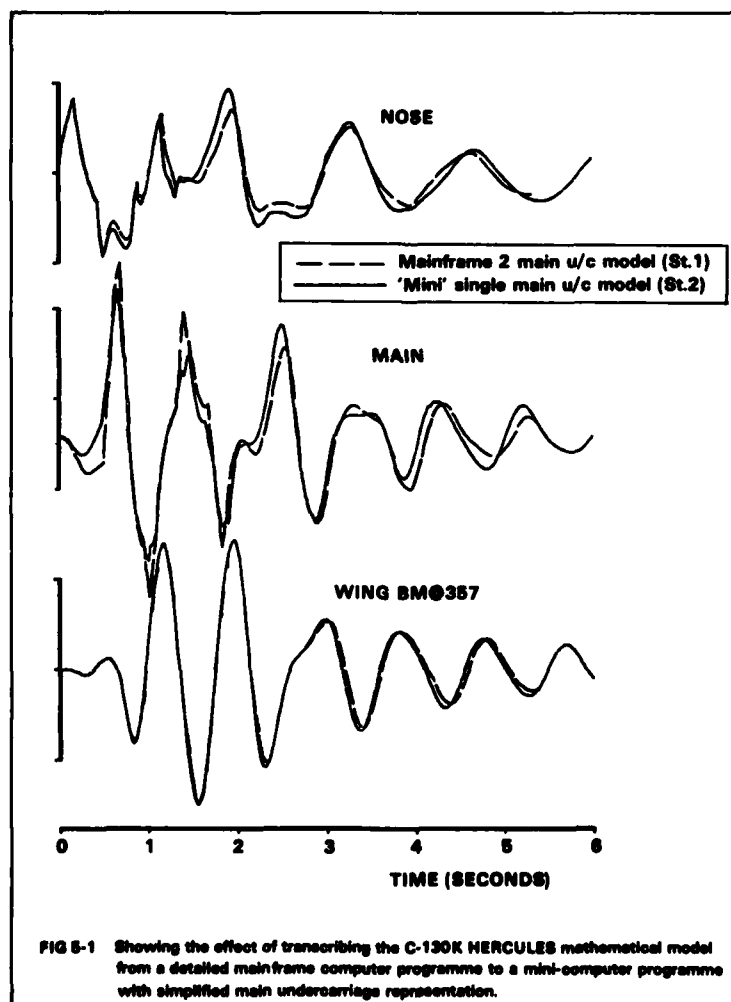
- o independent and geometrically correct main undercarriages
- o structural flexible modes of vibration up to at least 10 Hz.
- o accelerations, shears, bending moments and torques for many wing stations.

The integration method was fixed-step Runge-Kutta. Use was made of this model on a mainframe computer to evaluate potential problem areas prior to the trials and to identify safe trials schedules.

5.2 The trials programme confirmed the sensitivity of wing mid span bending and of nose undercarriage loads to runway roughness during taxi, as had been anticipated from initial studies. There was much evidence that main undercarriage loads were not sufficiently high to be of primary concern. Wing mid span bending was dominated by the fundamental wing bending mode and rigid aircraft heave. There were several aspects of oleo characteristics that displayed large inconsistencies with respect to theory and poor repeatability. These problems were ascribed to gas solubility in the hydraulic oil.

5.3 Costs associated with running the original detailed simulation model were high. With at least five aircraft weight and aerodynamic configurations over a minimum selection of repair profiles in any combination for aircraft speeds over a 100 knot range, it may be appreciated that the number of simulation runs necessary to estimate clearance limits can become very large. In view of the anticipated requirement for some 5000 operational clearance runs the overall computing cost could have been in excess of £75,000. It was perceived that there was a need for, and a potential for making major simplifications.

With some simplification it became possible to transcribe the mathematical model to the B.Ae in-house 'general purpose' taxi response programme, which was mounted on a 32K 16 bit word 'desk-top' mini-computer. This programme utilises a variable-step Kutta-Merson integration technique with potential for optimising tolerances in each degree of freedom. It was written originally to represent aircraft with typical 'Weybridge' telescopic strut undercarriages, single nose gear, one main gear per side, with account being taken of input by 2 axles on a main undercarriage bogie. Use of this model, which was fully detailed apart from the simplified main undercarriage representation, proved the benefit of such a move as it demonstrated little degradation of accuracy of response in the critical nose undercarriage load, and wing mid-span bending moment - see Fig.5-1.



## 5.3 - continued -

Main undercarriage load response plotted in Fig.5-1 is effectively an average for the twin main undercarriage. It is compared with twice the forward strut response of the more detailed model. Considering these factors, the principal features of the main undercarriage load response are successfully represented by the simplified model. The agreement of wing mid-span bending response testifies to the adequacy of the input representation from the main undercarriage. Even so, the more detailed mathematical model still provides the better representation of main undercarriage load peaks at repair mat leading and trailing edges.

Simplifications were progressively applied, and these are catalogued in Table 5-1.

	1	2	3	4	5
Computer	MAINFRAME	MINI	MINI	MINI	MINI
No. of Main u/c	2	1	1	1	1
No. of flex modes	8	8	8	1	1
D.o.F.	28	28	28	14	10
No. of IQ's	84/14	5	5	5	1
Integration step	FIXED	FIXED	VARIABLE	VARIABLE	VARIABLE
Minimum step size (seconds)	.0008	.0008	.00025	.00025	.00025
Steps/run	7,500	7,500	449	456	456
Elapsed time (minutes)	.	389	28.5	19.5	15.0
Cost	£15				< £1

Table 5-1 Progressive stages in the reduction of the C-130K HERCULES mathematical model running costs.

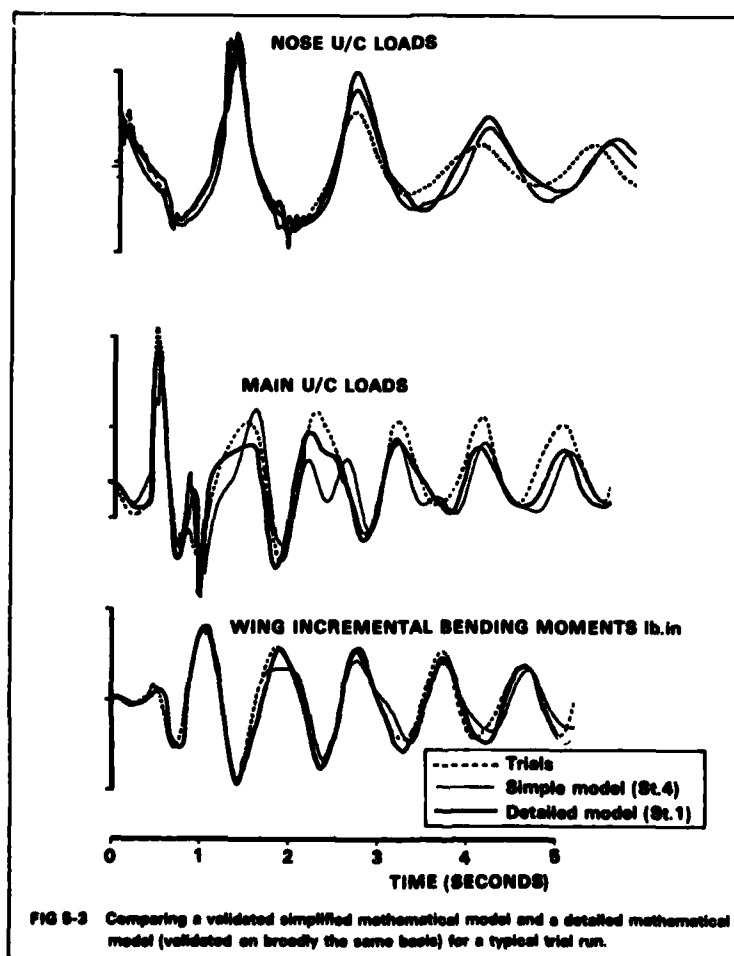
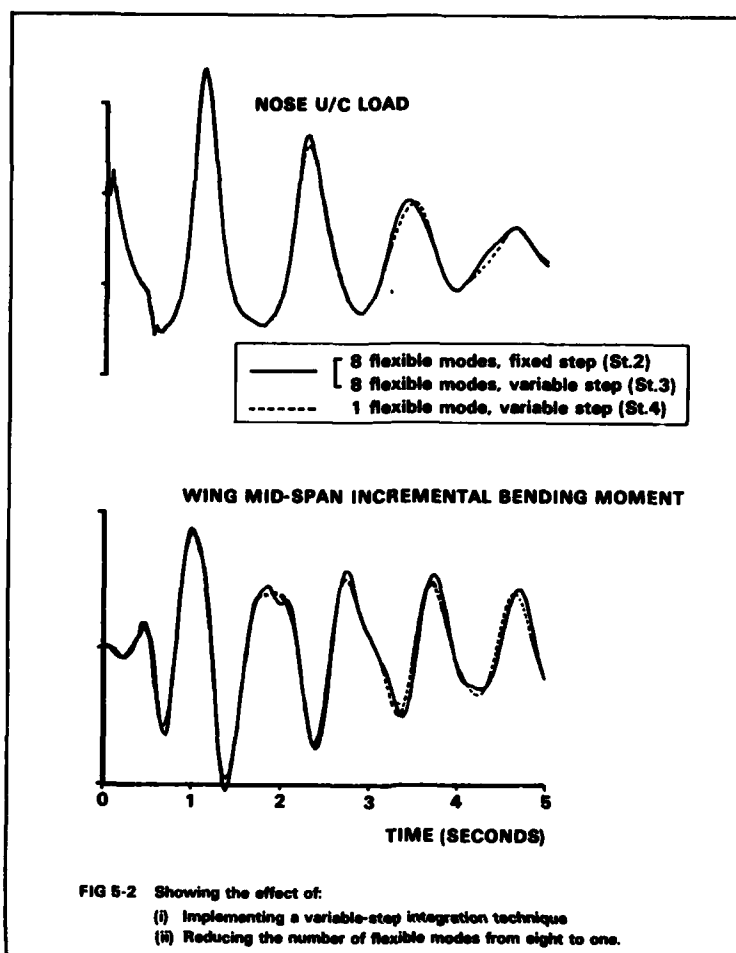
Implementation of a variable-step integration technique resulted in the most significant reduction in computation time, about 20:1, without compromise of the integration step size where it needed to be small (model standard 3). Reduction of the number of flexible aircraft modes from eight to one, a halving of the numbers of degrees of freedom, resulted in a further 50% reduction in run time (model standard 4). This brought the mathematical model to a manageable state to undertake validation against trials results, Fig.5-2.

5.4 The use of the simplified model for validation against trials results enabled very many detail model changes to be investigated. Considerable manipulation of oleo characteristics was necessary to match specific trials responses. In addition detail matching of quasi-static loads on nose and main undercarriage required a change in approach to the representation of aerodynamic forces.

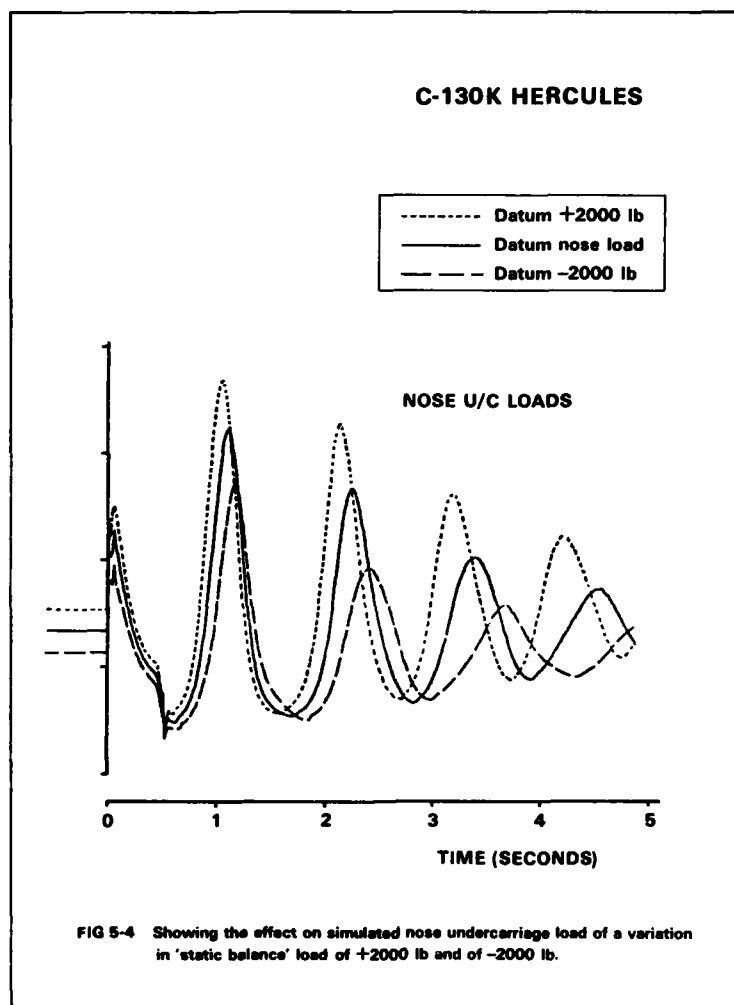
Fig. 5-3 illustrates the comparison that was eventually achieved in matching trials results. Also shown are responses of the mainframe detailed model validated broadly on the same basis. The element of the total aircraft response, due to the underlying runway profile and other extraneous inputs is obviously a cause for some of the remaining differences in the matching. Detail matching errors in the nose oleo load in particular are small in comparison with potential differences which would result if the quasi static load were to be in error. Fig. 5-4 indicates the magnitude of differences in response that could result from quasi-static nose load increments of  $\pm 2000$  lb. Such an increment to quasi-static nose undercarriage load could arise by any of the following mechanisms independently:-

- o different levels of friction load in front and rear main oleo pairs
- o five degrees of elevator at seventy knots
- o five inches shift in centre of gravity

5.5 The final simplification in preparation for operational clearance calculations involved removal of the forward translation degrees of freedom and also removal of superfluous coding from the computer programme. Much interpolation of time-history look-up table data was isolated in an independent pre-processor computer programme which also calculated forward translation. This produced a further reduction in elapsed time of the order of 25% without change to the basic representation of the aircraft.







## 6.0 CONCLUSIONS

The need to establish an operational capability for a number of military aircraft on damaged and repaired runways has brought about the need to examine the efficiency and running costs of our modelling and taxi response simulation procedures. It is found that:

- o experience gained during the modifying of our in-house general purpose digital simulation programme to suit a number of particular aircraft justifies this approach and proves a cost effective approach to the modelling requirements
- o such a simulation programme placed in a user-interactive mini computer environment is well suited for investigations at the feasibility study stage
- o cost effectiveness at the stage of production operational clearance calculations can best be achieved by
  - using a model with the minimum complexity necessary to evaluate the critical loads/accelerations
  - referring back to the more detailed model only for identified critical cases
  - using variable step integration techniques
  - using the interactive post processing capability of a dedicated mini-computer for the reduction of results

Status of Computer Simulations of USAF  
Aircraft and an Alternative Simulation Technique

Tony G. Gerardi  
AFWAL/FIBE  
Wright-Patterson AFB OH 45433

and

Dr Levon Minnetyan  
Asst. Professor, Clarkson College  
Potsdam NY 13676

## SUMMARY

This paper reports on the formulation of preliminary guidance and evacuation techniques for operating off of damaged runways using existing simulation methods and the status of final surface roughness criteria using the results of the USAF HAVE BOUNCE program. In addition, an alternate approach in simulating aircraft response to surface roughness will be discussed. The technique is to combine a conventional time history analysis using numerical methods to solve the coupled non-linear differential equations with a frequency domain analysis to solve the linear sub-structure equations of motion. In other words, the non-linear landing gear struts and linear structure are solved separately by different techniques and the solution combined to get the total aircraft response.

## PART ONE: STATUS OF SIMULATIONS

### I. INTRODUCTION

The requirement to determine the rough surface operational capability of front line aircraft is well understood. If an aircraft can operate on "rough" surfaces, a minimum operating strip (MOS) can be prepared in a shorter time. Efforts are underway in the United States and NATO countries to define the rough surface capabilities of their existing aircraft. The USAF has a program called "HAVE BOUNCE" to define the capability of each U.S. aircraft. The approach in HAVE BOUNCE is to:

Task I: Develop a computer program, for each aircraft, that is capable of simulating operations on rough surfaces.

Task II: Using this computer program, identify the aircraft's vulnerable components and provide guidance to the test director for Task III.

Task III: Validate the computer program with test data.

Task IV: Develop operational limitations.

Once the four tasks of HAVE BOUNCE are complete, surface roughness criteria are developed for each aircraft. The Operational Limitations generated by HAVE BOUNCE impact aircraft operational procedures such as takeoff, landing, takeoff configuration, special instructions for rough surface operations, etc. Surface roughness criteria are generated under the Rapid Runway Repair (RRR) program and define repair quality and spacing requirements. Finally MOS Selection Criteria developed are based on the operational limitations and surface roughness criteria.

Since the development of Operational Limitations and MOS Selection Criteria for each aircraft will require a considerable length of time, the USAF is also developing preliminary guidance to be used in the interim. This guidance will be developed using an existing computer program and any available test data. Emphasis is being placed on the front line fighter aircraft. In addition, evacuation procedures are being outlined in the event that the repair of a MOS for sustained operations is not practical. Table I contains the approximate schedule for delivery of the preliminary guidance, HAVE BOUNCE results, and final guidance. It is assumed that ten months are required to develop MOS Selection Criteria once the HAVE BOUNCE results are available and that an additional two months are assumed to get appropriate approvals of the final guidance and deliver it to the operational commands.

The preliminary guidance will be delivered in the form of an Air Force Wright Aeronautical Laboratories (AFWAL) Technical Memorandum (TM) and placed in the Base Commander's disaster preparedness file at each of the Operational Commands bases. Preliminary MOS Selection Criteria will be delivered to the repair crews two months after the TM is published.

The final Operational Limitations will be incorporated into each aircraft's appropriate technical order.

The final MOS Selection Criteria will be delivered to the repair crews.

### II. PRELIMINARY GUIDANCE:

Using a computer program developed in the Air Force Wright Aeronautical Laboratories, preliminary guidance is developed for operations on rapidly repaired bomb damaged runways. The program known as TAXI incorporates all of the non-linear characteristics of the landing gear as well as up to 15 flexible modes of vibration. Landing gear vertical loads are predicted and compared to limit values for failure

criteria. At the present time, pylon loads, wing moments, and shears, etc. are not monitored with this computer program. Generally, landing gear vertical loads can provide a good indication of the structural response of the entire aircraft structure, particularly fighter aircraft. The approach is to "validate" each aircraft specific TAXI model to the highest confidence level possible using any available test data. The computer model is then used to simulate each aircraft traversing the single and multiple "A" through "E" category repairs depicted in Figure 1. By evaluating aircraft response to this "range" of roughness, a good indication of the aircraft's capability can be obtained. This has been done for the A-10 aircraft for several gross weights.

Figure 2 shows a comparison of predicted response to A-10 test data. The test was a constant speed taxi over a 1-cos shaped dip. Comparison, such as that in Figure 2, provided enough confidence in the TAXI computer model to proceed with the development of preliminary guidance for operating on rough surfaces.

A single time history simulation is not sufficient to determine an aircraft's response over a given profile. The "tuning" effect of aircraft frequency(s) to bump wavelengths requires that all aircraft velocities from 0 to takeoff be considered. To accomplish this, a "do loop" is placed around the TAXI program and peak values of gear loads were stored for each velocity simulated. The results are then plotted. Figure 3 is a typical "velocity" analysis showing the results of an A-10 traversing a single "E" category repair. The resonate speed is clearly visible and as Figure 3 indicates "E" category repairs should be avoided at speeds around 30 knots. From Figure 3, it can also be seen that the A-10 responds primarily in pitch and the nose landing gear (NLG) is the critical component. Figure 4 points out that during takeoff, the NLG loading is compounded by the thrust moment acting above the waterline of the center of gravity.

The problem of multiple repairs is illustrated by Figure 5 which contains the plotted velocity analysis of the A-10 traversing two category "E" repairs 80 feet apart. It can be seen that a second pitch resonance occurs around 110 knots. The speed at which this second peak occurs is, of course, related to the spacing between the repairs.

In order to establish "repair spacing restrictions," a spacing or wavelength ( $\lambda$ ) analysis was performed. The results are shown in Figure 6. The spacing was varied from 40 to 300 feet between two "E" category repairs. For all spacings ( $\lambda$ ), a peak occurs around 20 knots. This corresponds to impacting the first class "E" repair. A second family of peaks occurs for a ( $\lambda$ ) of 40 to 100 feet. This family of peaks is due to the first rebound of the NLG. A third family of peaks occurs for a ( $\lambda$ ) of 120 to 280 feet and corresponds to the second rebound of the NLG. Finally, a fourth family of peaks begins to appear for a ( $\lambda$ ) of 200 to 300 plus. These peaks correspond to the third NLG strut rebound. It can be seen that considerable damping is achieved after each rebound. In fact, for ( $\lambda$ ) = 120 to 280 feet, the second repair can be treated as a single encounter.

Simulations are made of the A-10 in a hard braking condition as in landing rollout. Even though the aircraft weight is reduced (which reduces gear loads), high NLG loads can be produced over closely spaced "E" repairs when the brakes are applied at the main landing gear (MLG) and a subsequent pitch down moment is produced.

Since the A-10 speed versus distance down the runway can be easily predicted (Figure 7), several important facts can be deduced from the results of the wavelength analysis:

- Single "E" repairs (or better) are satisfactory beyond 40 knots.
- Multiple "E" repairs (or better) are satisfactory when spaced 300 or more feet apart.
- Additional simulations show that an "E" repair followed by a "C" repair is satisfactory when spaced 120 feet or more apart.

From this type of analysis, a Minimum Operating Strip (MOS) as shown in Figure 8, can be defined for an A-10 aircraft. Due to the lack of knowledge concerning the effect of landing on repairs, all repairs in the landing zone must be of high quality.

In addition, A-10 parametric studies show that a 25% increase in NLG strut preload pressure will reduce NLG peak loads by approximately 20% for all speeds.

Also, since the aircraft responds primarily in pitch, an aft stick takeoff will reduce NLG loads, although takeoff distances will increase.

Finally, in the event that runway damage is so severe that repairs for an MOS for sustained operations are not practical, aircraft evacuation may be the best option. By removing external stores and reducing gross weight, takeoff distance will be substantially shortened and rough surface capability will be increased. Also by reducing gross weight, tire pressures can be reduced which will substantially increase the tire flotation and perhaps permit operations on alternate surfaces.

Although preliminary guidance such as this is not complete and is not totally defined in a fashion to construct an "integrated" MOS, it does equip the Base Commander, aircrews, and runway repair crews with some direction.

### III. HAVE BOUNCE (HB) STATUS:

The end products of the USAF's HB program are:

1. A validated computer program capable of predicting airframe response at any potential critical component such as the gear, pylons, wing roots, etc.

2. Aircraft operating limitations; i.e., procedures affecting takeoff or landing techniques, gross weight limitations, etc.

The operating limitations are to be eventually incorporated into the flight manual by the appropriate system manager.

The validated computer programs are forwarded to the Air Force Engineering Services Center (AFESC) where surface roughness criteria is generated. Using the surface roughness criteria for each aircraft, MOS selection criteria are generated in a format that is capable of being integrated with other aircraft through a template overlay process. The continually updated MOS Selection Criteria will be sent to the runway repair crews as an amendment to the existing AF Manual 93-2 or other appropriate documents. Once the fully coordinated MOS selection criteria and operational limitations are delivered to the field, the preliminary guidance discussed in Section II will be discarded.

## PART TWO: AN ALTERNATE SOLUTION TECHNIQUE

### I. INTRODUCTION

Non-linear behavior often plays an important role in the transient structural response. Non-linearities may be due to inelastic material behavior, specially designed non-linear energy absorption and attitude control devices, or due to geometric non-linearities that result from large structural deformations. The structures addressed in this study are those that possess specifically designed non-linear energy absorption components. The time-history analysis is the accepted standard method for the simulation of non-linear dynamic response.

In theory, it is possible to simulate the total structural behavior by a direct dynamic analysis of a finite element model. However, the transient response analysis of the full finite element model is prohibitively expensive. Also, past experience has shown that such analyses of complex structures can be numerically unreliable.

Many complex systems contain both linear and non-linear structural components. The types of structures that are particularly addressed in this research are those with mostly linear characteristics. However, significant non-linearities exist in some limited regions of the structure. The most immediate and relevant example of such a dynamic system is an aircraft taxiing over an irregular surface. The vehicle superstructure may be assumed linear but the suspension system is highly non-linear. It is necessary to perform a time-history integration of the equations of motion to estimate the non-linear suspension response. To account for the vehicle flexibility during taxiing, the fundamental elastic vibration modes should also be included in the model. The modal superposition series can be truncated after a few modes since the higher frequency vibrations do not affect the suspension response. However, the time-history analysis is not a practical method to simulate the response of all critical aircraft components, especially those that are affected by the high frequency modes. It is not practical to include higher vibration modes with numerical reliability within the constraints of time-domain discretization. It would be necessary to decrease the time increment by several orders of magnitude to simulate the higher frequency modes consistently. Such refinement of the time step, with the addition of a greater number of modal coordinates, makes the time-history analysis approach prohibitively expensive for design calculations. A simple, efficient, and reliable method is needed to simulate aircraft total structural response for comparison with critical design limits to establish relevant runway repair criteria.

To accomplish this task, a hybrid analytical method is formulated, aimed at defining an optimal solution path that will reliably predict dynamic response. The method incorporates a time-history analysis for the non-linear response with a frequency domain analysis of the linear modes. First the time-history analysis including the non-linear components and a small number of linear modes is to be conducted. Partial decoupling of the non-linearities from the rest of the structure constitutes the second step. The remaining linear dynamic subsystem can be analyzed through the frequency domain under external forces and interactions from the non-linear components. The equations of motion can be written in modal coordinates

$$[M] \{\ddot{n}\} + [C] \{\dot{n}\} + [K] \{n\} = [\phi]^T \{P - P_{NL}\} \quad (1)$$

where

$[M]$  = generalized mass matrix

$[C]$  = modal damping matrix

$[K]$  = modal stiffness matrix

$[\phi]$  = modal transformation matrix

$\{P\}$  = generalized forces ( $P_{NL}$  - Non-linear)

The structures of interest in this research are composed of linear substructures that are joined together or to their surroundings by non-linear couplers. A taxiing aircraft can be regarded as a linear elastic vehicle structure connected to the unsprung suspension masses, tires, and the runway by means of highly non-linear suspension struts. When the linear vehicle structure is considered separately from the non-linear struts it becomes possible to formulate a stationary vibration problem.

## II. MODELING OF LINEAR SUBSTRUCTURES

In a general problem each linear substructure is considered separately from the surrounding non-linear and linear components. The interactive forces between a particular substructure and its surroundings are now considered as external loads at the substructure boundaries. The dynamic response of critical substructure components can be computed on the basis of a greater number of modes through the frequency domain.

The dynamic equations for free vibration of a linear substructure can be written as

$$[m] \{\ddot{u}\} + [k] \{u\} = 0 \quad (2)$$

where

$\{u\}$  = list of substructure nodal displacements

$[k]$  = stiffness matrix of the unconstrained substructure

$[m]$  = substructure mass matrix

The solution of the harmonic equations (Eq (2)) constitutes a generalized eigenvalue problem of the form:

$$[k] \{\phi\} = \omega^2 [m] \{\phi\} \quad (3)$$

where

$\omega$  = natural frequency of unconstrained substructure

$\{\phi\}$  = mode shape vector corresponding to

The solution to the vibration problem, equation 3, contains the natural frequencies and the vibration mode shape vectors  $\{\phi\}$ . These results are first used to evaluate the generalized orthogonal system properties as defined in Equation 1. Equation 1 is then integrated using a time history analysis program such as TAXI. Only the first few vibration modes which affect the non-linear components are used in the time history procedures. The results of this analysis yields the time histograms of non-linear forces. These forces are then used as external inputs for the detailed linear analysis of the remaining structure. The response analysis of a linear structure can be efficiently carried out through the frequency domain for each orthogonal mode.

## III. FREQUENCY DOMAIN ANALYSIS AND COMPUTATION OF TOTAL STRUCTURAL RESPONSE

The basic assumptions which permit a frequency domain analysis are that the non-linear substructure interaction forces are known and the linear systems are represented by orthogonal generalized coordinates. It was assumed that a few flexible modes were sufficient to estimate the non-linear coupling forces. In this section, a greater number of modes is assumed to represent the substructures in detail. The frequency domain analysis can also be used to compute the elastic forces when non-linear response is measured by testing.

To initiate the frequency domain analysis, all time history forces are transformed to the frequency domain by means of a fast Fourier transform algorithm. The resulting discretized harmonic amplitude coefficients are combined with the complex frequency response function of the generalized orthogonal vibration modes. The frequency response is transformed back to the time domain by an inverse Fourier transformation. The results are the separate time histories of the generalized modal displacements. Superposition of the modal displacement vectors yields the time histories of structural deflections. Other response parameters, such as stresses or loads developed in various structural components, can be evaluated directly from the displacements.

## IV. RELATIONSHIP TO THE STATE OF KNOWLEDGE IN THE FIELD

The new method relies on established methods of linear and non-linear analysis and strives to combine them in the best way to improve the solution efficiency. Formulation of the transient problem, in terms of a modal basis and substructuring to separate the non-linear and linear subsystems, are well established procedures. As an example, the AFWAL-TAXI program uses these techniques for the simulation of taxiing aircraft. More general applications of these methods are currently being investigated by other researchers. The hybrid solution method discussed here has not been previously addressed in the literature.

## V. EXTENT OF EFFORT

As a first step it is proposed that a rather simple model be used to compare the new hybrid method with direct time-history analysis. The first model will be a two-dimensional simulation of a simple beam vehicle taxiing over an irregular profile. The choice of a taxiing vehicle example is due to the availability of the AFWAL-TAXI program that will be used for time-history analysis.

The choice of a simple beam to represent an elastic vehicle is to have complete assurance and control on the finite element model in comparative parametric studies. The vehicle model to be used is depicted in Figure 9. The vehicle is represented by a collection of a finite number of beam elements. The suspension system consists of non-linear, oleo-pneumatic energy absorption devices. Typical non-linear landing gear load-deflection relationships will be used to represent the suspension gear properties. Each suspension strut force is represented as the sum of pneumatic spring force, hydraulic damping

force and strut friction force. The procedures in the existing AFWAL-TAXI program will be used to model the suspension system similar to that of a typical fighter aircraft.

## VI. CONCLUSION

Once an efficient and reliable numerical solution is established using the simple beam model, the method is further tested using actual aircraft data. The specific aircraft will be one for which extensive rough runway taxiing response test data is available.

Anticipated results of this research consist of:

(1) A computer procedure which will simulate the transient response of partially non-linear structures via an optimal solution path: There will not be any extensive software development as the computer program will rely heavily on existing computer programs of non-linear time-history analysis, such as TAXI and general purpose routines from computer libraries such as International Mathematical and Statistical Libraries (IMSL).

(2) Extensive comparative data between the new hybrid procedure and standard time-history non-linear analysis. Parametric comparisons of solution efficiency and reliability between the time-history and hybrid methods are helpful in guiding future solution techniques in an optimal direction.

(3) Validation of the new procedure by comparison of the simulated response for a specific aircraft to existing test data is obtained.

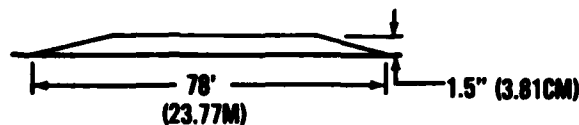
Table I. Approximate Schedule for Delivery of Guidance (Calendar Year)

	Preliminary Guidance (AFWAL Tech Memo) (To Operations)	MOS Selection Criteria	HAVE BOUNCE Completion (Final Report)	Final Guidance MOS Selection Criteria and Tech Order Change
F-4*	-----	October 1979	June 1980	April 1982
A-10*	completed June 1981	April 1982	March 1984	March 1985
C-5	-----	-----	October 1983	October 1984
F-15*	June 1982	August 1982	March 1983	March 1984
F-16*	March 1982	May 1982	June 1984	June 1985
F-111	March 1983	May 1983	October 1983	October 1984
B-747	-----	-----	July 1983	March 1985
DC-10	-----	-----	April 1983	January 1985
C-141	-----	-----	January 1982	September 1982
C-130	-----	-----	January 1982	January 1983

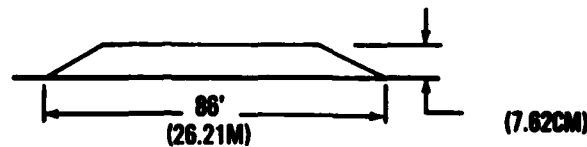
\* Priority

REPAIR  
CATEGORY

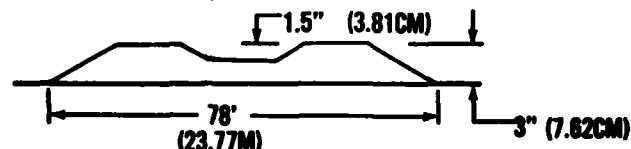
A



B



D



E

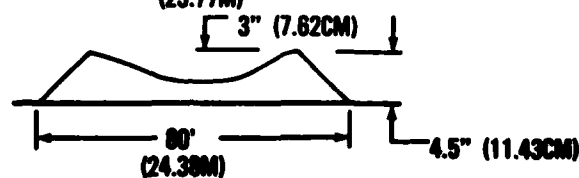


Figure 1. Repair Profiles

A-10A

30300 POUNDS GW (13744.08 KG)

40 KNOTS

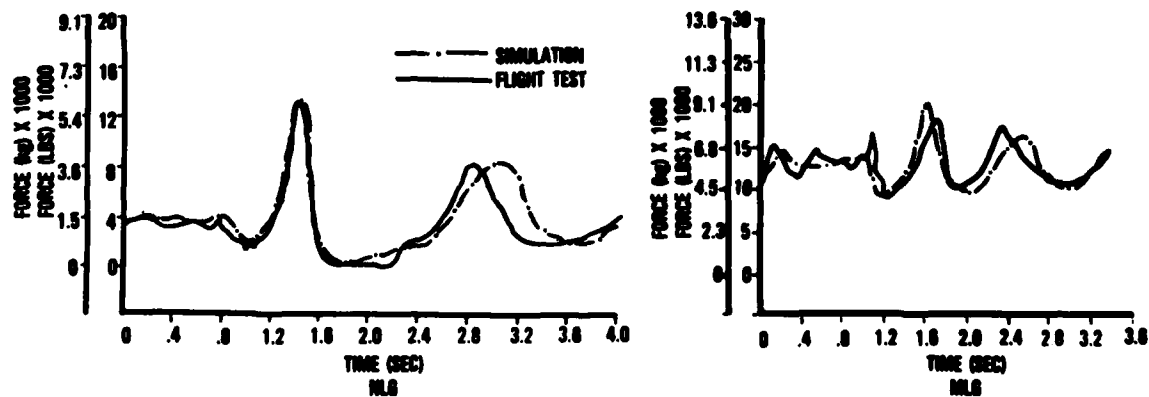


Figure 2. Comparison of A-10 Simulation to Test Data

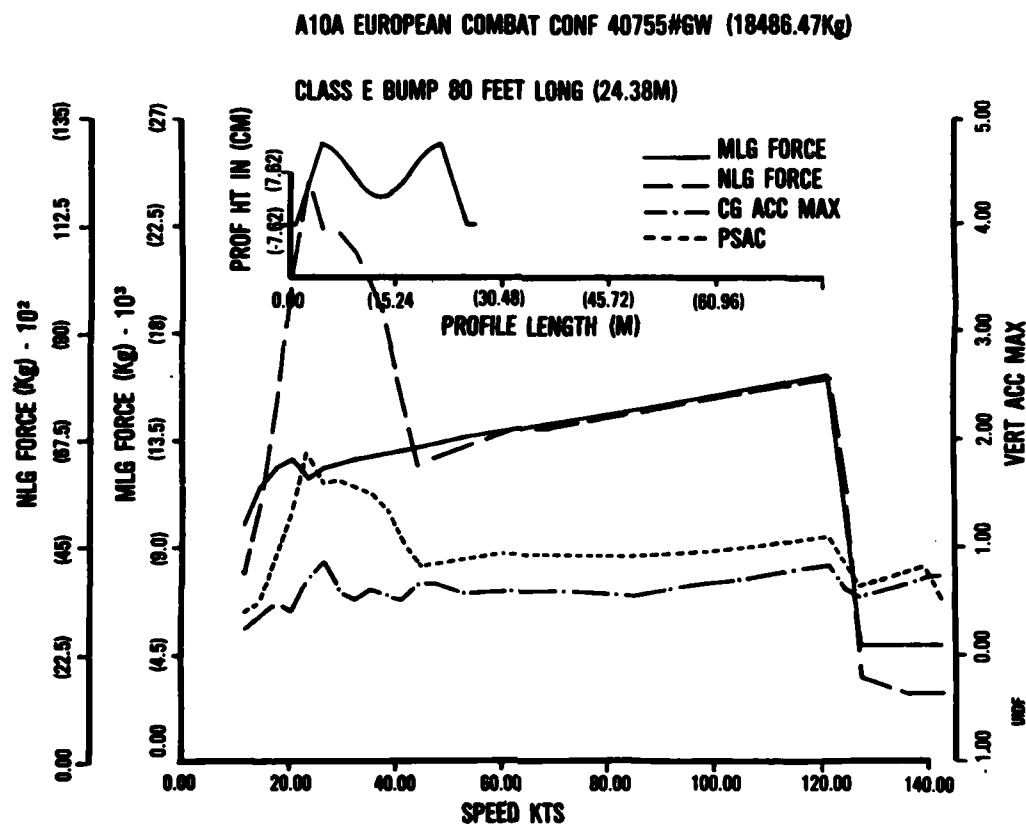


Figure 3. Typical "Velocity" Analysis

## RUNWAY INDEPENDENCE A-10 THRUST LINE

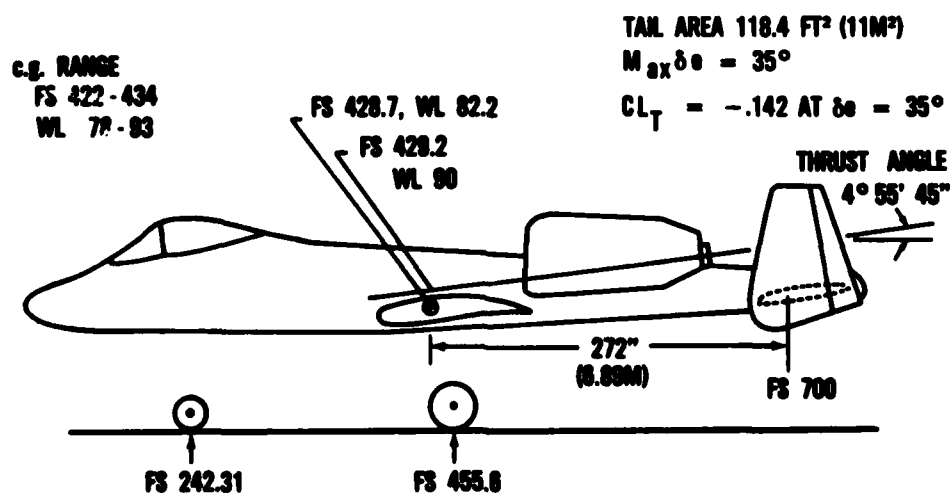


Figure 4. A-10 Thrust Line



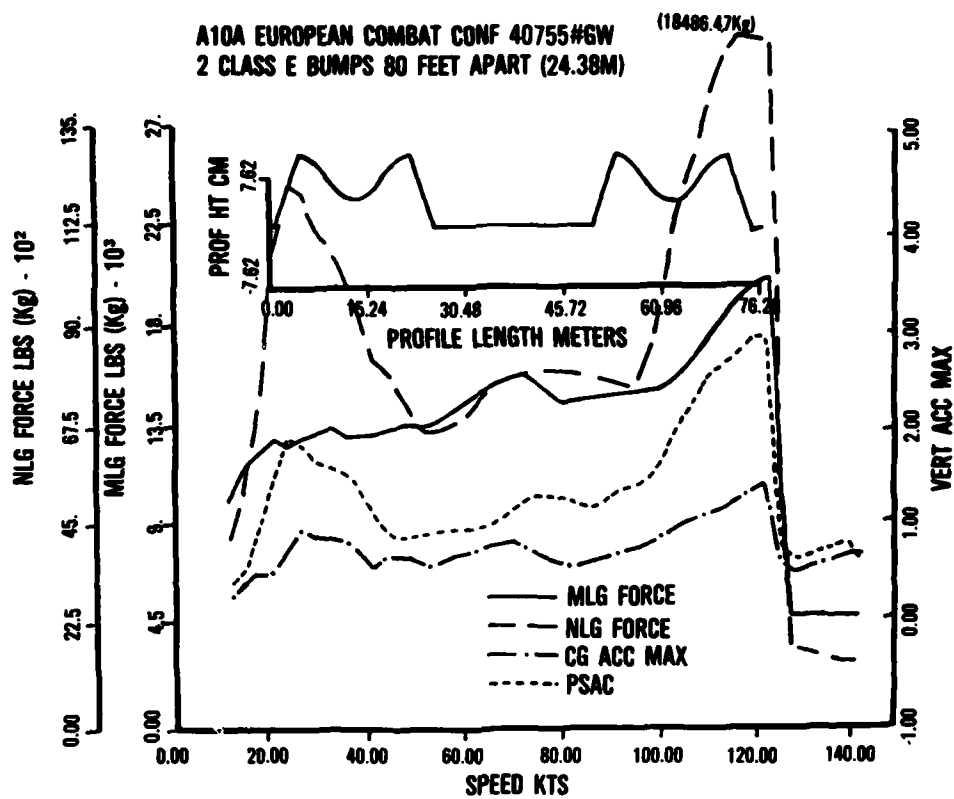


Figure 5. A-10 Response to Two "E" Repairs

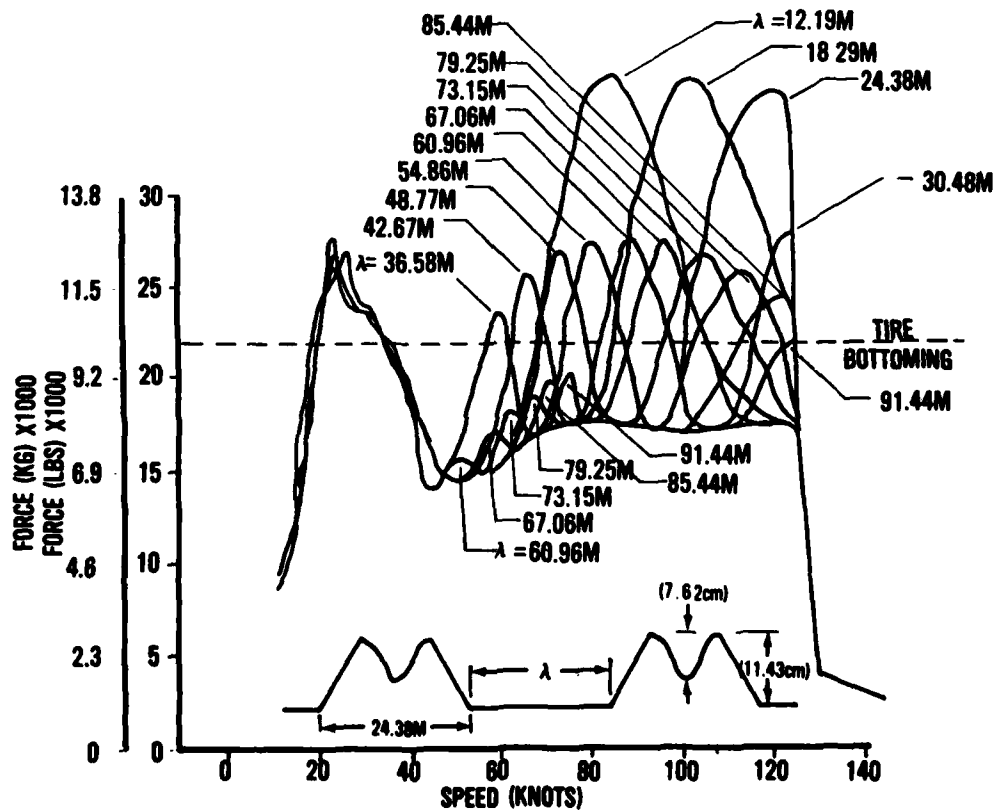


Figure 6. Mat Spacing Analysis

# A-10A THUNDERBOLT II DENSITY RATIO 1.000

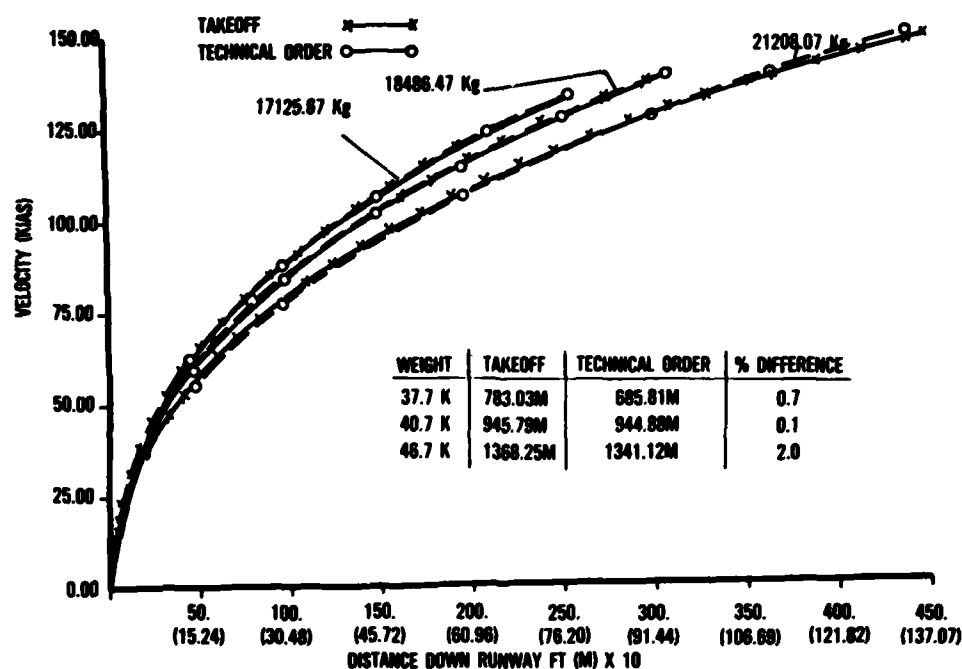
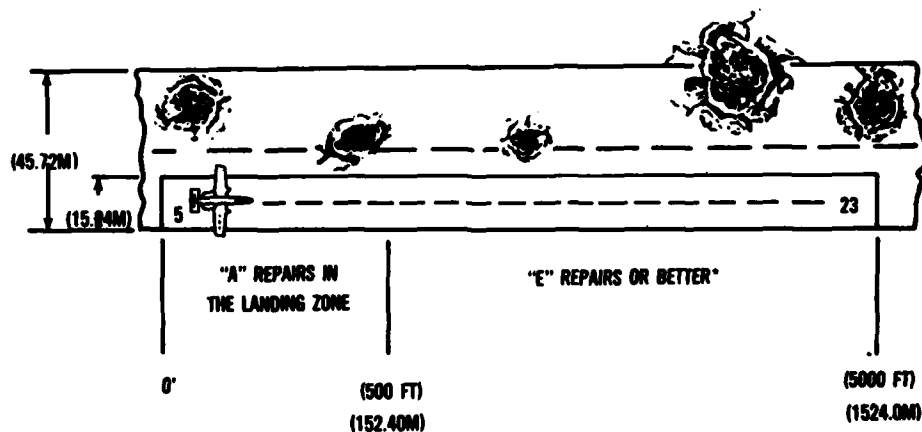


Figure 7. A-10 Speed vs Distance Down the Runway

## A-10 UNIDIRECTIONAL MINIMUM OPERATING STRIP (MOS)



- "A" QUALITY REPAIRS ARE REQUIRED IN FIRST (152.4M) (LANDING ZONE)
- MULTIPLE "E" QUALITY REPAIRS MUST BE SPACED (91.44M) APART
- AN "E" REPAIR FOLLOWED BY A "C" REPAIR CAN BE SPACED (36.58M) OR MORE APART
- MULTIPLE REPAIRS CLOSER THAN (36.58M) APART SHOULD BE MADE AS A SINGLE REPAIR
- TAXIWAYS REPAIRS MAY USE "E" QUALITY REPAIRS. TAXI SPEEDS OVER "E" REPAIRS SHOULD BE LIMITED TO 15 KNOTS

Figure 8. A-10 Unidirectional Minimum Operating Strip (MOS)

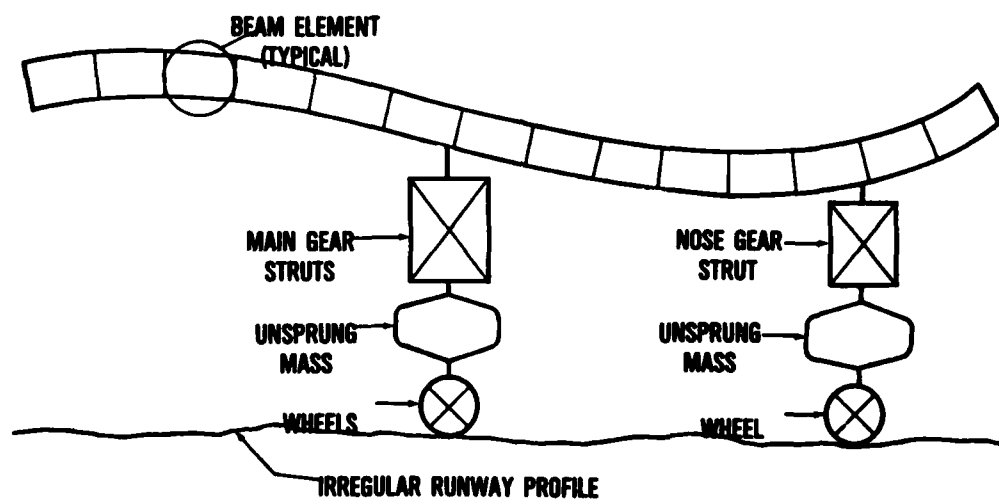


Figure 9. Beam Model to be used in the Hybrid

## METHODE DE SIMULATION NUMERIQUE DU SYSTEME AVION ATERRISSEUR

C. PETIAU et A. CELIER

AVIONS MARCEL DASSAULT- BREGUET AVIATION

78, Quai Carnot - 92214 - SAINT-CLOUD

ABSTRACT

Over more than ten years, a simulation method is being developed by AMD-BA for the dynamic calculation of landing, roll-off, taxiing, take-off and catapulting impacts. This method provides the landing-gear loads and the overall structural stresses as functions of time. The calculation takes account of the dynamic response of the structure and the non-linearities of the problem: large rotations, non-linear elasticity of tyres and shock absorbers, oil shearing, dry friction, etc. The implicit integration algorithm proceeds by elimination at different levels, of the freedom degrees of both the linear and linearized parts, leading, at each time step, to the solution of a non-linear equation system relative to the degrees of freedom associated with oil film shearing and dry friction. Shock absorber sticking due to friction can be taken into account. As the simulation cost is very low, statistical studies can be carried out, especially as regards the simulation of taxiing and take-off.

1 - INTRODUCTION

Les calculs de simulation du comportement dynamique des avions au sol présentent un caractère non linéaire accentué, intervenant sur un relativement faible nombre de degrés de liberté.

Par ailleurs l'aspect aléatoire de la plupart des entrées (profil de piste, condition initiale d'impact, coefficient de frottement des pneumatiques etc ...) exige de procéder à un grand nombre de simulations pour évaluer un système d'atterrisseur.

Avec le programme IMPACT nous effectuons ces simulations dynamiques à un prix raisonnable, sans simplification abusive des non linéarités.

L'idée directrice de la méthode est de procéder par 2 ou 3 niveaux de condensation des degrés de liberté selon les variantes :

- Etablissement des opérateurs de condensation de la structure élastique linéaire à la frontière des trains, préalablement à l'intégration,
- Linéarisation au voisinage du pas de temps précédent des non linéarités "douces" (géométrie, aplatissement des pneumatiques, etc...), condensation par couplage des non linéarités aigues (laminage d'huile, friction),
- Résolution "exacte" d'un système d'équation non linéaire ne portant que sur les degrés de liberté des non linéarités "aigues".

Nous présentons des applications de ces algorithmes sur des problèmes de roulement sur piste non plane, d'impact, et de catapultage.

## 2 - PRINCIPE THEORIQUE DE LA METHODE

### 2.1 - Degrés de liberté et variable du système

On se place dans un système d'axe entraîné par l'avion ce qui évite d'introduire dans le calcul de la réponse de la cellule la non linéarité due à la rotation en tangage et complique peu la modélisation des atterrisseurs.

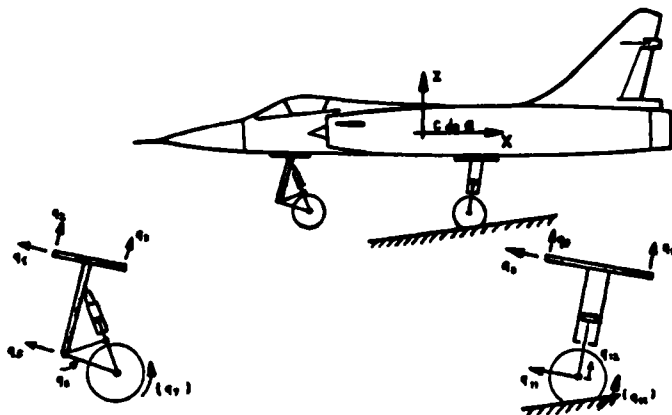
#### - Degré de liberté avion

Nous désignons par  $X$  les degrés de liberté de la structure avion excluant les atterrisseurs ; dans le cas général, on se place dans une base de mode propre calculé par éléments finis, complétée éventuellement par les déformées sous chargement unitaire aux points de couplage avec les trains.

Si on néglige la souplesse de la structure, on restreint  $X$  aux seuls modes rigides.

#### - Degré de liberté des atterrisseurs

Nous désignons par  $q$  les degrés de liberté des atterrisseurs (voir figure ci-dessous).



On décompose les degrés de liberté des atterrisseurs en 2 parties :

$$|q| = \begin{vmatrix} q_I \\ q_{II} \end{vmatrix}$$

$q_I$  représente les degrés de liberté atterrisseurs dépendants de  $X$  par l'opérateur constant  $[\partial q_I / \partial X]$  soit :

$$q_I = [\partial q_I / \partial X] X$$

$q_{II}$  représente les degrés de liberté atterrisseurs indépendants de  $X$ .

#### - Degré de liberté du système couplé

L'état du système couplé avion atterrisseur est défini par le vecteur :

$$y = \begin{vmatrix} X \\ q_{II} \end{vmatrix}$$

#### - Aplatissements des pneumatiques (vecteur $A$ plat. )

Ils sont fonction non linéaire de  $q$  et de la hauteur du sol, elle-même dépendant de  $q$  et de la forme de la piste.

Les non-linéarités sont essentiellement produites par les rotations (assiette et mouvement des balanciers).

#### - Enfouissement amortisseurs (vecteur $Enf.$ )

Ils sont fonction linéaire ou non linéaire (train à balancier) des composantes de  $q$ .

#### - Rotation des roues (vecteur $\omega$ )

Nous les prenons comme degrés de liberté indépendants intégrés aux  $q$  dans les problèmes d'impact et de freinage avec dérapage ; dans les problèmes de roulement elles sont fonction de  $q$ .

2.2 - Equations du problème

## - Mouvement d'avion

$$1) [M] X'' + [B] X' + [K] X = F_{\text{aéro}} + F_{\text{poussée}} + F_{\text{train}} / \text{avion}$$

Les matrices  $[M]$ ,  $[B]$  et  $[K]$  (masse, amortissement, rigidité) sont diagonales si on s'est placé dans la base des modes propres.

Les forces aérodynamiques  $F_{\text{Aéro}}$  sont fonction des paramètres aérodynamiques (incidence, braquage de gouverne, etc), eux-mêmes fonction de  $X$  et de ses dérivées par l'intermédiaire de l'équation de la mécanique du vol et éventuellement des lois du contrôle actif des commandes de vol.

La poussée réacteur  $F_{\text{poussée}}$  est fonction de la vitesse et des ordres pilote.

$F_{\text{train}} / \text{avion}$  représente l'action des trains sur l'avion.

## - Mouvement des trains (hors amortisseurs)

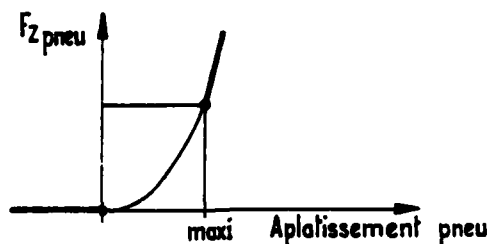
Nous les représentons par l'équation

$$2) [m] q(q) q'' + [b] q' + [k] q = f_0 + f_{\text{train}} / \text{avion} + f_{\text{amortisseur}} + (F_{\text{frein}}) + (F_X \text{ pneu})$$

qui est dérivée de l'équation de Lagrange en négligeant les termes issus de la dérivation de l'énergie cinétique  $T$  par rapport au  $q$  ce qui équivaut à ne pas tenir compte des forces centrifuges.

Les matrices  $[m] q(q)$ ,  $[k] q(q)$ , et le second membre  $f_0$  se déduisent de l'expression de l'énergie cinétique et de l'énergie élastique du train et des pneus.

L'énergie élastique provient en général de la flexion de la jambe de train et de la compression des pneumatiques dont la loi empirique non linéaire d'effort en fonction de l'aplatissement (voir figure ci-dessous) est linéarisée au voisinage de chaque état ; cette loi est prolongée par une droite à forte pente au-delà de l'écrasement maximal, et par une droite de pente nulle pour simuler le décollement.



Le terme  $F_{\text{avion}} / \text{train}$  correspond à l'action du reste de la cellule représenté par  $X$  soit :

$$F_{\text{avion}} / \text{train} = - \left[ \partial q_i / \partial X \right]_t F_{\text{train}} / \text{avion}$$

Le terme  $F_{\text{amortisseur}}$  représente les forces généralisées appliquées par les amortisseurs sur le reste des trains soit :

$$f_{\text{am}} = \left[ \partial \text{enf} / \partial q \right]_t q$$

représentant les efforts amortisseur.

Le terme  $F_X \text{ pneu}$  représente les forces généralisées dues au frottement des pneus, il n'apparaît que dans les calculs tenant compte du glissement ; dans les calculs sans glissement, la rotation des roues n'est plus un degré de liberté et le frottement des pneus est une force interne (voir § 2.3).

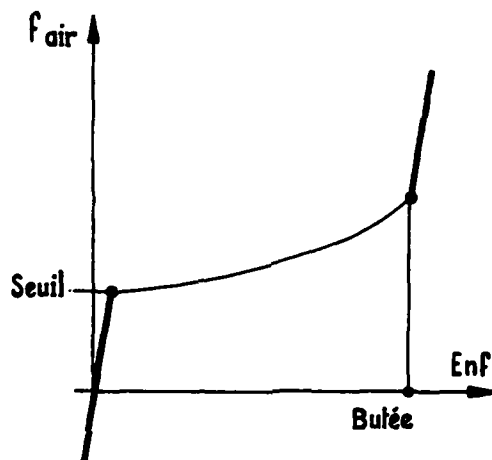
## - Forces amortisseur

Elles sont fonction de l'enfoncement et des efforts palier par des relations de la forme

$$\varphi_i = f_{\text{air}}(\text{Enf}_i) + S \left\{ f_{\text{rot}_i} + C_{\ell \text{ am}_i} \left( \partial \text{enf}_i / \partial t \right)^2 \right\}$$

$$S = -(\partial \text{Enf}_i / \partial t) / \left| \partial \text{enf}_i / \partial t \right| = \pm 1$$

$f_{\text{air}}(\text{Enf}_i)$  représente l'effort dû à la compression du gaz de l'amortisseur, nous prenons une courbe intermédiaire entre une loi isentropique et isotherme, les phénomènes de seuil et de butée sont pris en compte en prolongeant la loi par des droites de fortes pentes (voir ci-dessous).



$f_{\text{rot}_i}$  frottement sec. de Coulomb, est de la forme

$$f_{\text{rot}_i} \leq f_{\text{rot}_0 i} + \mu \left| f_{\text{palier}} \right|$$

L'égalité se produit en cas de glissement avec

$$\partial \text{enf}_i / \partial t \neq 0$$

$C_{\ell \text{ am}}$  : coefficient de laminage de l'huile, est différent entre la détente et l'enfoncement et peut varier pendant l'enfoncement.

## 2.3 - Intégration dans le temps

Nous utilisons la méthode implicite de Houbolt, dans laquelle les termes d'accélération et de vitesse apparaissant dans les équations sont discrétisés à un instant  $t$  sous la forme :

$$5) \quad \ddot{X}_t = \frac{1}{\Delta t^2} \left\{ 2 X_t - 5 X(t - \Delta t) + 4 X(t - 2 \Delta t) - X(t - 3 \Delta t) \right\}$$

$$6) \quad \dot{X}_t = \frac{1}{\Delta t} \left\{ \frac{3}{2} X_t - 2 X(t - \Delta t) + \frac{1}{2} X(t - 2 \Delta t) \right\}$$

Certains termes à variation lente sont posés comme étant égaux à leur valeur résultant de l'équilibre à  $t - \Delta t$ .

Cette procédure ramène l'intégration à une suite de résolution de système d'équation de la forme.

- Cellule

$$7) \quad [K_d] X = F_{dyn} + F_{aéro} + F_{poussée} + F_{train} / \text{avion}$$

avec :

$$[K_d] = \left\{ (K) + \frac{3}{2\Delta t} (B) + \frac{2}{\Delta t} (M) \right\} F_{dyn} = \frac{M}{\Delta t^2} \left\{ 5X(t-\Delta t) - 4X(t-2\Delta t) + X(t-3\Delta t) \right\} \\ + \frac{(B)}{\Delta t} \left\{ 2X(t-\Delta t) - \frac{1}{2} X(t-2\Delta t) \right\}$$

$F_{aéro}$  et  $F_{poussée}$  sont pris à leur valeur au pas précédent en fonction de  $X$  et de ses dérivées, du braquage de gouverne et des ordres pilotes et éventuellement de la fonction de transfert des commandes de vol électriques.

Il est possible à ce niveau de tenir compte des effets d'aérodynamique instationnaire.

- Trains

$$8) \quad [K_d] q = f_{...} + f_{\text{avion/train}} + f_{\text{amortisseur}} + (f_{\text{frot pneu}} + f_{\text{frein}})$$

avec :

$$[K_d] = \left\{ (K_{tg}(q)) + \frac{2}{\Delta t} (M_{tg}(q)) \right\} \\ f_{...} = f_0(q) + \frac{(M_{tg}(q))}{\Delta t^2} \left\{ 5q_{t-\Delta t} - 4q_{t-2\Delta t} + q_{t-3\Delta t} \right\}$$

- Couplage avion train

Dans la référence  $Y = \begin{vmatrix} X \\ q_{II} \end{vmatrix}$

avec  $q_I = [\partial q / \partial X] X$  la transposition des équations d'équilibre 2 et 3 conduit à une équation de la forme

$$[K_d] Y = F_{...} + F_{\text{amortisseur}}$$

$F_{...}$  rassemble les différents termes d'inertie, de linéarisation ; et de valeur d'effort prise à leur valeur au pas précédent (aérodynamique et poussée réacteur).

- Condensation des amortisseurs

En exprimant les forces généralisées amortisseur  $F_{\text{amortisseur}}$  en fonction des efforts amortisseur  $\phi_i$ , l'équation 9 devient :

$$9) \quad [K_d] Y = F_{...} + [\partial \text{enf} / \partial Y]_t \bar{\phi}$$

Les enfoncements s'expriment en fonction de  $Y$  par une relation linéarisée au voisinage de  $q$

$$\text{Enf} = \text{Enf}_0 + [\partial \text{Enf} / \partial Y] Y$$

En éliminant  $Y$  de 9 et exprimant les vitesses d'enfoncement par la formule 6 dans l'équation d'amortisseur 4, il vient le système

$$10) \quad \begin{cases} \text{Enf} = \text{Enf}_0 + [\partial \text{Enf} / \partial \phi] \phi \\ \phi_i = (a_1 + a_2 \text{Enf}_i) + S(F_{\text{rot}_i} + a_3 + a_4 \text{Enf}_i + a_5 \text{Enf}_i^2) \end{cases}$$

Le système 10 est résolu par relaxation sur chaque amortisseur consécutivement soit à résoudre en fixant les composantes  $\phi_j$  pour  $j \neq i$  des équations de la forme

$$11) \quad b_1 + b_2 \text{Enf}_i + S \left\{ f_{\text{rot}_i} + b_3 + b_4 \text{Enf}_i + b_5 \text{Enf}_i^2 \right\} = 0$$

$$\text{avec } f_{\text{rot}_i} \leq f_{\text{rot}_0} + \mu |f_{\text{palier}}(q(\text{Enf}))|$$



Les efforts palier se linéarisant en fonction de  $t - \Delta t$  au voisinage de l'état du pas de temps  $t - \Delta t$ .

Il apparaît que en cas de glissement l'équation 11 du second degré n'a qu'une seule racine satisfaisant aux relations

$$S = -(\partial \text{Enf} / \partial t) / |\partial \text{Enf} / \partial t|$$

et

$$F_{\text{rot}i} = F_{\text{rot}0} + \mu |F_{\text{palier}}|$$

Le blocage se détecte par l'inexistence de racine acceptable, dans ce cas  $\partial \text{Enf} / \partial t = 0$  ce qui entraîne

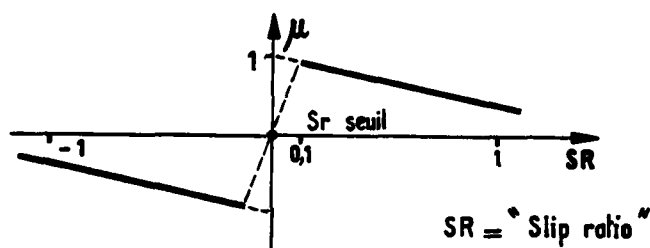
$$F_{\text{rot}i} = -b_1 + b_2 \text{Enf}_i(t - \Delta t)$$

pour assurer à  $q$  une valeur compatible avec  $\partial \text{Enf}_i / \partial t = 0$

#### - Frottement des pneumatiques

En dehors des problèmes de roulement ou de décollement dans lequel la rotation des roues n'est pas un degré de liberté, nous avons 2 approches :

a) asservissement du coefficient de frottement  $\mu$  sur la vitesse de glissement selon une loi du type ci-dessous :



$$S_r = 1 - \frac{V_{\text{périphérique roue}}}{V_{\text{centre roue}}}$$

Nous prenons  $f_x \text{ pneu}$  et  $\mu f_z \text{ pneu}$  à leur valeur au pas de temps précédent, il en résulte une condition de stabilité qui nécessite de fixer une valeur minimum à  $S_r \text{ seuil}$  en fonction du pas de temps d'intégration.

b) approche analogue à celle utilisée pour le frottement sec des amortisseurs, ce qui amène à compléter le système 10 par des équations où les inconnues sont les glissements du pneu  $g_l$  ou les efforts de frottement  $f_x \text{ pneu}$  soit :

$$g_{li} = g_{l0} + (\partial g_l / \partial p) F_x \text{ pneu}$$

$$|F_x \text{ pneu}| \leq \mu(S_r) F_z \text{ pneu}$$

qui sont résolus par relaxation à la suite, et de manière analogue, au frottement des amortisseurs.

## 2.4 - Organigramme

## A - donnée préalable

A1 - Calcul avion. souple par éléments finis

- . Calcul des modes souples  $[V]$
- . Calcul des déformations sous chargement unitaire aux points de couplage  $[D]$  (orthogonalisé par rapport au mode rigide).
- . Matrice de rigidité et de masse dans la base  $X'$  (modes rigides, modes souples, modes frontière).

$$(X_{EF} = [R, V, D] X')$$

$$[K'] = [R, V, D]^T [K_{EF}] [R, V, D] \quad [M'] = [R, V, D]^T [M_{EF}] [R, V, D]$$

. Mode propre de la base  $X' \longrightarrow$  base  $X$ 

$$\{K' - \omega_i^2 M'\} V_i = 0 \longrightarrow [V']$$

 $\longrightarrow$  Matrice de rigidité et de masse  $[K]$  et  $[M]$  diagonale dans la base réduite  $X$ .. Transposition de la base  $X_{EF}$  à la base  $X$  des opérateurs définissant les charges aérodynamiques et la poussée réacteur.. Déplacements des points de couplages trains dans la base  $X$ 

$$[\partial q_i / \partial X] = [\partial q_i / \partial X_{EF}] [R, V, D] [V']$$

. Opérateur donnant les contraintes efforts généraux, ou déplacement aux points sensibles de la structure

$$[\partial G / \partial X] = [\partial G / \partial X_{EF}] [R, V, D] [V']$$

A2 - Calcul avion rigide

Donnée directe de  $[M]$  par masse, centre de gravité et inertie principale calcul de  $[\partial q_i / \partial X]$  à partir des coordonnées des points de couplage.

A3 - Calcul avion souple à partir de mode souple obtenu empiriquement.

Donnée directe de  $[M]$ ,  $[K]$  et  $[\partial q_i / \partial X]$ (  $f_{aéro}$  et  $f_{poussée}$  peuvent être posées arbitrairement comme orthogonale au mode souple).B - initialisation  $t = 0$ - calcul des parties constantes des opérateurs  $[K_d]$  et  $[k_d]$ 

- équilibre statique initial

. avion en vol

calcul équilibre par résolution de la mécanique du vol

$$\longrightarrow X, X', X'' \longrightarrow X_0, X_{-\Delta t}, X_{-2\Delta t}$$

$$q_0 = q_{-\Delta t} = q_{-2\Delta t} = 0 \quad (\text{tout déformé})$$

. avion au sol

Itération de Newton Raphson sur l'algorithme d'intégration en supprimant les termes d'inertie, de viscosité et de frottement, et en prenant une loi isotherme de compression amortisseur (permet la résolution d'hyperstaticité éventuelle).

C - intégration

$$t = t + \Delta t$$

- calcul force intégrée "explicitement"

. mécanique du vol, ordre pilote, loi de commande de vol électrique

$$\rightarrow F_{\text{aéro}} = \text{fonction} (X_{t-\Delta t}, \dot{X}_{t-\Delta t}, \text{ordre pilote})$$

. loi de poussée réacteur

$$\rightarrow F_{\text{poussée}} = f(\text{ordre pilote})$$

- matrice de rigidité dynamique tangente et second membre des parties linéarisées au voisinage de  $t - \Delta t$

$$\rightarrow [k_d], f... \xrightarrow{\text{assemblage}} [K_d], F...$$

- factorisation de Gauss matrice  $[K_d]$

$$\rightarrow [K_d]^{-1}$$

- opérateur tangent d'enfoncement amortisseur (et éventuellement glissement de roue)

$$[E] = [\partial \text{enf} / \partial Y] [K_d]^{-1} [\partial \text{enf} / \partial Y]_t$$

$$\text{Enf}_0 = [\partial \text{enf} / \partial Y] [K_d]^{-1} F...$$

- résolution par relaxation du système d'équation non linéaire 10

$$\text{Enf} = \text{Enf}_0 + [E] \varphi$$

$$\varphi_i = \text{fonction de} (\text{Enf})$$

- restitution de  $Y, X, q$

$$Y = [K_d]^{-1} \left\{ F... + [\partial \text{Enf} / \partial Y]_t \varphi \right\}$$

$$\begin{Bmatrix} X \\ q_x \end{Bmatrix} = Y, \quad q_i = [\partial q_i / \partial X] X$$

- contraintes et efforts aux points sensibles de la cellule souple

$$D = [\partial D / \partial X] X$$

2.5 Variantes2.51 Variante 1 : intégration directe sur les degrés de liberté éléments finis

Cette méthode évite la troncature de la base modale, ce qui la rend plus précise en particulier dans les cas où le nombre de modes excitable est important

Elle diffère de la méthode de base par le fait que  $X$  représentant les degrés de liberté éléments finis est de rang élevé, ce qui nécessite, pour obtenir des temps de calcul raisonnables, une factorisation partitionnée de la matrice  $[K_d]$  en reportant en avant de l'intégration la confection des opérations permettant la condensation du problème sur les parties non linéarisées.

L'organigramme en est le suivant :

A - Calculs éléments finis préalables à l'intégration

- matrice de rigidité  $[K]$  et de masse  $[M]$
- factorisation de Gauss de la matrice de rigidité dynamique

$$\longrightarrow [K_{d_{EF}}]^{-1} = \left\{ [K_{EF}] + \frac{2}{\Delta t^2} [M_{EF}] \right\}^{-1}$$

(stockage en mémoire centrale sous forme creuse),

- déformée cellule sous chargement unitaire aux points de couplage avec les trains

$$[B] = [K_d]^{-1} [\partial q_i / \partial X_{EF}]_t$$

(résolution parallèle).

- matrice de flexibilité condensée à la frontière cellule train

$$[G] = [\partial q_i / \partial X]_t [B]$$

- matrice de rigidité cellule condensée à la frontière cellule train

$$[H] = [G]^{-1}$$

- opérateur creux donnant les contraintes et les efforts généraux en fonction de  $X_{EF}$

$$[\partial \sigma / \partial X_{EF}]$$

B - Initialisation  $t = 0$

Même principe qu'en 2-3 B.

C - Intégration

$$t = t + \Delta t$$

- calcul  $F_{aéro}$ ,  $F_{poussée}$  à partir de  $X_{t-\Delta t}$  (cf. § 2.2)

$$F_{dyn} = \frac{1}{\Delta t^2} [M] [5X_{t-\Delta t} - 4X_{t-2\Delta t} + X_{t-3\Delta t}]$$

- résolution cellule sans train

$$X' = [K_{d_{EF}}]^{-1} \{ F_{aéro} + F_{poussée} + F_{dyn} \}$$

(cette phase représente l'essentiel du temps de calcul)

- chargement cellule condensée sur les  $q_i$

$$f_{avion condensé} = [H] [\partial q_i / \partial X] X'$$

- calcul matrice dynamique tangente et second membre atterrisseur

$$\longrightarrow [k_d], f \dots$$

- couplage train-cellule dans base  $q$

$$[K_{tg}] = [k_{tg}] + [H]$$

$$F \dots = f \dots + f_{avion condensé}$$

- factorisation  $[K_d] \rightarrow [K_d]^{-1}$

- opérateur d'enfoncement amortisseur (et glissement roue)

$$[E] = [\partial \text{enf} / \partial q] [K_d]^{-1} [\partial \text{enf} / \partial q]_t$$

$$\text{Enf}_0 = [\partial \text{enf} / \partial q] [K_d]^{-1} F \dots$$

- résolution par relaxation du système d'équation non linéaire 10

$$\text{Enf} = \text{Enf}_0 + [E] \varphi$$

$$\varphi_i = \text{fonction de } [\text{Enf}]$$

- restitution de q

$$q = [K_d]^{-1} \left\{ F \dots + [\partial \text{enf} / \partial q]_t \varphi \right\}$$

- effort frontière cellule train

$$f_{\text{avion/train}} = [k_d] q - f \dots - [\partial \text{enf} / \partial q] \varphi$$

- déplacement cellule

$$X_{EF} = X' - [B] [\partial q_1 / \partial X]_t f_{\text{avion/train}}$$

- contraintes et efforts aux points sensibles de la cellule souple

$$\sigma = [\partial \sigma / \partial X] X$$

Cette approche a l'inconvénient de nécessiter la saisie à chaque pas de temps de la matrice de rigidité factorisée de la cellule  $[K]^{-1}$ , elle n'est raisonnablement praticable que si cette matrice tient en mémoire centrale (nombre de degrés de liberté n'excédant pas quelques milliers).

Pour une seule simulation d'impact, son coût est du même ordre que celui de la méthode de base, le prix des résolutions de calcul de  $X$  équilibre celui du calcul préalable des modes de la première méthode ; en pratique sur une même configuration de mode, on effectue un grand nombre de simulations ce qui rend la méthode de réduction modale préalable beaucoup plus avantageuse.

#### 2.52 - Variante 2 : Intégration sur base modale de rang élevé

L'algorithme à préconiser est alors identique à celui de la variante I,  $X$  représentant comme dans la méthode de base la composante dans la base des modes propres complétée des déformées sous chargement unitaire au point de couplage.

Son intérêt réside dans le fait qu'on ne procède au cours de l'intégration qu'à l'inversion d'une matrice  $[K_d]$  de rang nombre de degrés de liberté des trains, alors que dans la méthode de base cette matrice est du rang du nombre de degré de liberté total du système.

Son inconvénient est d'exiger que la matrice  $G$  de flexibilité de la cellule condensée au point de couplage soit régulière, ce qui évidemment exclut le cas d'avion rigide, ou conduit à de mauvais conditionnements en cas de base modale trop tronquée ou empirique.

Dans notre cas, cette méthode est la plus économique quand on s'intéresse particulièrement à la réponse dynamique de la cellule.

## 2.6 - Stabilité, convergence, coût

Notre méthode d'intégration est hybride, implicite explicite, elle est donc théoriquement soumise à des conditions de stabilité liées à la valeur du pas de temps, en fait les termes les plus contraignants, grande raideur élastique, laminage d'huile, friction sont traités en approche implicite ce qui efface pratiquement la condition de stabilité devant celle de convergence des résultats.

Le pas de temps assurant cette convergence est déterminé par :

- la méthode de Houbolt qui lisse les vibrations de période inférieure à quelques dizaines de fois le pas de temps,
- les diverses linéarisations dont l'hypothèse doit être acceptable pendant la durée d'un pas de temps,
- les évolutions de forces extérieures qui sont moyennées sur chaque pas de temps.

En pratique, le pas de temps  $\Delta t = 2 \times 10^3$  seconde assure une convergence sûre.

Il en résulte les ordres de grandeur de coût d'exploitation suivants sur IBM 3033 :

- simulation d'impact 5 sec.,
- simulation de roulement + décollage 20 sec.

Nous présentons planche 1 une étude de convergence de réponse en effort amortisseur sur un passage de bosse mettant en évidence les phénomènes de blocage pour des pas de temps de  $10^{-5}$  s,  $10^{-3}$  s et  $10^{-2}$  s.

## 2.7 - Organisation

Le programme IMPACT a évolué à partir de produits spécialement rédigés pour chaque type d'architecture vers un outil général susceptible de traiter toutes les configurations d'atterrisseur de nos avions.

Pour cela, nous avons défini une notion de "système" et de "sous-système" décrit à l'aide de données standardisées.

Les systèmes sont :

- . Les divers types d'atterrisseurs utilisés par AMD-BA (train "droit", train à "balancier"),
- . Les catapultes,
- . Le "Hold Back",
- . La crosse et le câble d'arrêt.

Les systèmes font appel à des modules plus généraux dits de "sous-système", ce sont principalement :

- . Les amortisseurs,
- . Les roues.

Les systèmes et sous-systèmes ont leur géométrie définie par correspondance à une liste de noeuds définit globalement.

## 3 - EXEMPLES D'APPLICATIONS

### 3.1 - Roulement, passage d'obstacle

Nous présentons à titre indicatif sur la planche 2 les efforts trains sur des simulations de roulement accélééré d'avion de combat sur la piste de notre centre d'essais en vol.

Ces excitations au roulement sont extrêmement délicates à établir :

- du fait de l'aspect aléatoire de l'excitation par le profil de la piste,
- par l'inadaptation du laminage des amortisseurs au roulement dû aux faibles vitesses d'enfoncement des amortisseurs (comparées à celles de l'impact) ; ce qui rend les résultats sensibles aux valeurs des autres amortissements (frottement pneumatique, structure ...) mal connues a priori.

Nous étudions planche 3, les effets de 2 bosses de 30 mm de hauteur et de 5 m de long abordées pendant le même roulement respectivement à 30 m/s et 60 m/s ; ces bosses qui pourraient être assimilées à des réparations sommaires, sont surimposées au profil de la piste d'Istres.

Il faut souligner que, même pour une vitesse avion identique, le niveau de réponse est sensible au point de la piste sur lequel est situé l'obstacle, ce qui nécessite de traiter pratiquement le problème par statistique.

On remarquera qu'aux vitesses envisagées, l'effet de la réparation n'est pas très important par rapport aux vibrations "naturelles".

### 3.2 - Impact

Nous présentons planche 4 des résultats de simulation d'impact typique d'avion de combat, avec une comparaison brute entre les résultats de simulation avec coefficient théorique et des essais de chute sur rouleau au CEAT qui font apparaître le degré de confiance qu'on peut avoir dans ce type de calcul.

Nous présentons planche 5, les comparaisons calcul essais en vol sur les impacts du Mercure, en particulier l'évolution des moments de flexion au droit des cadres principaux du fuselage.

Nous avons dans ce cas procédé par la méthode d'intégration directe sur modèle Eléments Finis.

### 3.3 - Catapultage

Nous en présentons planche 6 la simulation à titre anecdotique ; ce problème a exigé l'introduction de "système" particulier dans notre outil :

- . "Hold back" élément élastique se rompant quand l'effort catapulte est suffisant,
- . Elingue représentée par un ressort non linéaire de rigidité nul en compression,
- . Catapulte système complexe à modélisation élastique non linéaire (détente adiabatique) et caractéristique variable en fonction du temps (admission de vapeur et débit des fuites).

Notre outil permet de traiter dans la même approche le problème de transition rapide de la détente des élingues consécutifs à la rupture du Hold-back et celui d'oscillations plus lentes de la charge du train avant résultant de l'excitation du mode de tangage.

## 4 - CONCLUSION DEVELOPPEMENT

Aujourd'hui le programme IMPACT couvre l'essentiel de nos besoins de simulations en hypothèse de mouvement symétrique.

Les principales difficultés résultent de la mauvaise connaissance de certains paramètres citons :

- Loi d'air "polytropique" des amortisseurs,
- Laminage d'huile à faible vitesse,
- Frottement sec des amortisseurs,
- Frottement et hystérésis des pneumatiques,
- L'aérodynamique dans les effets de sol.

Il nous est apparu que les mesures directes de ces coefficients sont difficiles, ce qui nous amène à développer des méthodes d'identification indirecte basées sur la minimisation de distances calcul mesure.

Un autre aspect des simulations d'avion au sol est le caractère aléatoire de nombre de données :

- Conditions initiales et ordre pilote dans les effets d'impacts,
- Coefficient de frottement des pneumatiques,
- Profil de la piste,
- Conjonction variable des efforts dus à la piste et des surcharges de décollage (ou des effets des réparations).

Pour tenir compte de ces aspects aléatoires nous utilisons la méthode de Monté-Carlo par simulation sur des échantillons de donnée tirés au sort, les résultats sont analysés par histogramme.

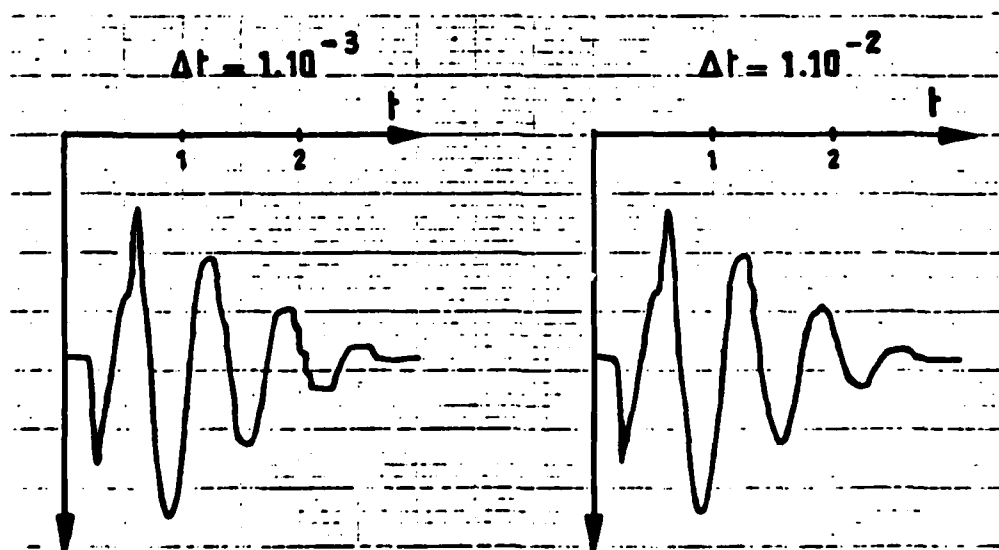
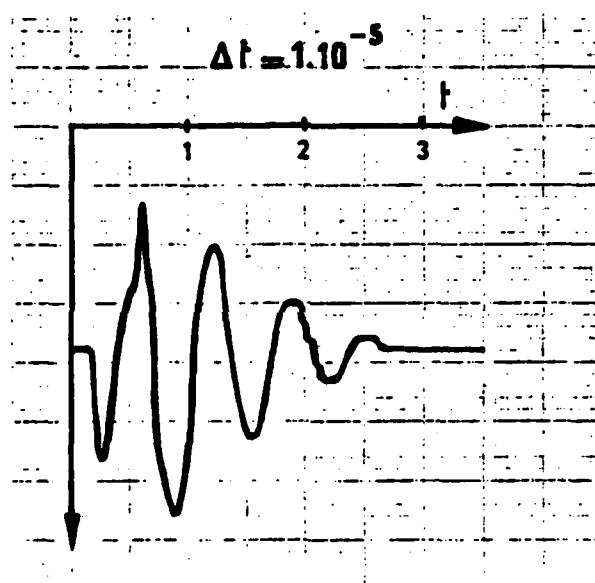
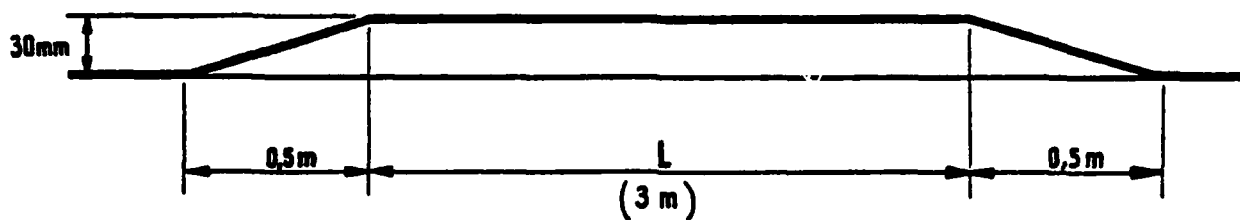
Nous envisageons deux voies principales de développement à venir :

- Extension aux impacts asymétriques qui pose le problème de la modélisation du ripé des pneumatiques, et renforce les effets de non linéarité géométrique,
- Prise en compte de systèmes d'amortissement actif, qui permettraient de résoudre le problème des insuffisances d'amortissement au roulement et d'optimiser l'absorption d'énergie pendant l'impact et l'abattée.

ETUDE DE CONVERGENCE

Enfoncement amortisseur pendant un passage de bosse

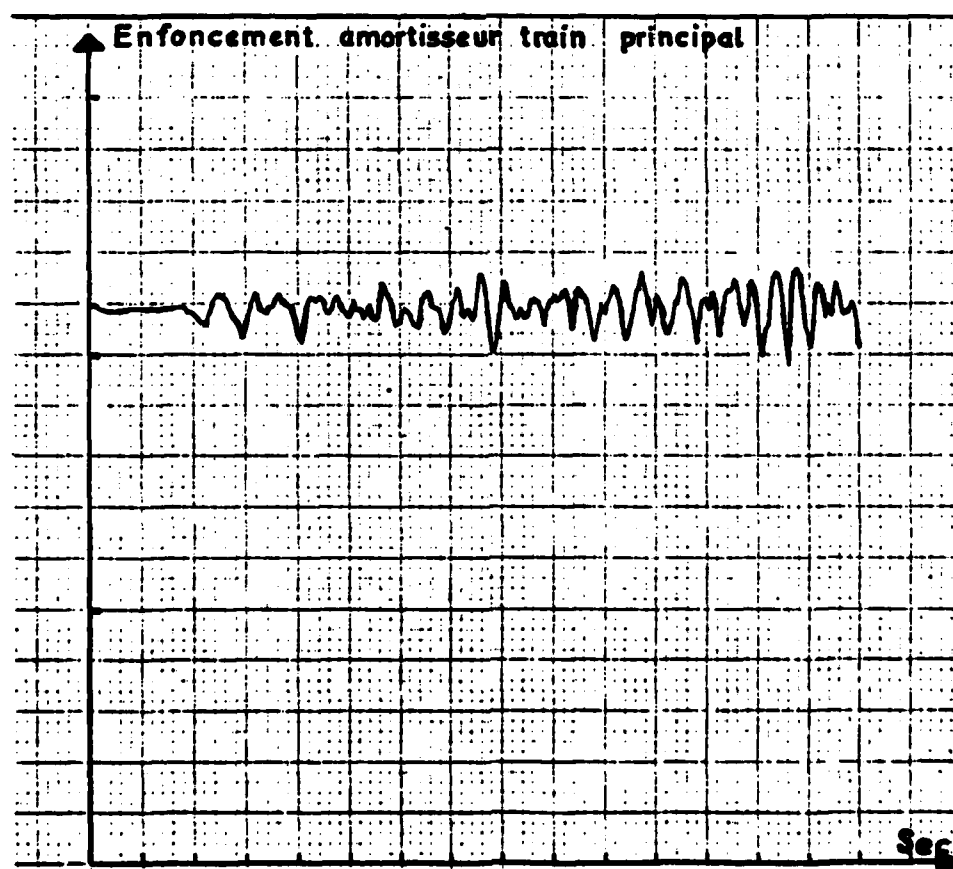
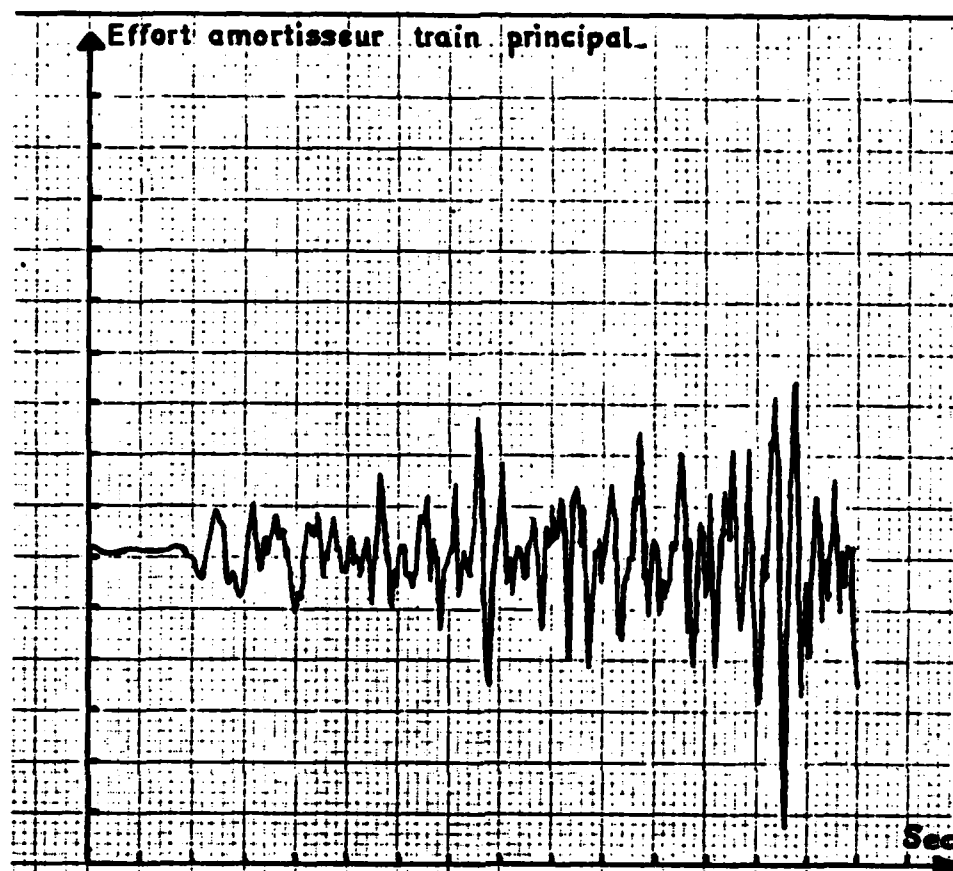
$$V = 10 \text{ m/s}$$





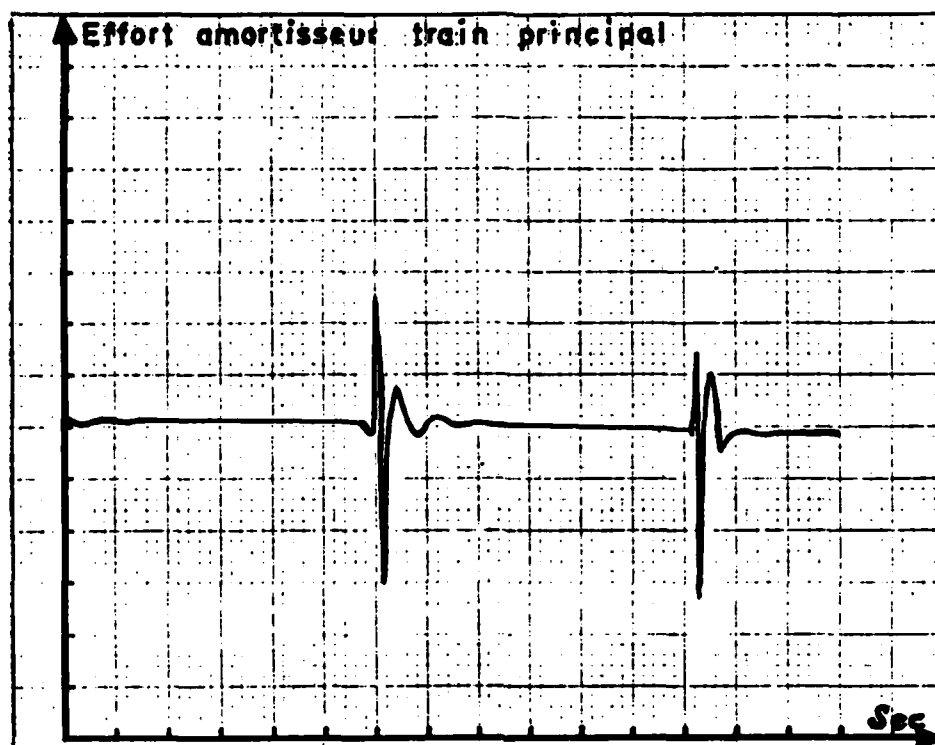
SIMULATION DE ROULEMENT AVEC ACCELERATION

(Piste d'Istres)

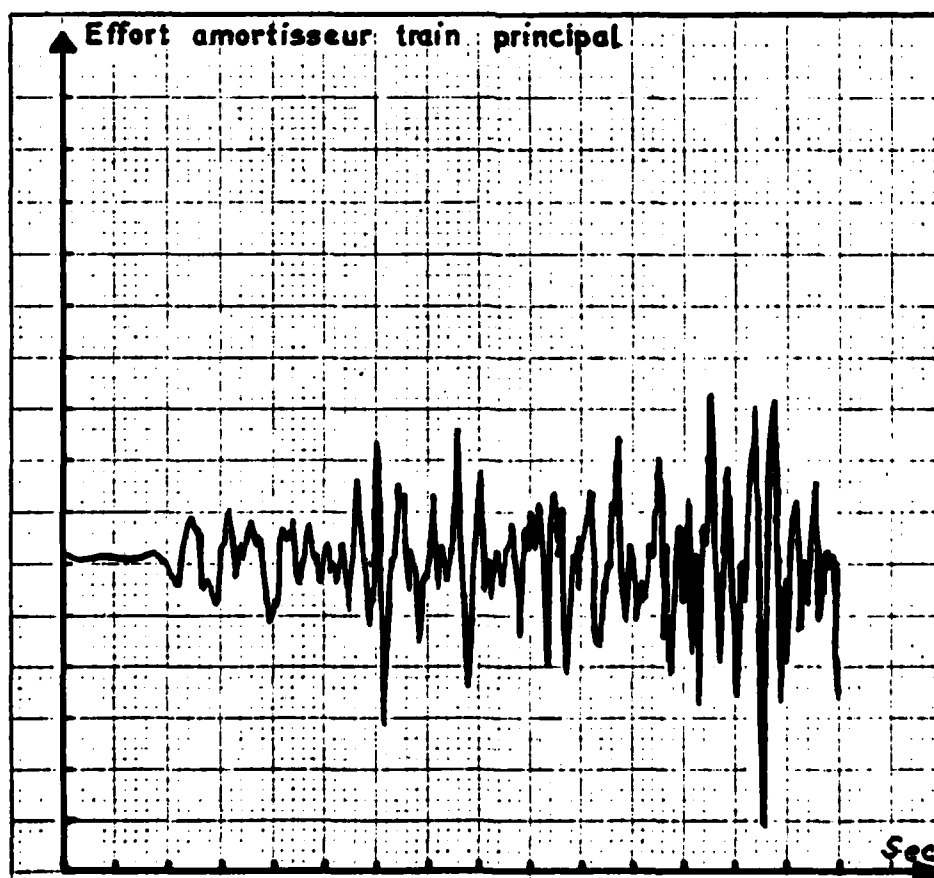


SIMULATION DE ROULEMENT AVEC ACCELERATION

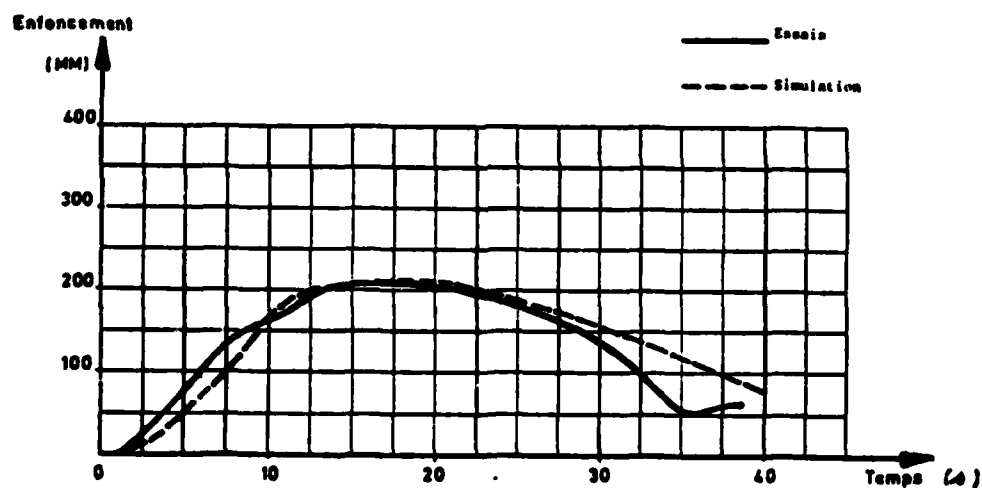
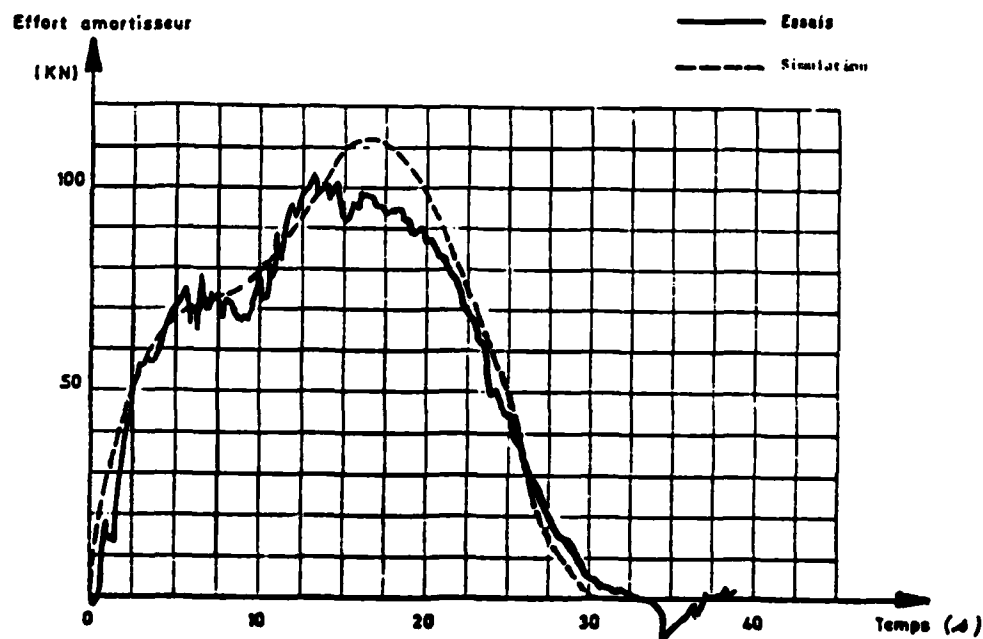
Piste lisse endommagée (2 bosses  $L = 5$  m,  $h = 30$  mm)



Piste d'Istres endommagée

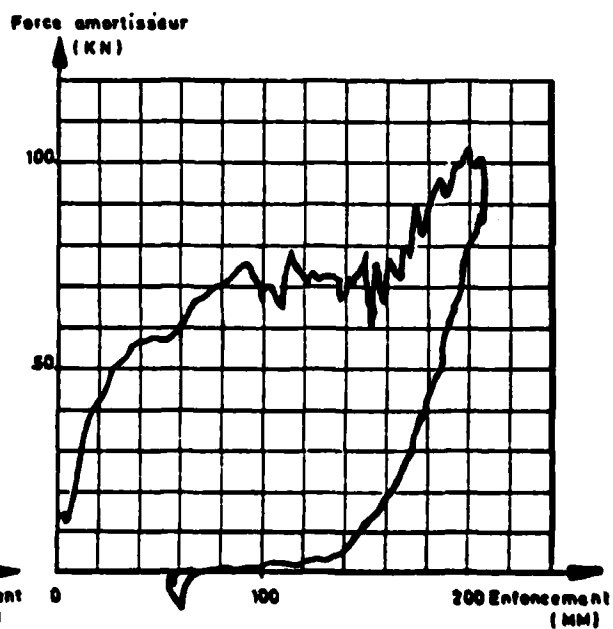
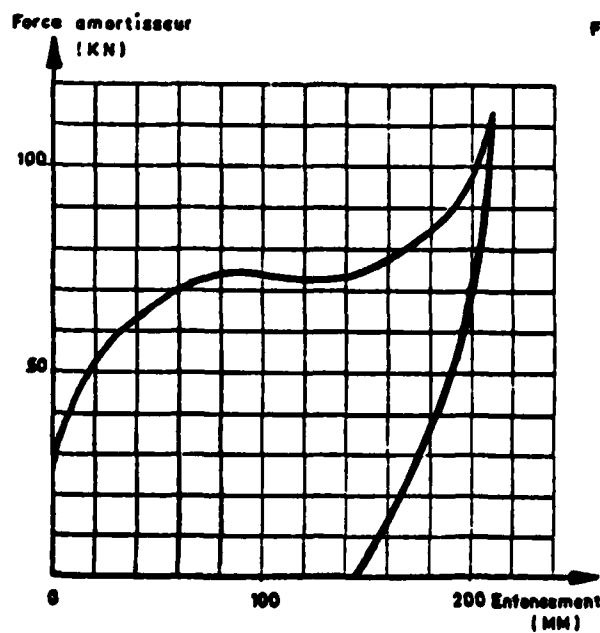


# ESSAIS DE CHUTE Comparaison calcul - essai



SIMULATION

ESSAI



MERCURE : ATTERRISSAGE DYNAMIQUE  
 Comparaison essais en vol - calculs

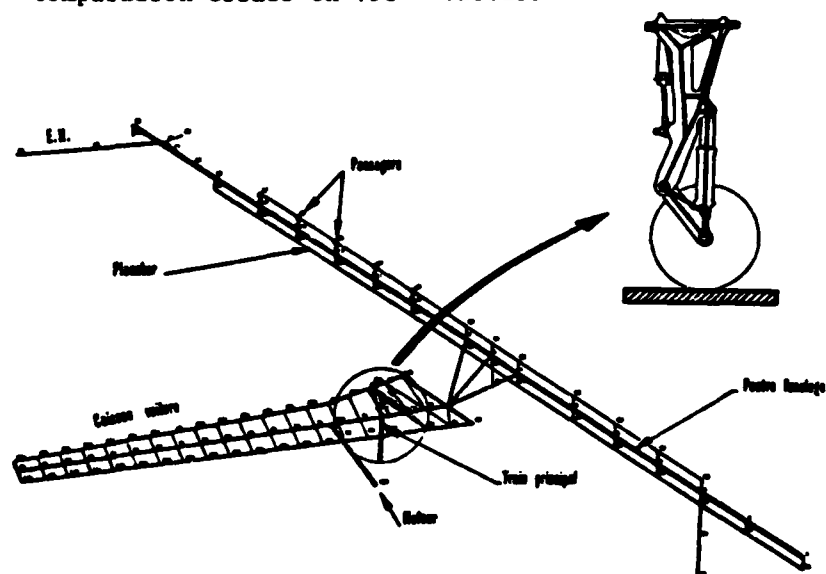
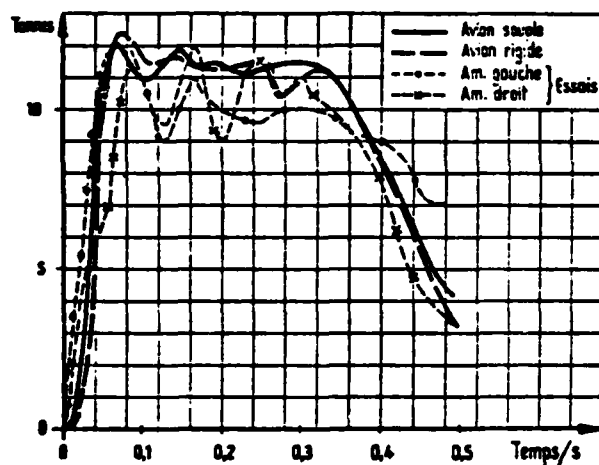
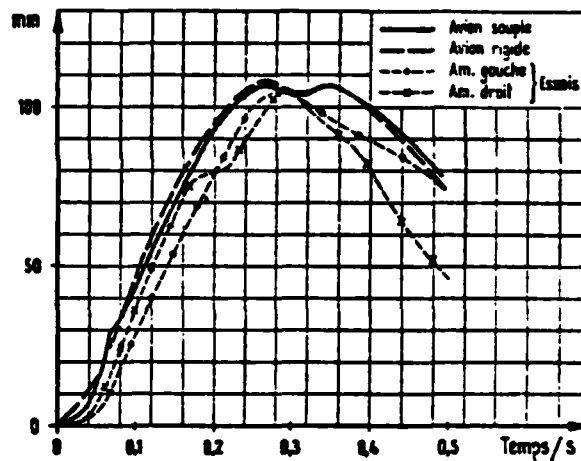


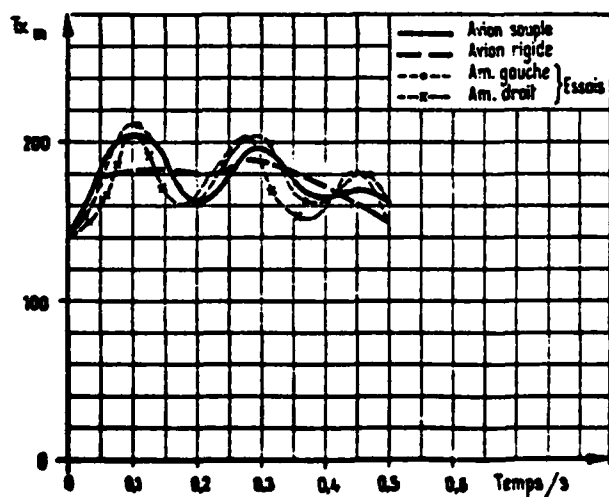
Schéma éléments finis simplifié



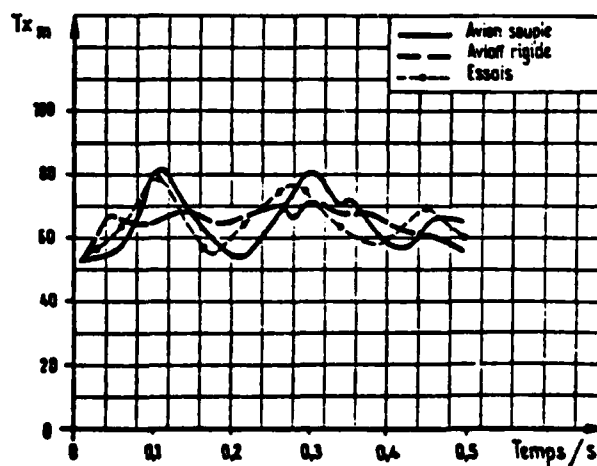
Effort amortisseur



Enfoncement amortisseur

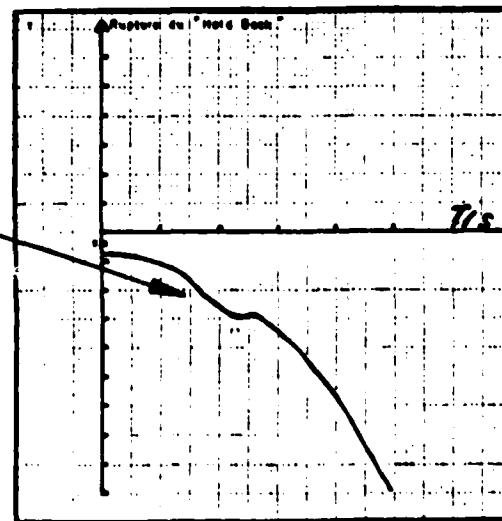
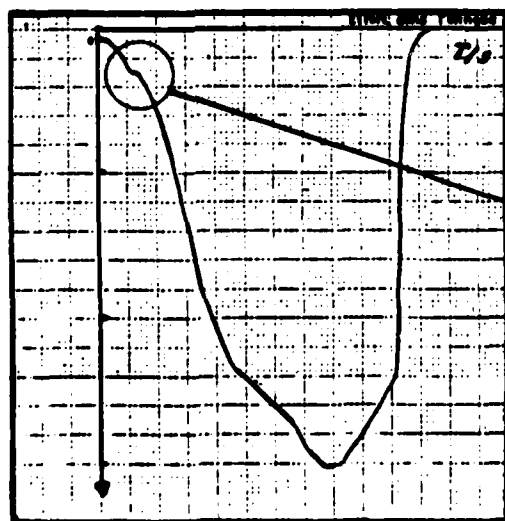
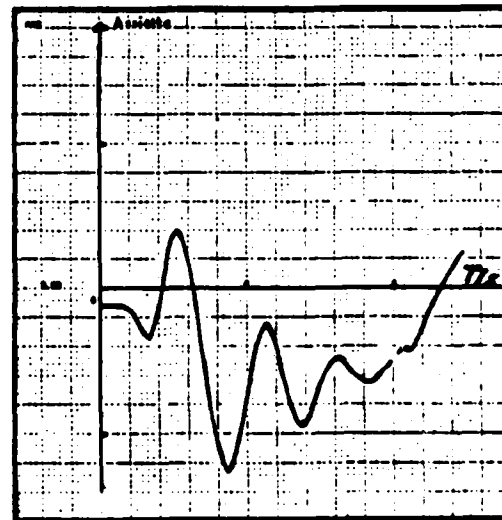
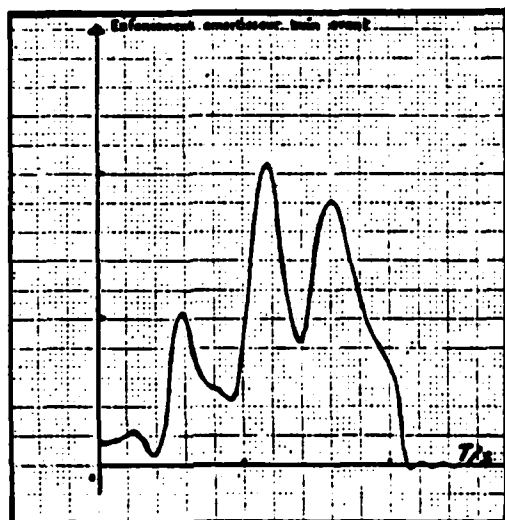
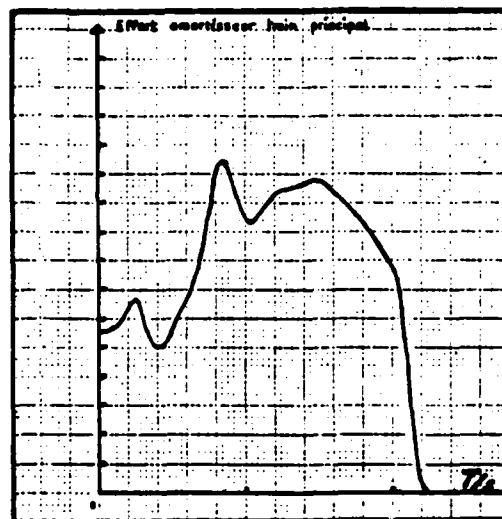
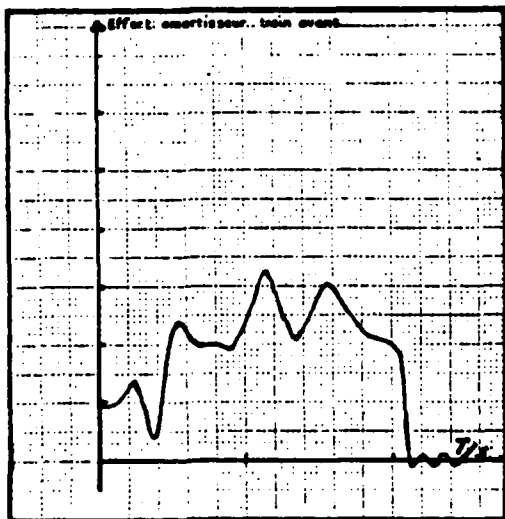
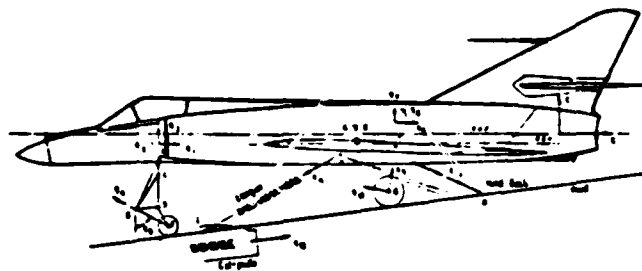


Moment de flexion au cadre  
principal arrière



Moment de flexion fuselage  
au cadre principal avant

## SIMULATION DE CATAPULTAGE



# PREDICTED AND MEASURED LANDING GEAR LOADS FOR THE NF-5 AIRCRAFT TAXIING OVER A BUMPY RUNWAY

by  
H.H. Ottens  
National Aerospace Laboratory NLR  
The Netherlands

## SUMMARY

A simple mathematical model of the NF-5A aircraft has been developed. The model has been validated using measured results. Landing gear loads have been calculated for the aircraft taxiing across a repaired runway using an AM-2 mat. The results depend strongly on the heaving and pitching motion of the aircraft when it meets the repair.

## 1. INTRODUCTION

Runway repair under wartime conditions requires quick repair procedures. These may introduce local runway irregularities that can lead to significant taxi loads on the aircraft and its undercarriage. Hence, repair procedures must be selected judiciously with regard to repair time and cost and to repair quality, in terms of runway roughness.

The damaged runway problem is being investigated by the NATO countries. Within that framework a working group of the AGARD Structures and Materials Panel investigates how the loads on an aircraft taxiing on a bumpy runway can be established. The results of this study may lead to criteria for repair procedures required. A number of pilot papers have been published by the AGARD panel (ref. 1).

The Netherlands contribution to this investigation is concentrated on two fighters operational for the Royal Netherlands Air Force viz. the NORTHROP NF-5 and the General Dynamics F-16. For both aircraft a simple mathematical model will be made to calculate the aircraft response.

Up to now the model of the NF-5 has been completed. Using this model the undercarriage loads have been calculated simulating a taxi run over a AM-2 mat which now is a standard repair procedure within NATO.

The main purpose of the Netherlands study is to investigate whether it is possible to express the loads in terms of a limited number of aircraft parameters viz. aircraft weight, location of the centre of gravity, heave and pitch resonance frequencies etc.

## 2. DESCRIPTION OF THE NF-5A MODEL

In figure 1 the NF-5A aircraft is shown. A simplified model of the NF-5A aircraft has been developed to analyse the aircraft response during taxiing on a runway. A full description is given in reference 2. Only symmetric motions of the aircraft are considered.

The model consists of a rigid aircraft structure supported by flexible landing gears. The model is shown in figure 2. There are one nose and two main landing gears. The two main landing gears are identical and as only symmetric motions are considered they act identical also.

Each landing gear is modelled into a rotational spring representing the dragstrut stiffness, a sliding member, a mass representing the axle, wheel and brake and a spring representing the tyre.

To describe the motion of the aircraft and the undercarriage deflections the following set of degrees of freedom, as shown in figure 3, has been chosen.

- i the coordinates of the aircraft c.g.
- ii the aircraft pitch angle
- iii the coordinates of the main and nose gear wheel axes.

As symmetric aircraft motions are considered only, one pair of coordinates is used for both main gear legs. Then, for any given runway profile and initial conditions these 7 degrees of freedom are sufficient to represent in the model.

- i horizontal, vertical and pitching motion of the aircraft
- ii dragstrut deflections
- iii tyre deflections
- iv travel of the spring damping system in the sliding members.

The equations of motion for the 7 degrees of freedom can be derived. These simultaneous differential equations are integrated numerically using a special purpose FORTRAN code, starting with given initial conditions.

The various components of the landing gear will be described in some detail in the next chapter. A more detailed description is given in reference 1.

### 3. DESCRIPTION OF A LANDING GEAR

The various landing gear components are:

#### (a) Drag strut

For simplicity reasons the stiffness of the drag strut and other structural elements of the landing gear attachments is represented by a linear rotational spring.

#### (b) Sliding member

In figure 4 a sketch of a sliding member is shown. It has three chambers. Chambers 2 and 3 are filled with oil completely whereas chamber 1 is partly filled with oil and partly with nitrogen gas. The oil flow between chambers 1 and 2 passes through an annular orifice the size of which is controlled by a variable diameter metering pin.

The oil flow between chambers 1 and 3 runs through an orifice that contains a recoil valve. This valve allows an unrestricted oil flow during the up-stroke of the landing gear, but during the down-stroke the restricted valve area increases the damping.

#### (c) Tyre

The tyre is represented by a non-linear spring. The spring coefficient depends not only on the tyre inflation pressure but also on the tyre deflection.

### 4. VALIDATION OF THE MODEL

The values of most parameters used in the mathematical model were established using design drawings and maintenance handbooks. Uncertain were the damping coefficients of the sliding members. These values were adjusted using data from measurements.

The model was checked experimentally at Gilze Rijen Airforce Base. The main runway was repaired and a secondary runway which crossed the main runway nearly perpendicularly was used. This crossing causes a bump in the secondary runway. The secondary runway profile is given in figure 5.

A number of taxiruns were made to check the operational usability of the secondary runway. These runs were performed with the instrumented NF-5A K-3001 aircraft of the Royal Netherlands Air Force. The measured results were compared with calculated results to validate the mathematical model.

The following parameters have been measured.

- i the compression of the nose gear sliding member
- ii the aircraft pitch angle
- iii the vertical acceleration of the aircraft c.g.
- iv the aircraft forward speed.

The pitch angle, the vertical acceleration and the forward speed have been measured using the standard aircraft measuring system. The compression of the nose gear sliding member was filmed using an ad-hoc aircraft mounted camera. On the runway surface a chalk line was painted as a reference for the aircraft position.

Taxi runs have been performed at 74, 98 and 116 knots. The measured results of the 98 knots run have been compared with calculated results.

The initial conditions for the integration were taken at the instant the chalk line was crossed. It proves very difficult to obtain values for the various degrees of freedom and their time derivatives and some approximation was involved in the process.

The comparison between measured and calculated results are shown in figures 6 to 8. This comparison shows a reasonably good agreement.

From these results it has been concluded that the model is sufficiently accurate to be used in runway roughness response analyses.

### 5. RESPONSE OF THE NF-5A AIRCRAFT TAXIING ACROSS AN AM-2 MAT

The response of the NF-5A aircraft taxiing at different speeds across a standard AM-2 mat has been calculated. The mat configuration used is given in figure 9.

The responses have been calculated for different aircraft configurations which are listed in table 1. In this table are also given the aircraft mass properties. In table 2 the resonance frequencies in heave and pitch are given. Configuration 2 is one of the heaviest configurations whereas configuration 6 is one of the lightest configurations.

Note that the heave frequency is nearly constant for all configurations. This is caused by the fact that the pressure of the nitrogen gas in the sliding member is adjusted in such a way that the static compression of the sliding member is constant and independent of the aircraft weight. The pitch frequency is different for the various configurations.

In figures 10 and 11 a typical response of the NF-5A (configuration 7) taxiing at low speed (10 knots) over an AM-2 mat is shown. The vertical forces from one main and from the nose gear are shown in figures 10 and 11 respectively. These responses look more or less like an amplitude modulated sine function. This is caused by the fact that both the aircraft heave and pitch motion contribute to the response. As the resonance frequencies of these motions are rather close ( $f_{\text{heave}} = 1.73 \text{ Hz}$ ,  $f_{\text{pitch}} = 1.33 \text{ Hz}$ ) the combined response is a kind of modulated sine function.

The main landing gear is located relatively close to the aircraft centre of gravity. Hence, its response curve essentially reflects heave motions only. The nose gear response, in contrast, reflects pitch motions mainly. Particularly, the nose gear response shows deviations from the sine function due to the non-linear behaviour of the gear.

From this it is concluded that taxiing at low speed over an AM-2 mat the NF-5 gear responses are affected by both the heave and the pitch motions of the aircraft.

In figures 12 and 13 similar results are shown for taxiing at higher speed (100 knots). The vertical force of the main gear reaches its maximum when the aircraft taxis onto the mat. The vertical force of the nose gear reaches its maximum when the aircraft has left the mat.

From this it is concluded that taxiing over a mat at high speed the main gear forces are determined by the mat ramp and therefore the aircraft weight and the taxiing speed are important parameters. For the nose landing gear, however, the aircraft dynamics (heave and pitch frequencies) are important since they determine the tuning of the aircraft motion with the ride-on and ride-off of the AM-2 mat.

It is rather difficult to present all the results in a clear way. Each taxiing speed and each aircraft configuration has its own particular response time history. The best way of presenting results may be presenting only the maximum values of each time history. This means that no information is available as to when the maximum occurred. This makes it sometimes difficult to interpret these "maximum value curves".

In figure 14 the maximum values of the main gear vertical force are shown as a function of the taxiing speed for six aircraft configurations (configurations 1 to 6). Above the taxiing speed of 50 knots these maximum values are roughly proportional to the taxiing speed. This is caused by the fact that these maxima occur at the mat approach. Below 50 knots the aircraft dynamics are of influence.

In figure 14 also the static vertical forces (aircraft at rest) are shown. It is seen that the taxiing response gives vertical forces up to twice the static values. Also, in the same figure the design limit load is shown. Up to 150 knots all response vertical forces remain below this design value.

In figure 15 the maximum values of the nose gear vertical force are shown, as a function of taxiing speed and aircraft configuration. This figure shows a more complex behaviour compared to the main gear response. The nose gear force is influenced more by the aircraft dynamics.

The static nose gear forces are also shown in figure 15. It can be seen that the maximum response forces can be up to three times the static forces. Only for the heaviest aircraft configurations the response force exceeds the design limit load up to the taxiing speed of 150 knots.

Finally, in figure 16 the maximum values of the vertical acceleration of the aircraft c.g. are shown. This figure is comparable with figure 14 showing the main gear vertical force. At higher taxiing speeds the response is roughly proportional to the speed. For lighter aircraft configurations smaller main gear vertical forces occur compared to heavier configurations. Nevertheless the vertical aircraft acceleration for the lighter configurations is higher compared to the heavier ones due to the smaller aircraft mass.

## 6. SENSITIVITY STUDY

The calculations described in the previous chapter were performed using "optimal" values of the parameters. That means that the values were taken according to the maintenance handbooks. In practice, however, for example the tyre pressure and the sliding member pressure are not adjusted for each change in aircraft configuration. This means that around all results there is a scatter band covering all kinds of deviations from prescribed values. These effects are not investigated in the present study.

In the calculations it was also assumed that the runway in front of the AM-2 mat was absolutely smooth. The aircraft had only a horizontal speed and no vertical or pitch velocity. From the measurements at Gilze Rijen it was observed that also the undamaged runway leads to aircraft responses. Typical response values measured taxiing on a normal runway were: vertical aircraft translations  $\pm 16 \text{ mm}$  ( $\pm .66 \text{ in}$ ) and aircraft pitch angles  $\pm .25 \text{ degr.}$  ( $\pm .0044 \text{ rad}$ ). The influence of these values on the aircraft response has been investigated.

Response calculations have been made for a NF-5A (configuration 1) taxiing over an AM-2 mat starting with different initial conditions. The results are shown in the figures 17 and 18.

The maximum vertical force from the main gear is shown in figure 17. It can be seen that the different initial condition affect the response but the maximum value increases 20 % at most.

In figure 18 the maximum nose gear vertical force is shown. Here a considerable influence from the initial conditions on the response is observed. Especially the perturbation of the pitch angle leads to increases of the nose gear force of up to 100 %.



## 7. DISCUSSION AND CONCLUSIONS

The aircraft response to taxiing over a damaged runway can be predicted with reasonable accuracy provided that some important items can be made available.

### i A dynamic model of the aircraft

This modelling has been demonstrated with sufficient accuracy for both fighter and civil transport aircraft. The setting of the various parameters used in the model may cause some inaccuracy. The parameter values for individual aircraft, such as tyre and sliding member pressure, are not always in accordance to the maintenance handbook values.

### ii The damaged runway profile

Standard repair methods lead to a well defined runway profile. For minor damages which remain unrepaired an estimation of the profile must be made. Not only the damaged or repaired runway profile is important, but also the undamaged runway profile. The undamaged runway profile leads to taxiing loads but also it determines the initial position of the aircraft approaching a damaged or repaired runway. The initial condition is the third important item that should be known.

### iii The aircraft initial condition

The aircraft initial position approaching a damaged or repaired runway patch is important as it determines the aircraft loads taxiing over that particular patch. In general these initial conditions result from taxiing over a smooth, undamaged runway. Unless the "smooth" runway profile is known in detail these initial conditions can only be estimated. The worst conditions with respect to the aircraft loading should be taken.

When these items have been made available the following procedure can be used in wartime conditions to decide in whether a damaged and repaired runway can be used for specific aircraft operations.

### i A handbook

A collection of calculated results for aircraft taxiing in different configurations over different runway profile starting with different initial conditions. From these calculations it is determined which combination of aircraft configuration, runway profile and initial condition is allowable with respect to landing gear loads, and for which combination the design limits are exceeded. These condensed results should be provided in a handbook format that allows a quick decision to be made with regard to operationability of a damaged runway.

### ii A computer code

The actual response calculation for an aircraft with a specific configuration taxiing over a specified runway can be performed almost instantaneously: the computer time required is less than a minute! It could therefore be considered to provide the operations room at each a force base with a computer code and a simple computer facility which can used to calculate the taxiing loads.

The proper aircraft and runway characteristics can then be inserted together with a conservative selection of initial conditions to yield a response curve. It is conceivable, even, to store standard aircraft configurations and runway repair profiles in a data bank.

The choice whether one of these possibilities can be used and which one is the most adequate is dependent on a number of operational considerations which are outside the scope of this study.

## 8. ACKNOWLEDGEMENT

The investigations described have been carried out under contract for the Research Branch of the Directorate of Materiel Air, Royal Netherlands Air Force. The kind permission to present this paper is gratefully acknowledged here.

## 9. REFERENCES

- 1 - "Aircraft dynamic response to damaged runways" AGARD report-685, October 1979.
- 2 H.H. Ottens and A. Nederveen: "Description of a model for taxi response calculations of the NF-5A aircraft". NLR TR 81103 C, 1981.

TABLE 1  
Characteristics of the analysed aircraft configurations








config.		internal	centrel.	inb.	outb.	tip	mass(lb)	$I_{pitch}$ (Lb in <sup>2</sup> )	cg (% MAC)
1		full	Mk 84	275 G full	-	full	21104	$2.03 \times 10^8$	9.1
2		full	150 G full	275 G full	Blu 1/B	full	21898	$1.99 \times 10^8$	13.6
3		full	150 G full	275 G full	-	full	19862	$1.82 \times 10^8$	16.4
4		full	-	150 G full	-	full	17405	$1.60 \times 10^8$	21.0
5		50 %	-	-	-	empty	12596	$1.73 \times 10^8$	11.3
6		5 %	-	-	-	empty	10183	$1.55 \times 10^8$	18.0
7		full	-	150 G full	-	full	17733	$1.90 \times 10^8$	11.2

TABLE 2  
Resonance frequencies of the different aircraft configurations

configuration	resonance freq. (Hz)	
	heave	pitch
1	1.71	1.65
2	1.70	1.38
3	1.71	1.37
4	1.72	1.31
5	1.78	1.32
6	1.78	1.08
7	1.73	1.33

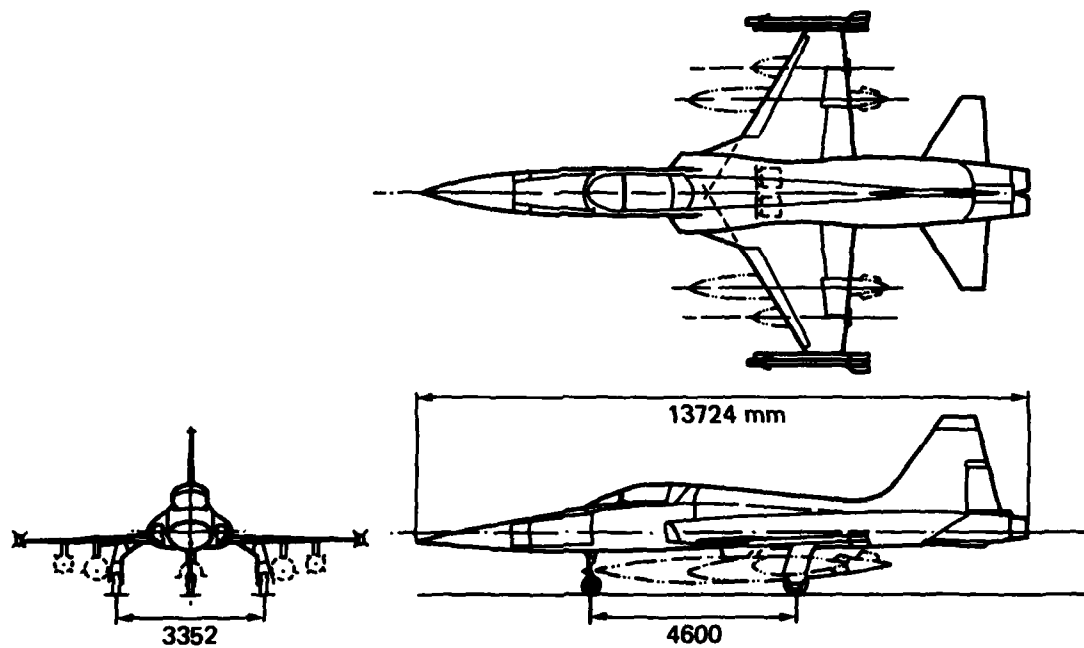
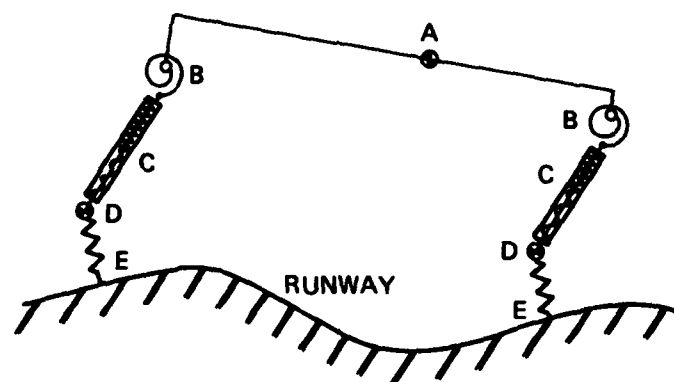


Fig. 1 General lay-out of the NF-5A aircraft



- |                            |  |
|----------------------------|--|
| <b>A RIGID AIRCRAFT</b>    | c.g. position and mass and inertia properties vary with payload and fuel configuration |
| <b>B TORSIONAL SPRINGS</b> | representing drag strut flexibilities  |
| <b>C SLIDING MEMBERS</b>   | with stiffness and damping properties derived from design drawings                     |
| <b>D WHEEL AXLES</b>       | lumped mass representing axles, wheels, tyres and brakes                               |
| <b>E SPRINGS</b>           | representing tyre flexibility  |

Fig. 2 Simple model of the NF-5A aircraft

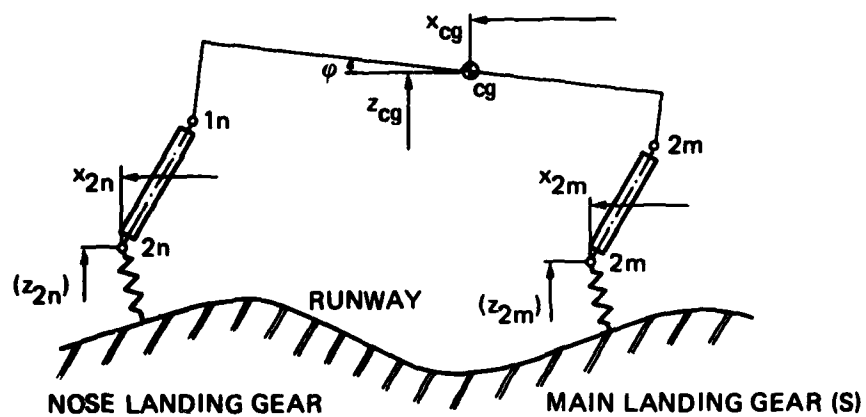


Fig. 3 Degrees of freedom selected for the NF-5A model

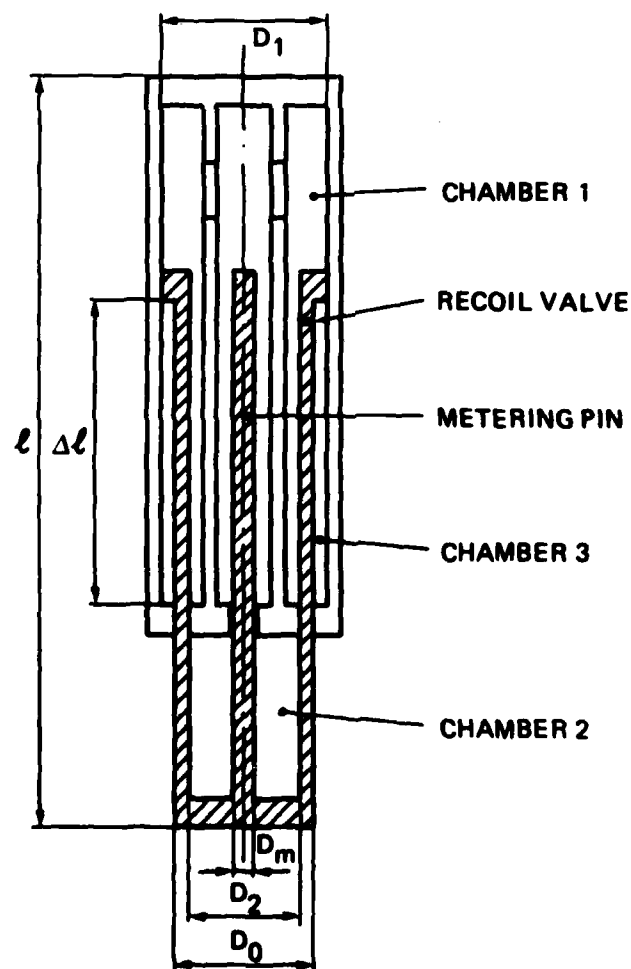


Fig. 4 Sketch of the sliding member

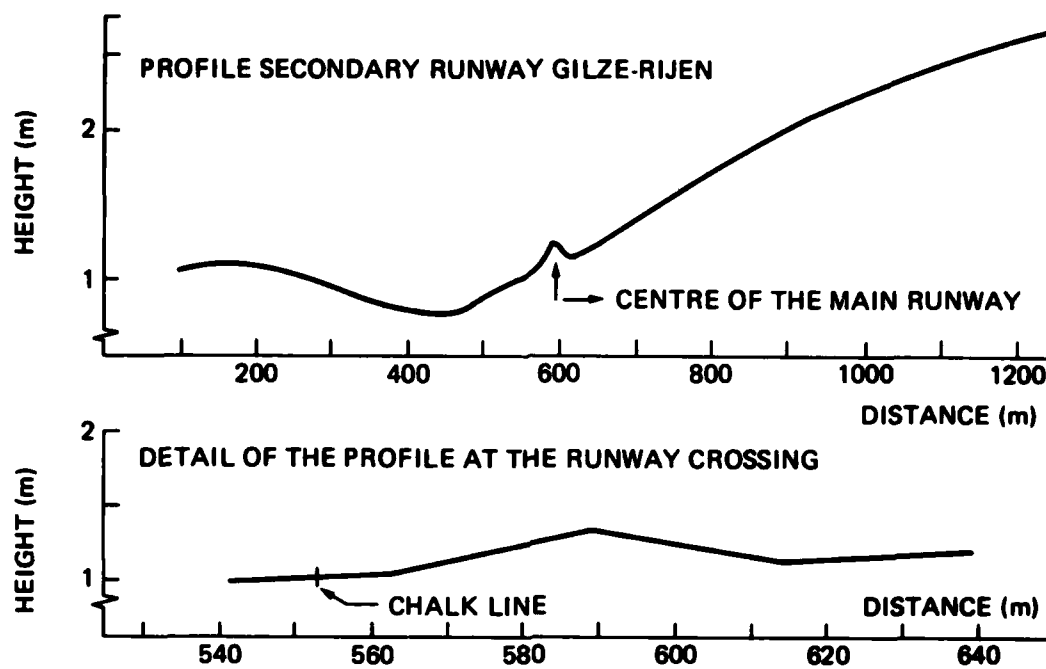


Fig. 5 Profile of the secondary runway at GILZE-RIJEN Airforce Base

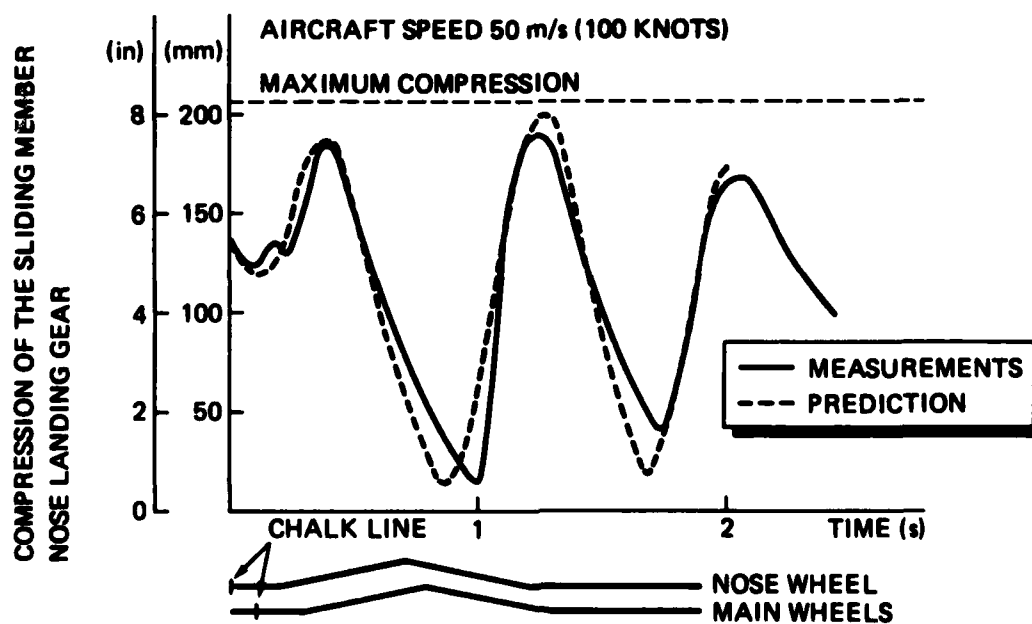


Fig. 6 Compression of the sliding member of the nose landing gear: comparison of the measured and predicted results

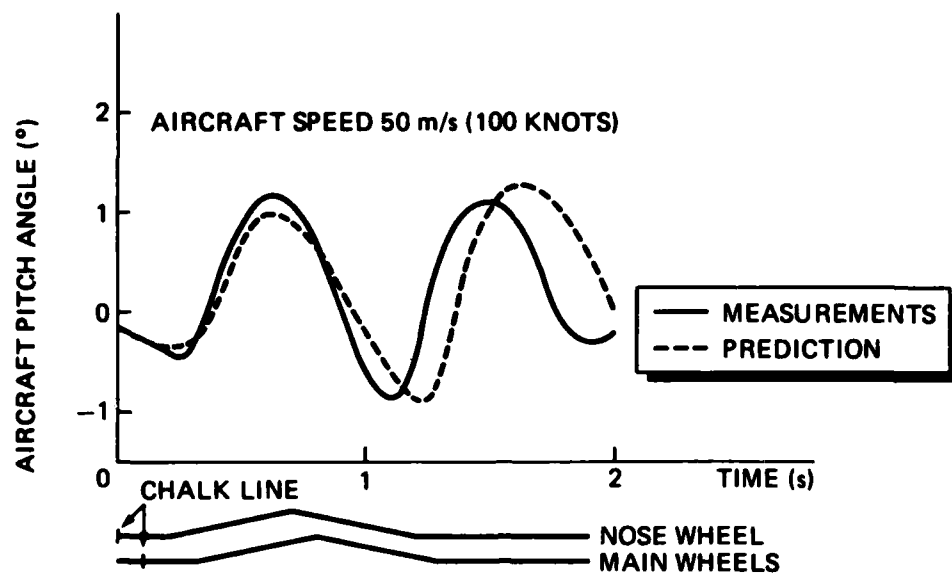


Fig. 7 Aircraft pitch angle: comparison of measured and predicted results

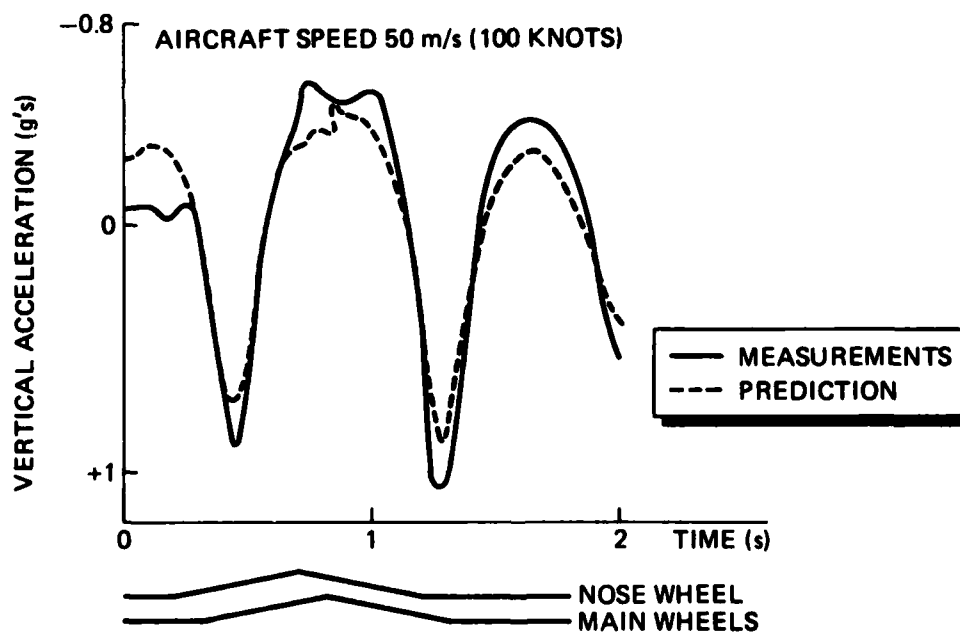


Fig. 8 Aircraft vertical acceleration: comparison of measured and predicted results

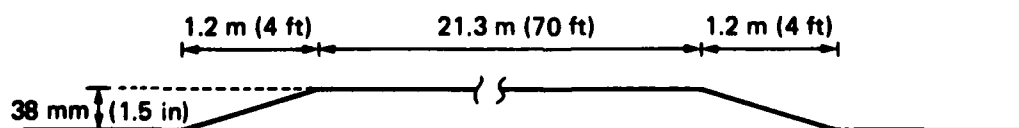


Fig. 9 AM-2 mat configuration

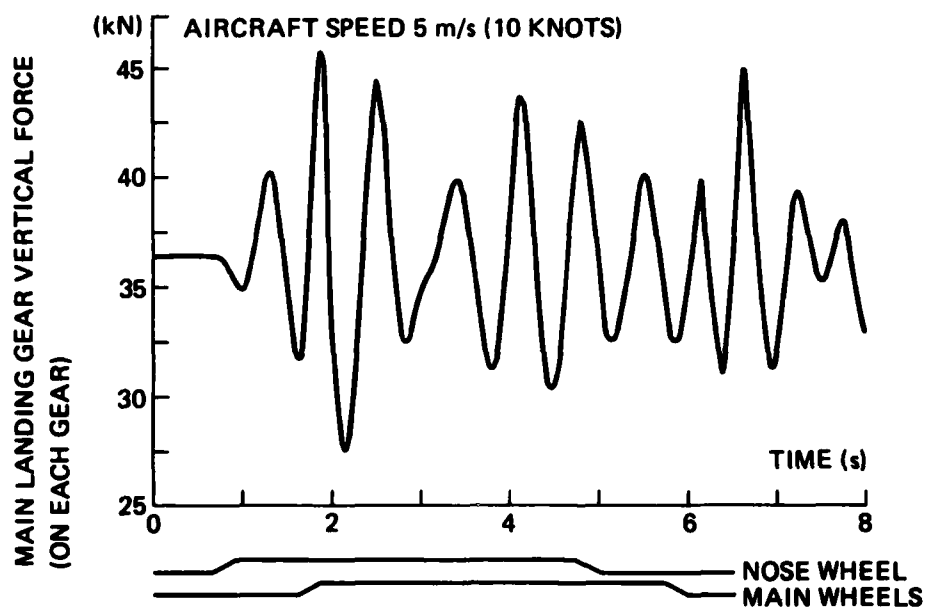


Fig. 10 Main landing gear vertical load generated by an AM-2 mat at  $V = 5$  m/s

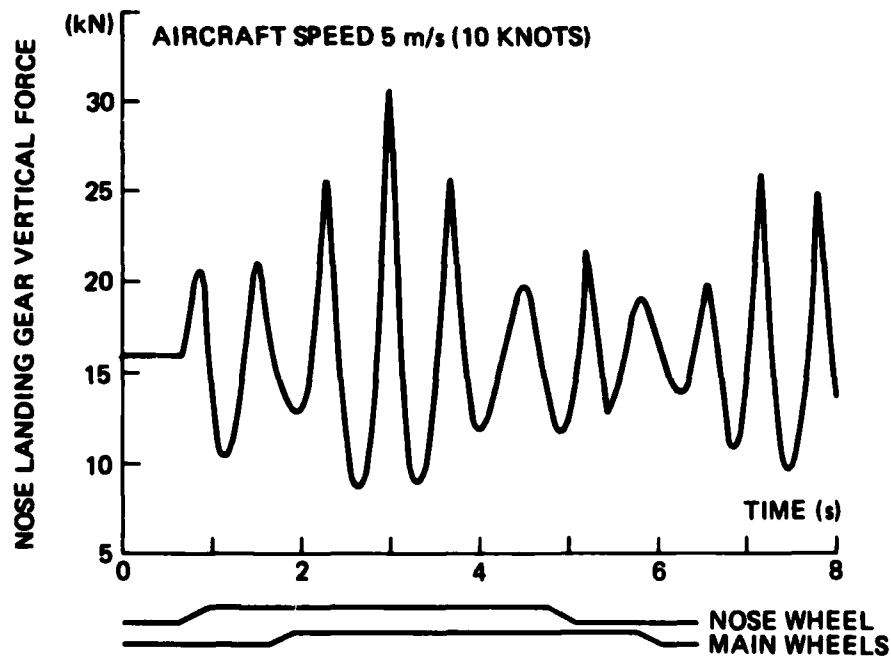


Fig. 11 Nose landing gear vertical force generated by an AM-2 mat at  $V = 5$  m/s

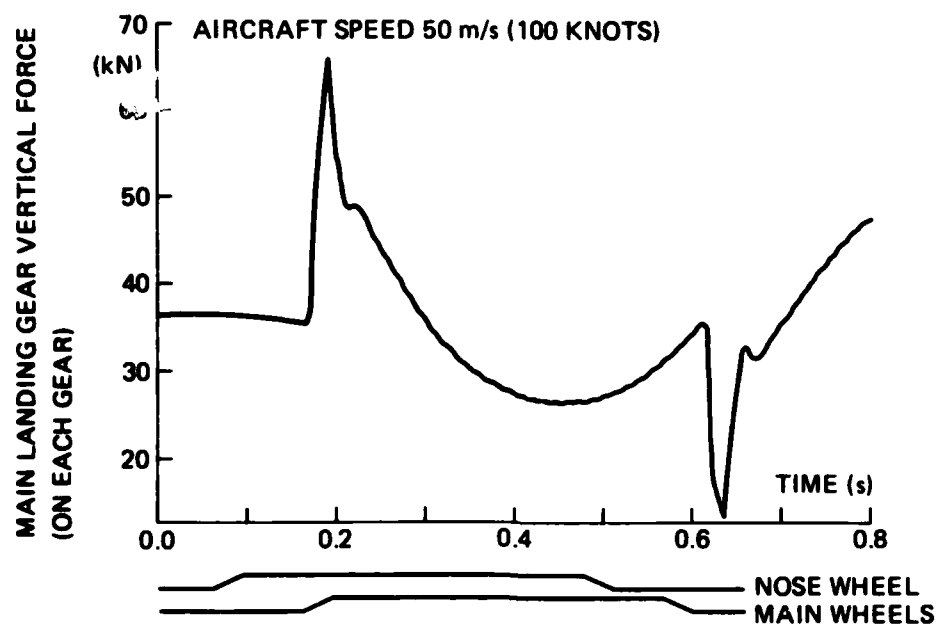


Fig. 12 Main landing gear vertical force generated by an AM-2 mat at  $V = 50$  m/s

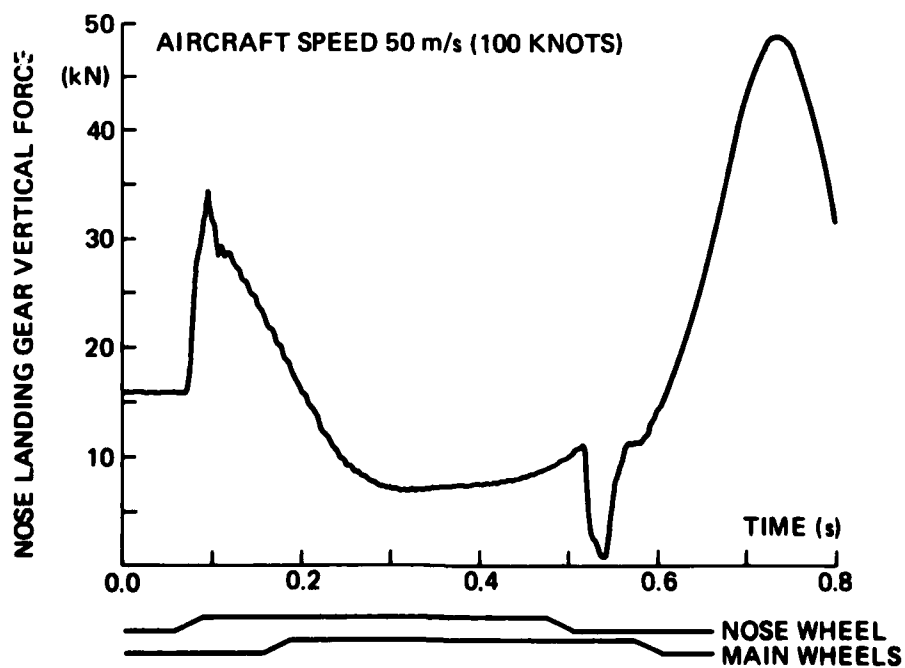


Fig. 13 Nose landing gear vertical force generated by an AM-2 mat at  $V = 50$  m/s



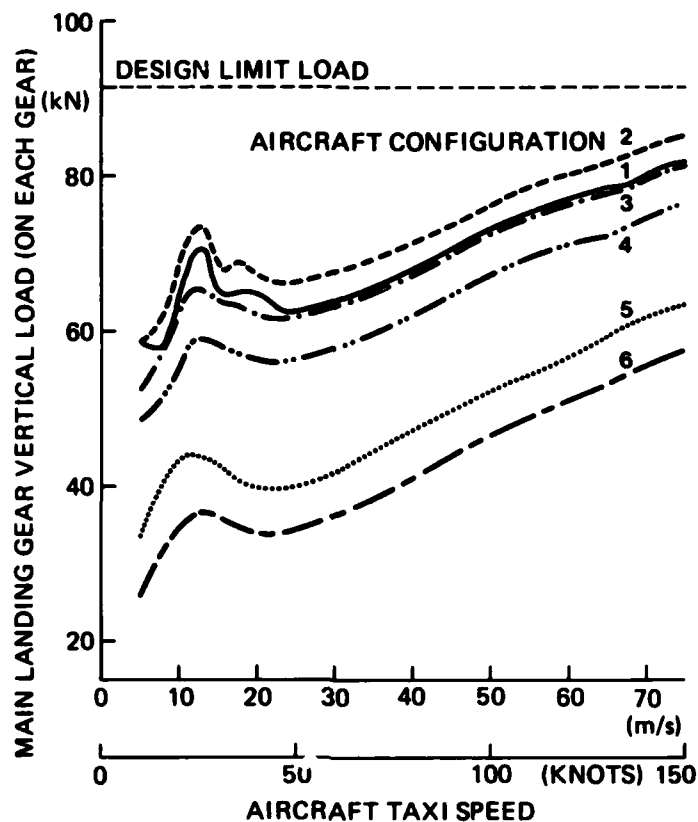


Fig. 14 Maximum load per landing gear during taxiing across an AM-2 mat

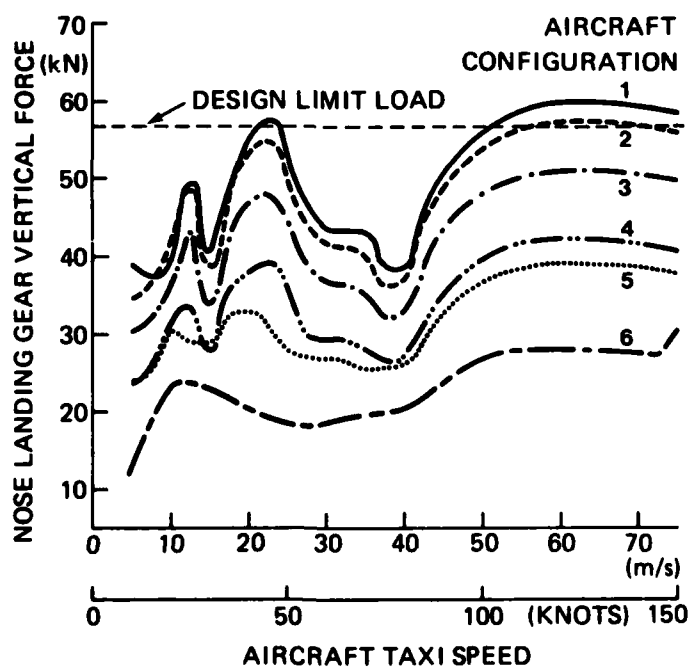


Fig. 15 Maximum load for the nose landing gear taxiing across an AM-2 mat

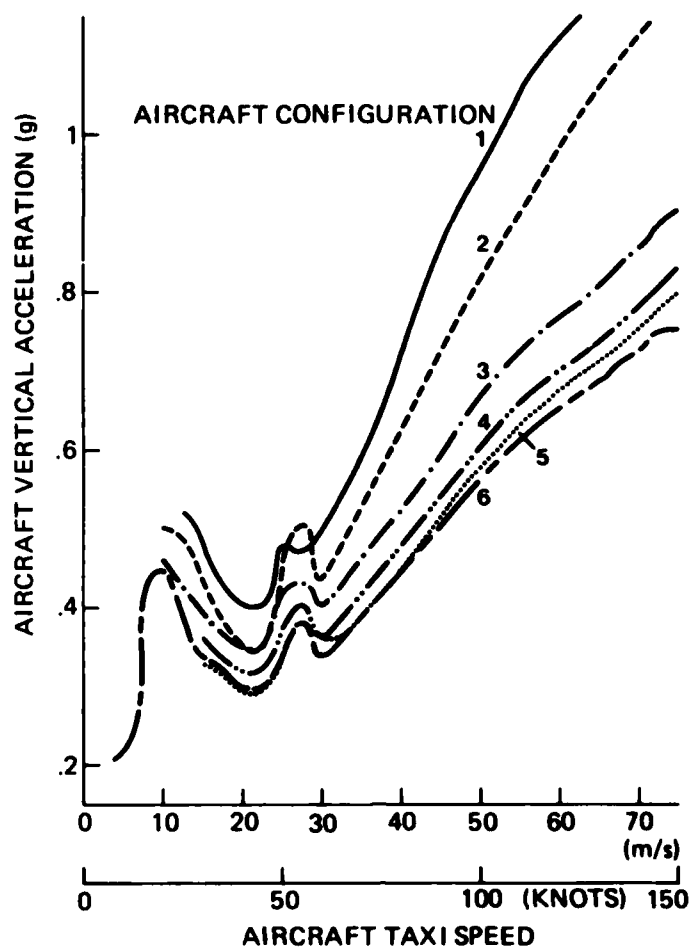


Fig. 16 Maximum aircraft vertical acceleration taxiing across an AM-2 mat

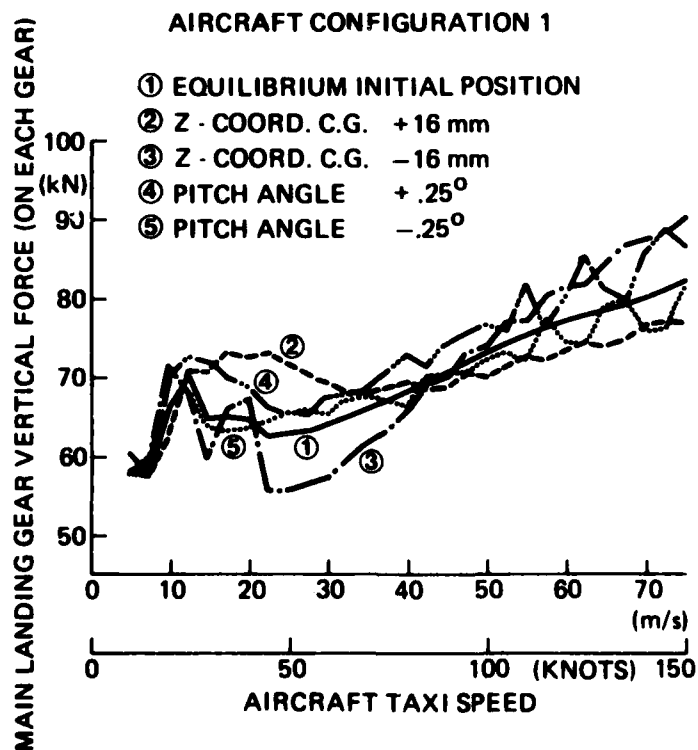


Fig. 17 Maximum load per main landing gear for different initial conditions

## AIRCRAFT CONFIGURATION 1

① EQUILIBRIUM INITIAL POSITION

② Z - COORD. C.G. +16 mm

③ Z - COORD. C.G. -16 mm

④ PITCH ANGLE +.25°

⑤ PITCH ANGLE -.25°

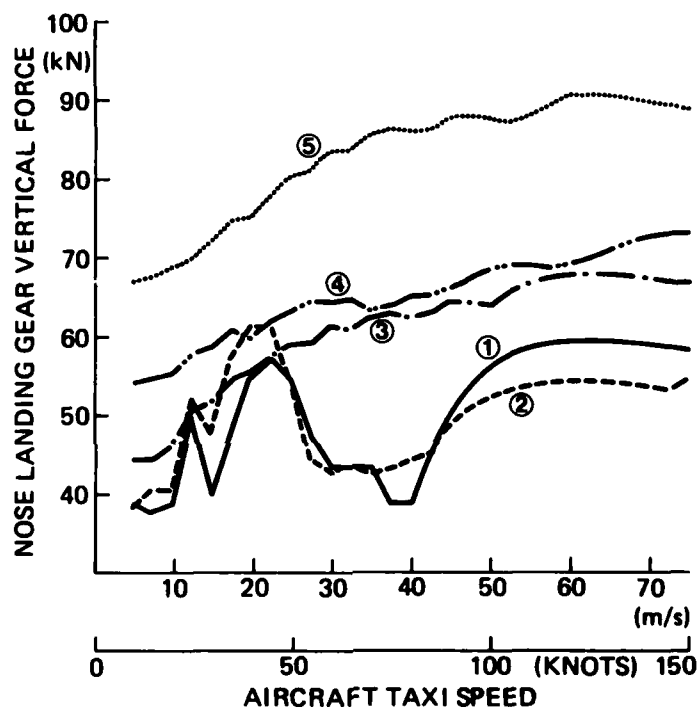


Fig. 18 Maximum nose gear vertical force for different initial conditions

# **Laboratory Testing Systems For Structural Dynamic Response To Large-Scale Disturbances**

**By  
John W. Piraino  
MTS Systems Corporation  
USA**

## ABSTRACT

Servo-hydraulic testing systems are successfully employed in the laboratory to simulate the environment of heavy-duty land vehicles. This paper will discuss the application of these testing techniques to investigate the dynamic structural response of aircraft operating in the damaged runway environment.

A general discussion of test objectives and test system configuration is included. A description of the control technique known as RPC™ is given. Examples of test data output for a typical test are provided for evaluation.

The contribution of this test method and its relationship to the computer modeling and field testing approach to the solution of the acceptable runway surface roughness definition is shown.

## INTRODUCTION

The definition of acceptable runway surface roughness criteria involves many participants. The civil engineer must know the minimal acceptable runway repair quality which will not compromise the structural integrity of various aircraft. The aircraft designer has to evaluate the fatigue damage imposed on his structure by ground-induced loads in this environment. Testing engineers have implemented numerous test programs to analyze the effects damaged/repared runways have on various aircraft. Computer simulation programs and environmental testing have been employed for this purpose.

This paper will present a dynamic test method for full-scale aircraft which can be combined with current modeling and analysis techniques to provide the Test Engineer with a comprehensive design tool. It is necessary to pay close attention to the selection and coordination of analytical and experimental approaches to provide an effective and efficient overall testing program.[1]

<sup>1</sup>Numbers in brackets designate References at end of paper.

## Test Design Objectives

Careful consideration must be made when designing the test program to assure that the test results are valid and appropriate to the specific program needs. [2]

Figure 1 depicts design support functions which are typically conducted in the testing laboratory. Figures 2 and 3 show a test design approach for full scale vehicle service history simulation in the laboratory. These figures are explained in detail reference 2.

### TEST DEFINITIONS (BROAD RANGE)

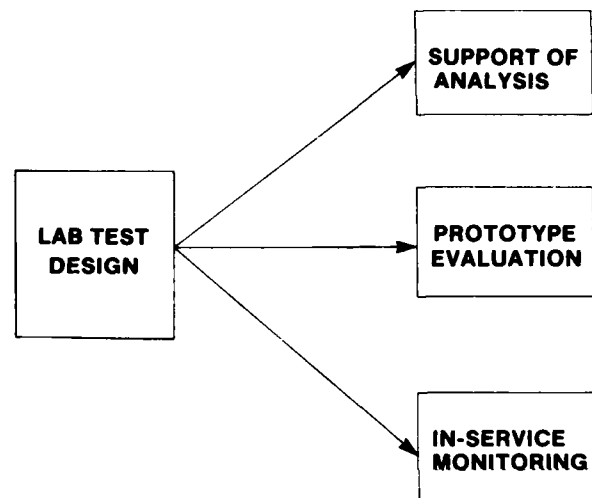


Figure 1. The required test results determine the test category.

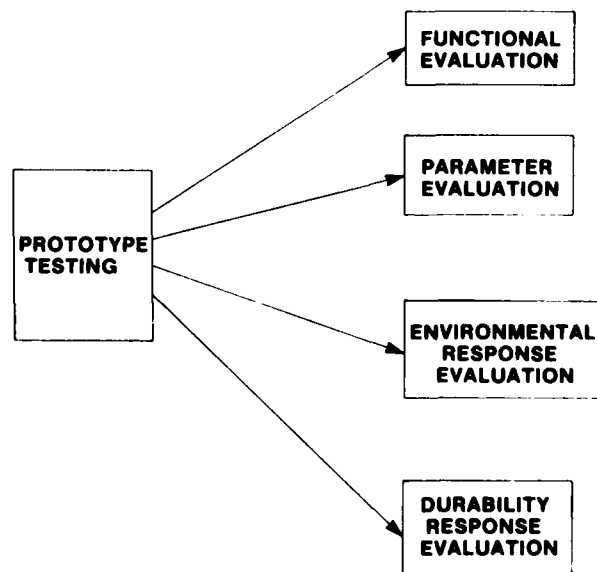


Figure 2. Runway Simulation Systems  
Prototype Testing Category

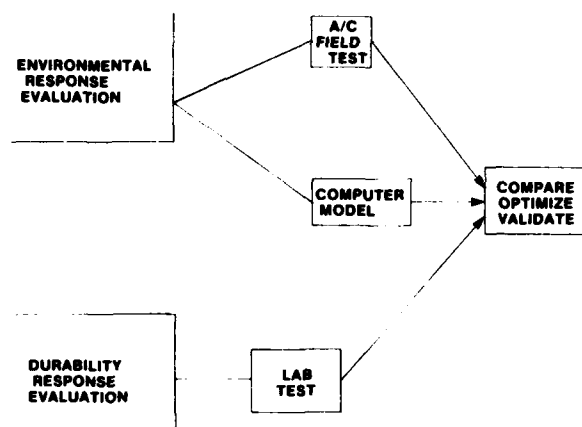


Figure 3. Test Communication

### Test Definition

To successfully reproduce, in the laboratory, the dynamic response of the aircraft structure in its operating environment.

Two requirements are necessary for successful simulation:

An understanding of the multiple-input multiple-output relationships of the system under test.

An accurate description of the environmental inputs.

An environmental description can be obtained from measured field data either in terms of measured structural response to the environmental excitation or by recording the actual environment itself. (Figure 4)

The literature contains numerous examples of the simulation of environmental inputs to the test structures through multiple electrohydraulic exciters. [3, 4, 5, 6].

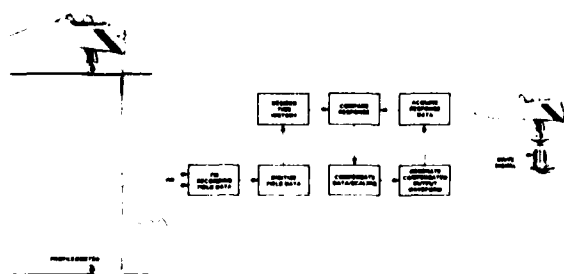


Figure 4.

### Test System Configuration

The system utilizes a digital computer with Fast Fourier Transform (FFT) capability to determine the drive signals to the servo hydraulics which excite the aircraft structure. Single-channel or multiple-channel tests may be conducted.

### Test Methods

Three major steps comprise the total test.

#### 1. Synthesize Effective Runway Surface Profiles

Considerations:

- Repair profiles
- Surface contours
- Superimposed ?
- Spacing ?
- Horizontal velocity ?

#### 2. Simulate Ground Loads on Aircraft Structure

- Excite aircraft with runway profiles through servo-hydraulic test system
- Monitor structural response
- Extended testing - durability

#### 3. Analyze Structural Response Data

- Determine surface repair roughness criteria

### Test Control Technique

Simulate the taxiing loads imposed on the wing structure through the landing gear and through distributed masses such as engines, fuel tanks and external stores using the MTS Remote Parameter Control™ (RPC) Technique.

The following is a step-by-step procedure for RPC:

Step 1: Actual service data is acquired on an analog FM tape.

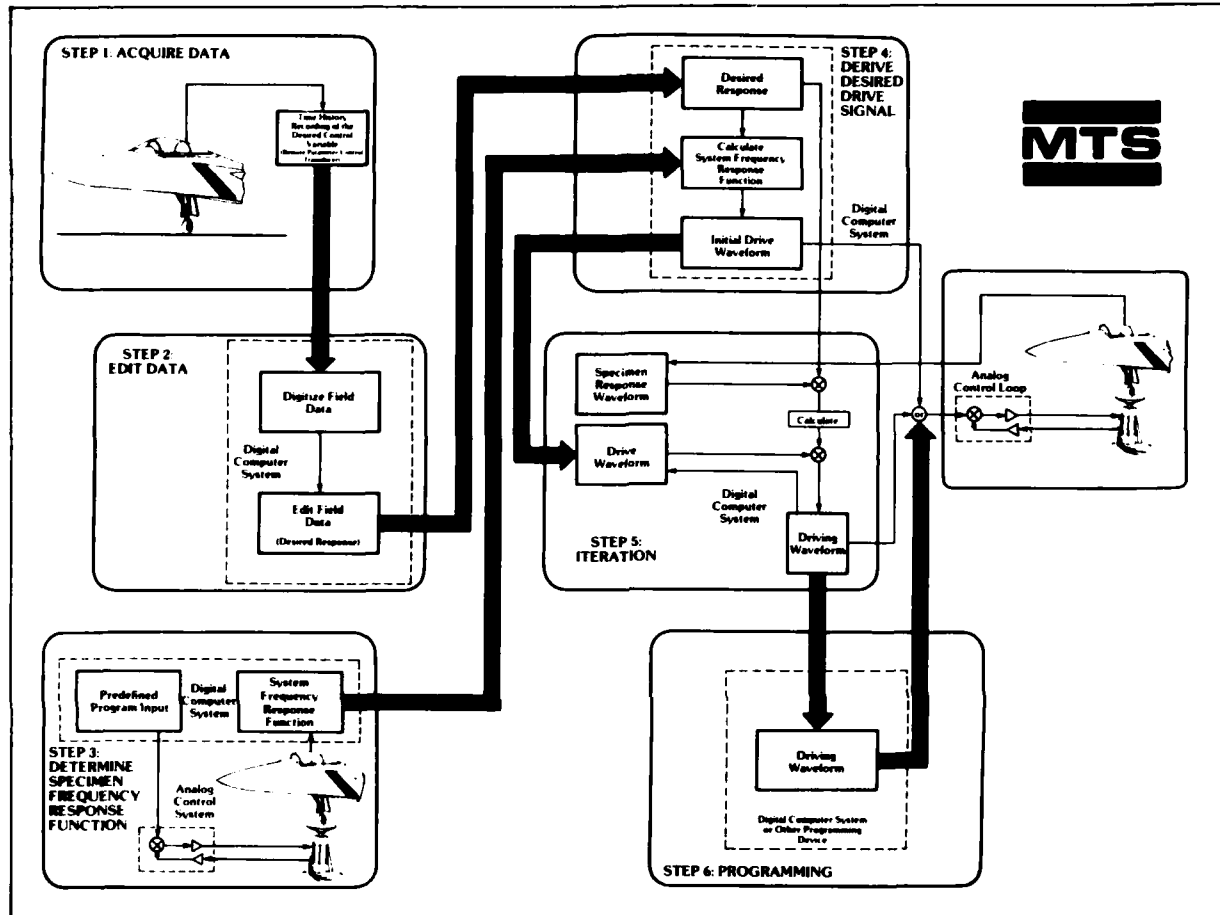
Step 2: The recorded field data is digitized, analyzed and edited to provide a representative laboratory response spectrum.

Step 3: The test system frequency response function is determined.

Step 4: The initial drive signal is calculated from computer evaluation of the field data and test system frequency response function.

**Step 5:** The computer alters the content of the drive signal by an amount determined from the difference between laboratory response and the desired response (field data). Further iterations provide an acceptable correlation between these two.

**Step 6:** The final drive signal is recorded for laboratory use.



# Test Results

The ability of the digital control algorithm to correct for test system distortion is shown in Figure 5. The example shown is for a sine wave testing signal. Figure

6 illustrates the method employed in correlating field response data with lab test response. Figure 7 shows a typical system response for the first iteration of the initial drive signal and the response after 7 iterations using the RPC® control technique.

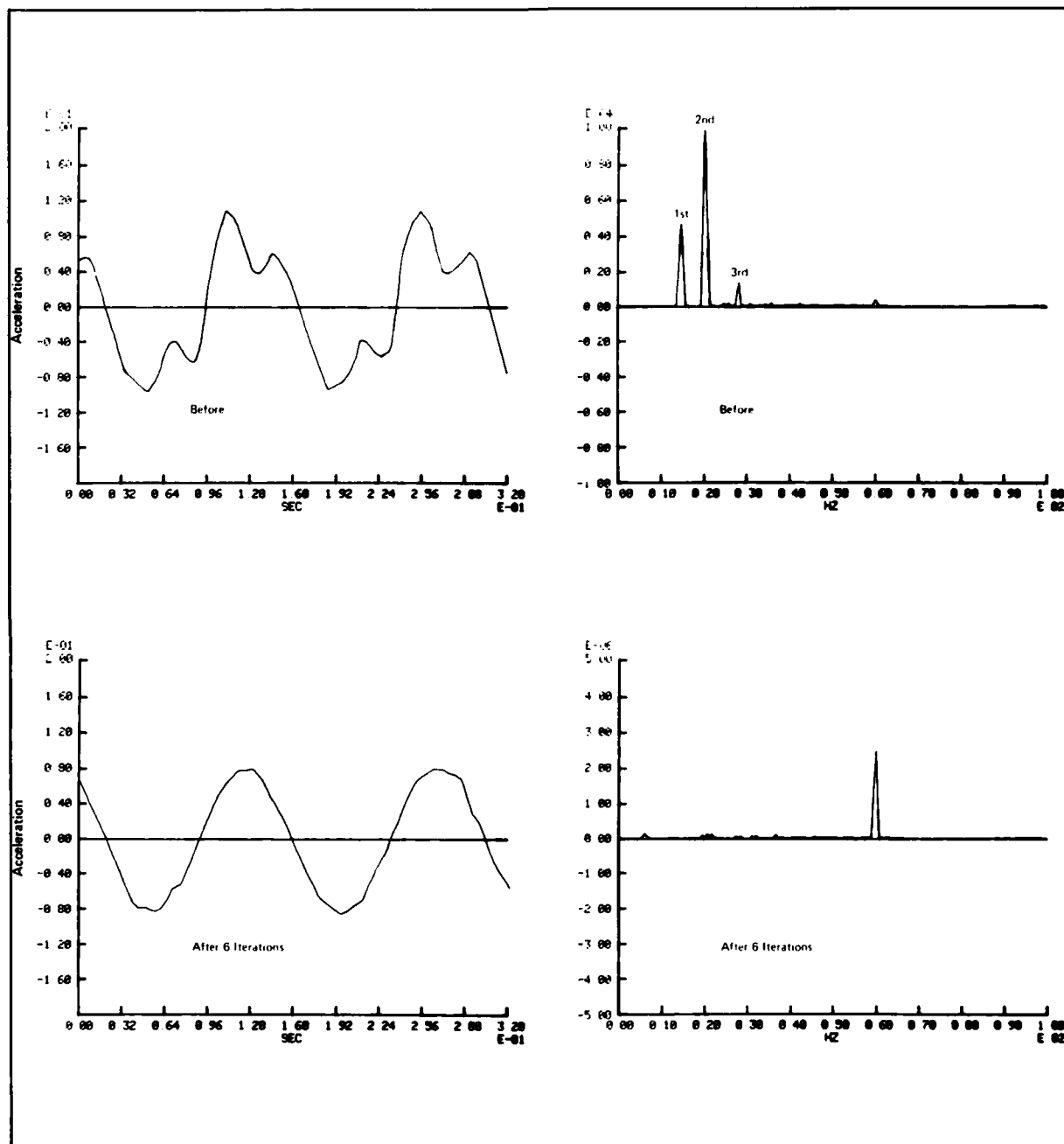


Figure 5.



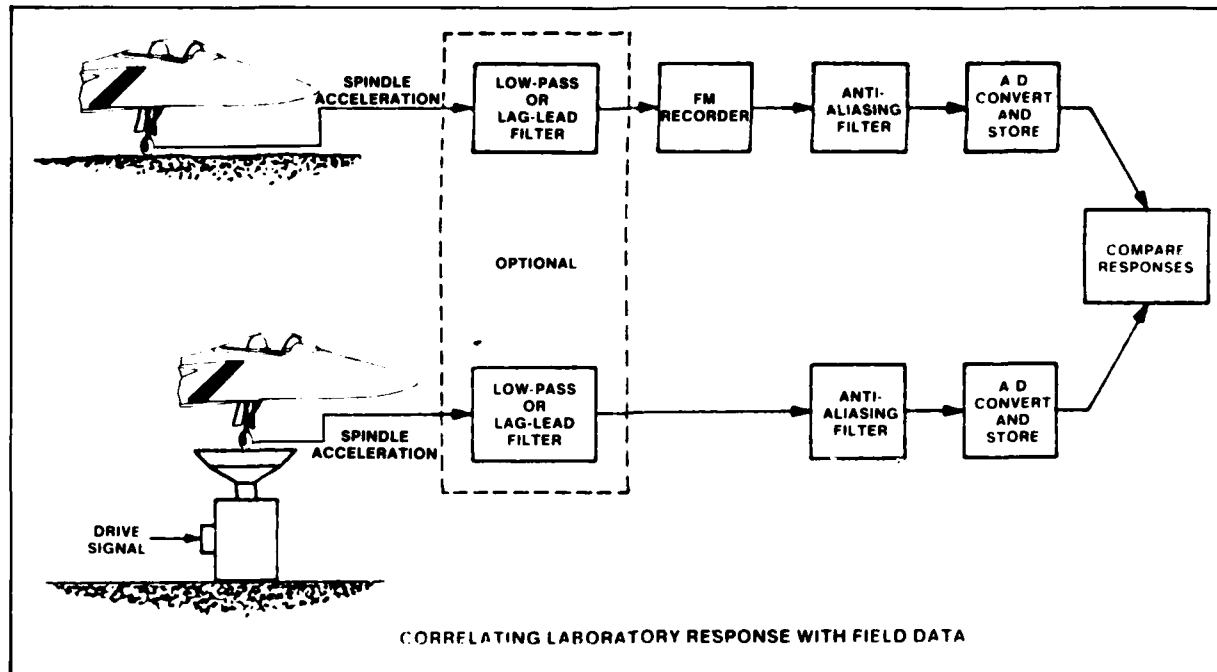


Figure 6.

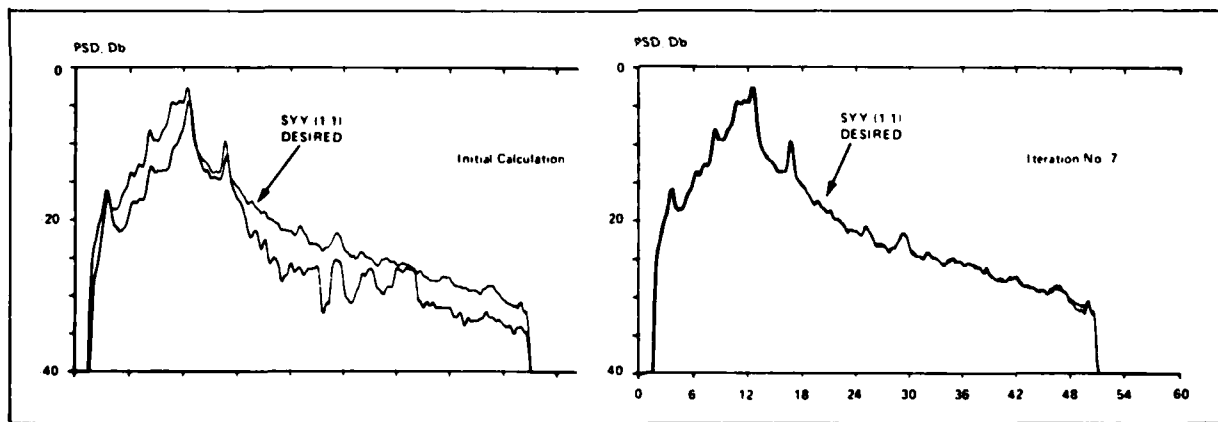
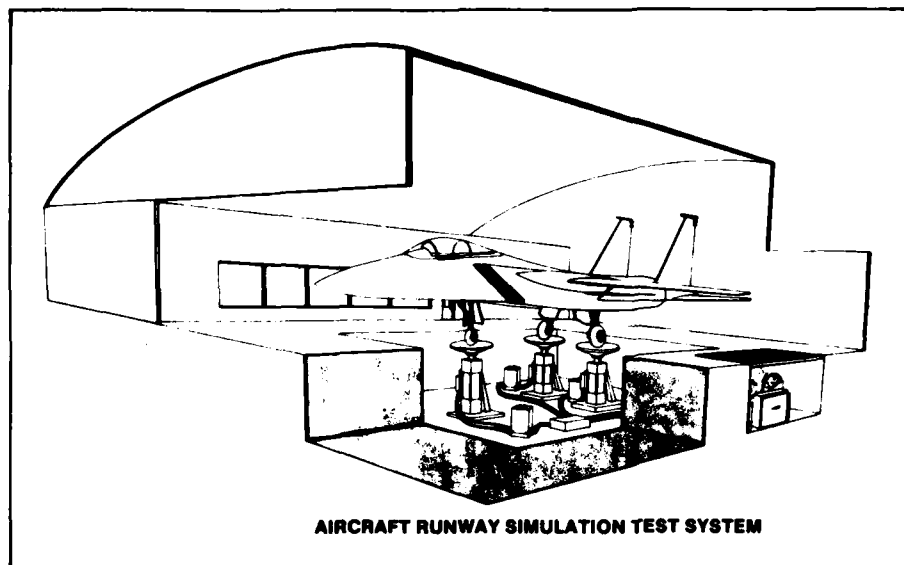


Figure 7.



#### Lab Testing Advantages

- Confirm Analytically Derived Computer Models
- Construct (Optimize) Difficult Dynamic Models
- Ground Vibration Testing
- Good Test Replication
  - Weather influences
  - Pilot influences
  - Better test parameter monitoring
- Timely Test Duration
  - Shortened aircraft turnaround
  - Maintained schedules
  - Equipment/manpower availability
- Cost Effective
  - Live aircraft operation
  - Personnel requirements

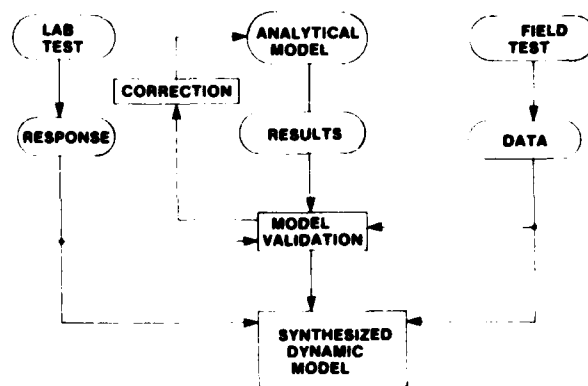


Figure 8.

#### SUMMARY/CONCLUSION

The employment of laboratory environmental simulation testing systems in conjunction with analytical methods will provide more realistic synthesized dynamic models. Similar systems have also been employed to conduct vibration testing and service life studies, as well as conduct prototype evaluations in the laboratory using the same equipment.

## References

1. R. M. Wetzel and K. H. Donaldson, Jr., "Experimental and Analytical Considerations in Service Life Estimation". Paper presented at the Society of Environmental Engineers Fatigue Group Conference on: Service Life - Calculation on Experimentation, The City University, London, England, February 23, 1977.
2. R. A. Lund and K. H. Donaldson, Jr., "Approaches to Vehicle Dynamics and Durability Testing". Paper 820092 presented at SAE Automotive Engineering Congress and Exposition, Detroit, February 22-26, 1982.
3. R. A. Lund, "Multiple Channel Environmental Simulation Techniques". Paper presented at Symposium on Experimental Simulation Tests on Motor Vehicles and Their Elements, Warsaw, Poland, October 1-2, 1979.
4. R. A. Lund, "Environmental Simulation with Digitally Controlled Servo-Hydraulics". Paper presented at IES 1976 Proceedings 22nd Annual Meeting. "Environmental Technology 76", Philadelphia, April 26-28, 1976.
5. B. W. Cryer, and P. E. Nawrocki, and R. A. Lund, "A Road Simulation System for Heavy Duty Vehicles". Paper 760361 presented at SAE Automotive Engineering Conference and Exposition, Detroit, February 23-27, 1976.
6. C. J. Dodds, "The Laboratory Simulation of Vehicle Service Stress". Paper 73-DET-24 presented at ASME Design Engineering Technical Conference, Cincinnati, September 9-12, 1973.

## THE PROBLEM OF DESIGN CRITERIA FOR AIRCRAFT LOADS DUE TO ROUGH RUNWAY OPERATION

by

Max Hacklinger  
BWB-ML, Dachauer Str. 128  
8000 München  
FRG

### SUMMARY

The problem of aircraft design criteria for the rough runway case is reviewed with emphasis on the initial design. The criteria are so divergent in the NATO countries that further design guidance is required to avoid excessively heavy undercarriages of new aircraft projects or shortfalls in interoperability. Nonlinearity and dynamic load cases from multiple obstacle encounter with sometimes adverse operational procedures are the two main problem areas. A compromise proposal of groundworthiness criteria is made for the repaired runway case which could provide a reasonable balance of normal operating and rough runway capability.

### 1. INTRODUCTION

At the time when the basic philosophy of our military airworthiness criteria was established, the process of aircraft development was quite different from now: specialized aircraft types were developed within a year or two and their eventual operational environment was not much different from that envisaged at the design stage. Now, combat aircraft take ten or more years to develop, they must be multi-role and eventually they are operated in an environment quite different from the original conditions. To take account of this by specifying an all-embracing design envelope however, would lead to enormous mass penalties. This is our dilemma with ground load design criteria – it is relatively easy to derive rational design loads from specific runway conditions, but very hard to find a good initial compromise for a range of conditions to cover the operational life of a weapon system.

How important it is to state the design specification in general terms, is demonstrated by certain carrier type aircraft: they have rather strong and heavy undercarriages because they were designed for high sink rate landing – yet they are susceptible to even minor runway obstacles when encountered with compressed legs.

Whereas most of the papers in this series deal with the behaviour of a given aircraft on a runway of known irregularity, I shall try to review the problem of design criteria in general which necessarily is less defined but quite important for new aircraft design.

### 2. DISCRETE VERSUS PSD

Rational design for "groundworthiness" under a variety of landing and runway conditions is as much a probability problem as airworthiness is for flight loads. Since PSD techniques have been so successfully applied to the problem of flight in turbulence it was only natural to investigate the hard ride on runways with the same tools. They have the great advantage of data handling – miles of real time tape can be reduced to a few power spectra in the frequency domain.

Reference 1 describes an attempt to apply this method in comparing two runways which had been surveyed for roughness. Both had similar roughness power spectra, hence one had expected similar aircraft reactions. In practice however, runway A was found to be quite smooth for transport aircraft operation whereas runway B raised numerous complaints of flight crews being shaken up and even worried about the structural integrity of their aircraft.

With hindsight, this failure of the PSD method can be explained. The beautifully simple relation between input spectrum from runway roughness  $\phi_R$  and aircraft response spectrum  $\phi_A$

$$\phi_A(\omega) = \phi_R(\omega) \cdot |H(\omega)|^2,$$

where  $H(\omega)$  is the aircraft frequency response, is the heart of all PSD application. But it is only valid for a linear system. This assumption holds reasonably well for flight loads, therefore the method is widely accepted for establishing design criteria for flight in turbulence. Undercarriages, unfortunately, are so strongly non-linear (see e.g. Reference 2) that loads derived from PSD analysis can be grossly misleading. In this case, there is no way around the tedious analysis in the time domain. PSD procedures may have some merit for the analysis of undercarriage fatigue, but design loads have to be determined from the time history of aircraft response to specified ground roughness.

### 3. REVIEW OF CRITERIA IN USE

#### (a) *United States*

The original US-specification for ground loads MIL-A-8862 (ASG) (Ref.3) did not contain specific ground roughness criteria. It has been replaced by MIL-A-8863 A (Ref.4), a much more rational and complete specification. This includes a new basic approach to the landing cases. Where previously the loading conditions were specified as limiting cases (deterministic approach), there are now envelopes of loading conditions with associated probabilities of exceedance (probabilistic approach). This is in line with the philosophy adopted in MIL-8861 for some flight load cases where the limit load conditions are no more specified in absolute terms but indirectly by stating a maximum probability of occurrence.

The probabilistic approach has not yet been carried over to the ground roughness specification which is still discrete – though it would be consistent to also specify probabilities for encountering roughness of various magnitudes. Table 1 gives a summary of the ground roughness criteria in MIL-A-8863 A. Single obstacles are covered by (1-cos)-bumps, steps and holes. Wavelength and height of the bump are to be varied over a wide range as shown in Figure 1. Repaired runways would be expected to fall into the area between  $H_3$  and  $H_4$ .

Steps and holes are discretely specified at 5 and 10 cm height. Continuous ground unevenness is given as an infinite sequence of identical (1-cos)-bumps, which may not be quite realistic. Height and wavelength of this series must be pessimised\* which in effect is a more severe requirement for finding aircraft resonances than real runways which are never completely tuned to the aircraft response. In addition to the symmetrical cases MIL-8863 A requires also that obstacles are traversed at  $45^\circ$  to the crest line. This could cause problems for large flexible aircraft – the resulting complex motions are difficult to analyse. It is less of a problem for the relatively stiff fighter type aircraft. There are no explicit requirements for repaired runways in MIL-8863 A.

#### (b) *United Kingdom*

AvP 970, Vol.1, Part 3 (Ref.5) is the new British Military Specification for aircraft undercarriages. Table 2 gives a summary of its rough runway criteria. Wavelength and height of the (1-cos)-bump are different from MIL-8861 A:

$$\left. \begin{array}{l} \text{the combination } L = 0.25 \text{ m} \\ H = 0.12 \text{ m} \end{array} \right\} \text{ represents a quite severe short obstacle}$$

whereas the US specification emphasises obstacles of longer wavelength.

AvP 970 also contains repaired craters; their dimensions obviously pertain to the UK class 60 mats and they would not be directly applicable to patches repaired with US-AM-2 mats. There is no sequence of repaired craters specified, but AvP 970 has a continuous runway profile of 1500 m length which has been derived from an actual runway, but biased towards wavelengths between 20 and 40 m. Figure 2 shows that basic profile; amplitude factors from 1 to 4 are specified to cover degraded conditions. With a factor of 2 (roughly corresponding to a mat-repaired runway) the critical area at B in Figure 2 represents a slope of 2%. At a touchdown speed of 100 Kt this would be equivalent to an increase of sink rate by 1 m/s, which is about 1/3 of the normal design sink rate of combat aircraft.

It is questionable whether amplitude amplification at constant wavelength is a realistic case. Usually higher amplitudes are correlated with longer wavelengths as was the case in Figure 1.

AvP 970 does not tie this continuous roughness criterion to specific aircraft design cases, following the general UK policy to provide detailed technical criteria as advisory information rather than the mandatory MIL-Specs. This criterion should be readily applicable to undercarriage fatigue. Rough runway cases are required in AvP 970 only for symmetrical encounter of obstacles.

#### (c) *France*

The new French military specification AIR 2004E (Ref.6) treats undercarriage design criteria differently from both the foregoing: Instead of specifying obstacle geometry from which by dynamic aircraft analysis design loads are derived,

\* = seeking the worst possible combination.

AIR 2004E specifies a simplified procedure whereby single wheel loading cases are given directly, see Table 3. This method had wide application in the old US specifications because it is easy to apply, but it has been gradually replaced by physically more realistic procedures where only the absolute environment is specified (gusts, runway roughness), but the aircraft reaction is derived analytically or by test.

No sequence of obstacles is specified in AIR 2004E but unsymmetrical loading cases are covered in some detail.

If we now try to compare these three major specifications for aircraft groundworthiness we must conclude that a common denominator cannot be found (with the exception of the simple step obstacle case). Since the concept of interoperability is now increasingly being emphasised, perhaps this is another case where AGARD has a task for standardisation within NATO-countries.

#### 4. SOME GENERAL OBSERVATIONS ON GROUND LOAD CRITERIA

##### (a) *Nonlinearity*

All our major codes of aircraft structural criteria, e.g. the MIL-8860 Series, rest on the basic concept of limit load. One specifies limiting conditions which during the operational life of the aircraft type are rarely exceeded (rarely being about  $10^{-5}$  per flight hour). Then a safety factor of 1.5 is applied to this load thus creating an ultimate condition up to which structural failure must not occur. For all flight cases this 1.5 is a comfortable margin to cover inadvertent overshoots, the rare "giant gust" or other singular events, because for a linear system  $j = 1.5$  means a real 50% reserve and structural deformation under flight load is not too far from linear.

Certification agencies recognise this in the establishment of operational limitations (Ref.8). Ground loads however, are the uncomfortable exception. Undercarriage characteristics are so strongly nonlinear that in the fully compressed condition even minor obstacles can cause critical load increments. So have carrier aircraft suffered severe damage from rolling over arrester cables 3.5 cm thick at the moment of maximum tyre deflection (Ref.7).

Another example is given in Figure 3 which is derived from simulated landings of a twin engined observation aircraft over (1-cos)-bumps (Ref.9). It can be seen that a 50% increase in obstacle height (5 to 7.5 cm), which appears similar to the  $j = 1.5$  mentioned above, would cause catastrophic failure. This obstacle size however, is in the very centre of the specifications of Tables 1 and 2. We can draw two conclusions from this:

- (a) The procedure to provide safety by strength margins can, in the undercarriage case, cause enormous mass penalties.
- (b) The wide range of obstacle heights given in the reviewed specifications entails an even wider range of undercarriage consequences due to the nonlinear load increase with the larger obstacles.

The alternative to (a) is to employ wherever possible design margins instead of strength margins, e.g. deep section tyres, load limiting devices acting at shock absorber bottoming. Such devices incidentally could also be utilized for monitoring landing overload, aircraft crew reports being unreliable for this purpose.

##### (b) *Multiple obstacle encounter*

Figure 3 is pessimised for one obstacle only. What can happen in a real case with more than one obstacle is shown in Figure 4. This is the test result of a 16 t combat aircraft rolling over two patches of simulated repair with AM-2 mats laid out on a regular runway. Obstacle encounter is after landing impact with fully deployed thrust reverser. Here the victim would be the nose gear, partly due to the effect of reverse thrust which causes the first load peak at A, in a similar way as hard braking would do. The point of interest is B where the pitching motion of the aircraft due to the first mat has caused a large nose gear compression when hitting the ramp of the second mat. This combination produces close to limit load of the nose gear. Without second mat, the nose gear load would have started decaying at B, similar to point C. The lower trace on Figure 4 shows that the case is insignificant for the main undercarriage (which has a limit load of 200 units).

##### (c) *Operational limitations*

The example of Figure 4 raises the question of operational limitations which are not covered in the reviewed criteria. Compounding all negative effects of pessimised runway obstacles, reverse thrust operation and braking would certainly lead to unrealistically severe design criteria. When reverse thrust is an integral part of the operational landing procedure, it should be included and at the early design stage the effect on nose gear loads may be held small. Dynamic braking on the other hand should be a separate case. The aircraft of Figure 4, according to the original MIL-8862 which does not cover dynamic braking, would have had a nose gear limit load of 55 units. With the introduction of a dynamic braking case this was raised to 78 units and still on it was found that with minor mass penalty the vertical design load could be raised to 120 units -- just about the load this aircraft had to suffer in the trial of Figure 4.

#### (d) *Design envelopes*

The basic undercarriage design criteria are quite different for US-Air Force and US-Navy aircraft; Figure 5 illustrates the situation: Air Force aircraft have overall lower design loads because of less stringent landing conditions. This gives lighter aircraft structures, but also a lesser rough runway capability (inner envelope). Navy aircraft due to the high design sink rate and severe unsymmetrical cases have overall higher vertical and horizontal design loads (outer envelope in Figure 5), heavier structure, but also better rough field capability – if the pitfalls mentioned under 4(a) are avoided by a good initial compromise of shock absorber design. The example of 4(a) above has shown that increasing the vertical design load can be very cost-effective for rough runway capability. What we propose therefore is a compromise between the Navy and Air Force extremes indicated by the dotted line in Figure 5. This should give a good initial design for rough runways without great mass penalty.

### 5. PROPOSED CRITERIA

The presently used major aircraft structural design criteria (References 4 to 6) are widely different in their treatment of the rough runway problem, in basic approach as well as in the numbers specified for obstacle height and wavelength. Reference 5 spans the whole range from regular paved runways to a sharp-edged 10 cm curbstone at a right angle to the aircraft path. This would have so drastic effects on undercarriage – and indeed whole aircraft – design that the designer of a new type needs more specific guidance. On the other hand, runway destruction and reconstruction techniques will certainly be in a state of flux for some more years.

To bridge the gap between too broad existing criteria and specific operational cases where the runway profile is known, we propose as an interim measure the following aircraft design criteria for the case of repaired runways:

- (a) Basic undercarriage design according to Figure 5 with increased vertical capability.
- (b) First landing impact on standard undamaged runway.
- (c) Three repaired craters, repair category A (Ref.2), standard length AM-2 mats, mat spacing to be pessimised for aircraft reaction.
- (d) Steady braking combined with (c), dynamic braking not combined with (c) but covered as a separate case. Reverse thrust to be combined with (c), if it is part of the operational landing procedure (as well as other operational retarding devices).
- (e) Symmetrical obstacle encounter.

Dynamic analysis with discretely specified ground roughness is of course required to optimise the shock absorbing system and to reveal possible airframe consequences:

- Combat aircraft being generally small and stiff exhibit mainly rigid body mode response; problems are confined to undercarriage and attachment structure.
- With high authority flight control systems the possibility of undesired coupling between runway-induced aircraft motion and control system reaction must be investigated.
- The integrity of external stores under rough runway inputs should be considered.

Transport aircraft, being large and flexible, have structural modes excited by runway obstacles. Short wavelength obstacles are critical for the undercarriage, but long bumps can become design cases for wings and external stores. In the example of Figure 3 (Ref.9) the introduction of wing flexibility gave smaller wing loads for short bumps than the rigid wing, but with longer bumps the flexible wing had 1.5 times the rigid wing load.

It may be operationally advantageous to introduce an emergency get-out-case: Since undercarriage loads depend so strongly on shock absorber characteristics, there could be a simple device for softening the shock absorbers at the cost of reduced landing sink rate. This device would be actuated for evacuation from a badly repaired runway if the aircraft will land on a regular airfield. MIL-8863 A has the probabilistic approach to the landing cases, but rough runway criteria still require pessimisation of discrete obstacle. It would be more rational to extend the probabilistic approach to obstacles. This would mean that probabilities for encountering obstacles of various height and length would be combined with the already specified probabilities for landing situations into one total probability for exceeding undercarriage limit load. We need analysis of a representative test case to see whether this alternative is a feasible one.

### 6. CONCLUSION

The design criteria available at present for the damaged runway case are so divergent that further design guidance is necessary to provide new aircraft designs with similar and reasonably balanced undercarriage capabilities. The proposal made here is intended to produce a basic undercarriage design capable of handling the expected range of runway conditions without excessive later modifications.

## REFERENCES

1. — *Implications of Recent Investigations on Runway Roughness Criteria*, AGARD Report 416, January 1963.
2. — *Aircraft Dynamic Response to Damaged Runways*, AGARD Report 685, March 1980.
3. Anon. *Airplane Strength and Rigidity, Landplane Landing and Ground Handling Loads*, MIL-A-8862 (ASG), May 1960.
4. Anon. *Airplane Strength and Rigidity, Ground Loads for Navy Procured Airplanes*, MIL-A-8863, July 1974.
5. Anon. *Design Requirements for Service Aircraft AvP 970*, Vol. 1, Part 3 Design of Undercarriages, August 1979.
6. Anon. *Résistance des Avions*. AIR 2004 E, March 1979.
7. Yeates, J.E.  
McHugh, Hewin *A Study of Rough-Terrain-Induced Structural Landing Loads*. TRECOM Tech. Rep. 63-68 (1963).
8. — *Factors of Safety Related to Structural Integrity*, AGARD Report 677 (1981).
9. Ebers, R.S.  
Sandlin, N.H. *V/STOL Landing Impact Criteria*, AD 855 103/8 SL, AFFDL-TR-68-96 (May 1969).



TABLE 1

## ROUGH RUNWAY CRITERIA MIL-A-8863 A (1974)

symmetrical and 45°

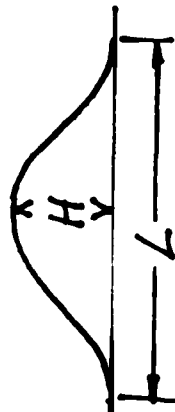
SEQUENCE OF OBSTACLES

INFINITE SERIES OF IDENTICAL (1-cos) -BUMPS  
H LINEARLY INCREASING WITH L  
L TO BE PESSIMISED FOR RESONANCES.

SINGLE OBSTACLE

(1-cos) -BUMP:  $L_{\min} = 0,61 \text{ m}$ 
 $L_{\max}$  = DISTANCE TRAVELED DURING COMPRESSION

STROKE OF SHOCK ABSORBER + TIRE



H = 5 to 127 cm, INCREASING WITH L

STEPS AND HOLES:  $L_{\min} = 10 \text{ cm}$  SEMIPREP. H = 5 cm  
UNPREP. H = 10 cm



CARRIER CABLE 1,5 cm Ø

TABLE 2

## ROUGH RUNWAY CRITERIA AvP 970 VOL 1 (1979)

symmetrical only

## SINGLE OBSTACLE

## SEQUENCE OF OBSTACLES

RECTANGULAR STEP:  $H = 2,5$  to  $10$  cm(1-cos) BUMP:  $L = 0,25$  m $H = 3$  to  $12$  cm

POTHOLE: (1-cos) BUMP INVERTED

REPAIRED CRATER:  $L = 10$  to  $25$  m $H = 5$  to  $13$  cm

CONTINUOUS RUNWAY PROFILE,  
DERIVED FROM ACTUAL RUNWAYS,  
BIASED FOR  $L = 20$  to  $40$  m.

4 CATEGORIES,  $H_{\max} = 68$  cm  
(over  $1500$  m)

TO BE USED FOR FATIGUE RATHER  
THAN DESIGN LOADS.

NO SEQUENCE OF REPAIRED  
CRATERS SPECIFIED.

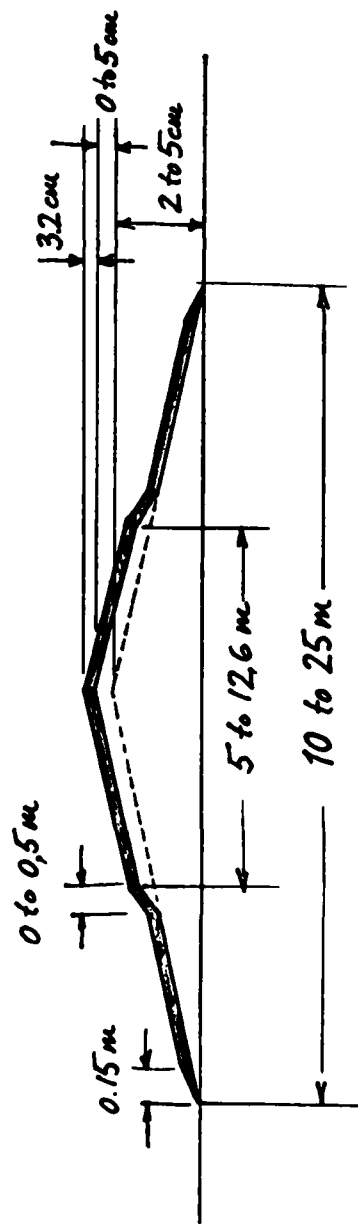


TABLE 3  
ROUGH RUNWAY CRITERIA AIR 2004 E (1979)

SINGLE OBSTACLE	SEQUENCE OF OBSTACLES
NO OBSTACLE GEOMETRY SPECIFIED, BUT SIMPLIFIED PROCEDURE TO DERIVE LOADS FROM ISOLATED WHEEL COM- PRESSION BY	NOT REQUIRED
H = 3 cm REGULAR HARD RUNWAY	
H = 6 cm GRASS OR MAT-PREPARED RUNWAYS	SYMMETRICAL AND UNSYMMETRICAL LOADING CASES
H = 10 cm CRUDELY PREPARED GROUND	

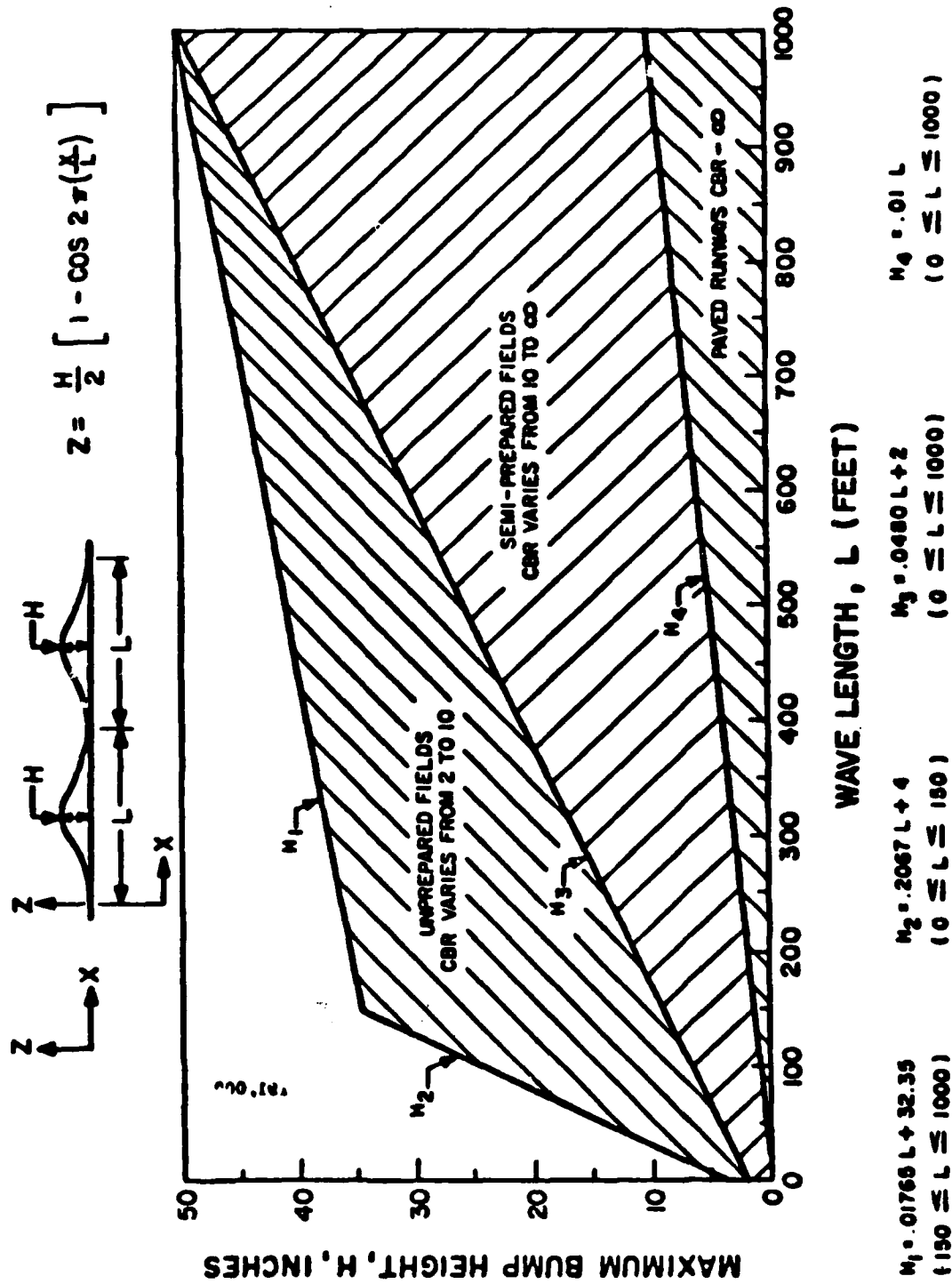


Fig.1 Obstacle dimensions MIL 8863 A

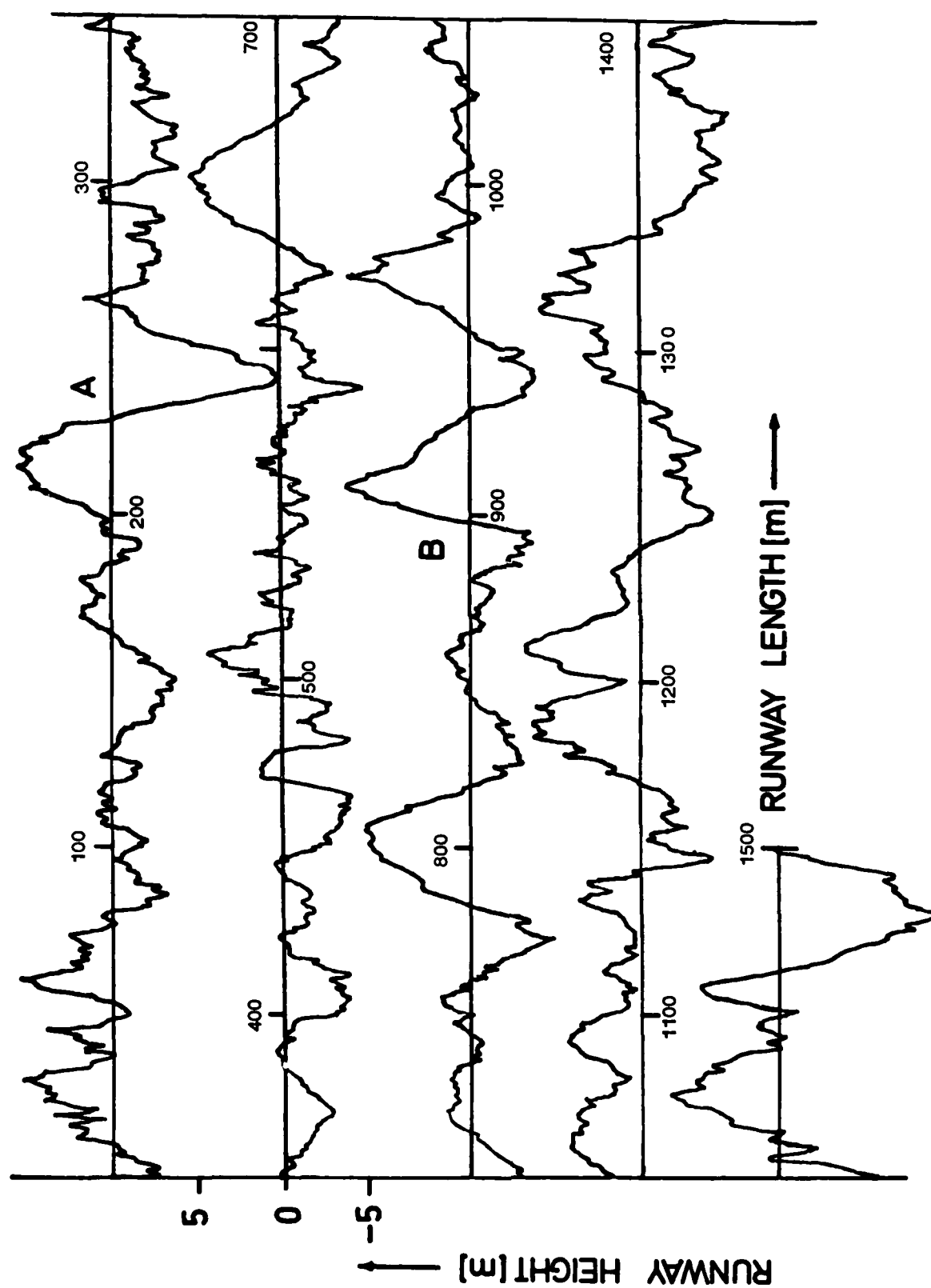


Fig.2 Continuous roughness profile AvP 970

SINK SPEED = 9.9 FPS  
 TOUCHDOWN SPEED = 87.4 KNOTS  
 BUMP SHAPE = 1 - COSINE  
 BUMP LENGTH = 30 INCHES (0,76 m)

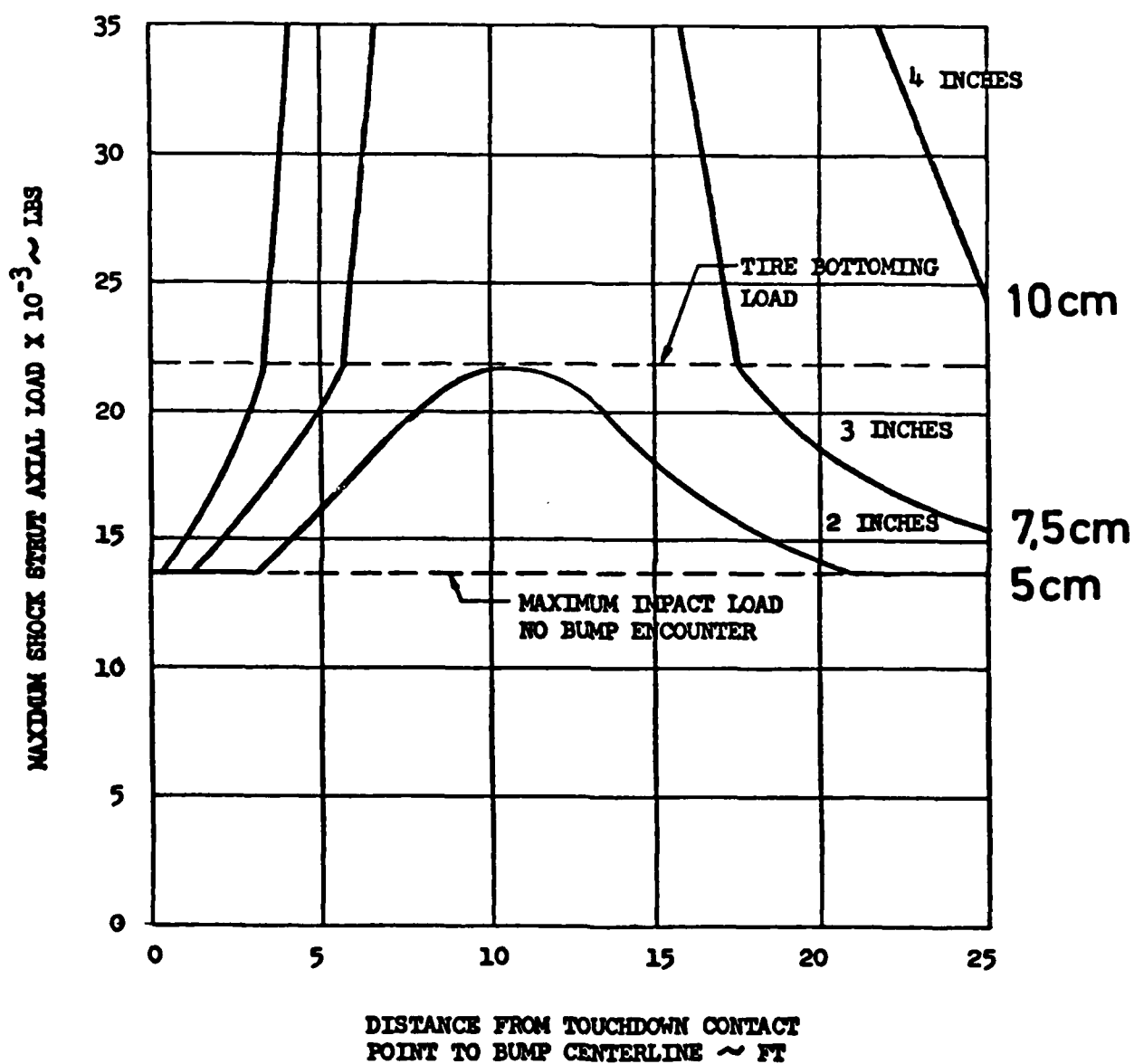


Fig.3 Effect of obstacle height variation

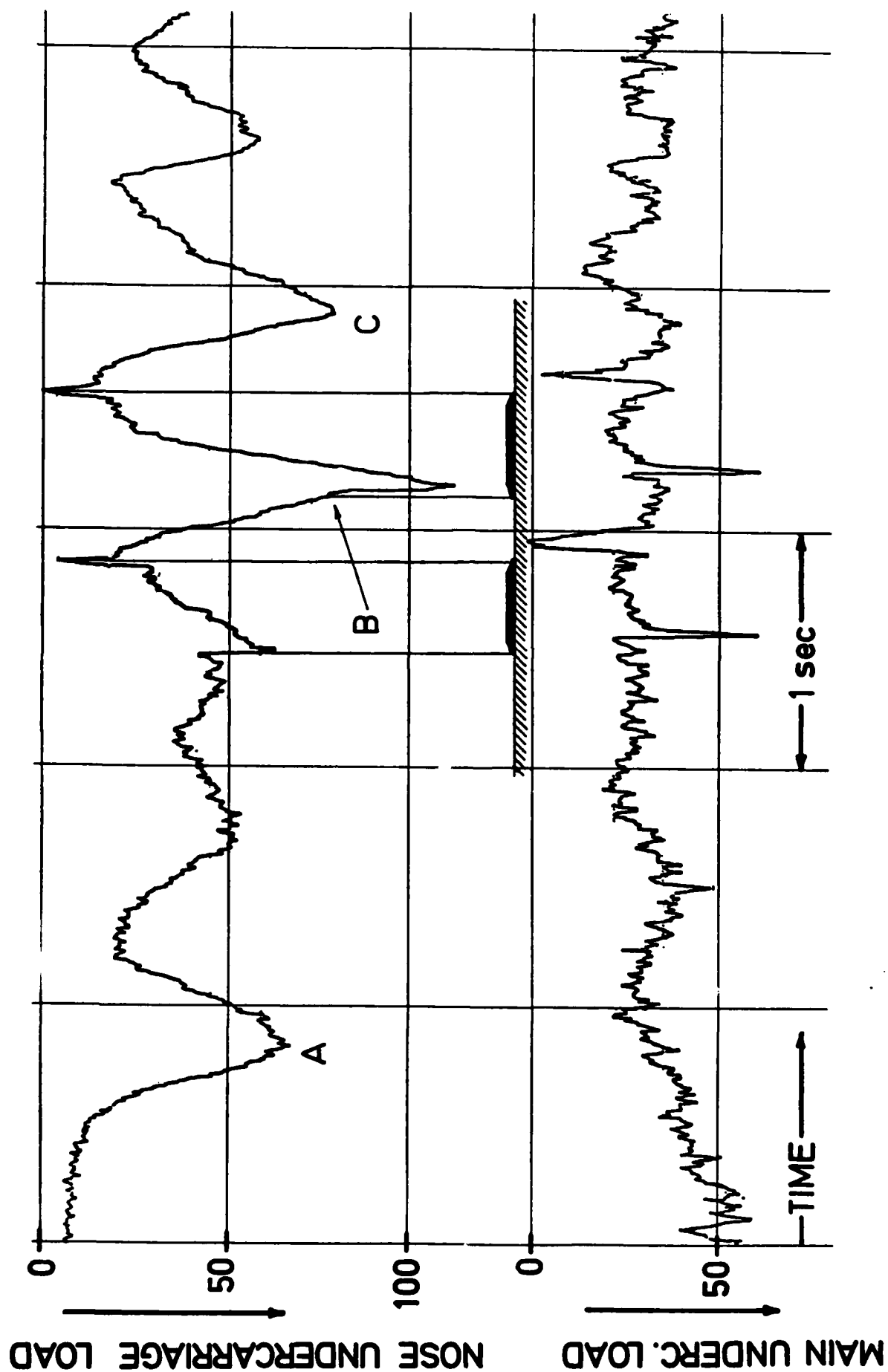


Fig.4 Landing tests over 2 AM -- 2 mats

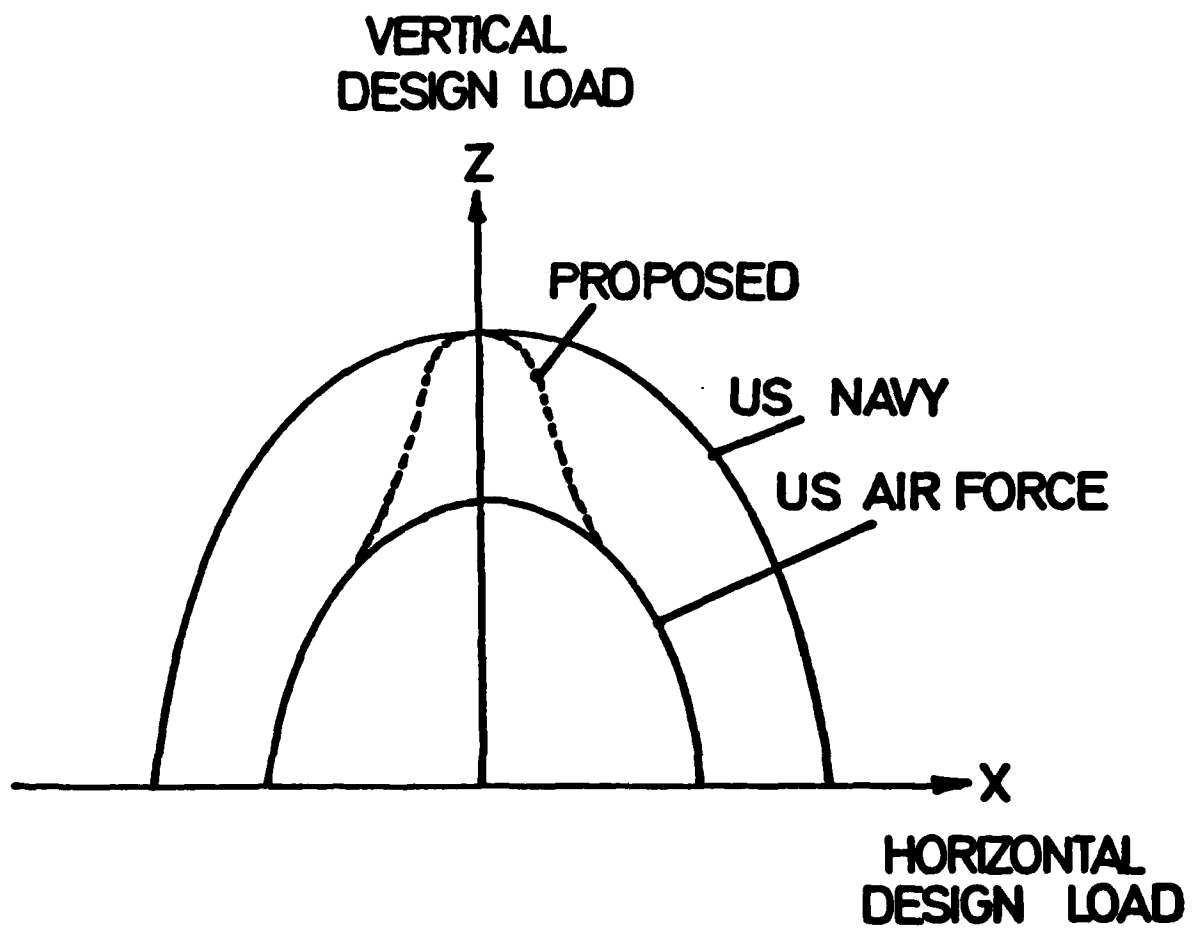


Fig.5 Undercarriage design load envelopes



LANDING GEAR SHOCK ABSORBER DEVELOPMENT TO IMPROVE  
AIRCRAFT OPERATING PERFORMANCE ON ROUGH AND DAMAGED  
RUNWAYS

G.H.Haines  
Chief Performance Engineer  
(Airframes)

DOWTY ROTOL LIMITED  
Cheltenham Road, Gloucester  
England  
GL2 9QH

#### SUMMARY

Aircraft landing gear shock absorber characteristics have been almost entirely dictated by landing impact energy absorption and suitability to support ground manoeuvring loads. To improve the performance of such systems when taxiing on rough or damaged surfaces requires further optimisation of the damping level and spring stiffness. Higher damping and softer spring-rate than generally used can reduce aircraft response when taxiing on typically rough ground. Shock absorber hardware developed at Dowty Rotol provides characteristics so modified and tests on single landing gears have demonstrated significant taxiing improvements without degrading the landing energy absorption capability. Similar improvements are predicted with such gears installed on an aircraft.

#### 1.0 INTRODUCTION

The great majority of aircraft undercarriage shock absorbers have been designed to meet the performance requirements of landing impact energy absorption, with relatively little attention being paid to the suspension characteristics when the aircraft is taxiing. Often the ability to provide a specified shock absorber closure under the static load and to withstand certain manoeuvring loads have been the only criteria considered. This limited consideration of the shock absorber characteristics has given rise to surprisingly few problems when operating from today's well prepared airfields. There is now however a growing awareness of the need to operate some civil aircraft on lower grade runways and to retain the operating capability of military aircraft in the presence of repaired or damaged runways. This increased awareness has led Dowty to look for ways of improving undercarriage capability and particularly to consider what potential improvement in taxi performance is available solely from changes to the characteristics of existing shock absorbers, without resorting to 'active' control with its associated increase in complexity.

Dowty's experience in the design of undercarriages over many years has thrown up a number of 'in-service' examples where the taxi performance of specific aircraft, with undercarriage characteristics arrived at substantially as described above, has been significantly improved by relatively simple modifications to the shock absorber spring and damping characteristics. This experience supplemented by theoretical analyses led to the formulation of some 'in-house' criteria for the design of shock absorber characteristics which remain equally pertinent when considered specifically for 'damaged' or 'repaired' runway operation. These criteria are:-

The shock absorber spring characteristics should provide adequate travel between the static loaded position and full closure to absorb, without 'bottoming', the specified obstacles or roughness.

The shock absorber spring within the travel range used when taxiing should be of relatively low stiffness.

The damping should effectively control the response of the undercarriage system at the velocities developed during taxiing.

Unfortunately these requirements are frequently found to conflict with those arrived at from the consideration of landing energy absorption.

To efficiently absorb landing energy and thereby reduce the shock absorber stroke to a minimum, the spring of an oleo-pneumatic shock absorber usually has little stroke between the static and fully closed positions and the spring stiffness increases rapidly beyond the static position. A typical static spring characteristic (Figure 1) shows a ratio of static load to preload of 4:1 and of closing load to static load of 2:1. The shock absorber damping is generally optimised to give efficient energy

absorption during the landing impact. However the damping level determined by this means generates relatively small damping forces when the shock absorber is closed at velocities appropriate to taxiing, damping in aircraft shock absorbers being most often the result of flow through orifices and therefore a function of velocity squared.

Such problems can be alleviated by the use of 'two-stage' or duplex springs and mechanical devices to control the damping. A 'two-stage' spring characteristic can be arranged to provide a low stiffness travel range within the total stroke required for landing energy absorption. The damping may be controlled by a simple pressure sensitive valve to provide different levels above and below a prescribed pressure (or closing velocity) level (Figure 2). By use of such devices the ground taxiing performance of a landing gear can be changed without greatly affecting the landing performance and while retaining the simplicity and reliability of a passive system.

Although a number of studies of the performance aspects of landing gear shock absorbers have been conducted including 'active' as well as 'passive' control devices little has been done, to the Author's knowledge, to evaluate the degree of improvement attainable with only 'passive' characteristics, a potentially very 'cost-effective' area of development. So Dowty, with MOD support, embarked upon a practical development programme to show the improvement which could be achieved, by optimising shock absorber characteristics for the ground taxiing considerations while at the same time incurring no penalty on landing energy absorption.

## 2.0 DOWTY ROTOL DEVELOPMENT PROGRAMME

The objectives of the development programme were:-

To establish the suspension characteristics of existing under-carriage equipment, then by a programme of test and development to define an improved suspension system.

To design and manufacture an 'improved' suspension system and demonstrate its effectiveness by aircraft trials on an in-service military aircraft.

It was decided after consideration of a number of aircraft to use Jaguar as the 'base-line' aircraft for the programme, for the following reasons;

Jaguar is an 'in-service' aircraft with a capability for rough and soft ground operation which has been well established by trials and computer simulation conducted by British Aerospace.

The landing gears are of lever suspension or trailing link design and have large low pressure tyres, each being features which improve the capability to absorb short wavelength roughness so making the undercarriages very suitable for the improvement programme which concentrates particularly on the responses due to longer wavelength roughness.

The suspension characteristics of the existing standard of undercarriages were determined by a programme of tests comprising frequency response tests and ground profile tests conducted under laboratory conditions and linear dynamometer tests in which the undercarriages were propelled across discrete ramps, repairs and craters.

The shock absorber characteristics were then modified as desired by utilising duplex or 'two-stage' springs to achieve different spring rates and pressure sensitive or 'two-stage' valves to provide different dampings for taxiing and landings. The suspension characteristics were then re-evaluated for the 'modified' shock absorbers.

The landing energy absorption capability was demonstrated by drop tests conducted on the undercarriages before and after modification.

The test programme to date has been conducted on individual undercarriages only and the results are therefore limited to the heave response of a single degree of freedom system. Computer simulation has been used to investigate the complete aircraft response and to show how improvements obtained by individual undercarriage development translate to total aircraft performance.

## 3.0 SHOCK ABSORBER CHARACTERISTICS

Both nose and main undercarriages of Jaguar have oleo-pneumatic capsule shock absorbers in levered suspension geometry configurations.

### 3.1 Nose Undercarriage Shock Absorber Characteristics

The nose shock absorber has a spring characteristic which results from compression of a volume of gas separated by a piston from the hydraulic fluid in the shock absorber. Because high pressure is developed during the final portion of shock absorber closure, hydraulic fluid compression becomes significant and modifies the spring curve which would result from gas compression alone. The wide range of steady loading occurring on the Jaguar nose undercarriage (Figure 3) is due to aircraft weight range, centre of gravity variation and the effect of main wheel braking.

Damping forces are generated within the shock absorber by restricting the flow of hydraulic fluid between chambers during compression and extension. Jaguar shock absorbers are arranged with completely separate compression and recoil damping chambers and directionally dependent damping is provided by use of mechanically simple plate valves in each chamber. This arrangement enables compression and recoil damping to be separately optimised and ensures that correct damping is maintained during continuous operation because the recoil chamber is completely filled with fluid during shock absorber compression as is the compression chamber during recoil.

### 3.2 Main Undercarriage Shock Absorber Spring Characteristics

The existing shock absorber utilizes a 'two-stage' spring which contains the static load range on the second stage of the spring (Figure 4). The mechanical arrangement to achieve this 'two-stage' spring system employs two separator pistons as shown in the schematic (Figure 5). The damping arrangement of the existing shock absorber of the Jaguar is similar to that already described for the nose undercarriage.

### 4.0 TRIALS PROGRAMME

A trials programme was promulgated to evaluate the suspension characteristics of individual undercarriages. The programme comprised:

#### Frequency Response Tests

In which the undercarriage system, loaded with a mass representative of the proportion of aircraft mass associated with the unit, was subjected to a sinusoidal ground input excitation and the response of the system measured. The amplitude and frequency of excitation were varied.

#### Rough Ground Profile Tests

In which the undercarriage system was subjected to measured ground profiles. The ground input was computer generated and was made representative of accelerating, decelerating and constant speed runs across profiles of various roughness.

#### Linear Dynamometer Trials

In which the undercarriage system mounted in a rig could be propelled along a track at various forward speeds. Ground obstructions were situated in the path of the rig and the response of the undercarriage to particular ground inputs was measured. Triangular ramps (long wavelengths), rectangular planks (short wavelengths) and craters were used as ground inputs.

Measurements of loads and displacements were made so that performance comparisons could be made of the different standards of shock absorbers tested. Limitations in the hydraulic power available to the test rig for the frequency response and ground profile testing made it necessary to use a 'scaled down' version of the Jaguar main undercarriage. A new shock absorber was manufactured and used in a 2/3 scale model undercarriage geometrically representative of the Jaguar main undercarriage, the spring characteristic and damping levels were suitably adjusted.

### 5.0 TEST RESULTS FOR STANDARD SHOCK ABSORBERS

Frequency response tests were conducted on nose and main undercarriages using a number of different unit loads, input frequencies in the range 0.1 to 10 Hz and input amplitudes of 13 to 38 mm. The results were obtained in the form of amplitude ratio and phase lag characteristics. Figure 5 for nose and Figure 6 for the main undercarriage show results for representative unit loads.

Ground profile tests were conducted using a representative rough ground profile and a range of applicable unit loads. A velocity range of 20 to 160 knots was considered and constant speed, accelerating and decelerating runs were included. The results were obtained as time history measurements of the various parameters. Typical results for the standard shock absorber equipment are shown in Figures 8 and 9 for the nose and main undercarriages respectively. These results correspond to the aircraft speed which generates the greatest response at the particular weight condition being considered.

Dynamometer tests were performed throughout the aircraft forward speed range at different unit loads. Pairs of triangular ramps, series of planks and single craters were used as ground inputs. Again a number of relevant parameters were recorded as functions of time. Typical results using a pair of triangular ramps as the ground input at forward speeds which produce maximum response are shown for the nose and main undercarriages in Figure 10 and 11 respectively.

## 6.0 IMPROVED SHOCK ABSORBER CHARACTERISTICS

### 6.1 Nose Undercarriage Shock Absorber

Possible modifications to the nose shock absorber spring characteristic were considered which according to our experience could be expected to lead to improvements in taxiing performance. It is not possible with a 'passive' spring system to significantly reduce the spring stiffness throughout the total loading range and still meet the other constraints of spring stroke, closing load and pre-load. A 'two-stage' spring modification was therefore made which reduced by half the stiffness at the take-off weight static load position, retained the minimum weight static load on the low stiffness portion of the second stage spring but had little effect on the stiffness at the 'steady-braked' load. The residual travels at other than the 'steady-braked' load were also improved significantly (Figure 11). Practically this was achieved by incorporating a second annular separator piston within the shock absorber which contained the supplementary low pressure gas spring.

General experience with landing gear shock absorbers for which the damping has been based on landing energy absorption suggests that they are under damped during taxi induced motion at the predominant, rigid body heave and pitch frequencies. On Jaguar specifically, pitch response predominated during aircraft taxi trials and it was evident that higher damping in the nose shock absorber could reduce the response. A pressure sensitive valve has been used in the modified shock absorber to provide higher damping during taxiing without significantly affecting the landing impact performance of the shock absorber. With such an arrangement a secondary damping orifice system becomes operative when the damping pressure due to flow through the primary orifice reaches a prescribed value (Figure 13). Provided the velocities developed during taxiing do not exceed the level set for the valve to operate then the higher damping will apply at all conditions other than landing impact. On landing at design vertical velocities the shock absorber velocity exceeds that at which the valve operates and landing impact optimisation can be performed with the valve in its open condition.

### 6.2 Main Undercarriage Shock Absorber

Because the existing main undercarriage shock absorber already has a 'two-stage' spring arrangement which situates the static load range on a portion of the second stage spring, of relatively low stiffness, it would not be expected that significant reduction in stiffness could be achieved without violating the other spring design constraints. It was therefore decided that no change would be made to the main shock absorber spring characteristic. However, changes to the main undercarriage shock absorber damping were made in a similar way to that employed on the nose shock absorber. A pressure sensitive damping valve was again used to provide different levels of damping under taxiing and landing conditions (Figure 14).

## 7.0 TESTS USING 'MODIFIED' SHOCK ABSORBERS

Similar tests were performed using the modified shock absorbers as already described for the existing standard shock absorbers.

Figure 15 compares the typical frequency response of the standard and modified nose undercarriages where the improvement exceeded 30% in amplitude ratio when expressed in decibels, equivalent to almost a 40% reduction in response amplitude with the modified undercarriage, while Figure 16 shows the reduced response of the modified shock absorber to the rough ground profile. The responses of the two standards of shock absorber to the triangular ramps are compared in Figures 17 and 18, which show sprung mass response and vertical reaction factor improvements of 31% and 25% respectively.

The main undercarriage results show less performance improvement due to modified characteristics than did the nose undercarriage. The frequency response shown in Figure 19 is reduced by 11% and the ground profile taxi response is little changed (Figure 20). The response to the triangular ramps is improved by 29% on sprung mass response and 17% on reaction factor (Figures 21 and 22). The reasons for this lesser improvement in performance are thought to be:

The standard maingear shock absorber has a 'two-stage' spring which provides relatively low stiffness under static load.

The 'two-stage' valve introduced into the modified maingear shock absorber operated at a lower velocity than intended and during some of the trials the damping was switched to the lower landing damping level.

Probably the most striking performance comparison occurred during linear dynamometer tests with the nose undercarriage. With the standard shock absorber and 90 mm ramps the undercarriage system response was so great that the programme was aborted at 70 kts speed to avoid damage. The modified undercarriage completed the same test programme with no sign of distress.

## 8.0 LANDING ENERGY ABSORPTION

The existing and modified undercarriages were subjected to a limited programme of drop tests to demonstrate the capability of the modified units to meet the landing impact energy requirements. A typical comparison of the results obtained is shown in Figure 23.

One aspect of the modified shock absorber design which led to concern was the operation of the 'two-stage' damping valve during the tests. The sudden loss of effective damping control which occurred on the main undercarriage when the valve opened at the instant when the undercarriage response was at its most severe was clearly undesirable and potentially dangerous. A modified valve was developed which has a gradual or 'progressive' change from one damping level to the other (Figure 24). Such a valve was incorporated into the main undercarriage shock absorber and a limited amount of testing showed a general improvement in performance when compared with the standard shock absorber (Figures 25 and 26), without displaying the sudden damping discontinuity characteristic of the 'two-stage' valve. It is considered that with further development this type of valve may prove more suitable than the simple 'two-stage' design.

## 9.0 AIRCRAFT PERFORMANCE

The programme of tests conducted by Dowty has been supplemented by theoretical predictions of the complete aircraft performance conducted by BAe. Warton using their Jaguar aircraft model. The undercarriage theoretical models were first validated using the single undercarriage linear dynamometer test results and then the complete aircraft performance was predicted over various rough ground inputs. The undercarriage data was changed to represent the 'improved' shock absorber characteristics and the aircraft performance re-evaluated. Two improved undercarriage standards were considered, the first with a 'two-stage' spring characteristic in the nose shock absorber and 'two-stage' damping in both main and nose units, and the second with a further change to introduce the 'progressive' type of damping valve into the main undercarriage shock absorber. Comparison of the results shows that a significant improvement in performance is retained when evaluated in terms of the complete aircraft. The vertical reactions for each of the shock absorber standards when crossing a section of the rough ground profile are shown in Figure 27.

## 10.0 CONCLUSION

The development programme so far has confirmed that even with an aircraft such as the Jaguar, which already has a good ground taxiing capability, significant improvements can be made by re-optimising the undercarriage shock absorber characteristics for ground taxiing. Further it has been demonstrated that, for the degree of roughness considered, optimised characteristics can separately be obtained for taxiing and landing by the use of well established techniques of 'two-stage' or duplex springs and pressure sensitive damping control valves. We hope to proceed in the near future to the second part of our planned trials programme, when a Jaguar aircraft with suitably modified shock absorbers will give a practical demonstration of the improvements attainable.

Dowty believes that of the many factors which influence the ability of a military aircraft to operate from rough or damaged runways improved undercarriage performance is potentially very significant. Furthermore it has been demonstrated that modifications made to the 'passive' characteristics of existing conventional shock absorbers can lead to very worthwhile improvements. It is probable that such improvements can be made on many 'in-service' aircraft or incorporated into new designs at little cost and Dowty look forward to being able to demonstrate the effects of such improvements by aircraft trials in the next phase of the development programme.

### Acknowledgement:

Dowty Rotol wishes to thank the Ministry of Defence and British Aerospace Public Ltd. Co. - Warton for their support and assistance in the completion of this development project, and to acknowledge the use of undercarriage equipment for the Jaguar designed by Messier Hispano Bugatti which formed the basis of the studies.

## TYPICAL UNDERCARRIAGE GROUND SPRING WITH 8:1 COMPRESSION RATIO

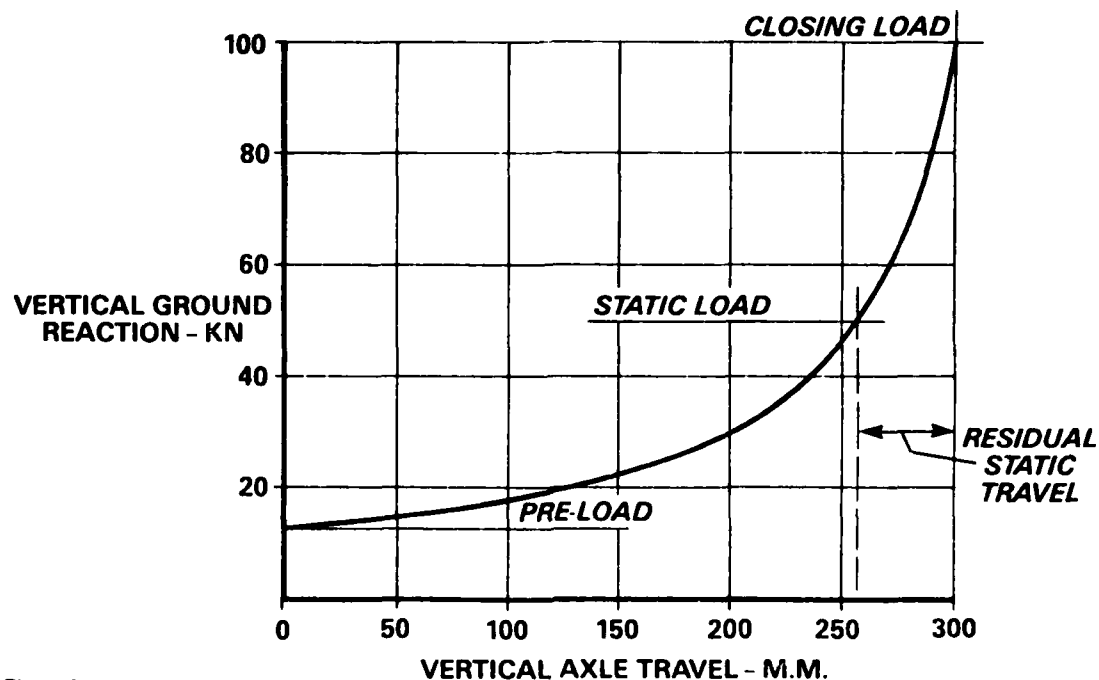


Figure 1

## PRESSURE VERSUS FLOW CHARACTERISTIC OF A TWO-STAGE DAMPING VALVE

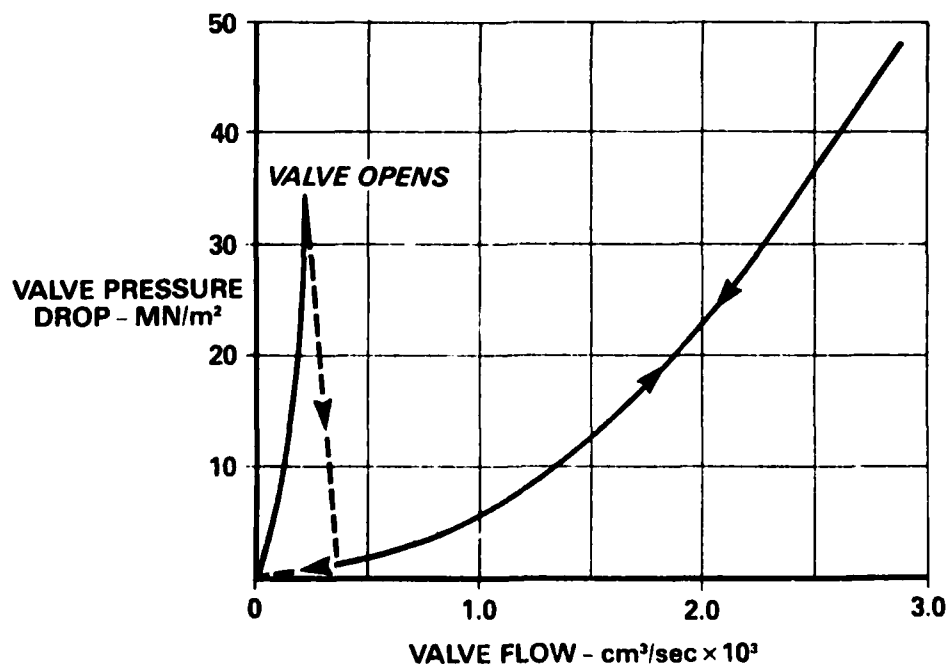


Figure 2

## NOSE UNDERCARRIAGE GROUND SPRING CURVE

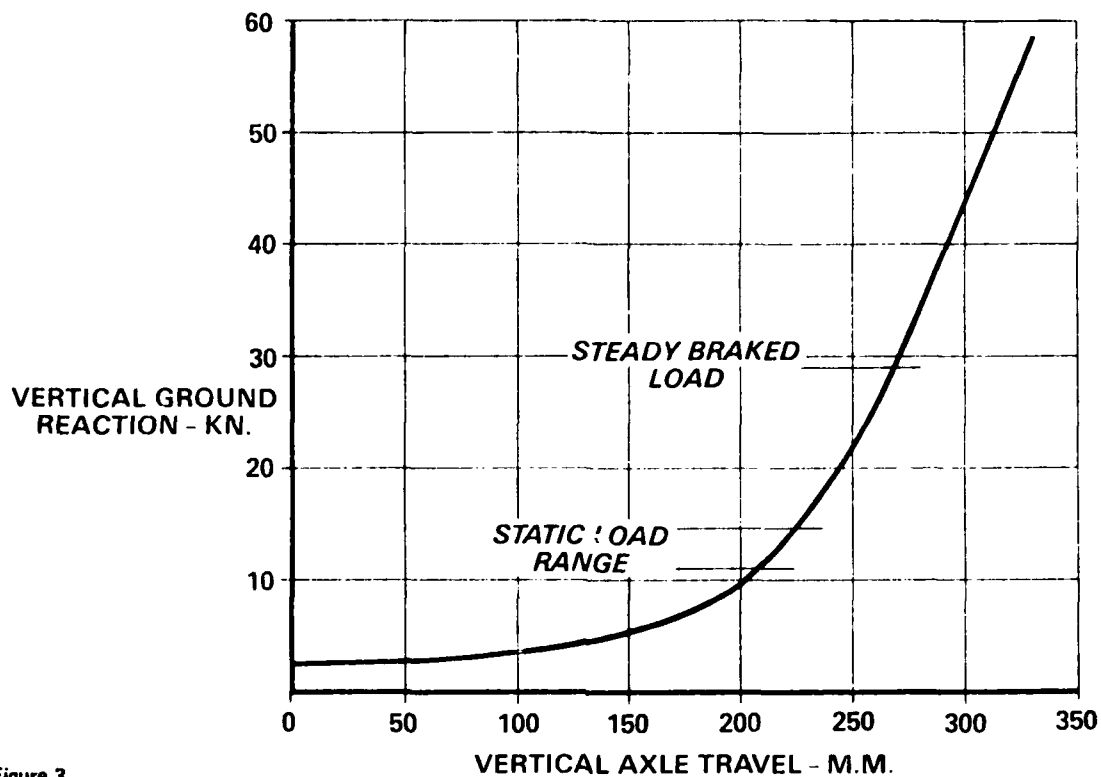


Figure 3

## MAIN UNDERCARRIAGE GROUND SPRING CURVE

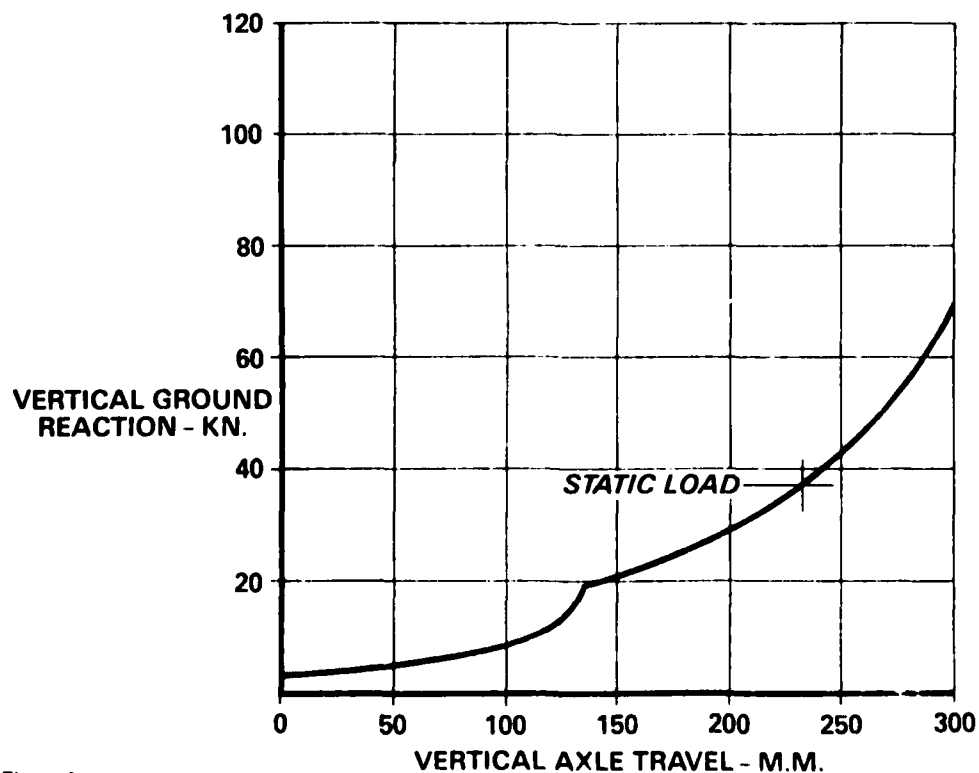


Figure 4

## DIAGRAMMATIC ARRANGEMENT OF JAGUAR MAIN SHOCK ABSORBER

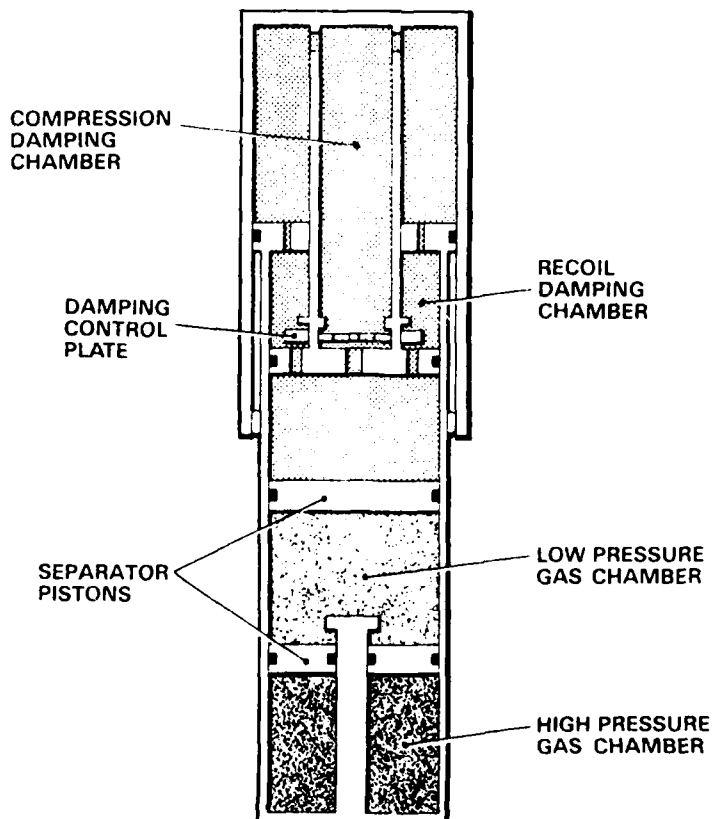


Figure 5

## NOSE UNDERCARRIAGE FREQUENCY RESPONSE TEST

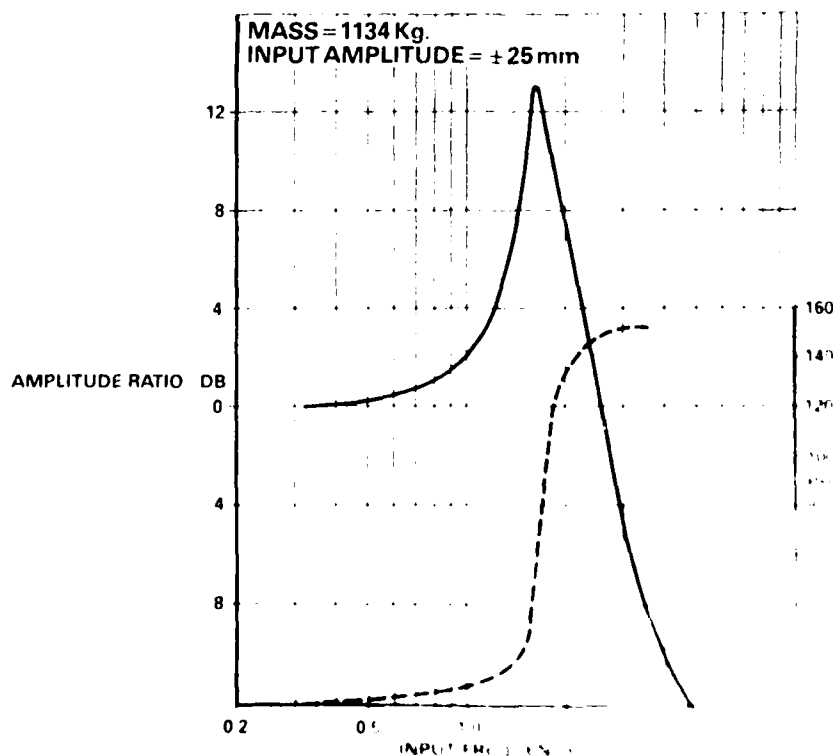


Figure 6



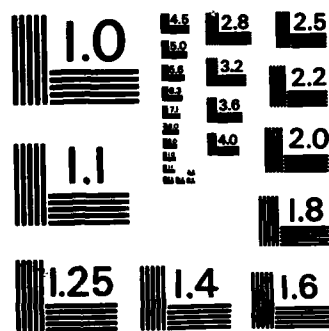
AIRCRAFT DYNAMIC RESPONSE TO DAMAGED AND REPAIRED  
RUNWAYS(U) ADVISORY GROUP FOR AEROSPACE RESEARCH AND  
DEVELOPMENT NEUILLY-SUR-SEINE (FRANCE) AUG 82  
AGARD-CP-326 F/G 1/5

NL

F/G 1/5

## FILMS

GIVE



MICROCOPY RESOLUTION TEST CHART  
NATIONAL BUREAU OF STANDARDS-1963-A

## MAIN UNDERCARRIAGE FREQUENCY RESPONSE TEST

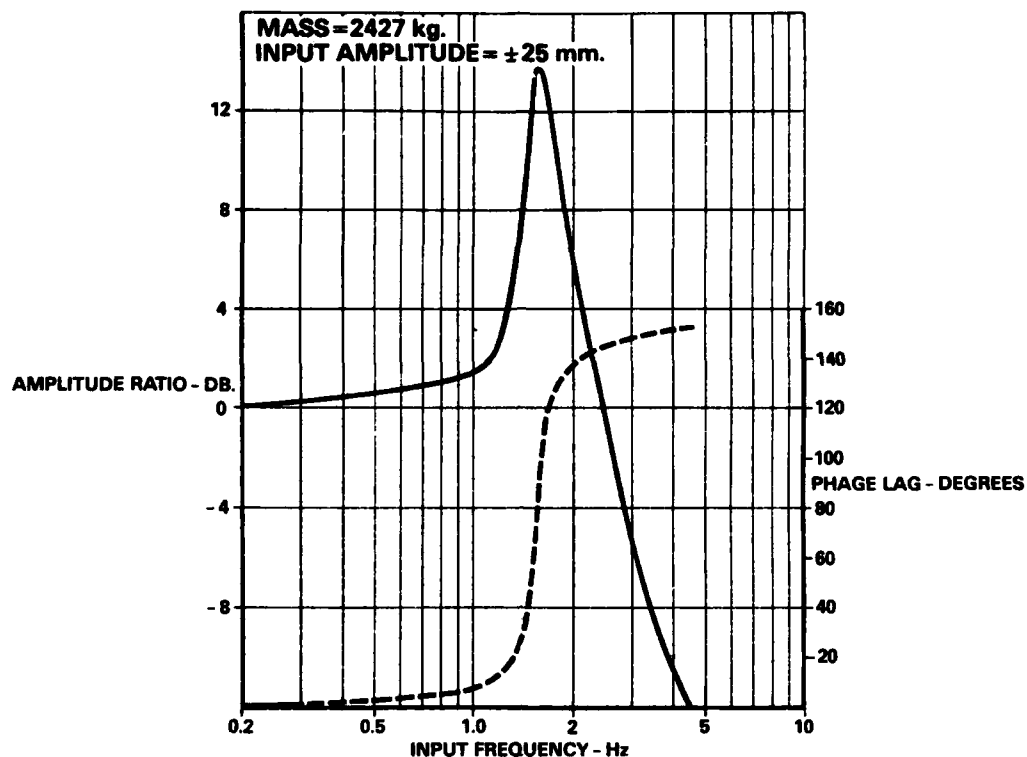


Figure 7

## STANDARD NOSE GEAR UNIT LOAD = 2948 kg, SPEED = 100 kts.

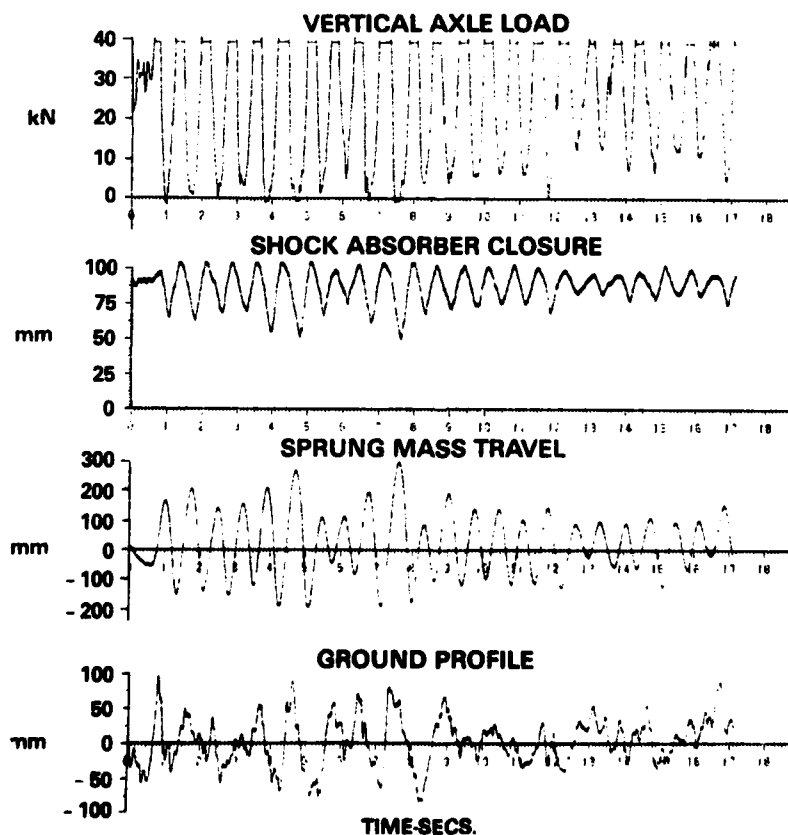


Figure 8

# STANDARD MAIN GEAR

UNIT LOAD = 2427 kg SPEED = 120 kts.

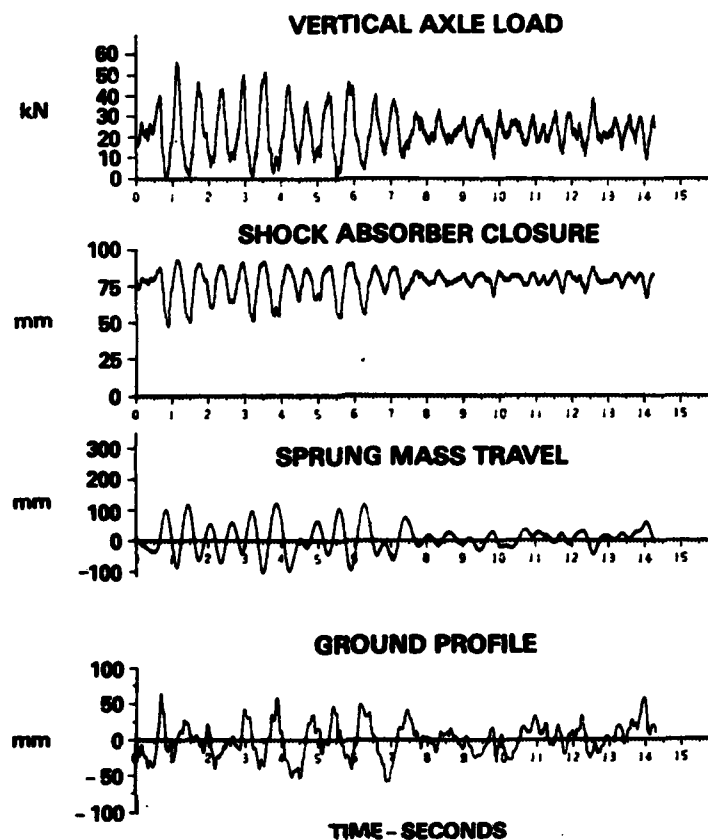


Figure 9

## NOSE UNDERCARRIAGE SPRUNG MASS RESPONSE TO TWO RAMP INPUT

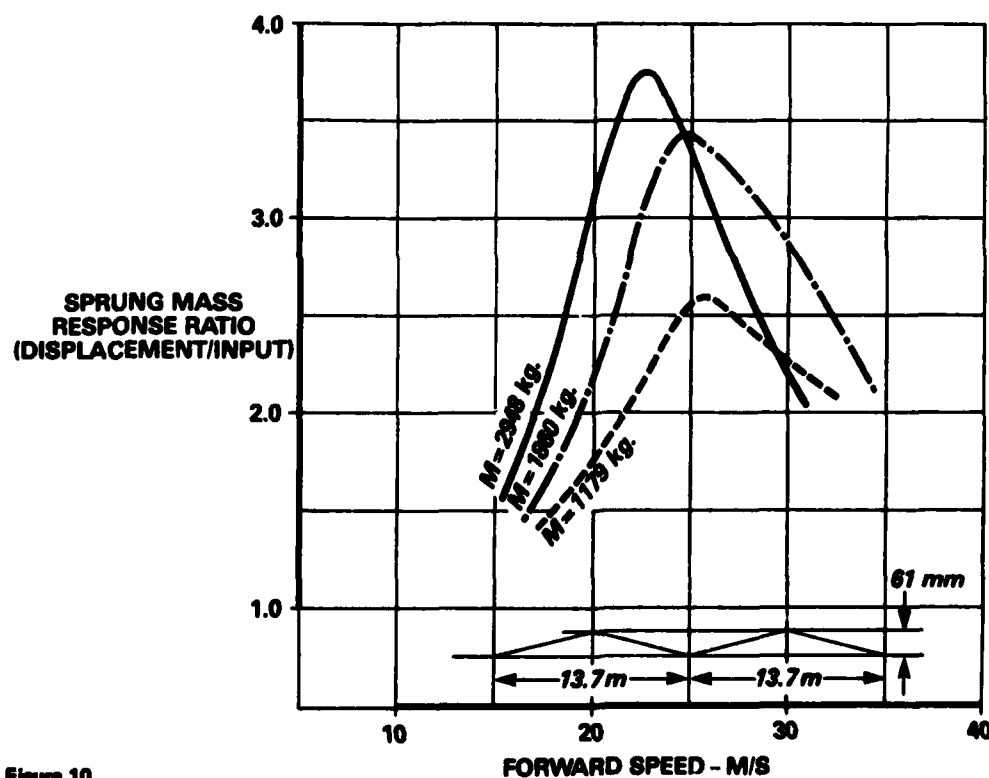


Figure 10

## MAIN UNDERCARRIAGE SPRUNG MASS RESPONSE TO TWO RAMP INPUT

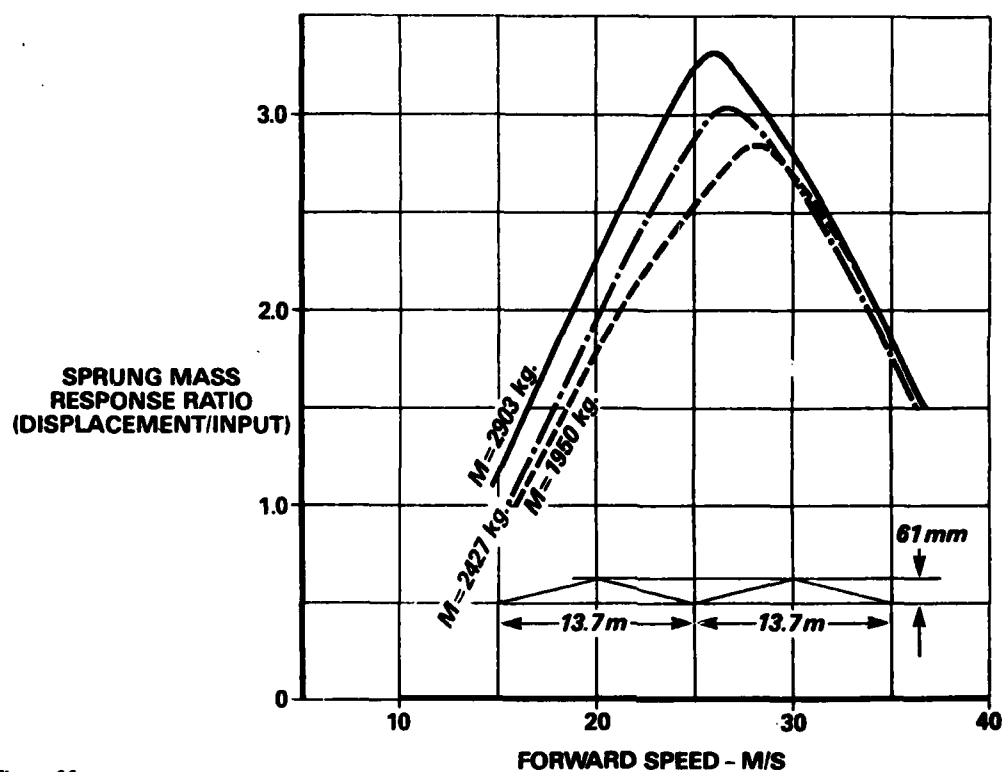


Figure 11

## NOSE UNDERCARRIAGE TWO-STAGE GROUND SPRING CURVE

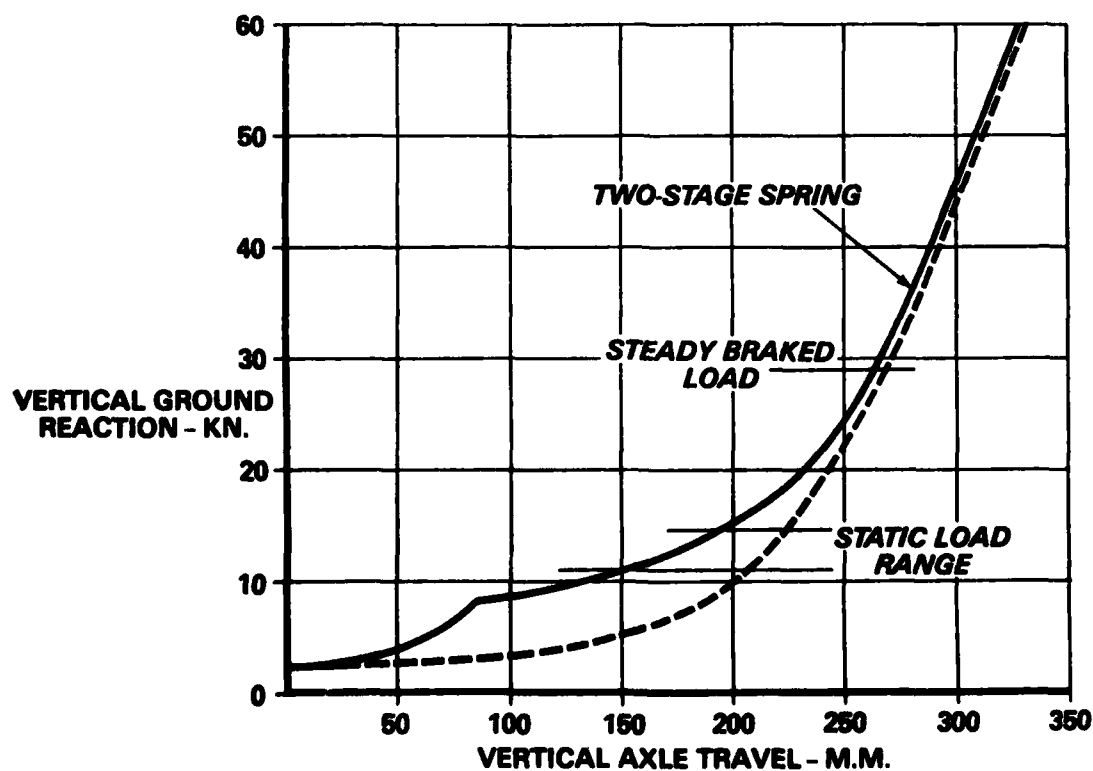


Figure 12

# **NOSE UNDERCARRIAGE SHOCK ABSORBER DAMPING CHARACTERISTIC COMPARISON OF STANDARD AND MODIFIED**

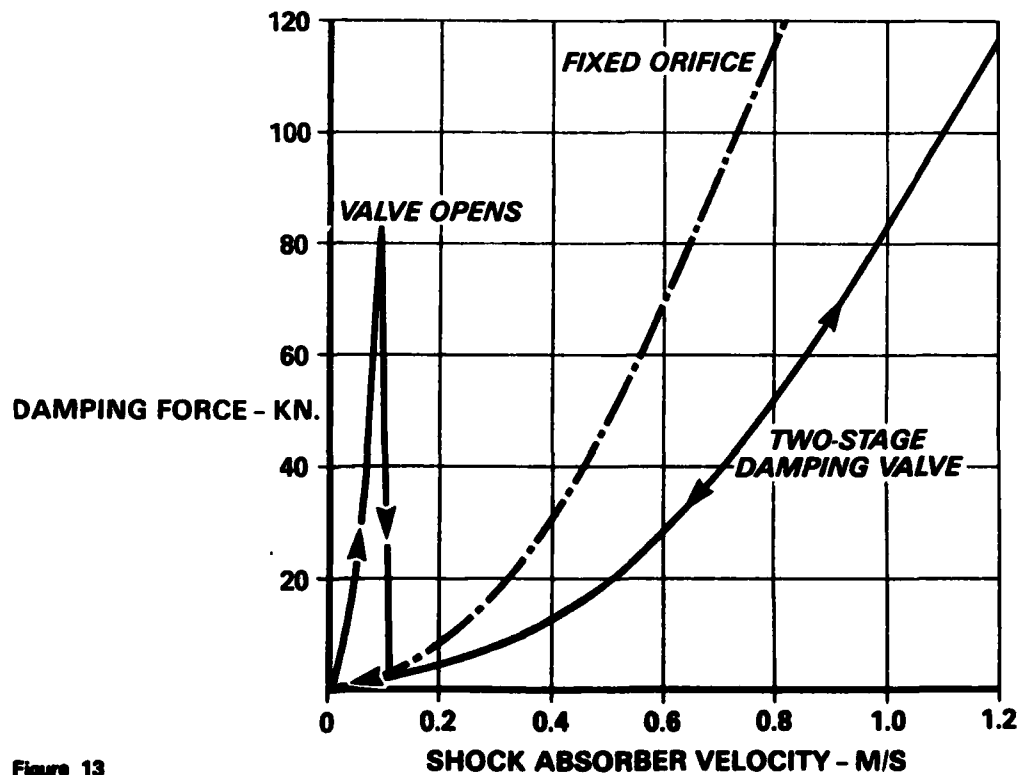


Figure 13

# **MAIN UNDERCARRIAGE SHOCK ABSORBER DAMPING CHARACTERISTIC COMPARISON OF STANDARD AND MODIFIED**

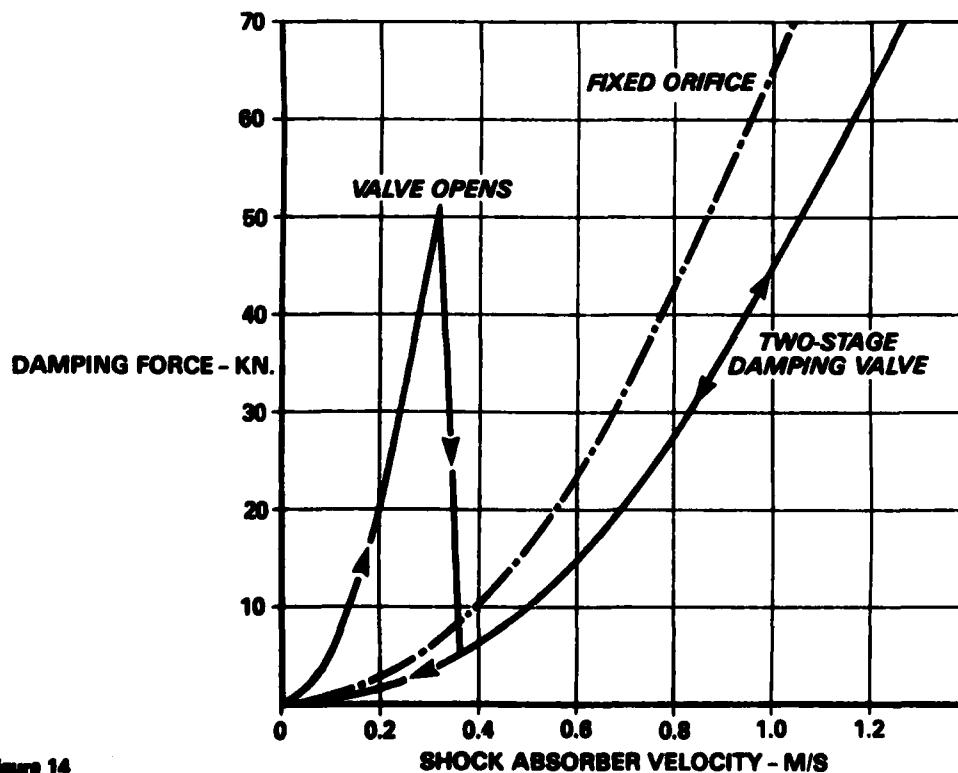


Figure 14

# **NOSE UNDERCARRIAGE FREQUENCY RESPONSE TEST COMPARISON OF STANDARD AND MODIFIED SHOCK ABSORBERS**

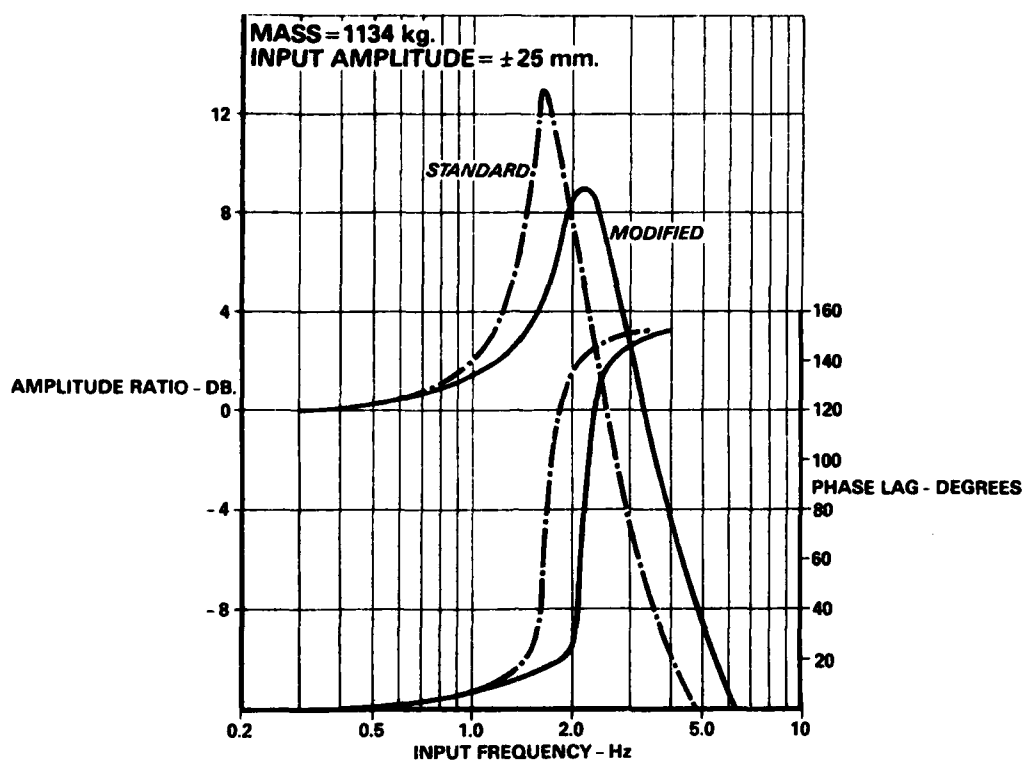


Figure 15

## **MODIFIED NOSE GEAR UNIT LOAD = 2948 kg    SPEED = 100 kts.**

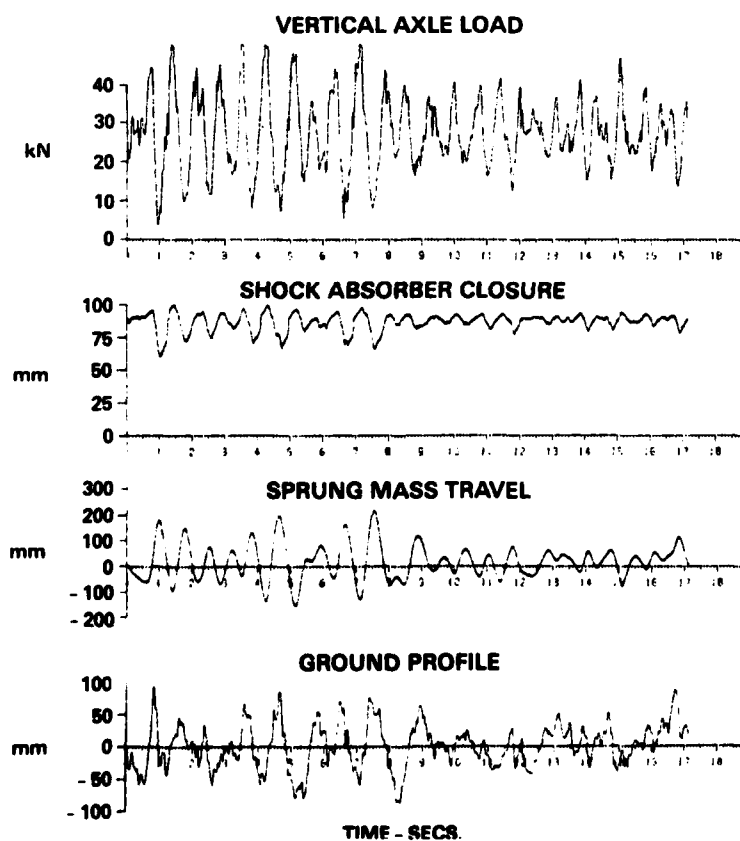


Figure 16

# **NOSE UNDERCARRIAGE SPRUNG MASS RESPONSE TO TWO RAMP INPUT COMPARISON OF STANDARD AND MODIFIED SHOCK ABSORBERS**

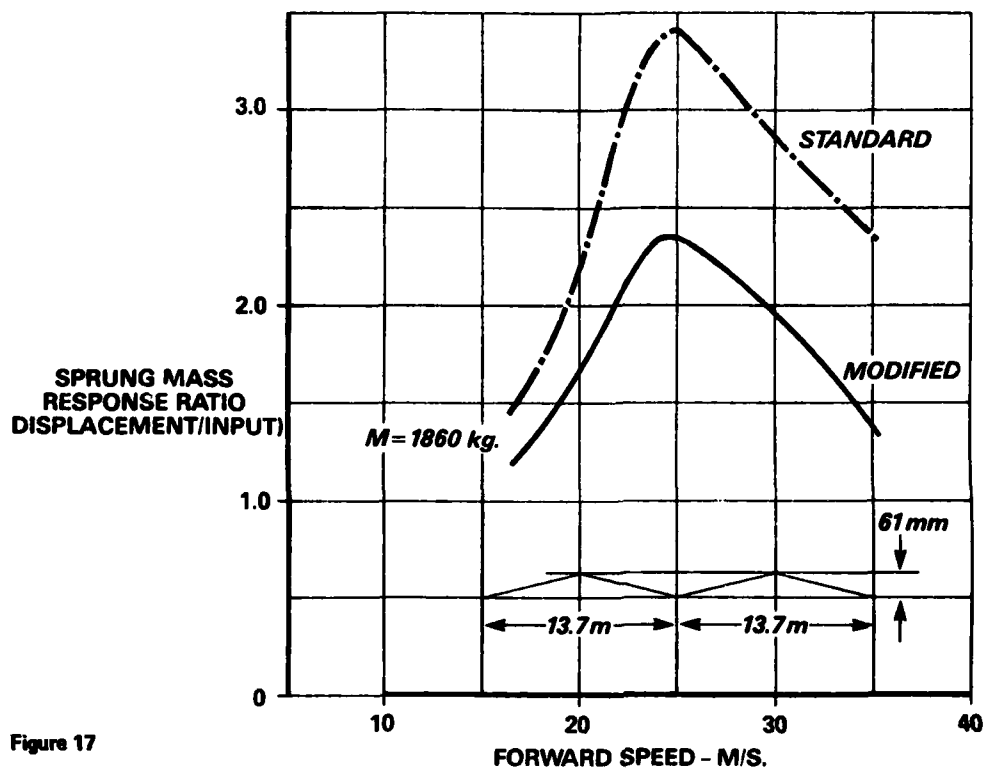


Figure 17

# **NOSE UNDERCARRIAGE REACTION FACTOR FOR TWO RAMP INPUT COMPARISON OF STANDARD AND MODIFIED SHOCK ABSORBERS**

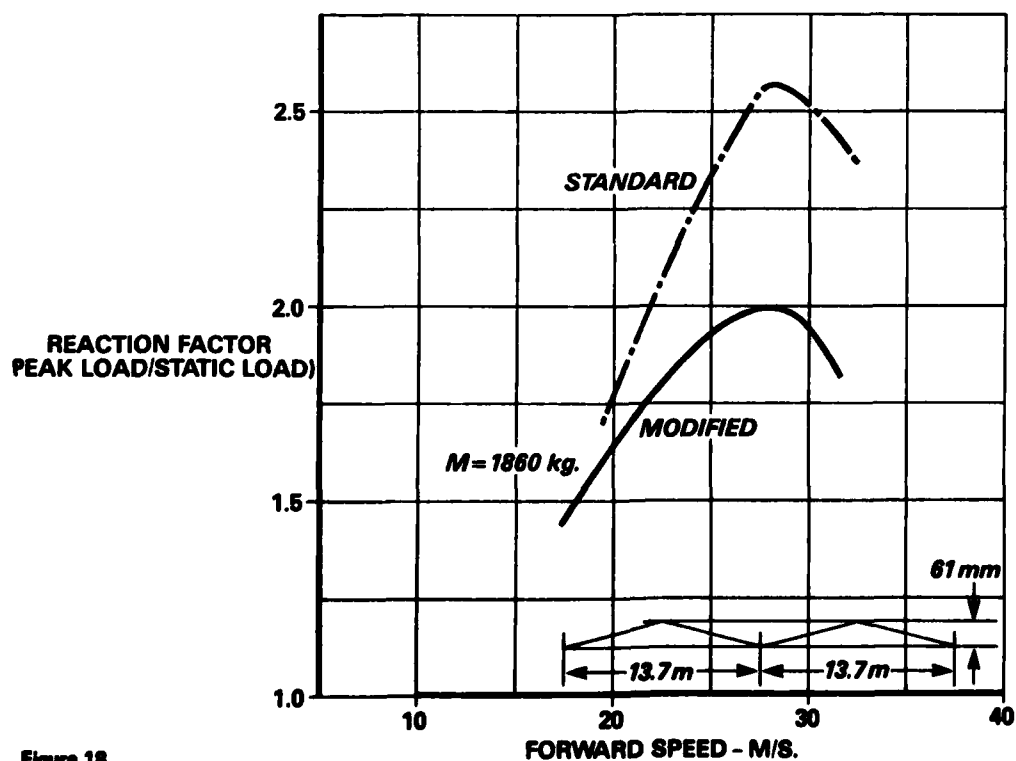


Figure 18



# **MAIN UNDERCARRIAGE FREQUENCY RESPONSE TESTS COMPARISON OF STANDARD AND MODIFIED SHOCK ABSORBERS**

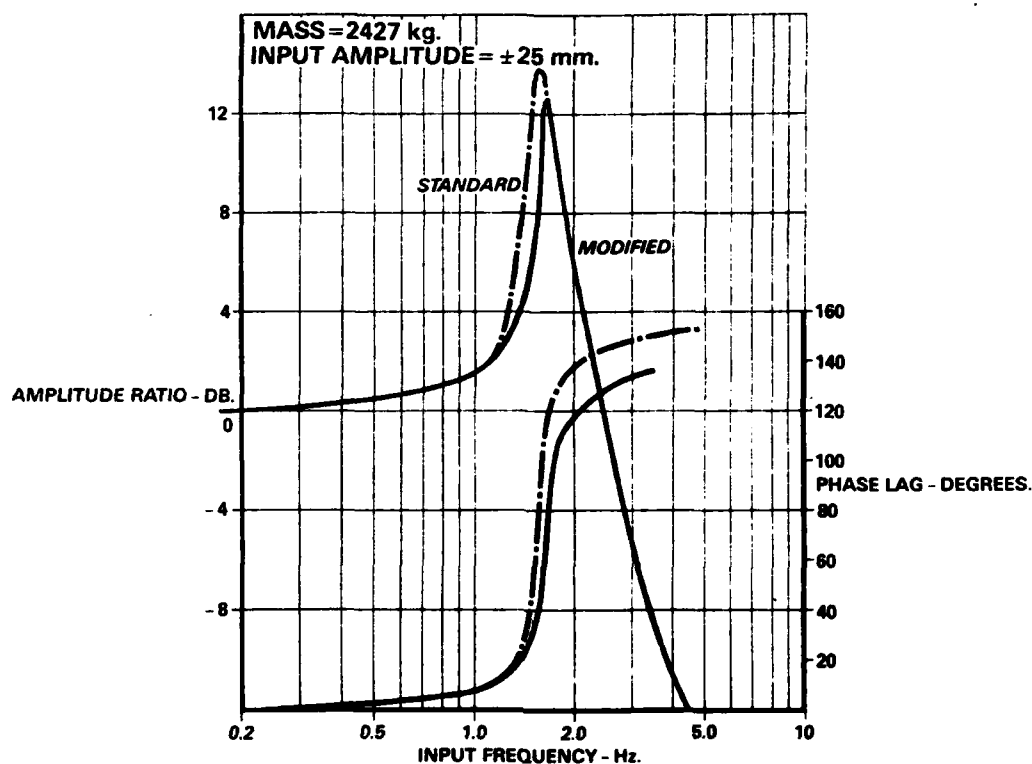


Figure 19

## **MODIFIED MAIN GEAR UNIT LOAD = 2427 kg SPEED = 120 kts.**

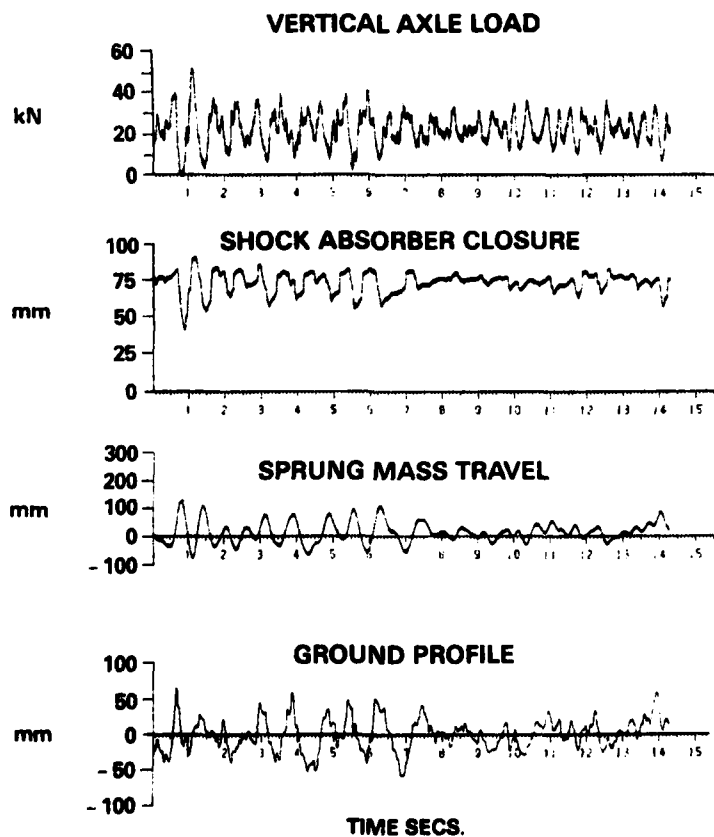


Figure 20

# **MAIN UNDERCARRIAGE SPRUNG MASS RESPONSE TO TWO RAMP INPUT COMPARISON OF STANDARD AND MODIFIED SHOCK ABSORBERS**

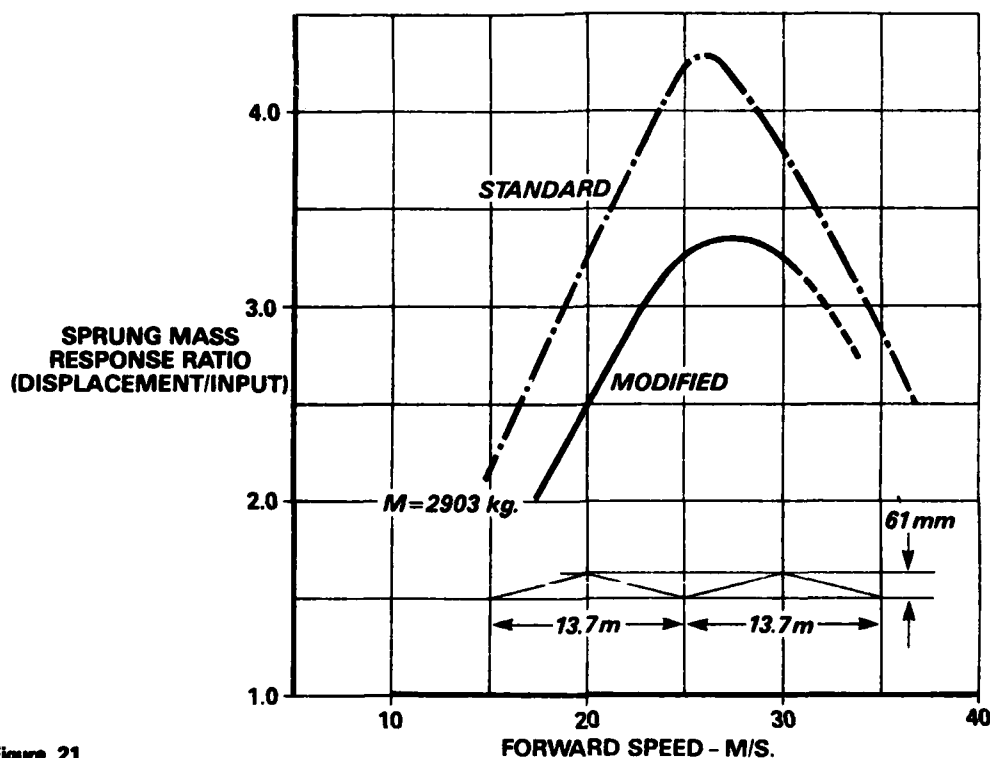


Figure 21

# **MAIN UNDERCARRIAGE REACTION FACTOR FOR TWO RAMP INPUT COMPARISON OF STANDARD AND MODIFIED SHOCK ABSORBERS**

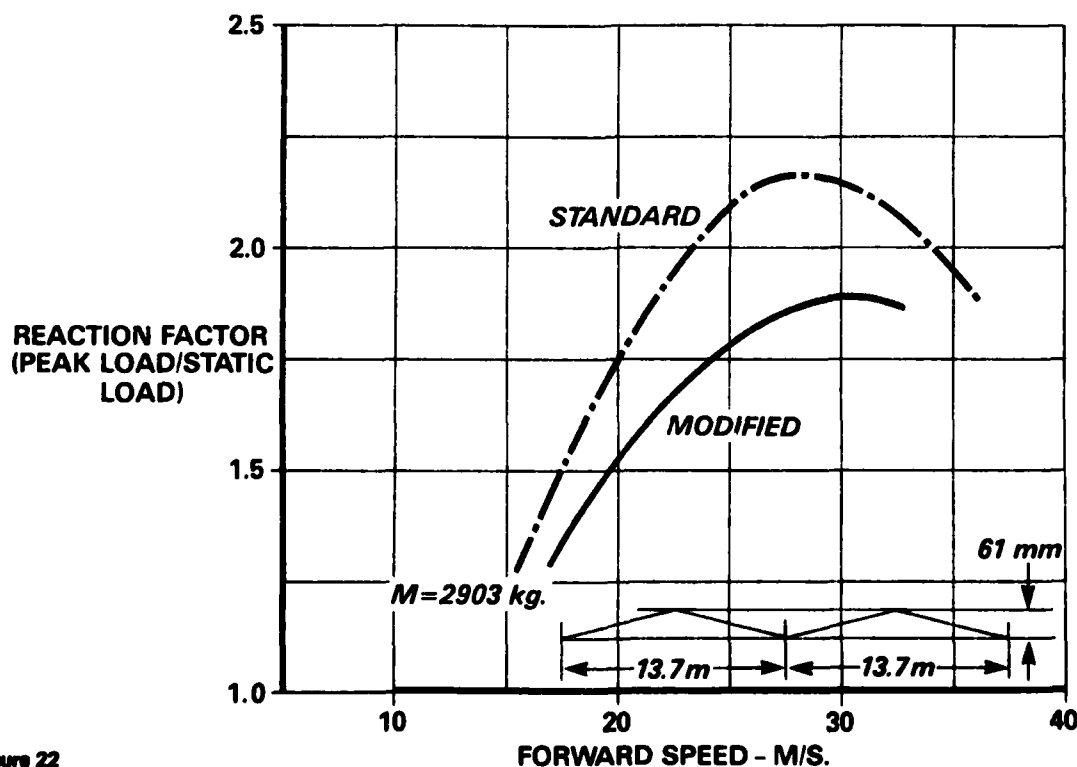


Figure 22

# **MAIN UNDERCARRIAGE DROP TEST AT 3.6 M/S VERTICAL VELOCITY DROP MASS=1105 kg.**

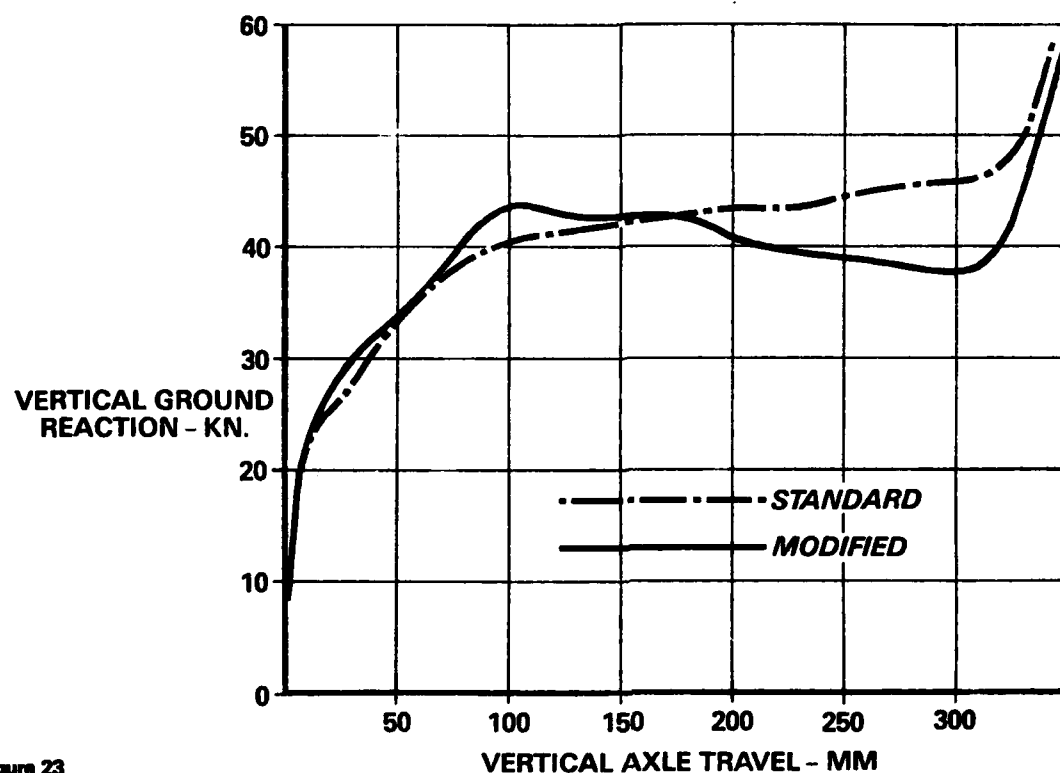


Figure 23

# **MAIN UNDERCARRIAGE SHOCK ABSORBER DAMPING CHARACTERISTIC COMPARISON OF STANDARD AND PROGRESSIVE**

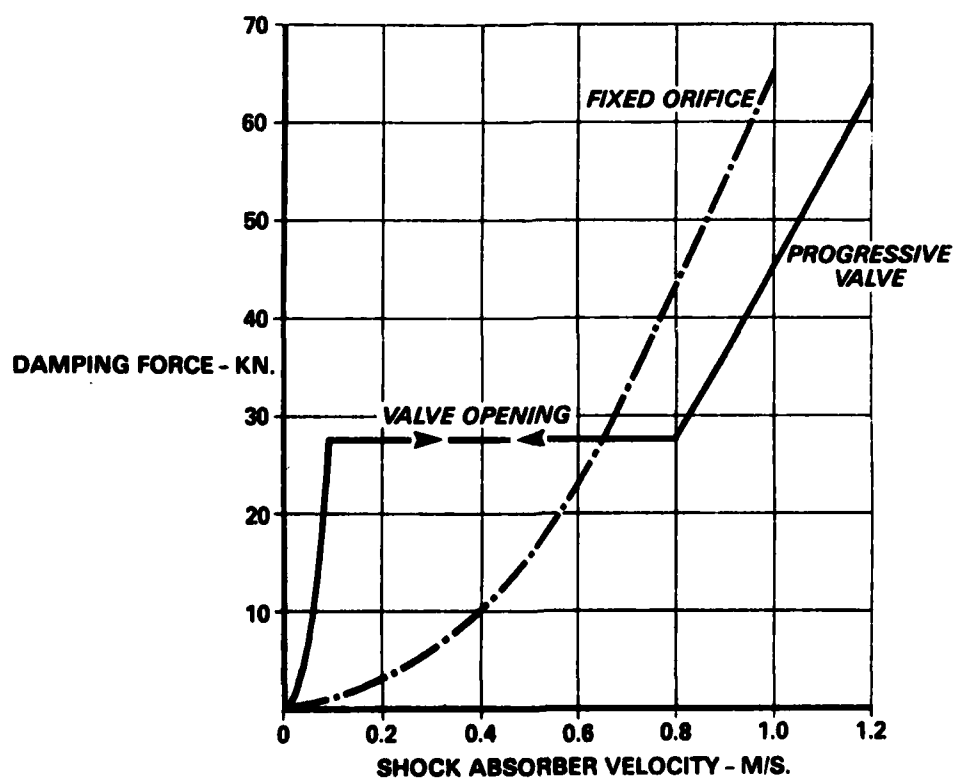


Figure 24

# **MAIN UNDERCARRIAGE SPRUNG MASS RESPONSE TO TWO RAMP INPUT COMPARISON OF STANDARD AND PROGRESSIVE VALVE SHOCK ABSORBERS**

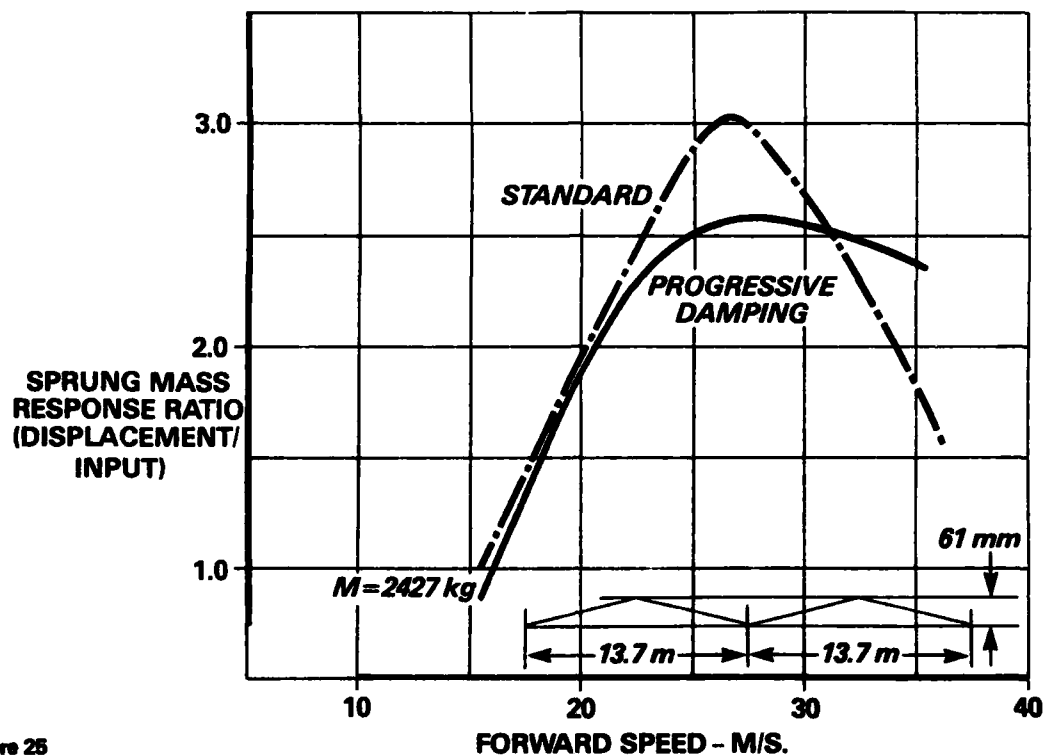


Figure 25

# **MAIN UNDERCARRIAGE REACTION FACTOR FOR TWO RAMP INPUT COMPARISON OF STANDARD AND PROGRESSIVE DAMPING SHOCK ABSORBERS**

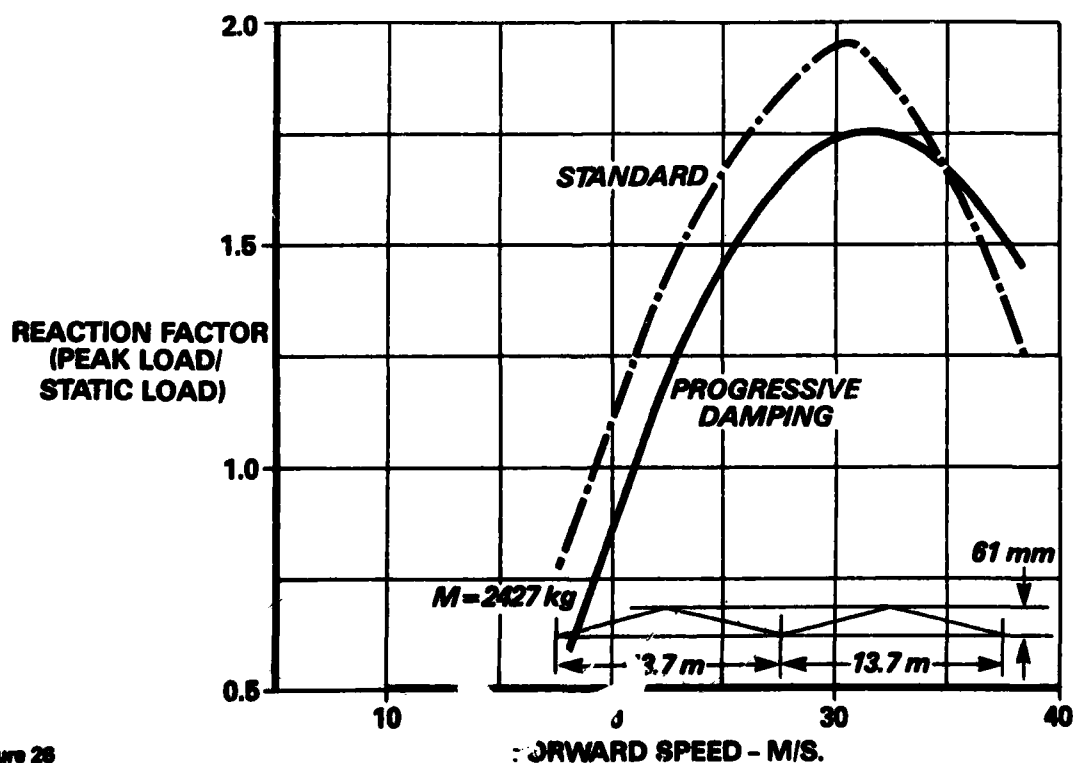


Figure 26

## TAKE-OFF RUN OVER ROUGH GROUND PROFILE. NOSE GEAR VERTICAL AXLE LOADS

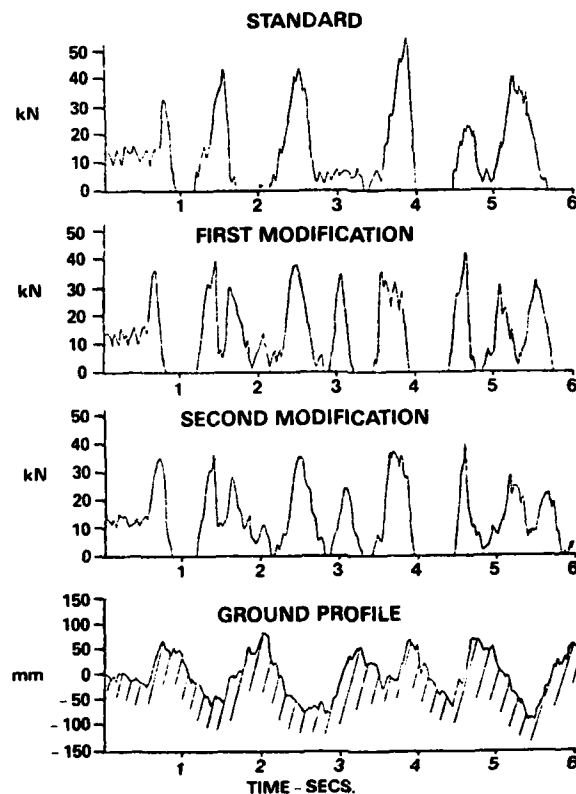


Figure 27

## TAKE-OFF RUN OVER ROUGH GROUND PROFILE. MAIN GEAR VERTICAL AXLE LOADS

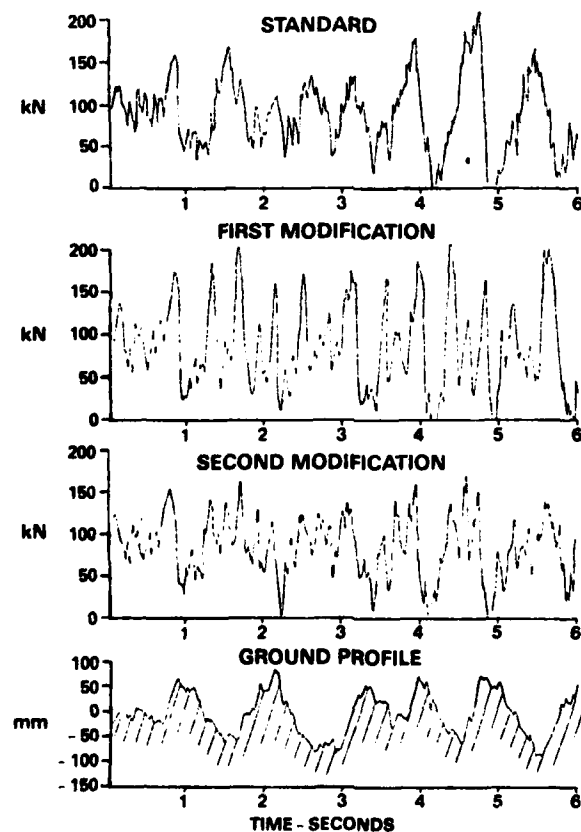


Figure 28

## ROUGHNESS CONSIDERATIONS FOR TRANSPORT AIRCRAFT

B. M. Crenshaw  
Staff Engineer  
Lockheed-Georgia Company  
Marietta, Georgia 30063  
USA

### SUMMARY

A requirement exists for accurate calculations of landing gear and structural loads which could occur from taxi, takeoff, and landing on repaired bomb-damaged airfields. Collection of applicable test data has been accomplished for two transport aircraft, and is being collected for a third. A joint US/UK test program utilizing the C130MK1 Hercules aircraft was carried out during the summer of 1980 in the United Kingdom. Simultaneously, tests of the C-141B aircraft were conducted at Edwards AFB, California and Whiteman AFB, Missouri. To date, C-5A roughness testing has consisted of traversing (1-cosine) shaped bumps at low speeds. Additional C-5A testing is planned for 1982 to obtain structural response near landing and takeoff speeds. Results from these tests are used to validate computer simulation predictions of loads and to assist in the development of operating techniques.

### 1. INTRODUCTION

If operational recovery of battle damaged airfields is to be accomplished, transport aircraft may be required to deliver vital equipment and supplies utilizing repaired runways or perhaps adjacent unpaved areas. Ground handling design requirements for transports historically have been 2.0g static and later a roughness amplitude which produced a 0.5g increment over a (1-cosine) shaped undulation at a frequency corresponding to the first wing bending mode. The 2.0g condition designed the inner portion of the wing and the 0.5g flexible analysis became a consideration on the outer wing. These rather arbitrary requirements provide for some capability for runway roughness, as proven by the years of successful operation of conventional transport aircraft.

Other pertinent design parameters include landing gear load factor and strut stroke which are established to meet a specified sink rate. Nose gear maximum vertical load is likely to be established from sudden application of brakes. Tire size is usually selected on the basis of flotation requirements and storage pod constraints.

Aircraft growth at least through the time of the C-5A has resulted in increased landing gear complexity, size, and weight. Comparisons of main landing gears for the C-130, C-141B, and C-5A are shown in Figure 1. In most cases these design approaches have resulted in gears which perform well on maintained runways and have capability for operation on unpaved surfaces. Some unpaved surface and landing mat exploratory testing has been accomplished for all the Lockheed-Georgia transport aircraft. Tests from unpaved surfaces were made on C-130 aircraft starting in 1956 and continuing on an infrequent basis through a 1981 test of a stretched model of the C-130. Numerous flights are routinely made by commercial and military operators into remote airstrips including landings on snow/ice surfaces with ski equipped models.

The operating concepts associated with "Project HAVE BOUNCE" added to the roughness requirements faced by transport aircraft. Roughness amplitude is generally more severe than that encountered on most unsurfaced airstrips. The airfield dimensions defined for minimum operating strips are expected to preclude taxi to a smooth area, and time may not allow surface refurbishment to the standards expected for normal conditions.

### 2. STRUCTURAL MODEL COMPUTER SIMULATION DESCRIPTION

Digital computer simulation programs have been written to predict aircraft loads resulting from operating over repaired runways. These programs use time history integrations of aircraft accelerations to produce displacements and loads in the aircraft structure. Modifications of initial programs have been made to produce a more accurate representation of aircraft behavior.

#### a. Runway Model

The runway is represented either as discrete repairs on an otherwise smooth surface or as surveyed profile amplitudes with repairs superimposed. The profile elevation may be constant across the gear track width or may be three separate profiles representing the nose, left main, and right main gears for unsymmetric encounter by wheels on one side of the aircraft. Amplitude point spacing is arbitrary but must be constant.

#### b. Tire and Strut Models

Tire load deflection characteristics are based on manufacturer's load-deflection data represented as a point contact with the surface. The tire deflection therefore must follow the surface profile without "smoothing" within the tire footprint. Differences introduced by the point contact approximation were found to be more significant on the British Class 60 profiles where erroneously high strut velocities were observed in simulations of the C-130 over the six inch repair approach ramp. Since these velocities were sharp spikes, aircraft response is not significantly affected and the point contact errors can be compensated for by a modification of the strut damping coefficients. Provision is made in the C-141B and C-5A simulations to account for landing gear bogie effects on the main landing gear struts and multiple tandem tires, although the point contact model for each tire is retained.

Comprehensive instrumentation on the C-130 nose gear and one main gear allowed the generation of dynamic pressure/stroke curves. Pressure measurements above and below the orifices allowed calculation of effective damping values. When test results were compared to the theoretical isothermal pressure/stroke relation, pressures were found to be lower than expected for both nose and main struts even though the gears were repeatedly serviced correctly and were at their proper static extensions prior to starting taxi. Hysteresis in the load-stroke relation was observed and the nose gear strut bottomed repeatedly as indicated by both instrumentation and post test disassembly of the strut.

It was also found that on the accelerating or takeoff tests different pressure/stroke characteristics were produced than on the constant speed or decelerating tests. This behavior was observed on both the nose and the main gears. During takeoff the pressure/stroke relation also shifted to a new characteristic following repair encounter.

Figures 2 and 3 show these two types of behavior, with Figure 2 illustrating typical load-stroke characteristics during deceleration and Figure 3 illustrating typical behavior for accelerating and takeoff. This behavior is attributed to a portion of the strut inflation air going into solution in the hydraulic oil. Since the struts were checked for proper extension prior to starting taxi, air loss must be related to strut motion and flow through the damping orifice. Pressure rises following takeoff showed that the underinflation was not caused by leakage.

The hysteresis found during constant speed and deceleration tests is believed to be air going into and out of solution in response to the strut internal pressure variations. In the characteristics seen on takeoff, a pronounced shift in the pressure/stroke curve occurs. Vertical load reduces on the strut as aerodynamic lift builds up and rapid compression of the partially extended strut at repair encounter appears to cause a large portion of the dissolved air to come out of solution. Figure 3 shows that following repair encounter the strut is operating along its correct theoretical pressure/stroke curve. Some results from previous laboratory studies of air solubility in liquids were found. Reference 1 reports experiments with several oils under varying pressures and agitation which support the conclusion that a rapid decrease in dissolved air could cause the observed pressure variations during takeoff.

A fitted isothermal curve passing through the average of measured pressure/stroke relations was found to produce satisfactory load comparisons with test for constant speed and decelerating tests. To simulate acceleration and takeoff tests, a computer program to calculate isothermal curves consisting of several segments was developed. Results for typical computation are illustrated in Figure 4. The pressures and volumes shown with Figure 4 do not represent actual values which could be measured in the strut, but are the values necessary to define each of the fitted isothermal segments.

C-130 measured strut damping values were found to be significantly lower than those measured from drop tests or calculated from the theoretical damping equation for both main and nose gears. These differences are believed to be caused by hydraulic fluid foaming. Corrections to the damping coefficients were developed from measured data.

Similar pressure and stroke data are not available for the C-141B and C-5A; however, it is suspected that since the strut designs are similar in that there is no separation between the air and oil, some air is going into solution. Though the effect seems to be less pronounced on these aircraft, there was evidence of the C-141B nose gear strut bottoming at loads less than predicted during the HAVE BOUNCE testing.

Development of more exact simulations will require laboratory testing to define the conditions producing strut load/deflection hysteresis, underinflation and loss of damping.

#### c. Aircraft Structural Model

The allowable aircraft rigid body motions are vertical translation and pitch. Roll is allowed in the option which includes unsymmetric repair encounter.

Only wing flexibility is included in the C-130 analysis since the large diameter, short fuselage was considered to be essentially rigid in its response to ground roughness, and no evidence of fuselage flexibility affecting the response at critical locations was seen in the test data. The wing is represented as a beam model with 20 lumped masses, free to move in bending and torsion about an assumed elastic axis. Engines and external fuel tanks are treated as lumped masses. From this model and the associated bending and torsion stiffness, coupled bending and torsion orthogonal modes are calculated. The eight lowest frequency modes were selected to use in the time history calculations.

The C-141B and C-5A aircraft models use complete aircraft mode shapes including a flexible fuselage representation. In order to include a sufficient number of wing and pylon modes, a larger number of whole aircraft modes are required. Both the C-141B and C-5A simulations used 15 flexible modes.

#### d. Aerodynamic Model

Because of propellers on the C-130, aerodynamics at high power settings played a significant role in establishing nose gear loads. Figure 5 shows variations in nose gear loading on the stretched C-130 MK3 aircraft as a function of forward aircraft speed for two cycles of speed variations produced by thrust changes between takeoff power and full reverse. This figure illustrates the influence of thrust even at low speed.

Correct determination of the aerodynamic behavior of this aircraft on the ground proved to be a most difficult and challenging task. Difficulties arose because of a lack of aerodynamic coefficients for the thrust/speed combinations tested and poor definitions of ground effect. Most previous taxi testing over

(1-cosine) bumps was done at speeds below about 30 knots using constant throttle settings close to ground idle, and reasonable comparisons were possible without the necessity of including aerodynamics in the computer model.

To simulate landing and takeoff, it was necessary to derive appropriate aerodynamic coefficients from test measurements. A computer program was written which utilized time histories of measured gear loads, throttle setting, elevator position, brake pressure, strut positions, longitudinal acceleration, and wheel speed. From these quantities, along with known aircraft geometry and engine characteristics, external aerodynamic lift and pitching moments were calculated.

It was necessary to include propeller slipstream effects as well to obtain reasonable values for lift and pitching moment coefficients. It is assumed that positive propeller slipstream dynamic pressure adds directly to forward motion dynamic pressure for that portion of wing area between the tip of the inboard propeller and the tip of the outboard propeller. In reverse thrust, slipstream dynamic pressure is subtracted from forward motion dynamic pressure but is not allowed to result in a negative flow over the wing. It is also assumed that slipstream dynamic pressure can be added to forward motion but does not reduce net dynamic pressure below that due to forward motion at the horizontal tail and elevator.

A first order lag on throttle motion in the engine thrust calculation was included. An additional time delay was used to calculate elevator input and is proportional to the amount of time required for the aircraft to move a distance equal to that from the wing quarter chord to the horizontal tail quarter chord.

Wing damping following repair encounter in the 80 to 100 knot range for both landing rollout and takeoff simulations of the C-130 failed to achieve the desired level of accuracy. This underdamped response has been partially offset by increasing the structural mode damping as speed increases. Improvements can probably be achieved by adapting an aerodynamic representation similar to that now used in gust analysis.

### 3. ANALYSIS AND TEST CORRELATIONS

Before the start of testing, preliminary simulations were used to identify aircraft critical load components and to estimate the effects of speed on loads for all of the repair profiles tested. Nose gear vertical load during braking, wing bending with high fuel loads, plus engine pylon response for the fan jet powered transports were identified as the critical loading conditions. Testing verified that the component selections were correct.

Preliminary analysis showed that the C-130 has sufficient brake capacity to overload the nose gear during repairs if maximum brake pressure is used. Initial measurements verified the expected braking coefficients; therefore, remaining tests were conducted with light to medium braking.

#### a. C-130 Comparisons

Figure 6 (a), (b) and (c) shows an example comparison of the computer simulation with test results for the C-130 nose gear vertical load, front main gear vertical load, and wing station 357 bending moment for a 42-knot taxi speed. Good agreement was obtained as was the case for most constant speed tests. Those test conditions showing the largest variation contained transient pitch response following thrust changes just prior to the repair encounter.

Figure 7 illustrates the difficulties encountered when simulating decelerating tests. Nose gear vertical load accuracy was largely dependent upon obtaining the precise vertical load at the repair leading edge. To calculate this load as closely as possible, C-130 simulations were started well ahead of the repair, and included time history inputs of engine thrust, elevator motion, and braking drag.

#### b. C-141B Comparisons

No structural problems were encountered and all measured loads from C-141B tests were below design limits. The highest load responses with respect to design limit were nose gear vertical loads and outboard nacelle pylon accelerations. A total of eleven tests were compared on a time history basis. They were selected as high load cases, aircraft resonant conditions, or cases where poor peak loads correlations occurred.

The largest differences in simulation and measurement were for outboard pylon accelerations. Maximum accelerations occurred in a landing configuration with spoilers deployed. Vertical response frequency was around 3 Hz and lateral response was a complex oscillation with components at 1.8, 3, 13, and 15 Hz. Maximum vertical response occurred in the 80 to 110 knot range. High frequency lateral responses were also seen in this speed range, particularly when brakes and reverse thrust were applied.

Figure 8 (a) and (b) shows comparisons for a case where poor pylon acceleration agreement was obtained. Since there are some questions as to the reliability of accelerometer measurements as an accurate assessment of pylon loads, further attempts at a refined simulation were not made. A conservative factor was applied to the vertical acceleration simulation data when used to establish aircraft capability.

#### c. C-5A Comparisons

At this time, only low speed test data over (1-cosine) roughness is available for the C-5A aircraft. Correlations with this information have been excellent. Figure 9 (a), (b), and (c) show nose gear, front main gear, and rear main gear vertical loads over three 3-inch amplitude bumps at a 25-knot forward aircraft speed.



Figure 9 (d), (e), and (f) shows comparisons for outboard pylon lateral, vertical, and torsion moments, and agreement is considered to be excellent. At 25 knots, aerodynamic forces are negligible.

Since no C-5A data exists for taxi with braking or reverse thrust, and in light of the higher than expected C-141B pylon accelerations found at high speed, additional testing has been recommended. Particular emphasis is being placed upon verifying acceleration measurements by including strain gages to determine if frequencies measured with accelerometers are transmitted through the pylon structure.

#### 4. LESSONS LEARNED

"Project HAVE BOUNCE" test programs have shown that low speed testing previously used to validate the 0.5g center of gravity dynamic load factor criterion cannot be counted on to reveal all of the aircraft response characteristics associated with landing and takeoff from repaired bomb-damaged runways.

Among the findings are:

- o High speed tests of landing and takeoff configurations are advisable. Both thrust reversal and braking effects need to be tested for the landing configuration.
- o Thorough instrumentation is vital to interpretation of unexpected results and for establishing precise test conditions. Additional instrumentation would have been useful in the derivation of aerodynamic data for the C-130, and also in interpreting acceleration measurements on the C-141.
- o Conventional aerodynamic coefficients obtained from wind tunnel tests are inadequate for simulations in ground effect at low speeds and high power settings for the prop-powered C-130.

#### 5. RECOMMENDATIONS FOR MINIMIZING AIRCRAFT RESPONSE TO ROUGHNESS

Pilot actions can affect aircraft loads during operation over bomb damage repairs. For example, an aft control column can be used for nose gear load relief at speeds above approximately 40 knots on the C-130. Pilot actions can also adversely affect nose gear loads as in the case of sudden braking near repairs. This section summarizes general guidelines for minimizing loads while operating on repaired airfields.

##### a. Parking Area and Taxiway Operations

An aircraft speed limitation of 10 knots or less can usually be relied on to prevent loads from exceeding design limits on taxiways. Even so, sudden stops should not be made where the nose or main wheels might encounter a leading edge ramp while experiencing high combined vertical and drag loads or while the aircraft is pitching. Turning or pivoting of the aircraft should also be avoided where a gear could encounter repairs during the turn.

##### b. Takeoff

Takeoff roll should not be started immediately before a repair ramp because significant pitch motion is induced by engine run-up and brake release. If repairs cannot be avoided in this situation, positioning the nose gear at the level portion of the repair, or traversing the repair at a low throttle setting, is recommended. Elevator and power settings should be held steady to avoid pitch oscillations.

Using an aft control column position can sometimes reduce nose gear loads and is recommended if no adverse aircraft response occurs. Forward movement of the control column to delay aircraft rotation should be done smoothly to minimize pitch oscillation. Abrupt aircraft rotation at liftoff could momentarily cause high main gear vertical loads additive to those generated by repairs and should also be avoided.

##### c. Landing and Rollout

Landing impact should be made on a smooth surface to avoid spinup on a repair ramp and to avoid combining aircraft sink rate with the equivalent sink rate generated while passing over a repair. To minimize possible aircraft dynamic response and loads following impact, sink rate should be kept as low as possible.

The C-130 has sufficient brake capacity to cause excessive nose gear loads over some repair profiles if maximum braking is applied. Testing showed that limited braking of the proper levels can be achieved through practice.

In summary, the general recommended landing and rollout procedure is: Land with a low rate of sink in an area clear of repairs, and follow through by a smooth transition to reverse thrust. Move the control column to an aft position and apply braking at the minimum level necessary to stop the aircraft within the distance available.

##### d. Weight and Center of Gravity Effects

Since nose gear vertical load, wing bending moment, and pylon response have been determined to be the critical components, any aircraft cargo/fuel loading which can reduce these loads will be beneficial. Wing fuel should be minimized and loaded inboard consistent with flight restrictions. Nose gear loading will be reduced as the center of gravity is moved aft. In all cases aircraft weight should be minimized during operation from repaired runways.

#### e. Landing Gear Strut Servicing

There is a tendency for landing gear struts to become underinflated without any evidence of leakage on the C-130. A similar effect may be occurring on other aircraft having struts with air and oil in contact. Since the most likely time for this to occur is immediately after the strut has been opened to the atmosphere and filled with fresh unsaturated fluid, strut position should be carefully observed after the first few flights following any servicing. Overinflation for operation over repairs is less dangerous than underinflation. The primary adverse effect of a reasonable amount of overinflation would be a slight reduction in the maximum landing impact sink rate capability.

#### 6. CONCLUSIONS AND RECOMMENDATIONS

A large amount of test data has been gathered to establish behavior of transport aircraft operating over bomb damage repair patches.

It is concluded that:

a. Overall comparisons of simulations and test data are considered to be excellent with the exception of differences generated by variations in strut pressure/stroke relations, some differences in predicted pylon accelerations at high speeds, and variations due to poor definitions of aerodynamic inputs. The computer models now account for these differences by the use of appropriate test-derived factors.

Computer simulation programs for the C-130 and C-141B have been sufficiently validated to predict aircraft response over other repair configurations and spacings. Plans are being made to verify C-5A pylon response prior to release of the computer simulation model.

b. Tests revealed apparent air/oil mixing in the landing gear struts which caused underinflation and premature strut bottoming. Empirical landing gear strut characteristics and damping values have been established for the C-130.

c. Previous methods of accounting for aerodynamics during ground operations were found inadequate for the prop-jet-powered C-130. A revised aerodynamic model was developed which includes simulation of propeller slipstream effects during transition from forward to reverse engine thrust.

d. A limitation on maximum braking effort is required for the C-130 in order to remain within limit loads for the maximum amplitude repairs tested. Abrupt braking using any of these aircraft must be avoided in the vicinity of repair profiles because of the danger of traversing the repair with high nose strut and tire deflections.

Also the following recommendations are made:

o Pilots should receive training in correct procedures for minimizing loads when operating over repairs. Techniques for use of up elevator to reduce nose gear loads, practice for minimum braking on rollout, and smooth transitions into reverse thrust should be included.

o Future transport landing gear designs can achieve improved capability through the addition of separator pistons to eliminate mixing of air and hydraulic oil.

o Specifications for new aircraft designs which are expected to operate over repaired runways should address roughness encounter during braked roll for maximum capability.

#### REFERENCE

1. Schweitzer, P. H., and Szebehely, V. G., "Gas Evolution in Liquids and Cavitation," Journal of Applied Physics, Volume 21, December, 1950.

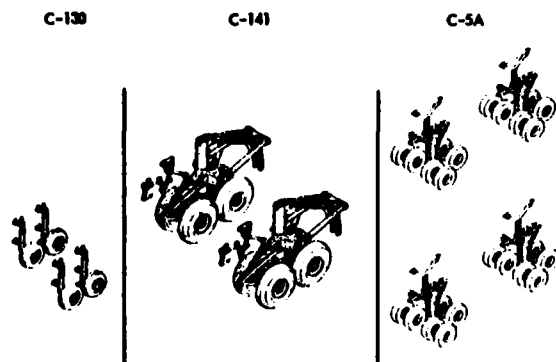


FIG. 1 LANDING GEAR STRUT AND TIRE ARRANGEMENTS FOR THE C-130, C-141, AND C-5A TRANSPORT AIRCRAFT MAIN GEARS

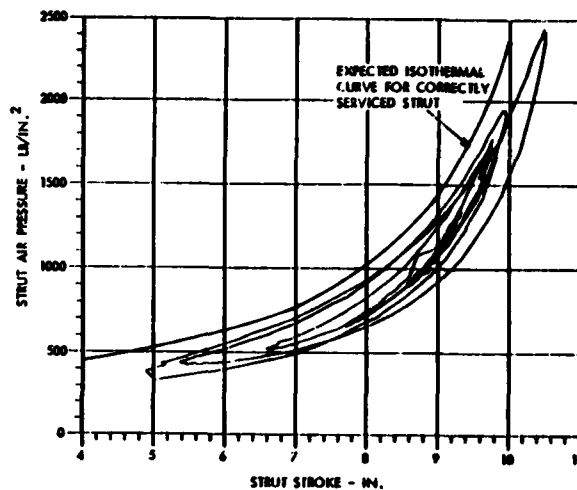


FIG. 2 TYPICAL C-130 NOSE GEAR PRESSURE/STROKE CURVE REPRESENTING CONSTANT SPEED TAXI OR DECELERATING TESTS

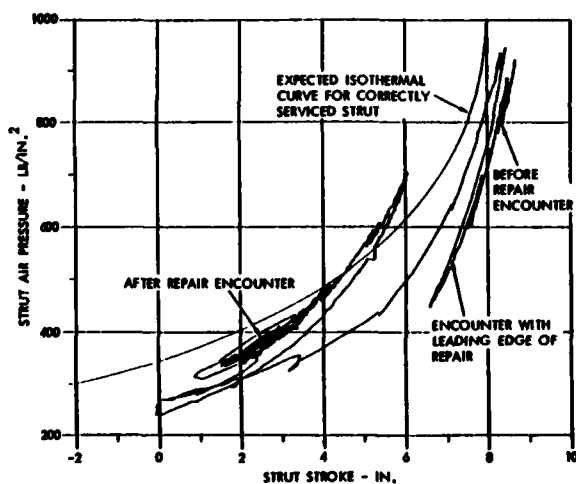


FIG. 3 TYPICAL C-130 NOSE GEAR PRESSURE/STROKE CURVE REPRESENTING TAKEOFF TESTS

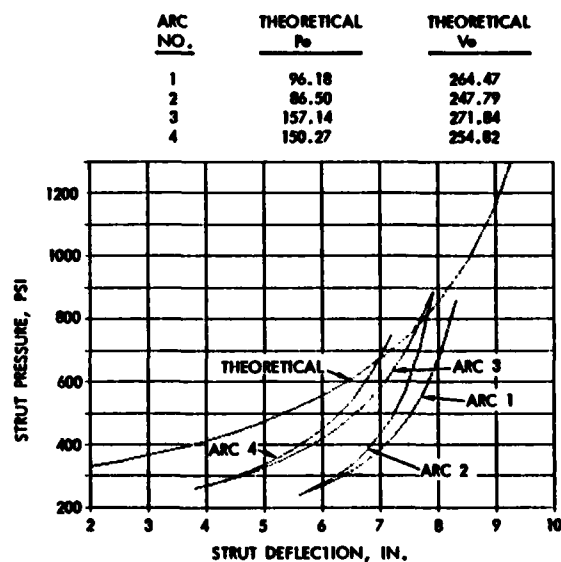


FIG. 4 CALCULATION OF SEGMENTED APPROXIMATIONS OF STRUT BEHAVIOR DURING TAKEOFF - C-130 MAIN GEAR

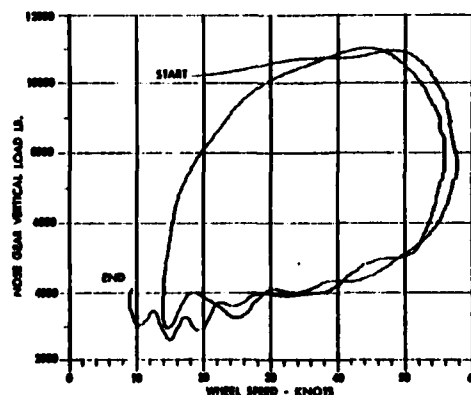
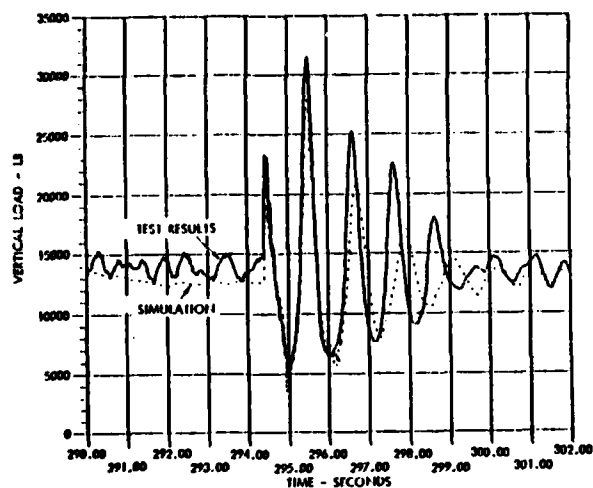
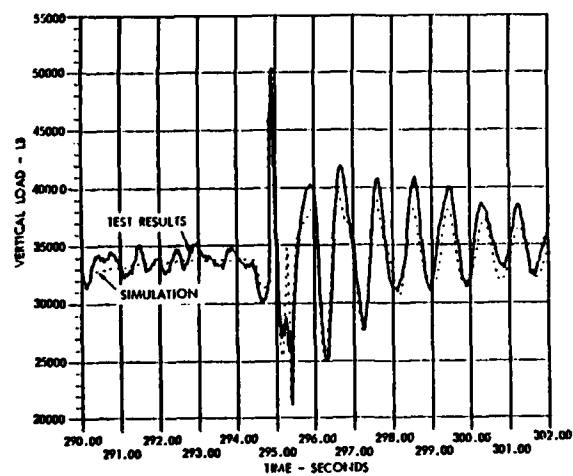


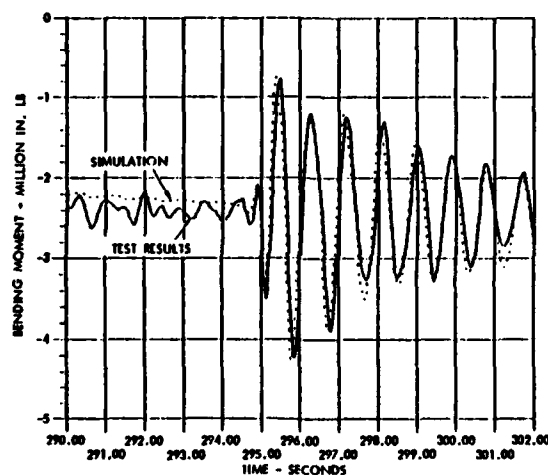
FIG. 5 NOSE GEAR VERTICAL LOAD VARIATIONS THROUGH 2 CYCLES OF ENGINE THRUST CHANGE - C-130 STRETCH MK3 AIRCRAFT



(a) NOSE GEAR VERTICAL LOAD



(b) FRONT MAIN GEAR VERTICAL LOAD



(c) WING STATION 357 BENDING MOMENT

FIG. 6 COMPARISONS OF C-130 COMPUTER SIMULATIONS  
AND TEST RESULTS - CONSTANT SPEED TAXI

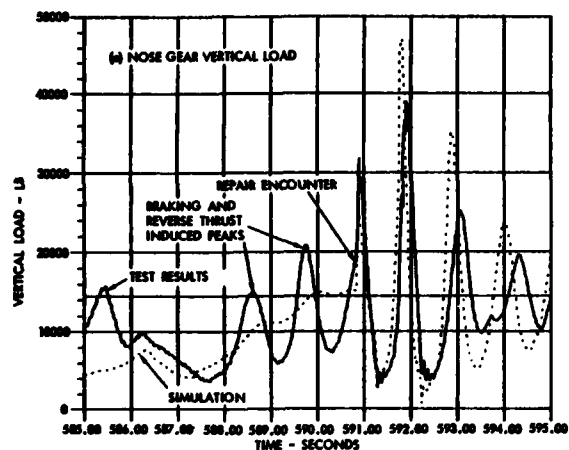
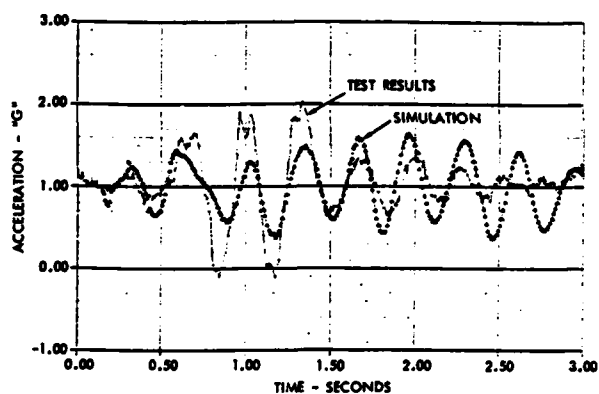
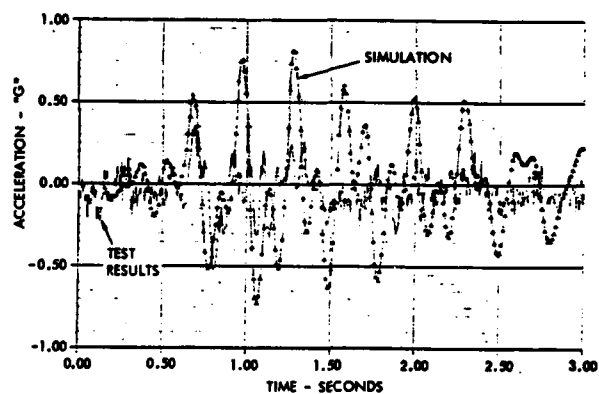


FIG. 7 COMPARISON OF C-130 NOSE GEAR VERTICAL LOAD COMPUTER SIMULATION AND TEST RESULTS - REVERSE THRUST AND BRAKING

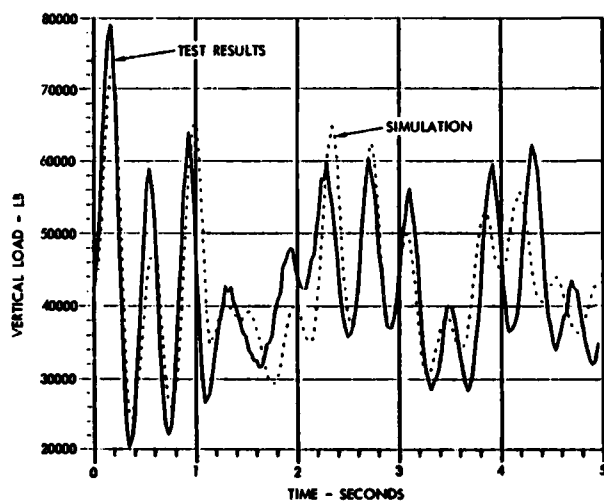


(a) PYLON VERTICAL ACCELERATION

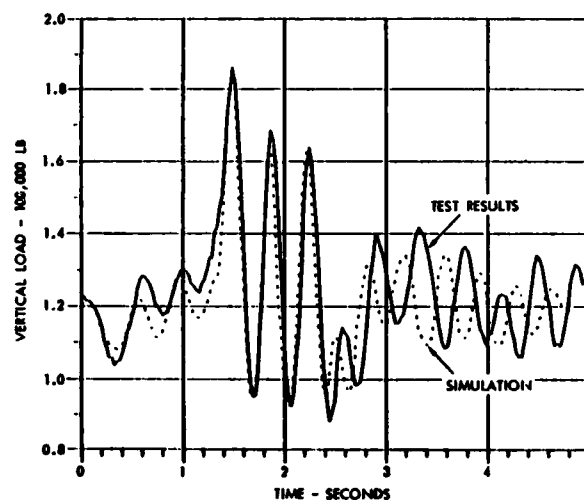


(b) PYLON LATERAL ACCELERATION

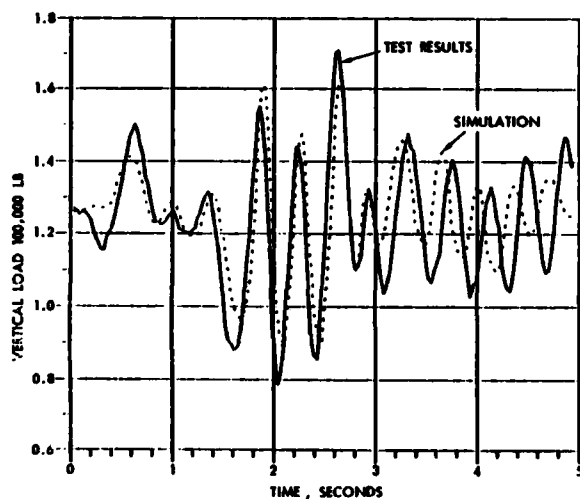
FIG. 8 C-141B OUTBOARD ENGINE PYLON ACCELERATIONS



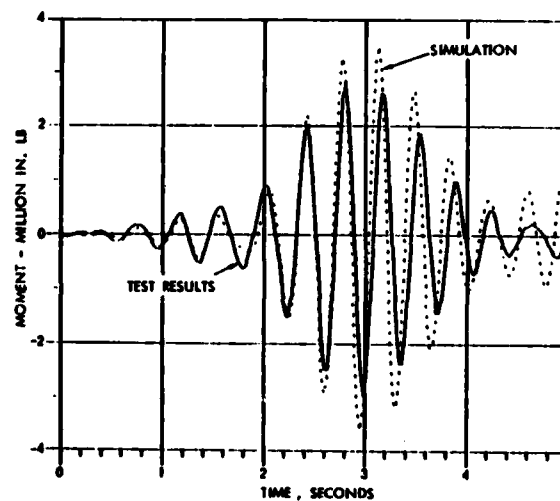
(a) NOSE GEAR VERTICAL LOAD



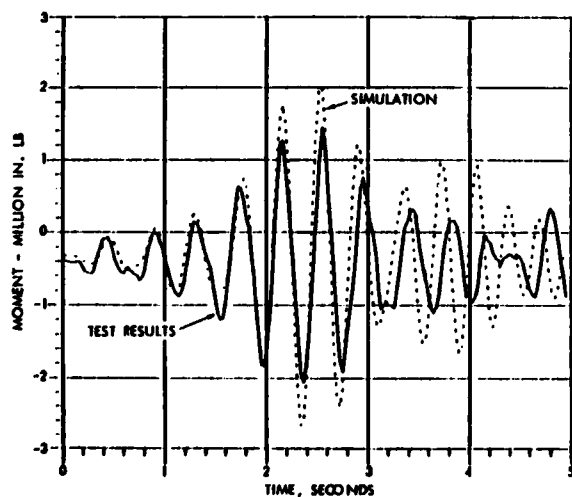
(b) FRONT MAIN GEAR VERTICAL LOAD



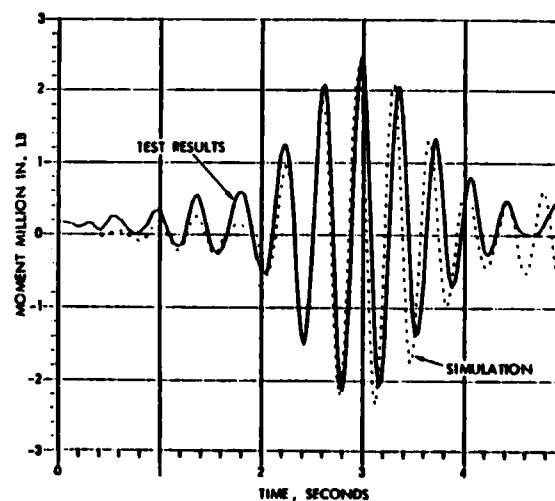
(c) AFT MAIN GEAR VERTICAL LOAD



(d) OUTBOARD PYLON LATERAL MOMENT



(e) OUTBOARD PYLON VERTICAL MOMENT



(f) OUTBOARD PYLON TORSION MOMENT

FIG. 9 COMPARISONS OF C-5A COMPUTER SIMULATIONS AND TEST RESULTS OVER THREE (1 - COSINE) BUMPS AT 25 KNOTS

## A FIGHTER LANDING GEAR FOR THE 1980's

R. F. BUTTLES  
MANAGER, F/A-18L SYSTEMS DESIGN

R. D. RENSHAW  
SR. TECH. SPECIALIST, F/A-18L LANDING GEAR

SUMMARY

Airfields, particularly forward airstrips, are envisioned to receive early aggressor strikes causing damaged runways whose rapid repair results in rough fields with restricted takeoff and landing distances and taxi areas of the soft field category.

This paper presents a discussion of design considerations for a landing gear incorporating soft field, damage/repared runway, and increased sink speed capabilities over that of current USAF design in a present day fighter/attack aircraft. The establishment of the design criteria and constraints are discussed, and the resulting configuration is defined as applied to the Northrop F/A-18L aircraft. Shock strut weight and stroke comparisons are shown of various fighter landing gears to illustrate trends and philosophy differences between land based and carrier based aircraft. The effects of oil loads, air loads, and friction are discussed as design parameter considerations. Shock strut internal geometry philosophy is discussed. The resulting reduced loads transmitted to the aircraft are illustrated in various figures concluding the text.

I. INTRODUCTION - DESIGN PHILOSOPHY AND BACKGROUND

Landing gear for military fighter-bomber type aircraft is undergoing a design philosophy and criteria evolution. Present aggressor action scenarios indicate that airfields will be primary first attack targets and that considerable taxi/runway cratering may be experienced. The results of this kind of aggressor action is an airfield that would be classified as semi-prepared, or rough field, as opposed to the undamaged prepared type (hard surfaced) airfield. Land based military fighter aircraft designed prior to 1978 were considered to operate from prepared surfaces as defined in U.S. Government Military Specification MIL-A-8862 Airplane Strength and Rigidity Landplane Landing and Ground Handling Loads or MIL-A-8863 Airplane Strength and Rigidity Ground Loads for Navy Procured Airplanes.

The U.S. Air Force has been conducting hasty repair type runway tests to determine the effects of filled and/or matted runways on landing gear loads. The tests included evaluating shock struts with longer strokes from static to compressed lengths and modified oleo air pressures.

In the 1960's, extensive testing and evaluation was conducted on the OV-1 Mohawk and OV-10A Bronco airplanes to determine landing gear loads and response during landing and taxi over rough runways. The rough field design and capability of the C-5A was thoroughly investigated and proven in the mid 1960's. More recently, British Aerospace mounted a rough field program for the Jaguar with considerable success.

The Northrop Corporation is currently engaged in marketing a multi-role land based fighter, the F/A-18L, designed to operate in the above noted environment. This paper documents Northrop's approach to the design challenges encountered which involved studying several design configurations to arrive at the solution chosen for the F/A-18L. Consideration was given to operational requirements, weight, cost, reliability, and integration with the airframe. Single bump criteria from the existing USN MIL-A-8863 semi-prepared field capability, additional damage/repared runway profiles, and limited STOL capability were used in the design. This chosen approach involves compromises between extremes of field roughness and soil softness to achieve reasonable weight and simplicity (enhanced reliability) in the gear design. These compromises were evaluated and prioritized in order to track their effects across the landing and taxiing spectrums.

A look at current USAF and USN landing gears reveal significant differences as could well be expected when the operating environment is taken into account. Typical land based aircraft successfully use a 10 foot per second sink speed at landplane landing design weights whereas carrier based aircraft require up to 24 feet per second to operate successfully in a carrier type landing which includes a rolling and pitching deck. Also, differences in ground handling are apparent when the Navy launching and arresting conditions are added.

The imposition of the very stringent USN requirement for carrier operations is very clearly shown in comparison of landing gear weights as a percent of the airframe weight, shown in Figure 1; of shock strut stroke, shown in Figure 2; and of tire pressures shown in Figure 3; for several USN and USAF airplane types. It can be seen that without exception the carrier suitable gears are heavier than the land based designs as a result of the more stringent design requirements. The USAF and USN F-4 aircraft use the same shock strut stroke and operating characteristics but the USAF F-4 tire construction has

been altered from that of the USN aircraft thus permitting the different tire pressures indicated in Figure 3. Using the same approach, the F/A-18A tire pressures could also be reduced for land based use. It is well known that landing gears designed to the USN carrier based aircraft criteria impose cost, weight, complexity, and stiffness requirements detrimental to an optimized land based aircraft.

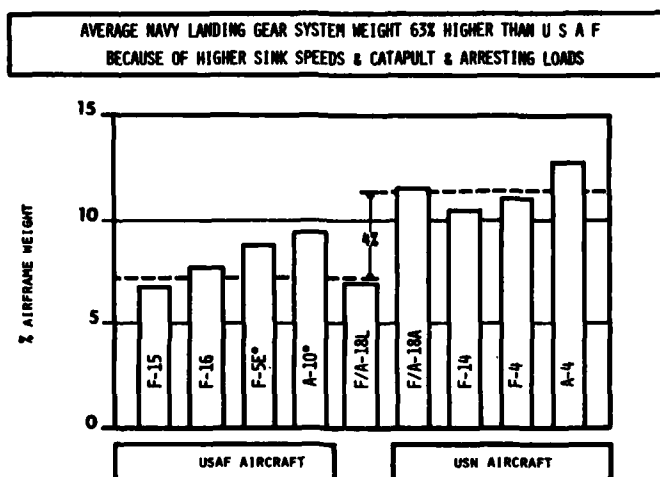


FIGURE 1. COMPARISON OF LANDING GEAR SYSTEM TO AIRFRAME WEIGHT

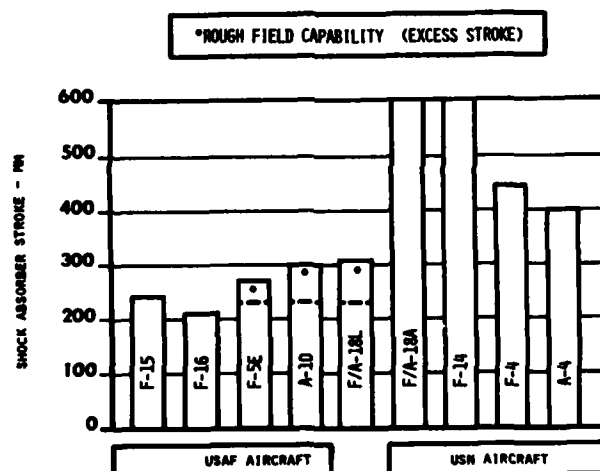


FIGURE 2. MAIN GEAR SHOCK ABSORBER COMPARISON

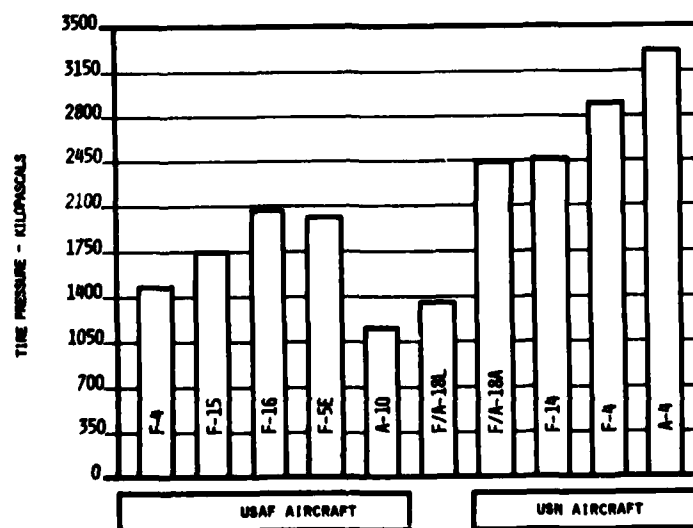


FIGURE 3. MAIN GEAR TIRE PRESSURE COMPARISON



## II. APPROACH AND DESIGN CONSIDERATIONS

Starting with a design to current USAF criteria, the first step taken at Northrop to cater for damage/repai red runways was to lengthen the stroke of the shock struts from 250mm to 330mm. We then increased the stroke remaining between static and compressed positions and modified the trapped air volume to reshape the air curve for taxi stability and static servicing of the strut. The effect of the changes on the air curve (load stroke) is depicted in Figure 4.

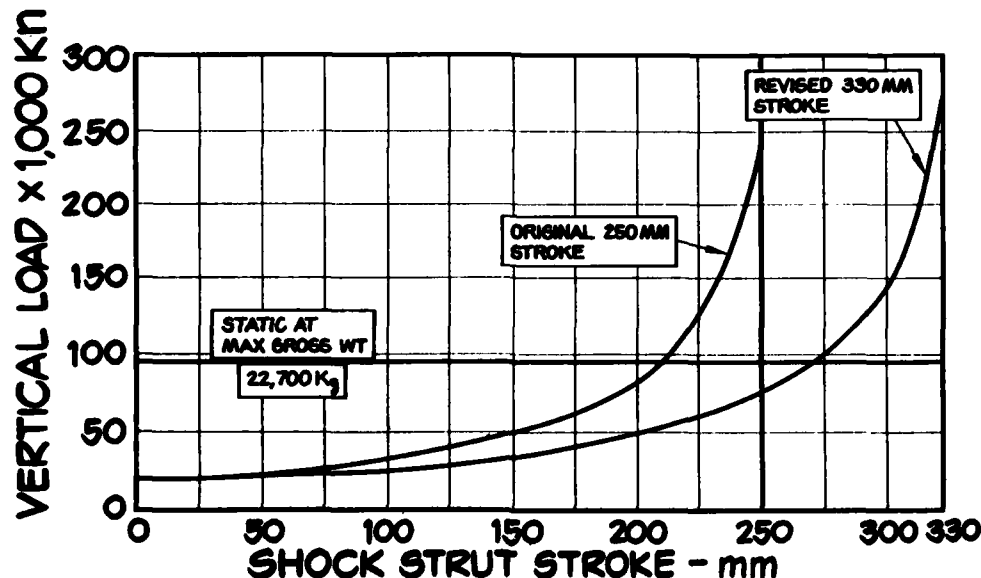


FIGURE 4. EFFECT OF INCREASED STROKE

Reviews of the USN and USAF specs - MIL-A-8863 and MIL-A-8862 show little difference in design requirements for their land-based operations. The areas of major difference being sink speeds (3.3M/sec USAF versus 7.2M/sec Navy), rough field criteria, and the Navy use of limit loads in their landing cases. During the preliminary design phases of the F/A-18L, because of the high inherent external load carrying capability, it became apparent that taxi, towing, and jacking loads and not landing loads would design the gear if the sink speed was limited to the current USAF 3.3M/sec at the design landing weight. Increasing the length of the shock struts for enhanced rough field operations increased the imbalance between landing and ground handling loads. It was decided to make use of the excess landing load capability now inherent in the design. Investigation into the maximum attainable sink speed that could be achieved on the F/A-18L without exceeding the airframe design load criteria of 2.25 G for the main gear and 3.0 G for the nose gear resulted in a design limit sink speed of 4.3M/sec. Indicating that a very adequate landing gear can be designed for an airplane with a limited STOL (increased glide slope) performance inside the existing MIL-A-8862 and MIL-8863 envelopes.

During a conventional land-based landing, the pilot will invariably perform a flare-out at the end of the normal glide slope approach and ease the airplane into a gentle touchdown. This kind of landing technique, reduces predictability of touchdown point and might be unacceptable on a damaged runway. With this approach path, the F/A-18L would use approximately 415 meters after passing over a 15 meter obstacle and before touching down. Substantial improvements can be made using approach paths with steeper glide slope angles, minimal flare or no-flare touchdowns, and approach end arrestor cable engagements with less than 305 meters of roll distance.

Figure 5 shows the variation in touchdown distance with approach angle and terminal sink speed for the Northrop F/A-18L.

It can be seen that considerable improvement in short field performances can be made by allowing the maximum limit sink speed to increase to 4.3M/sec and using a higher glide slope angle than the usual 2° to 3° for present fighter aircraft. Studies of the proposed landing gear configuration for the F/A-18L show minimal impact on the landing gear design by increasing the sink up to the 4.3M/sec condition.

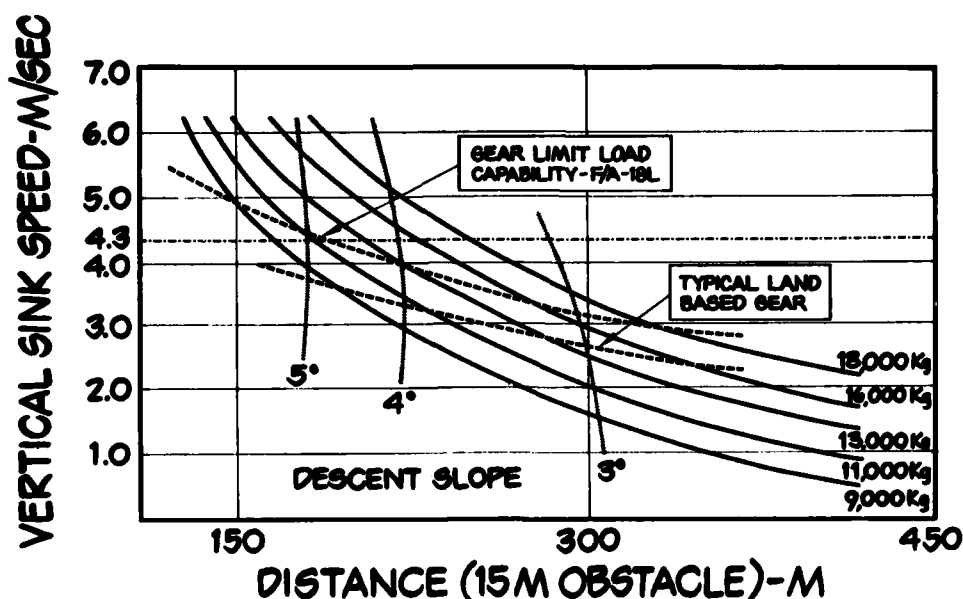


FIGURE 5. TOUCHDOWN DISTANCES VERSUS SINK SPEED

The requirement that the airplane be capable of operating off semi-prepared airstrips was of primary importance in the design of the F/A-18L landing gear. Some years earlier, Northrop designed the F-5A/B airplane with a limited degree of rough/soft field capability. This experience was enlarged upon in the A-9 (USAF close support aircraft prototype) design, and criteria and design preferences were established.

Northrop Corporation uses an analytical model for determining airplane dynamic responses during landing and taxi conditions. It is a combination of the usual linear system airframe model coupled with nonlinear models representing the nose and main landing gears.

The methods are general and may be used to calculate dynamic landing responses for specified initial conditions. These conditions are sink speed and initial airplane attitude corresponding to a specified approach speed and weight. The airplane landings may be either three point or symmetrical two wheel landing with subsequent nose gear touchdown. In addition to landing, taxi over a specified rough field or bumps and dips are included in the equations of motion.

Twenty-four modes (rigid and elastic), described by up to one hundred forty-four control point motions, may be included in the dynamical model. The coefficient of friction may be constant or a function of slip ratio.

The nonlinear forces considered are orifice damping, air spring, strut friction, tire spring, tire damping, ground tire friction, and forces due to the variable length of the strut produced in the landing process.

Studies of the main landing gear configuration determined that the simplest and lightest approach is a cantilever gear design with a double-skew-axis trunnion. There is a school of thought that a levered suspension gear has significant advantages over a cantilever gear for semi-prepared field operation. To investigate this, a study was made of the operating characteristics of the simple cantilevered design and more complex levered suspension designs. Three characteristics of the lever suspension gear surfaced in this investigation.

1. In lever suspensions, the shock strut friction is minimal and is not affected by the horizontal force created by traversing a bump.
2. In a full lever suspension, gear bending loads are not induced in the piston. However, it was found that strut friction is not important, provided strut bending loads do not cause excessive deformation of the piston.
3. Levers at a significant angle to the horizontal have an advantage when traversing very short wavelength and step bumps due to the rearward movement of the tire. Over longer wavelengths, the advantage is minimal. This effect is illustrated in Figure 6.

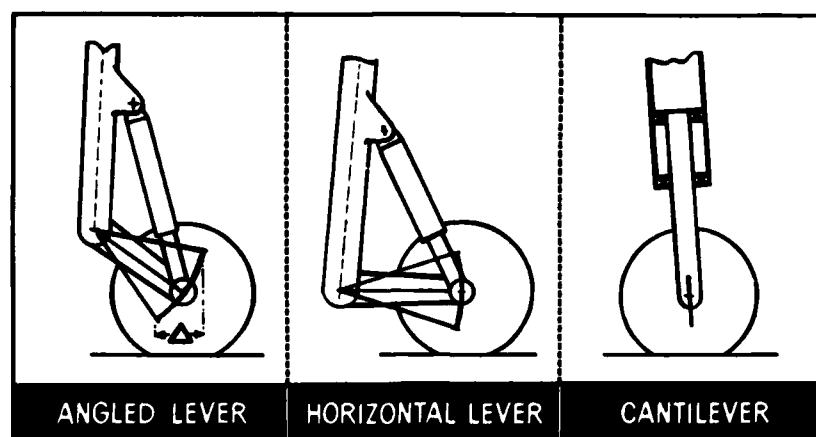


FIGURE 6. AXLE MOTION OVER SHORT BUMPS

The major conclusion of the investigation was that a simple, well designed landing gear with a cantilevered shock strut (at less weight, lower cost, and considerably less complexity) would provide comparable capability to that of a levered gear. Confidence in the structural integrity of landing gears designed to the land based requirements of MIL-A-8862 or MIL-A-8863, coupled with the extremely low hard landing incident rate, contributed to Northrop's choice of a simple, single stage cantilever shock strut. This shock strut has the capability to absorb landing energies of 4.3 meters per second sink speeds at land plane landing design weights giving a reasonable solution for obtaining shorter landing distances over obstacles yet still permitting good semi-prepared field damping efficiencies. The configuration of the main gear is shown in Figure 7.

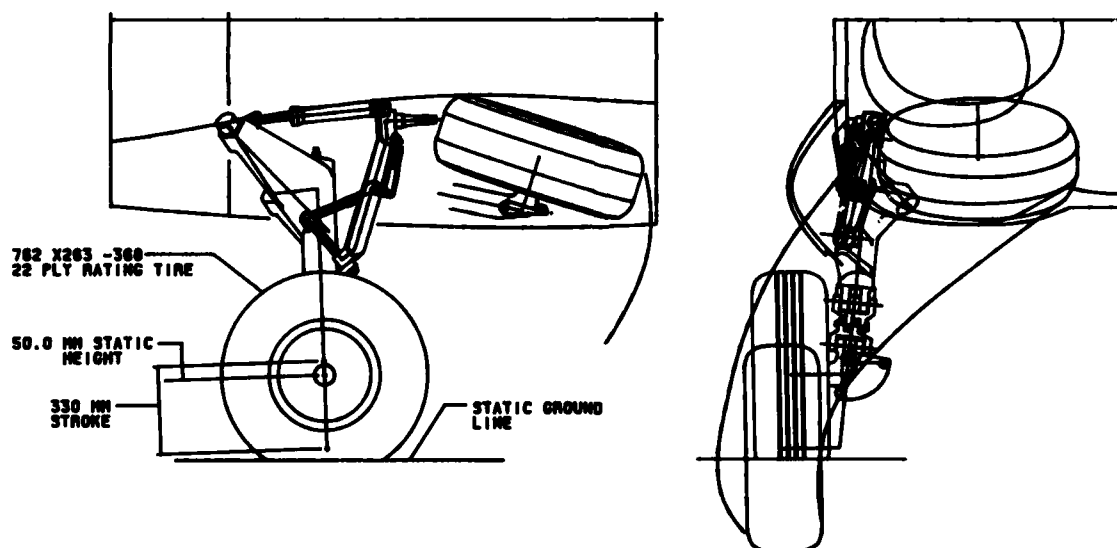


FIGURE 7. MAIN LANDING GEAR CONFIGURATION

A cantilever shock strut was also chosen for the nose gear, based on the above investigation and the desire to keep the design as simple as possible and close to the known F-5/YF-17 configurations and retraction/extension characteristics.

### III. CONFIGURATION AND CHARACTERISTICS

The load input into the airplane structure during the crossing of bumps comes from a combination of strut oil load, air load, and strut friction.

Northrop has undertaken studies of methods that could be used to contain the above loads within the overall design limitations of the airplane.

(a) Oil loads. Two methods of controlling the oil loads were considered:

1. Overload relief valve. The purpose of the overload relief valve integral with the metering pin, as depicted in Figure 8, is to open during

traversing the bump allowing the shock strut to increase its stroke rate while maintaining a high load within the strength envelope of the gear.

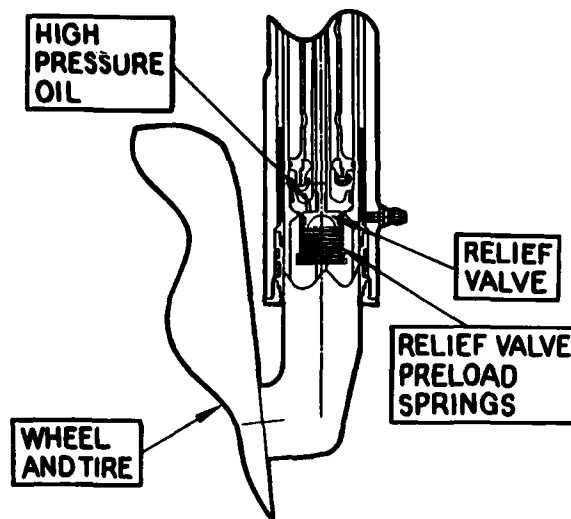


FIGURE 8. OVERLOAD RELIEF VALVE

2. Tailored metering pin. The tailored metering pin, as depicted in Figure 9, takes advantage of the excess stroke in the shock strut over that required to meet the landing energy requirements.

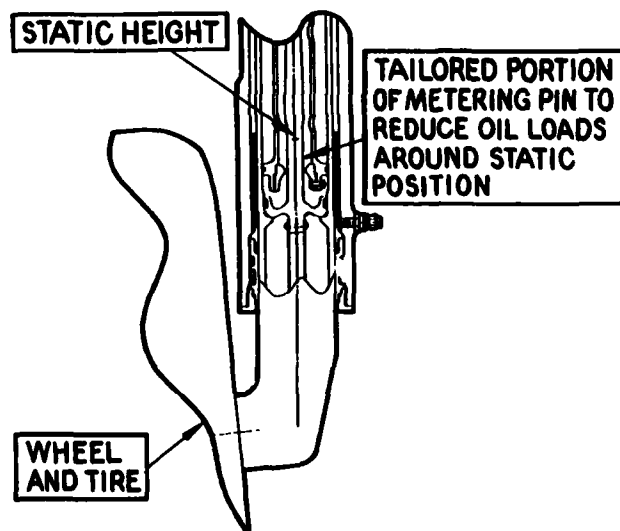


FIGURE 9. TAILORED METERING PIN CONCEPT

By tailoring the metering pin shape to reduce the oil loads in the taxi area, when taxiing over bumps beyond the tire capability, oil loads can be significantly lowered, thus permitting the gear to follow the air curve more closely. More than thirty differing metering pin shapes have been evaluated in the analytical models to arrive at a design that permits the 4.3 M/sec sink speed and the bump capability desired. Varying the metering and rebound snubbing between main and nose gears also controls the pitch and heave tendencies of the airplane. Figure 10 illustrates the magnitude of the oil load for a typical MIL-A-8863 1-cosine bump.

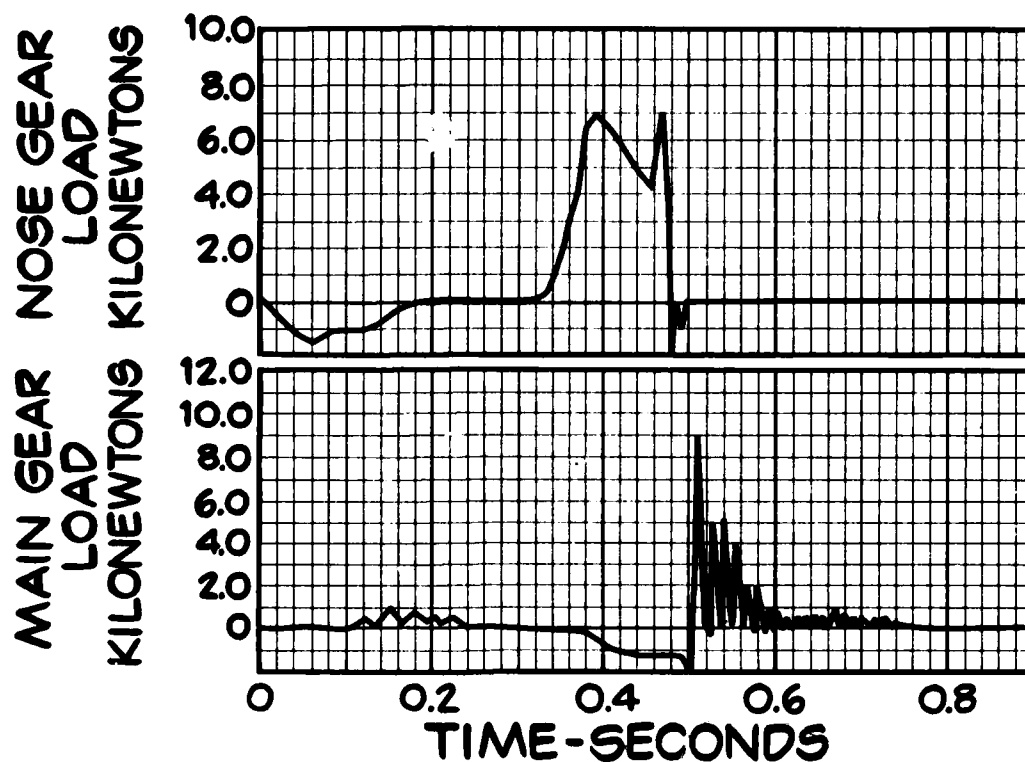


FIGURE 10. OIL METERING LOADS FOR A 234mm BUMP HEIGHT @ 76M/SEC

The simplicity and versatility of the tailored metering pin was sufficient for Northrop to decide to use that approach.

- (b) Air loads. The major load input to the airplane structure during the crossing of a bump is from the airspring. Consequently, the shape of the air spring is of critical importance.

Figure 11 shows a comparison of the aircurves for a single stage and a dual stage strut for the main gear.

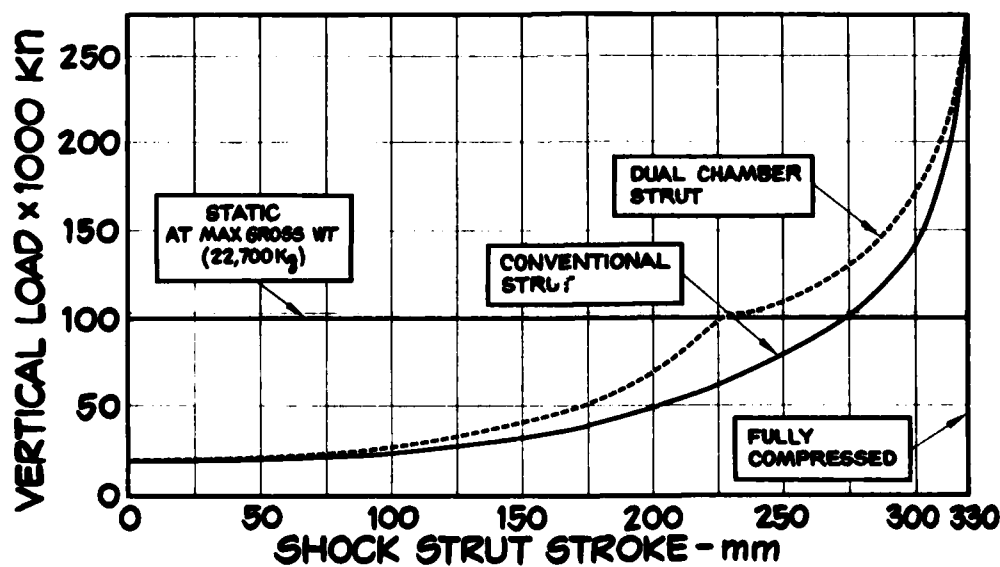


FIGURE 11. AIR SPRING COMPARISON

Figure 12 shows the single stage shock strut configuration, and Figure 13 shows a modification to a dual chamber, multistage configuration. Analysis of the airplane behavior when traversing single and multiple 1-cosine bumps showed that the loads could be contained inside the design envelope using the single stage configuration. However, in the event that a dual chamber configuration would be required, the proposed design can be easily modified. Figure 14 illustrates the magnitude of the air spring load for a typical MIL-A-8863 1-cosine bump.

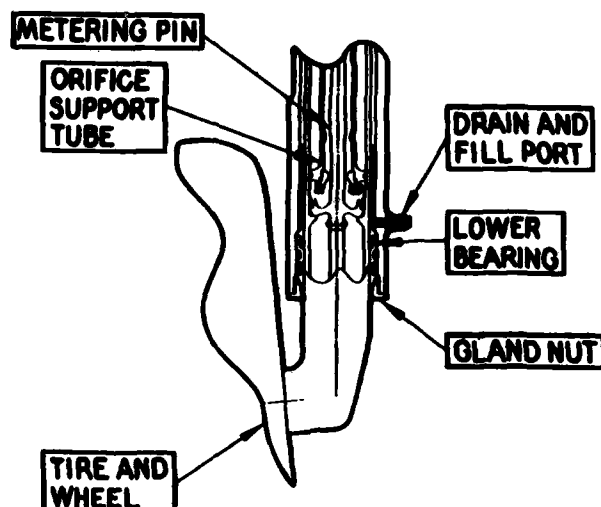


FIGURE 12. SINGLE STAGE SHOCK STRUT

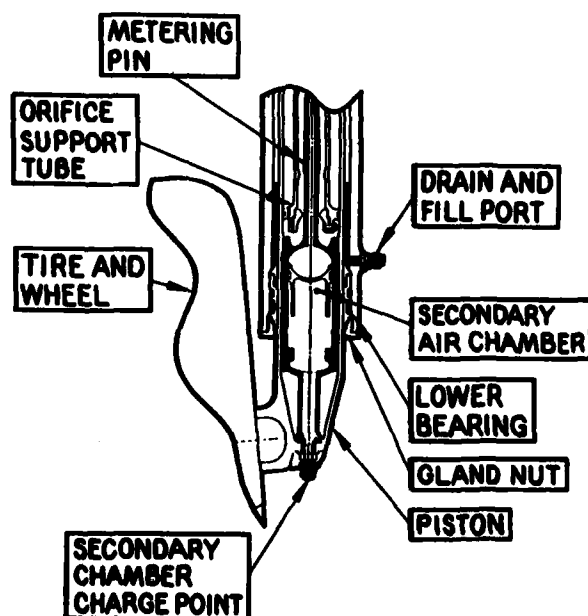


FIGURE 13. DUAL CHAMBER, SHOCK STRUT

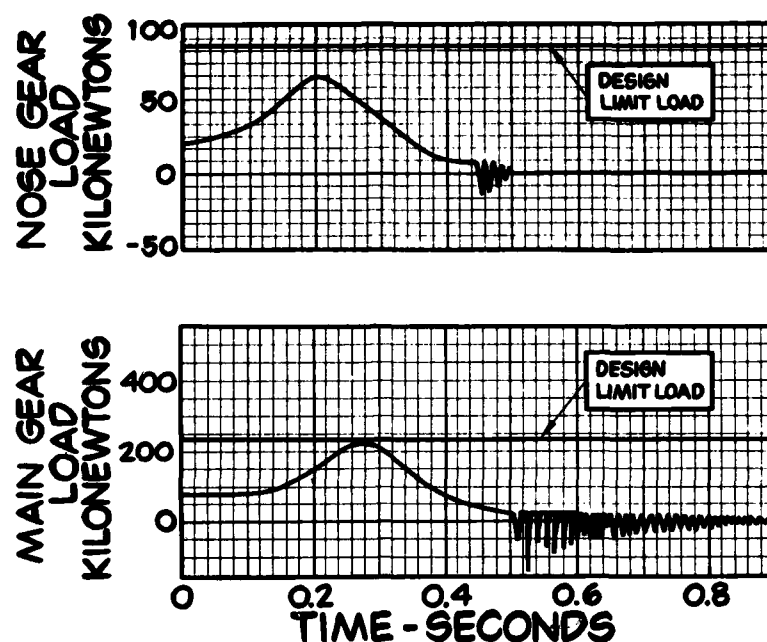


FIGURE 14. AIR SPRING LOAD FOR A 234mm BUMP HEIGHT @ 76M/SEC

In addition, to the oil and air load considerations, the strut bearings and wheel/tire sizes must be given proper attention.

- (c) Bearing overlap and material. The design of the shock strut bearings for the F/A-18L landing gear incorporate large bearing overlaps and use of low friction material liners. The resulting low internal friction loads caused by reaction to drag and side loads permit unhindered strut operation. Figure 15 shows the internal strut friction loads for a typical MIL-A-8863 1-cosine bump.

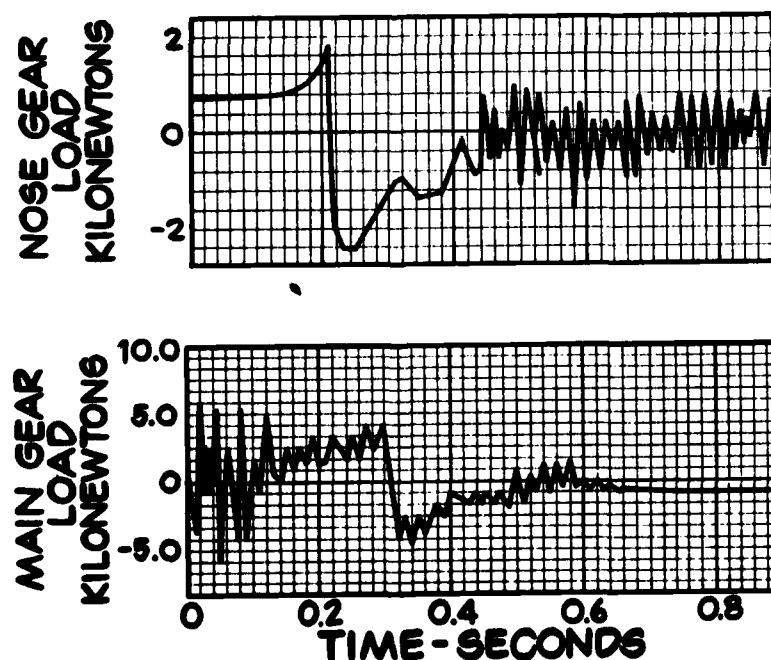


FIGURE 15. STRUT FRICTION LOADS FOR A 234mm BUMP HEIGHT @ 76M/SEC

From early configuration studies, it became evident that a major decision in configuring an airplane for semi-prepared field operation is -- how many and what size tires?

MIL-A-8863 requires that the airplane be capable of absorbing a 53mm step bump. The airplane crosses this type of roughness so fast that the upsprung mass does not have time to react. Either the tire has to "swallow" the bump or it will bottom out, ruining the tire. To aid in crossing the longer wavelength bumps, tire stiffness should be kept as low as possible, i.e., one deep section tire as opposed to two shallower section tires. Thus, for a given load more bump height can be "swallowed" by the single tire/shock strut combination than by the dual tire/shock strut combination. The choice of the tire size also greatly affects the soft field (flotation) characteristics of the airplane and the choice is the result of a balance between the soft and rough field requirements.

To permit a balance between both the rough and soft field operations for the F/A-18L, analytical studies were conducted to determine appropriate tire and wheel sizes.

This resulted in a 508 x 165-203 nose wheel and tire and a 762 x 267-368 main gear wheel and tire. Adequate brake space is allowed by the choice of a 368mm rim on the main gear wheel.

The flotation characteristics of this running gear combination are shown in Figure 16. The nose wheel is not critical for flotation in any aircraft configuration including maximum gross weight.

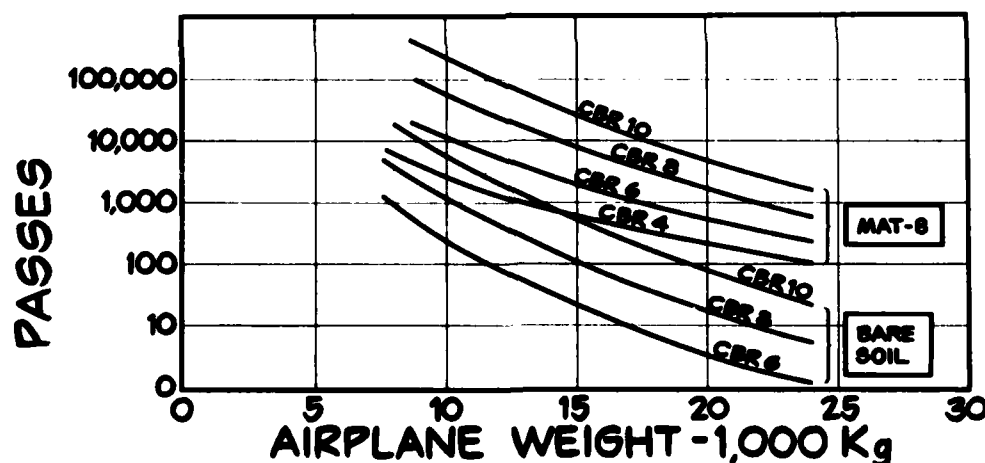


FIGURE 16. FLOTATION CHARACTERISTICS

To achieve the flotation characteristics as in Figure 16, the tires are designed to operate at 35% sidewall deflection. Most current fighter aircraft tires are designed to operate at 32% sidewall deflection, with the exception of the F-16 tire. By designing to 35% deflection, the tire becomes capable of limited operations at sidewall deflections up to 45%. This results in a 55% increase in runway pass capability on soft ground. For example, an 18,000 kilogram airplane on soil rated at CBR 10 would have a pass capability of 280 at 45% sidewall deflection in place of 180 passes at 35% deflection.

To further enhance the ground operating characteristics of the aircraft, the landing gear geometry provides a turnover angle best suited to semi-prepared airfield operations. Studies show that high turnover angles give increased adverse braking stability because the wheel track width is narrow, however, this has the effect of decreasing taxi roll stability. Low turnover angles give increased roll stability; but at the same time, decreases adverse braking stability. USN aircraft require low turnover angles because of operating on carriers subject to pitching and rolling. Since carrier landings are arrested landings, braking stability is less important than rolling stability. USAF aircraft, on the other hand, operate from fixed bases where long landing rolls and long taxi runs dictate higher turnover angles to emphasize braking stability at the expense



of rolling stability. The turnover angle of the F/A-18L was established at  $56^\circ$  as a balance between roll stability and braking stability. Figure 17 shows comparative turnover angles for current aircraft.

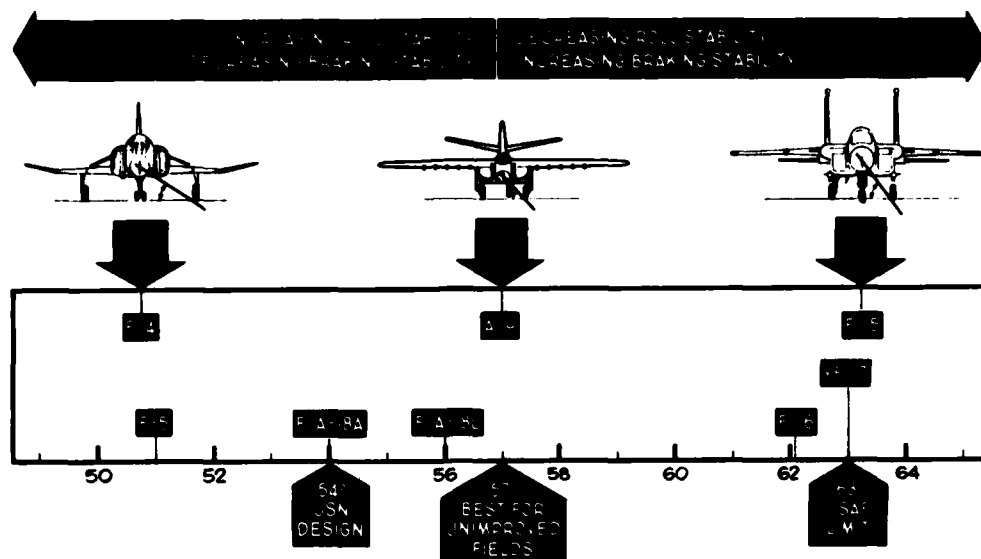


FIGURE 17. TURNOVER ANGLE ASSESSMENT

The F/A-18L is provided with a paired wheel fully modulated anti-skid braking system for use with normal braking and will provide stable braking for most runway conditions. A low speed dropout deactivates anti-skid braking for velocities below 25 knots.

Roll stability on semi-prepared airfields is obtained through the selection of the moderately low turnover angle and by tailoring the lower portion of the main gear shock strut air curve. This results in a natural roll stability without having to resort to dual chamber shock struts.

#### IV. CONCLUSION

In conclusion, we have a landing gear design with extended stroke and tailored metering pin which keeps the vertical loads below the gear and aircraft structure design limits when traversing 1-cosine bumps that would have been catastrophic with the conventional design criteria. The improvement in bump capability is shown in Figure 18.

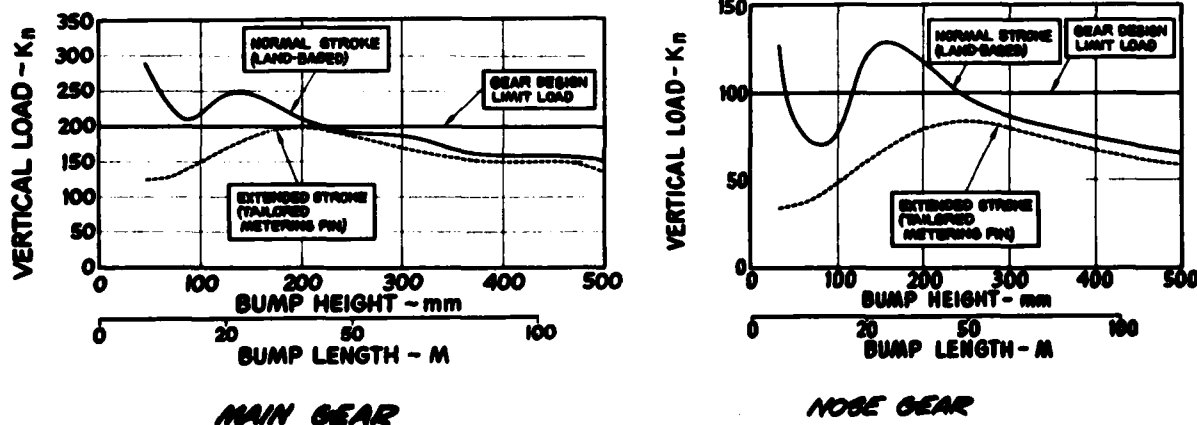


FIGURE 18. VERTICAL LOAD VERSUS BUMP HEIGHT

Improvements in pitching acceleration and wing torsional moments are depicted in Figures 19 and 20.

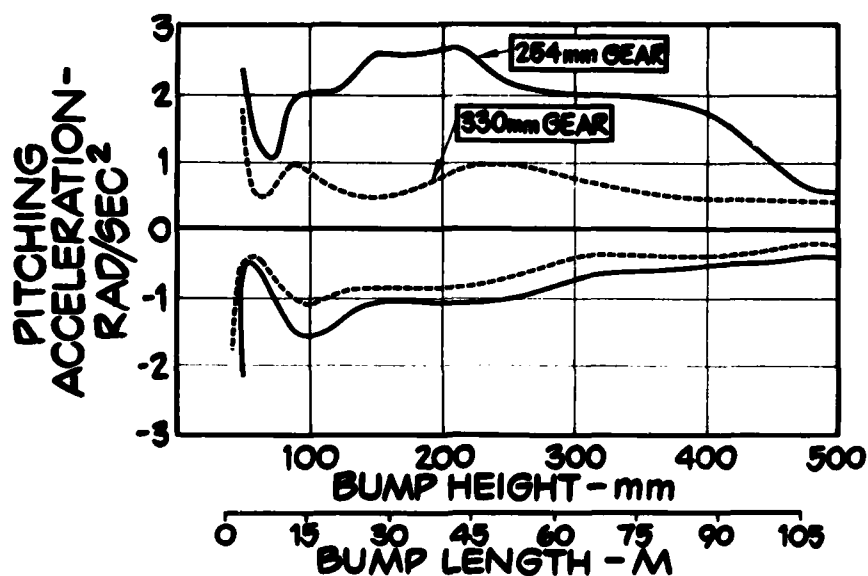


FIGURE 19. PITCHING ACCELERATION OF 23,500 KG AIRPLANE AT 76M/SEC

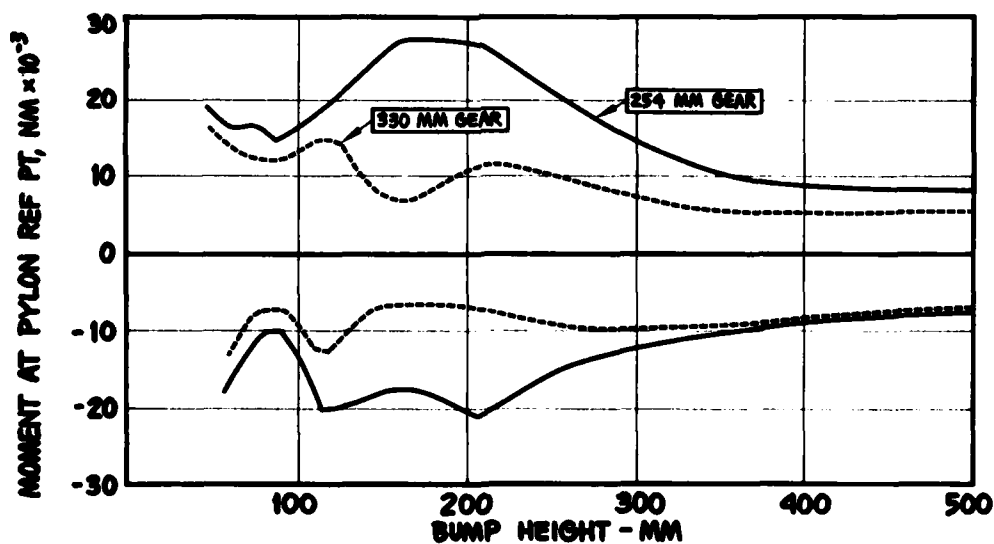


FIGURE 20. WING TORSIONAL MOMENTS FROM PYLON MOUNTED 2310 LITER FUEL TANK

In addition to 1-cosine bump capability, the landing gear design was checked against computer-simulated runway profiles to confirm adequacy of the design as shown in Figure 21.

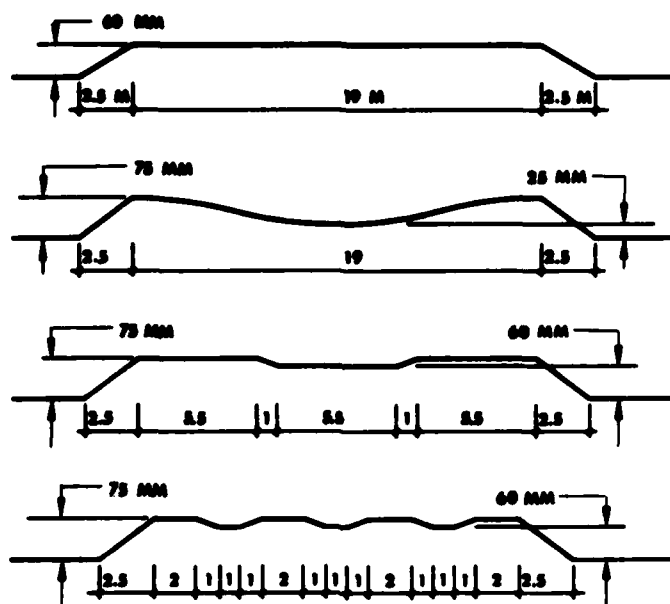
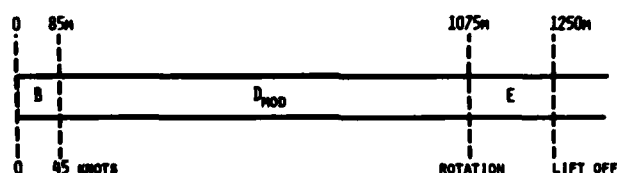


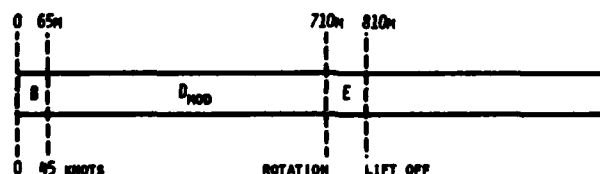
FIGURE 21. REPRESENTATIVE RUNWAY PROFILES

As a result of the analytical survey, the damage/repared runway category of repair for a 20,000 KG F/A-18L aircraft is estimated to be as shown in Figure 22 with degree of roughness B, Dmod, and E defined as follows:

	B	Dmod	E
MAXIMUM UPHEAVAL	38MM	76MM	76MM
MAXIMUM SAG	0	50MM	76MM
MAXIMUM LENGTH OF CRATER	Any	Any	Any
MAXIMUM LENGTH OF MAT	23.5M	23.5M	Any
CHANGE IN SLOPE	3%	3%	3%
MINIMUM SPACING OF REPAIR	30M	Any	Any



### MILITARY POWER TAKEOFF



### MAXIMUM POWER TAKEOFF

FIGURE 22. RUNWAY CATEGORY OF REPAIR

By combining the results of the various studies, a landing gear has been designed that will meet a logical balance of rough field and soft field handling requirements and yet satisfying weight and cost constraints that result in a more combat efficient aircraft.

**REPORT DOCUMENTATION PAGE**

<b>1. Recipient's Reference</b>	<b>2. Originator's Reference</b>	<b>3. Further Reference</b>	<b>4. Security Classification of Document</b>
	AGARD-CP-326	ISBN 92-835-0316-2	UNCLASSIFIED
<b>5. Originator</b>	Advisory Group for Aerospace Research and Development North Atlantic Treaty Organization 7 rue Ancelle, 92200 Neuilly sur Seine, France		
<b>6. Title</b>	AIRCRAFT DYNAMIC RESPONSE TO DAMAGED AND REPAIRED RUNWAYS		
<b>7. Presented at</b>	the 52nd Meeting of the AGARD Structures and Materials Panel in Çeşme, Turkey on 5-10 April 1981 and at the 54th Meeting in Brussels, Belgium on 4-9 April 1982.		
<b>8. Author(s)/Editor(s)</b>			<b>9. Date</b>
Various			August 1982
<b>10. Author's/Editor's Address</b>			<b>11. Pages</b>
Various			232
<b>12. Distribution Statement</b>	This document is distributed in accordance with AGARD policies and regulations, which are outlined on the Outside Back Covers of all AGARD publications.		
<b>13. Keywords/Descriptors</b>			
Aircraft Taxiing Dynamic response Runways		Surface properties Maintenance Damage	
<b>14. Abstract</b>			
<p>During 1981 and 1982 the AGARD Structures and Materials Panel held two technical meetings on "Aircraft Dynamic Response to Damaged and Repaired Runways". The 1981 meeting focused on the environment of damaged airfields, while the 1982 Specialists' Meeting focused on aircraft dynamic response. The meetings had two main goals: (1) to review the programs and methods within the AGARD countries for dynamic analysis and testing of taxiing aircraft, and (2) to encourage the exchange of information on aircraft dynamic response, thereby improving the interoperability of NATO military aircraft. The publication consists of the papers presented at these meetings.</p>			

<p>AGARD Conference Proceedings No.326 Advisory Group for Aerospace Research and Development, NATO AIRCRAFT DYNAMIC RESPONSE TO DAMAGED AND REPAIRED RUNWAYS Published August 1982 232 pages</p> <p>During 1981 and 1982 the AGARD Structures and Materials Panel held two technical meetings on "Aircraft Dynamic Response to Damaged and Repaired Runways". The 1981 meeting focused on the environment of damaged airfields, while the 1982 Specialists' Meeting focused on aircraft dynamic response. The meetings had two main goals: (1) to review the programs and methods within the AGARD countries for dynamic</p> <p>P.T.O.</p>	<p>AGARD-CP-326</p> <p>Aircraft Taxiing Dynamic response Runways Surface properties Maintenance Damage</p>	<p>AGARD Conference Proceedings No.326 Advisory Group for Aerospace Research and Development, NATO AIRCRAFT DYNAMIC RESPONSE TO DAMAGED AND REPAIRED RUNWAYS Published August 1982 232 pages</p> <p>During 1981 and 1982 the AGARD Structures and Materials Panel held two technical meetings on "Aircraft Dynamic Response to Damaged and Repaired Runways". The 1981 meeting focused on the environment of damaged airfields, while the 1982 Specialists' Meeting focused on aircraft dynamic response. The meetings had two main goals: (1) to review the programs and methods within the AGARD countries for dynamic</p> <p>P.T.O.</p>	<p>AGARD-CP-326</p> <p>Aircraft Taxiing Dynamic response Runways Surface properties Maintenance Damage</p>
<p>AGARD Conference Proceedings No.326 Advisory Group for Aerospace Research and Development, NATO AIRCRAFT DYNAMIC RESPONSE TO DAMAGED AND REPAIRED RUNWAYS Published August 1982 232 pages</p> <p>During 1981 and 1982 the AGARD Structures and Materials Panel held two technical meetings on "Aircraft Dynamic Response to Damaged and Repaired Runways". The 1981 meeting focused on the environment of damaged airfields, while the 1982 Specialists' Meeting focused on aircraft dynamic response. The meetings had two main goals: (1) to review the programs and methods within the AGARD countries for dynamic</p> <p>P.T.O.</p>	<p>AGARD-CP-326</p> <p>Aircraft Taxiing Dynamic response Runways Surface properties Maintenance Damage</p>	<p>AGARD Conference Proceedings No.326 Advisory Group for Aerospace Research and Development, NATO AIRCRAFT DYNAMIC RESPONSE TO DAMAGED AND REPAIRED RUNWAYS Published August 1982 232 pages</p> <p>During 1981 and 1982 the AGARD Structures and Materials Panel held two technical meetings on "Aircraft Dynamic Response to Damaged and Repaired Runways". The 1981 meeting focused on the environment of damaged airfields, while the 1982 Specialists' Meeting focused on aircraft dynamic response. The meetings had two main goals: (1) to review the programs and methods within the AGARD countries for dynamic</p> <p>P.T.O.</p>	<p>AGARD-CP-326</p> <p>Aircraft Taxiing Dynamic response Runways Surface properties Maintenance Damage</p>

<p>analysis and testing of taxiing aircraft, and (2) to encourage the exchange of information on aircraft dynamic response, thereby improving the interoperability of NATO military aircraft. The publication consists of the papers presented at these meetings.</p> <p>Papers presented at the 52nd Meeting of the AGARD Structures and Materials Panel in Çeşme, Turkey on 5-10 April 1981 and at the 54th Meeting in Brussels, Belgium on 4-9 April 1982.</p>	<p>analysis and testing of taxiing aircraft, and (2) to encourage the exchange of information on aircraft dynamic response, thereby improving the interoperability of NATO military aircraft. The publication consists of the papers presented at these meetings.</p> <p>Papers presented at the 52nd Meeting of the AGARD Structures and Materials Panel in Çeşme, Turkey on 5-10 April 1981 and at the 54th Meeting in Brussels, Belgium on 4-9 April 1982.</p>
<p>ISBN 92-835-0316-2</p> <p>analysis and testing of taxiing aircraft, and (2) to encourage the exchange of information on aircraft dynamic response, thereby improving the interoperability of NATO military aircraft. The publication consists of the papers presented at these meetings.</p> <p>Papers presented at the 52nd Meeting of the AGARD Structures and Materials Panel in Çeşme, Turkey on 5-10 April 1981 and at the 54th Meeting in Brussels, Belgium on 4-9 April 1982.</p>	<p>ISBN 92-835-0316-2</p> <p>analysis and testing of taxiing aircraft, and (2) to encourage the exchange of information on aircraft dynamic response, thereby improving the interoperability of NATO military aircraft. The publication consists of the papers presented at these meetings.</p> <p>Papers presented at the 52nd Meeting of the AGARD Structures and Materials Panel in Çeşme, Turkey on 5-10 April 1981 and at the 54th Meeting in Brussels, Belgium on 4-9 April 1982.</p>
<p>ISBN 92-835-0316-2</p>	<p>ISBN 92-835-0316-2</p>